



Wissenschaftszentrum Weihenstephan

Lehrstuhl für Biotechnologie der Nutztiere

Role of Sod2 in Pancreatic Carcinogenesis

Christin Ruoff

Vollständiger Abdruck der von der Fakultät Wissenschaftszentrum Weihenstephan für Ernährung, Landnutzung und Umwelt der Technischen Universität München zur Erlangung des akademischen Grades eines

Doktors der Naturwissenschaften

genehmigten Dissertation.

Vorsitzender: Univ.-Prof. Dr. H. Luksch

Prüfer der Dissertation:

1. Univ.-Prof. A. Schnieke, Ph.D.
2. Univ.-Prof. Dr. R. M. Schmid

Die Dissertation wurde am 27.11.2014 bei der Technischen Universität München eingereicht und durch die Fakultät Wissenschaftszentrum Weihenstephan für Ernährung, Landnutzung und Umwelt am 30.03.2015 angenommen.

TABLE OF CONTENTS

TABLE OF CONTENTS	I
LIST OF FIGURES	IV
LIST OF TABLES	VI
LIST OF ABBREVIATIONS	VII
I. Abstract	1
Zusammenfassung	3
II. Introduction	5
1. <i>Biology of the Pancreas</i>	5
1.1. Anatomy and Physiology of the Pancreas	5
1.2. Diseases of the Pancreas	6
1.2.1. Diabetes	6
1.2.2. Pancreatitis	7
1.2.3. Pancreatic Cancer	8
1.3. Pancreatic Ductal Adenocarcinoma (PDAC)	10
1.3.1. Mouse Models of PDAC	11
1.3.2. Open Questions in PDAC Research	12
2. <i>Oxidants, Antioxidants and Oxidative Stress</i>	13
2.1. Oxidants	13
2.2. Reactive Oxygen Species (ROS)	14
2.2.1. Types of ROS	14
2.2.2. Sources of ROS	16
2.3. Biological Effects of ROS	19
2.3.1. ROS-Mediated Modifications of Biomolecules	19
2.3.2. Physiological Role of ROS	22
2.4. Antioxidants	24
2.4.1. Antioxidant Enzymes	24
2.4.2. Accessory Antioxidant Enzyme Systems	27
2.4.3. Non-enzymatic Antioxidants	30
2.5. Oxidative Stress	34
3. <i>Aims of the Study</i>	34
III. Material and Methods	37
1. <i>Chemicals, Buffers and Solutions</i>	37
1.1. Standard Chemicals	37
1.2. Standard Buffers and Solutions	37
2. <i>Mice</i>	38
2.1. Transgenic Mouse Strains	38
2.2. Mouse Husbandry	38
2.3. High Fat Diet (HFD) Feeding Experiments	38

2.4. Intraperitoneal Glucose Tolerance Test (IP-GTT).....	39
2.5. Analysis of Stool Samples.....	39
2.5.1. Collection of Stool Samples.....	39
2.5.2. Assay for Total Proteases in Stool.....	39
2.5.3. Assay for Total Lipases in Stool.....	40
2.6. Tissue Harvesting and Preparation of Formalin-Fixed, Paraffin-Embedded (FFPE) Tissue Blocks.....	40
2.7. Histological Analyses.....	40
2.7.1. Hemalaun-Eosin (H&E) Staining.....	41
2.7.2. Masson's Trichrome Staining.....	41
2.7.3. Immunohistochemistry.....	41
2.7.4. Immunofluorescence.....	43
2.7.5. Image Acquisition and Preparation.....	44
2.7.6. Image Analysis.....	45
3. <i>Cell Isolation and Culture</i>	45
3.1. Equipment and Supplies.....	45
3.2. Murine Primary Acini.....	46
3.2.1. Isolation of Murine Primary Acini.....	46
3.2.2. Analysis of Murine Primary Acini.....	47
3.3. Murine PDAC Cell Lines.....	48
3.3.1. Isolation and Maintenance of Murine PDAC Cell Lines.....	48
3.3.2. Culture of Murine PDAC Cell Lines.....	49
3.3.3. Treatment of Murine PDAC Cell Lines.....	49
3.3.4. Mycoplasma Testing.....	50
4. <i>Molecular Biological Methods</i>	50
4.1. DNA-based Methods.....	50
4.1.1. DNA Isolation.....	50
4.1.2. Polymerase Chain Reaction (PCR).....	51
4.1.3. Mitochondrial DNA Damage Quantitative PCR (qPCR) and Copy Number Assay.....	52
4.1.4. Agarose Gel Electrophoresis.....	54
4.2. RNA-based Methods.....	54
4.2.1. RNA Isolation from Murine Pancreas.....	54
4.2.2. Reverse Transcription-Polymerase Chain Reaction (RT-PCR).....	54
4.3. Protein-based Methods.....	56
4.3.1. Protein Isolation from Murine Tissues, PDAC Cell Lines and Primary Pancreatic Acini.....	56
4.3.2. Immunoblot Analysis.....	57
4.3.3. Ras Activity Assay.....	58
4.4. Oxidative Stress Methods.....	59
4.4.1. Carboxy-H ₂ DCFDA and MitoSOX Plate Assay.....	59
4.4.2. Spin Trap and Electron Spin Resonance (ESR) Spectrometry.....	59
5. <i>Statistical Analysis</i>	60
IV. Results.....	61
1. <i>Characterization of the Pancreas-Specific Sod2 Knockout Mouse</i>	61

2. Role of <i>Sod2</i> in Pancreatic Cancer.....	71
2.1. Role of <i>Sod2</i> in <i>Kras</i> ^{G12D} -Mediated PDAC.....	71
2.2. Role of <i>Sod2</i> in <i>Trp53</i> ^A ; <i>Kras</i> ^{G12D} -Mediated PDAC	89
V. Discussion.....	96
1. Characterization of the Pancreas-Specific <i>Sod2</i> Knockout Mouse	96
1.1. Effects of <i>Sod2</i> Deletion on Pancreatic Development and Function.....	96
1.1.1. Influence of the Genetic Background on <i>Sod2</i> Deletion	97
1.2. Loss of <i>Sod2</i> and Oxidative Stress	97
1.3. Loss of <i>Sod2</i> and Cell Fate Determination	100
1.4. Loss of <i>Sod2</i> and Mitochondrial Function	101
1.5. Effects of Heterozygous Pancreas-Specific <i>Sod2</i> Deletion	101
1.6. The Neurological Phenotype Observed with <i>Ptf1a-Cre</i> ^{ex1} -Mediated <i>Sod2</i> Deletion	101
2. Role of <i>Sod2</i> in Pancreatic Cancer.....	103
2.1. Influence of <i>Sod2</i> Status on Ras Signaling in <i>Kras</i> ^{G12D} Pancreata	104
2.2. Influence of <i>Sod2</i> Status on Trp53 Signaling in <i>Kras</i> ^{G12D} Pancreata	104
2.3. Gender-Specific Effect of <i>Sod2</i> Deletion in Pancreatic Carcinogenesis	105
2.4. <i>Trp53</i> -Dependency of the Gender-Specific Benefit of <i>Sod2</i> Deletion in Pancreatic Cancer	107
2.5. Possible Implications for Human Disease	108
VI. Conclusions	110
VII. References.....	111
APPENDIX	VIII
ACKNOWLEDGEMENTS.....	XII
CURRICULUM VITAE	XIII

LIST OF FIGURES

Figure II.1:	Anatomy and physiology of the pancreas.....	5
Figure II.2:	Tumor progression model for PDAC.....	11
Figure II.3:	Formation of the most important ROS from $O_2^{\cdot-}$	14
Figure IV.1:	<i>Sod2</i> -loss is confirmed in pancreata of <i>Sod2</i> ^{ΔPanc/ΔPanc} mice on RNA and protein level.	61
Figure IV.2:	Body weights and survival are reduced in <i>Sod2</i> knockout compared with wt mice.	62
Figure IV.3:	Histomorphologically, <i>Sod2</i> knockout are indistinguishable from wt pancreata.	64
Figure IV.4:	Endocrine function of <i>Sod2</i> knockout is not different from wt pancreata. ...	65
Figure IV.5:	Exocrine function of female <i>Sod2</i> knockout might be slightly reduced compared with female wt pancreata.	66
Figure IV.6:	ROS are mildly increased in <i>Sod2</i> knockout pancreata.	69
Figure IV.7:	Proliferation and apoptosis are not affected by pancreas-specific <i>Sod2</i> knockout.....	70
Figure IV.8:	Body weights are reduced in <i>Kras</i> ^{G12D/+} ; <i>Sod2</i> ^{ΔPanc/ΔPanc} compared with <i>Kras</i> ^{G12D/+} mice.	71
Figure IV.9:	<i>Sod2</i> knockout prolongs tumor-free, but not overall survival in female <i>Kras</i> ^{G12D/+} mice.	73
Figure IV.10:	There is a partly significant trend towards less intact pancreatic tissue and a higher number of PanIN lesions comparing <i>Kras</i> ^{G12D/+} ; <i>Sod2</i> ^{ΔPanc/ΔPanc} with <i>Kras</i> ^{G12D/+} mice.	74
Figure IV.11:	Male <i>Kras</i> ^{G12D/+} ; <i>Sod2</i> ^{ΔPanc/ΔPanc} deposit slightly, but not significantly more collagen than male <i>Kras</i> ^{G12D/+} pancreata.	76
Figure IV.12:	<i>Kras</i> ^{G12D/+} ; <i>Sod2</i> ^{ΔPanc/ΔPanc} might express less Amy1 and more Ck19 than <i>Kras</i> ^{G12D/+} pancreata.	77
Figure IV.13:	<i>Kras</i> ^{G12D/+} ; <i>Sod2</i> ^{ΔPanc/ΔPanc} acinar explants transdifferentiate faster than <i>Kras</i> ^{G12D/+} acinar explants.	79
Figure IV.14:	Concomitant <i>Sod2</i> knockout slightly increases ROS in <i>Kras</i> ^{G12D/+} pancreata.	80
Figure IV.15:	<i>Sod2</i> knockout might reduce proliferation and increase apoptosis in <i>Kras</i> ^{G12D/+} pancreata.	81
Figure IV.16:	<i>Sod2</i> knockout might reduce Ras activity in <i>Kras</i> ^{G12D/+} mice.....	83
Figure IV.17a:	Esr1, but not Esr2 signaling might be altered by <i>Sod2</i> knockout in <i>Kras</i> ^{G12D/+} mice.	85
Figure IV.17b:	Expression of several potential Esr1 target genes is altered by <i>Sod2</i> knockout in <i>Kras</i> ^{G12D/+} mice.....	87
Figure IV.18:	Trp53 target gene expression is probably unaffected by <i>Sod2</i> knockout in <i>Kras</i> ^{G12D/+} mice.....	88
Figure IV.19:	Pancreas-specific <i>Sod2</i> knockout significantly prolongs survival in female <i>p53</i> ^{ΔPanc/+} ; <i>Kras</i> ^{G12D/+} , but not <i>p53</i> ^{ΔPanc/Panc} ; <i>Kras</i> ^{G12D/+} mice.	89

Figure IV.20: <i>Sod2</i> deletion does not prevent loss of the second <i>Trp53</i> allele in <i>p53^{ΔPanc/+};Kras^{G12D/+}</i> derived PDAC or PDAC cell lines.....	90
Figure IV.21: <i>Sod2</i> deletion does not increase expression of the remaining <i>Trp53</i> allele in <i>p53^{ΔPanc/+};Kras^{G12D/+}</i> derived PDAC.	92
Figure IV. 22: <i>Sod2</i> deletion might reduce mitochondrial function in <i>Kras^{G12D/+}</i> , but not in <i>p53^{ΔPanc/+};Kras^{G12D/+}</i> and <i>p53^{ΔPanc/ΔPanc};Kras^{G12D/+}</i> PDAC cell lines. ...	93
Figure IV. 23: <i>Sod2</i> deletion increases sensitivity of <i>Kras^{G12D/+}</i> , <i>p53^{ΔPanc/+};Kras^{G12D/+}</i> , and <i>p53^{ΔPanc/ΔPanc};Kras^{G12D/+}</i> PDAC cell lines to SIN-1 but does not alter mitochondrial DNA damage or copy number.	94

LIST OF TABLES

Table III.1:	Standard chemicals.....	37
Table III.2:	Antibodies and conditions for immunohistochemistry.	42
Table III.3:	Sequences and amplicon sizes of primers used in PCR.	51
Table III.4:	Sequences, amplicon sizes and efficiencies of primers used in Mitochondrial DNA Damage Quantitative PCR (qPCR) and Copy Number Assay.	53
Table III.5:	Sequences, amplicon sizes and efficiencies of primers used in RT-PCR.	55
Table III.6:	Primary antibodies, target protein sizes and conditions used for immunoblot analysis.....	57
Table Appendix.1:	Gene symbols and names.....	VIII
Table Appendix.2:	Brands and companies.	X

LIST OF ABBREVIATIONS

4-HNE	4-hydroxy-2-noneal
8-oxo-dG	8-hydroxyguanine
ACC	acinar cell carcinoma
ADM	acinar-to-ductal metaplasia
ALS	amyotrophic lateral sclerosis
AP	acute pancreatitis
BrdU	5-Bromo-2-deoxyuridine
CNS	central nervous system
CP	chronic pancreatitis
DSB	double-strand DNA break
ESR	electron spin resonance
ETC	electron transport chain
FFPE	formalin-fixed, paraffin-embedded
GSH	(reduced) glutathione
GSSG	glutathione disulfide
H ₂ O ₂	hydrogen peroxide
HCC	hepatocellular carcinoma
H&E	hemalaun-eosin
HFD	high fat diet
HOCl	hypochlorous acid
IP-GTT	intraperitoneal glucose tolerance test
IPMN	intraductal papillary mucinous neoplasm
LDL	low density lipoprotein
LPO	lipid peroxidation
MCN	mucinous cystic neoplasm
MMP	matrix metalloproteinase
MDA	malonyldialdehyde
•NO	nitric oxide
O ₂ ^{•-}	superoxide
•OH	hydroxyl radical
ONOO ⁻	peroxynitrite anion
PanET	pancreatic endocrine tumor
PanIN	pancreatic intraepithelial neoplasia
PDAC	pancreatic ductal adenocarcinoma
PUFA	polyunsaturated fatty acid
rcf	relative centrifugal force
ROS	reactive oxygen species
SOD	superoxide dismutase
SSB	Single-strand DNA break
TBARS	thiobarbituric acid-reactive substances
wt	wild-type

Gene symbols and names can be found in Table Appendix.1.

I. Abstract

Pancreatic ductal adenocarcinoma (PDAC) is one of the deadliest human cancers and kills over 94 % of patients within the first year of diagnosis. Despite extensive research and tremendous advances for other cancer types, prognosis of PDAC has hardly improved in the last decades creating a desperate need for novel early diagnosis and therapeutic strategies.

Oxidative stress caused by reactive oxygen species (ROS) generated in the cells' power plants, the mitochondria, has been implicated in the development and progression of neoplastic diseases - and in particular of PDAC.

Superoxide dismutases (SODs) are a class of antioxidant enzymes, which protect cells from ROS. Of the SODs, mitochondrial SOD2 is the only essential isoform and *Sod2* knockout mice succumb early after birth. Although a body of evidence suggests a positive correlation between *SOD2*-loss and PDAC, the nature of this association has never been investigated *in vivo*.

Making use of a pancreas-specific *Sod2* knockout mouse line, the present thesis first shows that *Sod2* is fully dispensable to physiological pancreatic development and function and the only significant pancreas-related phenotypic aberrations noted were a slight increase in ROS and a decrease in body weight.

To gain insight into the role of *Sod2* in PDAC, the effects of pancreas-specific *Sod2* deletion were then investigated in three common PDAC mouse models: the relatively mild *Kras*^{G12D/+} mouse model, which harbors pancreas-specific, mono-allelic activation of the proto-oncogene *Kras* and the faster and more stringent *Trp53*^{ΔPanc/+}; *Kras*^{G12D/+} or *Trp53*^{ΔPanc/ΔPanc}; *Kras*^{G12D/+} mouse models, which combine pancreas-specific, mono-allelic *Kras* activation with concomitant pancreas-specific, mono- or bi-allelic deletion of the tumor suppressor gene *Trp53*, respectively.

In the *Kras*^{G12D/+} mouse line, pancreas-specific *Sod2* deletion mildly accelerated acinar-to-ductal metaplasia, one of the key initiatory events of PDAC formation, potentially due to an increase in ROS.

Yet, conversely, *Sod2* deficiency also significantly prolonged tumor-free survival of female *Kras*^{G12D/+} mice. Strikingly, the protective effect of *Sod2* deletion extended to female *Trp53*^{ΔPanc/+}; *Kras*^{G12D/+} mice, but was absent in male *Kras*^{G12D/+} mice, male *Trp53*^{ΔPanc/+}; *Kras*^{G12D/+} mice, or *Trp53*^{ΔPanc/ΔPanc}; *Kras*^{G12D/+} mice of both genders. While the lack of protection seen with the *Trp53*^{ΔPanc/ΔPanc}; *Kras*^{G12D/+} mice indicates that the beneficial effect of *Sod2* deletion requires at least one functional *Trp53* allele, neither proliferation, nor apoptosis, nor *Trp53* signaling were found to be affected by *Sod2* status. However, *Sod2* deletion was found to increase sensitivity to oxidative stress. Furthermore, differential estrogen receptor 1 expression indicated that sex hormone signaling might, at least partly, account for the gender-specificity of this benefit.

Taken together, to my knowledge, the present thesis suggests for the first time that *Sod2* has tumor-inhibitory capacity in the early, but tumor-promoting capacity in the late stages of PDAC carcinogenesis. In addition, it provides the first evidence of a gender-specific effect of *Sod2*. While the first aspect is supported by recent findings in skin cancer and lymphoma, gender-specific effects have never been reported for any other antioxidant enzyme or tissue before.

The clinical relevance of the presented findings may be illustrated by the failure of antioxidant supplementation in the treatment or supportive treatment of human cancers. The present study is in concert with these reports. Moreover, it indicates that gender may impact the effects of antioxidants and that this may affect cancer progression and survival.

Zusammenfassung

Das duktale Adenokarzinom der Bauspeicheldrüse (PDA) ist eine der tödlichsten Krebserkrankungen des Menschen und über 94 % der Patienten versterben bereits innerhalb eines Jahres nach Diagnosestellung. Trotz intensiver Forschung und wesentlichen Fortschritten bei anderen Krebsarten, hat sich die Prognose für das PDA in den letzten Jahrzehnten kaum verbessert. Es besteht daher dringlicher Bedarf nach neuen diagnostischen und therapeutischen Ansätzen.

Oxidativer Stress, welcher durch reaktive Sauerstoffspezies (ROS) verursacht wird, die in den Mitochondrien, den Energielieferanten der Zelle, produziert werden, wird oft mit der Entstehung und dem Fortschreiten neoplastischer Erkrankungen – und insbesondere PDA – in Verbindung gebracht.

Superoxiddismutase (SOD) beschreibt eine Klasse antioxidanter Enzyme, welche Zellen vor ROS schützen. Die mitochondriale Isoform SOD2 ist die einzige essentielle Isoform der SOD und *Sod2*-Knockoutmäuse versterben kurz nach der Geburt. Obwohl eine Reihe von Hinweisen für einen positiven Zusammenhang zwischen dem Verlust von *SOD2* und PDA spricht, wurde dies niemals hinreichend *in vivo* untersucht.

Mittels einer auf die Bauspeicheldrüse beschränkte *Sod2*-Knockoutmauslinie, zeigt die vorliegende Arbeit zunächst, dass *Sod2* für die physiologische Entwicklung und Funktion der Bauspeicheldrüse nicht notwendig ist. Ein geringes Ansteigen der ROS-Level sowie ein leicht verringertes Körpergewicht blieben die einzigen gewebespezifisch feststellbaren phänotypischen Auffälligkeiten.

Um einen Einblick in die Rolle von *Sod2* bei PDA zu gewinnen, wurden anschließend die Auswirkungen der bauchspeicheldrüsen-spezifischen Deletion von *Sod2* in drei gebräuchlichen Mausmodellen für das PDA untersucht: Das relativ milde *Kras*^{G12D/+}-Modell, welches durch eine bauchspeicheldrüsen-spezifische, monoallelische Aktivierung des Protoonkogens *Kras* gekennzeichnet ist, sowie die schnelleren und stringenteren *Trp*^{ΔPanc/+};*Kras*^{G12D/+}- und *Trp*^{ΔPanc/ΔPanc};*Kras*^{G12D/+}-Modelle, in denen bauchspeicheldrüsen-spezifische, monoallelische Aktivierung von *Kras* mit bauchspeicheldrüsen-spezifischer, mono- oder biallelischer Deletion des Tumorsuppressorgens *Trp53* kombiniert wird.

In der *Kras*^{G12D/+}-Mauslinie, beschleunigte gleichzeitige auf die Bauspeicheldrüse beschränkte Deletion von *Sod2* geringfügig die azinoduktale Metaplasie, eines der Schlüsselereignisse der frühen PDA-Entstehung. Dies geschah möglicherweise durch ein Ansteigen von ROS.

Andererseits verlängerte die *Sod2*-Defizienz jedoch ebenfalls signifikant das tumorfreie Überleben weiblicher *Kras*^{G12D/+}-Mäuse. Dieser protektive Effekt manifestierte sich ebenfalls bei den weiblichen *Trp*^{ΔPanc/+};*Kras*^{G12D/+}-Tieren, jedoch nicht bei den männlichen *Kras*^{G12D/+}-Mäusen, den männlichen *Trp*^{ΔPanc/+};*Kras*^{G12D/+}-Mäusen oder den *Trp*^{ΔPanc/ΔPanc};*Kras*^{G12D/+}-Mäusen beider Geschlechter. Die Abwesenheit eines protektiven

Effekts bei den $Trp^{\Delta Panc/\Delta Panc};Kras^{G12D/+}$ -Mäusen deutet darauf hin, dass für den positiven Effekt der *Sod2*-Deletion mindestens ein funktionelles *Trp53*-Allel vonnöten ist. Der *Sod2*-Status beeinflusste aber weder die Proliferation, noch die Apoptose, noch das *Trp53*-Signaling. Hingegen vergrößerte der *Sod2*-Verlust die Sensitivität gegenüber oxidativem Stress. Des Weiteren deutete veränderte Östrogenrezeptor 1-Expression darauf hin, dass Sexualhormon-Signalwege eine Rolle bei der Geschlechtsspezifität der beobachteten Protektion spielen könnten.

Nach meinem besten Wissen legt die vorliegende Arbeit zum ersten Mal den Schluss nahe, dass *Sod2* tumorhemmende in der frühen, jedoch tumorfördernde Eigenschaften in der späten Phase der Krebsentstehung haben könnte. Weiterhin liefert sie den ersten Hinweis darauf, dass *Sod2* eine geschlechtsspezifische Wirkung haben könnte. Während kürzlich veröffentlichte Studien mit Mausmodellen für Hautkrebs und Lymphom den ersten Punkt stützen, wurde noch niemals zuvor und in keinem Gewebe schon einmal von einer geschlechtsspezifischen Wirkung eines antioxidanten Enzyms berichtet.

Dass die hier vorliegenden Ergebnisse durchaus klinische Relevanz besitzen könnten, wird möglicherweise darin deutlich, dass die Gabe von Antioxidanzien bisher weder bei der Behandlung noch bei der unterstützenden Behandlung humaner Krebserkrankungen nennenswerte positive Effekte nach sich zog. Die vorliegende Arbeit legt einen ähnlichen Schluss nahe. Darüber hinaus könnten sie andeuten, dass das Geschlecht die Wirkung von Antioxidanzien beeinflussen könnte und dass dies Auswirkungen haben könnte auf das Fortschreiten und Überleben von Krebserkrankungen.

II. Introduction

1. Biology of the Pancreas

1.1. Anatomy and Physiology of the Pancreas

The pancreas is an organ of the upper abdomen that stretches quasi transversally from the loop of the duodenum to the spleen ([1]; see Figure II.1A). It has two histomorphologically and functionally distinctive compartments: The endocrine compartment predominantly secretes hormones that control carbohydrate metabolism, the exocrine compartment, on the other hand, mainly produces enzymes and bicarbonate and transports them to the duodenum for digestion of foods (Figure II.1B).

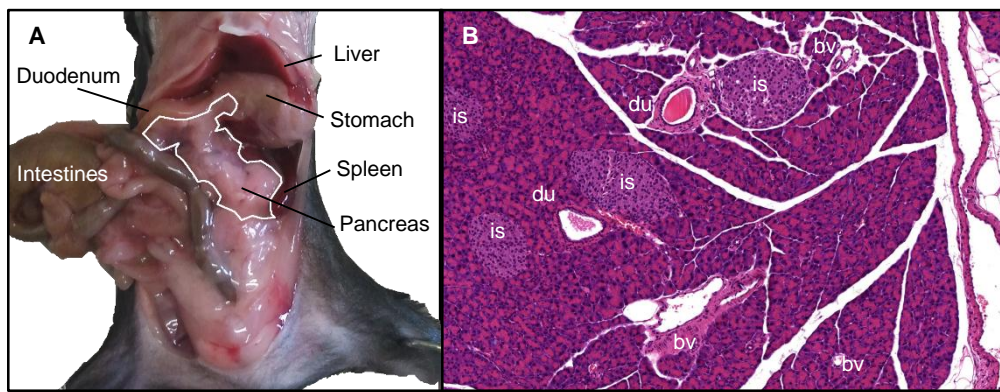


Figure II.1: Anatomy and physiology of the pancreas.

(A) Anatomic position of the pancreas.

(B) Microscopic appearance of the pancreas. is=islet of Langerhans, du=duct, bv=blood vessel.

The endocrine compartment, which only represents about 1 % of the organ volume, is covered by the islets of Langerhans. These spherical structures are scattered throughout the organ and composed of tens to hundreds of cells of five different types:

α -cells comprise 15 to 20 % of the Langerhans islets and produce glucagon after stimulation by cholecystokinin, insulin, or low blood glucose levels. This hormone induces glycogenolysis/gluconeogenesis in the liver and subsequent glucose transport into the blood stream [2, 3].

With 50 to 80 %, β -cells represent the majority of the Langerhans islet cells. Functionally, they counteract the α -cells and secrete insulin, a hormone which lowers blood glucose levels by stimulating glucose uptake into the cells in response to increased blood glucose levels, e.g. after a meal [2, 3].

Somatostatin-producing δ -cells, ghrelin-producing ϵ -cells, and pancreatic polypeptide-producing PP-cells, engage predominantly in regulating and fine-tuning α - and β -cell function [2, 4, 5].

The second functional entity of the pancreas, the exocrine compartment, is primarily composed of lobules of glandular cells, the acini, and ducts.

Acinar lobules, which consist of approximately 40 to 50 pyramidal acinar cells each, constitute the majority of the exocrine pancreas. Acini produce and store in granules a whole

range of digestive enzymes, mostly as inactive pro-enzymes. These include lipases, proteases (e.g. trypsin, chymotrypsins, carboxypeptidases, aminopeptidase, elastase), amylolytic amylases, and nucleases (deoxyribonucleases, ribonucleases). After food intake, acinar cells release these digestive pro-enzymes towards the center of the acinar lobules. From there, they enter the pancreatic ducts system, which is connected to the acini by centroacinar cells. The pancreatic enzymes are enriched with bicarbonate and water from the ductal lining and secreted into the duodenum. When the pancreatic juices enter the duodenum, enteral kinases activate the enzymatic precursors, which then participate in digesting the food while the bicarbonate neutralizes the acidic pH of the chyme and facilitates nutrient absorption by enterocytes [1, 2].

In addition to the aforementioned ones, stellate cells are another cell type of the pancreas. Under normal conditions, these fibroblast-like cells reside quiescently next to the vasculature and the acinar and ductal structures. However, during inflammatory processes, such as pancreatitis (see II.1.2.2), stellate cells become activated and start proliferating and producing collagen type I. This process is the main cause of fibrosis observed in pancreatitis and pancreatic cancer [2].

Blood supply of the pancreas is achieved by branches of the celiac and mesenteric superior, as well as the splenic and hepatic arteries, while splenic and mesenteric superior veins arrange for venous drainage towards the portal hepatic system [2]. The close connection of the splenic and portal veins to the pancreas may account for the early and extensive metastasis observed with pancreatic cancer [1].

1.2. Diseases of the Pancreas

Besides congenital disorders that arise due to defective organogenesis and may result in disturbed function or completed absence of single pancreatic cell types, the endocrine or exocrine compartment as well as the whole pancreas (see [1]), several acquired pancreatic pathologies exist. The most important ones are diabetes, pancreatitis, and pancreatic cancer.

1.2.1. Diabetes

Diabetes, or more correctly diabetes mellitus, is a disease involving the blood glucose regulatory function of the endocrine pancreas. Due to insufficient insulin secretion or insulin resistance, blood glucose levels can reach abnormally high levels, which may lead to macro- and microvascular complications (e.g. stroke, neuropathy, nephropathy, and retinopathy) as well as an impaired immune defense. Consequently, common long-term consequences may include loss of sight, exigency for limb amputation or kidney transplantation, or, at worst, death. Clinically, diabetes presents with high plasma glucose levels, polyuria, polyphagia and increased thirst, loss of weight, weakness and fatigue [3]. In 2010, about 7 % of the adult population were estimated to have diabetes, worldwide. In the next 20 years, this number is expected to rise by more than 50 %, meaning that about 440 million people will suffer from the disease. With a fatality rate of up to 25 %, diabetes constitutes a serious health problem [6].

Type 1 and 2 diabetes are the most common forms of diabetes.

Type 1, or insulin-dependent diabetes, is usually diagnosed in childhood and early adulthood (< 35 years). In most cases, it is an autoimmune disease, where activated CD4⁺ and CD8⁺ T cells and macrophages infiltrate the pancreatic Langerhans islets and destroy the insulin-producing β -cells resulting in complete loss of insulin production. Due to the total lack of insulin, treatment for type 1 diabetes is insulin supplementation via injection or oral administration [3, 7].

Up to 90 % of diabetic patients worldwide suffer from type 2 diabetes. In this type, insulin resistance precedes insufficient insulin synthesis and secretion. It is considered mostly a metabolic disease and associated with obesity, hypertension, and dyslipidemia. While normally diagnosed after the fourth decade of life, the incidence in children and young adults is rapidly increasing due to the stark rise in obesity. Although in type 2 diabetes progressive β -cell destruction is common, it rarely progresses to a point of complete insulin deficiency, as it is not immune mediated. Therefore, type 2 diabetes can often be managed by a change in lifestyle, diet, weight control and a more stringent control of blood pressure and blood glucose levels. In patients that do not respond to these measures, oral anti-diabetic drugs are used [3, 7].

1.2.2. Pancreatitis

Acute pancreatitis (AP) is an acute inflammatory condition of the pancreas that affects about 1 to 5 per 10,000 people worldwide each year. Patients usually present with sudden onset of abdominal pain, nausea, and vomiting. While 80 to 90 % of patients have mild disease and uneventfully recover without any long-term complications or recurrences, some patients may develop severe AP. In these instances, AP is associated with local and/or systemic complications, including necrosis, abscess, pseudocyst, and infection and/or multi organ failure and death, respectively. Notably, while in general, AP has a fatality rate of 2 to 5 %, severe AP may have a mortality of up to 20 % [8].

The pathogenesis of AP can be divided into an early inflammatory and a late regeneration phase. The early inflammatory phase is initiated, when, in response to a triggering insult, acinar digestive pro-enzymes become prematurely activated already in the pancreas. If their secretion is inhibited, the activated digestive enzymes lead to an auto-digestion of the pancreas and a destruction of the parenchyma. Thereafter, the injured pancreas (presumably the acinar cells; [9]) starts producing cytokines (e.g. tumor necrosis factor and platelet-activating factor), chemokines (e.g. chemokine (C-C motif) ligand 2) and cell adhesion molecules (e.g. intercellular adhesion molecule 1), which attract and activate neutrophils (and potentially macrophages) and promote pancreatic inflammation [8]. These cytokines might not only activate pancreatic stellate cells, but also be responsible for the distant organ injury observed with severe AP, when released into circulation [10].

After the acute inflammatory phase, anti-inflammatory cytokines (e.g. interleukin 10 or transforming growth factor, β ; [11]) allow for pancreatic regeneration. While complete remission is common, after severe AP, full pancreatic recovery may take up to one year [10].

The most common etiologies of AP include biliary stones (30 to 50 %) and alcohol abuse (20 to 40 %). However, both conditions rarely cause AP, and only about 2 % of gallstone patients and 5 % of alcohol abusers develop AP. In up to 30 % of patients, no clear etiology can be identified [8, 10].

Recurrent episodes of AP are most commonly related to alcohol abuse (60 %) or untreated biliary stones (19 %), while about 17 % of cases appear idiopathic [10].

Chronic pancreatitis (CP) is characterized by persistent pancreatic inflammation that results in progressive parenchymal injury and fibrosis. These confer irreversible damage to the pancreas, potentially resulting in destruction of the whole organ. Patients usually suffer from maldigestion, diabetes and severe unremitting pain often requiring hospital admission [12]. AP is a common etiology of CP and about 50 % of patients with recurrent AP develop CP [11]. Other etiologies include alcohol abuse and genetic predisposition. In about 20 % of cases, no clear etiology can be discerned. Notably, CP is one of the biggest risk factors for pancreatic cancer and it is estimated to confer a 15 to 20-fold elevated risk for developing the disease ([13]; rev. in [11]).

1.2.3. Pancreatic Cancer

Pancreatic cancer is only among the 9th (women) to 10th (men) most commonly diagnosed human cancers in the US; however, ranking fourth leading cause of cancer deaths among both genders, it is one of the deadliest and kills 94 % of patients within the first year of diagnosis. The poor prognosis is largely due to the fact that the disease is usually not detected until advanced stages when the cancer has spread and surgery - the only treatment that offers a chance of cure - is no longer an option. Even in those rare cases when surgery is still possible, prognosis is poor with a 5-year survival rate of only 20 to 25 % [14].

Cancers may arise in both endocrine and exocrine pancreatic compartment. In addition, the pancreas might also be origin of primary lymphoma or site for distant metastasis of tumors of other organs or organ systems. However, both of the latter are rare conditions.

Pancreatic lymphoma may account for 2.8 % of pancreatic cancers and generally affects patients in their sixties [15]. Primary treatment involves chemo- and radiotherapy according to non-Hodgkin's lymphoma protocols and may be curative in up to 30 % of patients [16].

Almost any type of cancer may spread to the pancreas, but Adsay and colleagues report, that most pancreatic metastases originate from tumors of the lung, the gastrointestinal tract, and lymphomas. Notably, in one third of cases, pancreatic metastases were initially suspected to be primary pancreatic cancers ([17]; rev. in [18]).

Pancreatic endocrine tumors (PanETs) constitute 1 to 2 % of pancreatic cancers and affect about one out of 100,000 people per year. In some cases, they arise in the context of a hereditary tumor-predisposing syndrome, such as multiple endocrine neoplasia type I and von Hippel-Lindau disease [18].

Different types of PanETs are distinguished and diagnosed by the hormones they produce. They include glucagonomas, insulinomas, gastrinomas, somatostatinomas, adrenocorticotrophic hormone producing tumors, and growth hormone releasing factor

secreting tumors. Additionally, about 15 to 30 % of PanETs are classified non-functional PanETs as they are clinically inert but produce neuroendocrine cell markers such as chromogranin-A and somatostatin receptors. The type of PanET is not only relevant to clinical presentation, but also to course of treatment, and prognosis. Often, a combination of surgical and medical measures provides the best approach with respects to symptom treatment and prognosis. Of note, metabolic irregularities, which are common in these tumors, should be corrected prior to treatment. Median survival of PanETs lies between 40 and 60 months [18].

Pancreatic exocrine tumors are classified predominantly according to their histological appearance. Pancreatic ductal adenocarcinoma (PDAC), as the name states, primarily exhibits a glandular pattern with duct-like structures and accounts for more than 85 % of pancreatic cancers [19].

Pancreatic intraepithelial neoplasms (PanINs) are the most common type of ductal neoplasia and occur in up to 30 % of pancreata [19]. While these microscopic lesions of the smaller ducts (< 5 mm) are never invasive *per se*, they are well-recognized as precursor lesions to invasive PDAC (see below; [20, 21]).

Other types of ductal neoplasms include serous, mucinous, and papillary cystic lesions, which represent less than 10 % of pancreatic neoplasms. Two common types of are serous cystadenomas and mucinous cystic neoplasms (MCNs). Both types are most frequently found in women. While serous cystadenomas are almost uniformly benign, 8 to 33 % of MCNs represent invasive carcinomas. Surgical removal is the predominant course of action for both [18].

Intraductal papillary mucinous neoplasms (IPMNs) are another type of cystic ductal neoplasms and occur in patients older than 60. Again, surgical resection is the treatment of choice and about 50 % of resected specimens contain invasive carcinoma. Median survival depends on tumor stage and ranges from 77 to 100 % for noninvasive and 43 to 65 % for invasive IPMNs [18].

Solid pseudopapillary tumors of the pancreas are rare and predominantly affect young women in their twenties. In approximately 20 % of cases, metastases are present at time of presentation, nonetheless, cure rates after surgical resection are higher than 95 % [22].

About 1 % of pancreatic cancers are classified acinar cell carcinoma (ACC). These tumors are generally well differentiated and express the pancreatic digestive enzymes. About 50 % of ACC patients exhibit metastatic disease at time of diagnosis and stage of disease correlates well with prognosis. Surgery might not be sufficient in treating the disease as many patients develop distant recurrences after primary tumor resection. Median survival of ACC lies at about 19 months [23].

Moreover, squamous cell carcinoma may arise from squamous metaplastic cells that may appear in the pancreas in the course of inflammation. This type affects patients at approximately 62 years, represents 0.5 to 2 % of pancreatic cancers and has a very poor prognosis with median survival of three to seven months for non-resectable or resectable disease, respectively [24].

Tumors of mixed types are extremely rare and include e.g. pancreatoblastoma, a tumor that is usually found in children [25], mixed acinar-endocrine [26], and mixed acinar-ductal

carcinoma [27]. Generally, median survival times are low in these instances and therapy might involve surgery as well as chemotherapy.

1.3. Pancreatic Ductal Adenocarcinoma (PDAC)

PDAC is not only the most prevalent type of pancreatic cancer, but also the one with the worst prognosis, which is reflected in a median survival of only 4 to 6 months [28, 23]. Besides CP, the most common predisposing factors of PDAC include smoking, diabetes, obesity, and familial cancer syndromes [14].

In 2000, data from postmortem examination, clinical studies, and molecular genetic analyses prompted Hruban and colleagues to propose a tumor progression model from precursor lesions to invasive PDAC, which is analogous to the adenoma-carcinoma tumor sequence of colorectal cancer and involves the stepwise accumulation of genetic and morphological changes [29]. Today, this model is well-accepted and various mouse models have reinforced its validity [28, 30, 31, 32, 33, 34].

Besides potentially already representing invasive carcinomas on their own (see II.1.2.3), MCNs and IPMNs are also well-accepted precursor lesions for PDAC. However, by far the best-established and most prevalent precursor lesions for PDAC are the so-called pancreatic intraepithelial neoplasias (PanINs; rev. in [35]). The current perception of the PDAC progression model from PanIN to invasive carcinoma is shown in Figure II.2.

As can be seen in Figure II.2, one of the earliest genetic events in PDAC development is the acquisition of activating mutations in the *Kirsten rat sarcoma* (*KRAS*) oncogene. These can be found in over 90 % of pancreatic cancers, occur almost exclusively as point mutations in codon 12 and result in substitution of glycine with aspartate, valine, or arginine [36]. As a consequence, the small GTPase KRAS is trapped constitutively in its active, GTP-bound state and triggers persistent stimulation of downstream signaling pathways, which in turn drive many of the key events of cancer initiation and progression, including sustained proliferation, anti-apoptosis, metabolic reprogramming, remodeling of the tumor microenvironment, immune evasion, cell migration and metastasis [37].

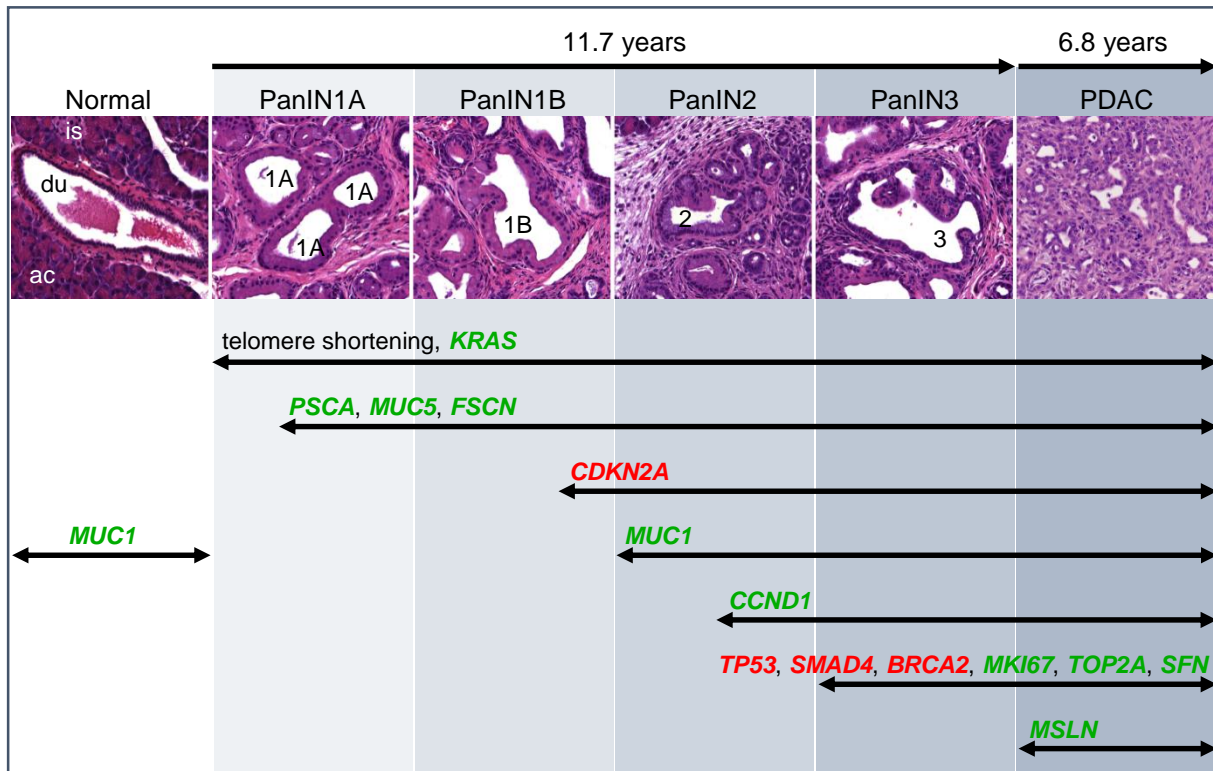


Figure II.2: Tumor progression model for PDAC.

According to the general opinion, progression from pancreatic intraepithelial neoplasia (PanIN) lesions to PDAC is accompanied by the stepwise accumulation of specific histologic, genetic, and epigenetic alterations. The most frequent alterations are herein described.

Histologically, the lowest grade PanINs, which can be flat (1A) or papillary (1B) progress via an intermediate grade (2) to high-grade PanINs (3) and finally to PDAC. PanIN1 is characterized by columnar, mucin1-containing cells with basal, unvaried nuclei, while PanIN2 presents with first nuclear alterations, including loss of polarity, nuclear crowding, enlarged nuclei, pseudo-stratification and hyperchromatism. PanIN3 demonstrates prominent nuclear atypia, frequent mitosis and potentially budding off of small clusters of epithelial cells into the lumen and/or luminal necroses, but are still contained within the basement membrane [21].

The most important genetic and epigenetic alterations as well as their time of occurrence can also be found in the figure (see Table Appendix.1 for gene symbols and names). Gain-of-function mutations are written in green, loss-of-function mutations in red letters.

Images of normal duct and PanINs were taken with the same magnification, image of PDAC was taken with half the magnification of the first.

Data are taken from [38], [21], [39], [40], [41], and [35]. ac=acini, du=duct, is=islet of Langerhans.

1.3.1. Mouse Models of PDAC

In line with the pivotal role of *KRAS* activating mutations in the initiation of precursor lesions, mice engineered with a prenatal pancreas-specific *Kras*^{G12D} mutation develop classical PanIN lesions and, at a low frequency and after a long latency, PDACs [30, 28]. These findings suggest that besides the importance of the *KRAS* activating mutation for the initiation of precursor lesions, other rate-limiting events are required to drive progression of these neoplasms towards high-grade PanINs and pancreatic cancer [19].

This was further confirmed by experiments putting the prenatal pancreas-specific *Kras*^{G12D} mutation into backgrounds of pancreas-specific inactivation of tumor suppressor genes

known to be mutated frequently in human pancreatic cancers, such as biallelic deletion of the *Cdkn2a* [30] or *Stk11* [42], mono- or biallelic deletion of *Trp53* [32], or conditional expression of the *Trp53*^{R172H} dominant negative allele ([31]; see also Figure II.2). Notably, all of these experiments gave rise to mouse strains developing full-blown metastatic disease with short latency and very high penetrance that faithfully recapitulated the human disease. However, not only inactivation of tumor suppressor genes, but also inflammation cooperates with oncogenic *Kras* to promote pancreatic cancer as demonstrated in a *Kras*^{G12V} transgenic mouse subjected to cerulein-induced pancreatic inflammation [43]. This further underscores the importance of CP as a risk factor for pancreatic cancer.

1.3.2. Open Questions in PDAC Research

Despite the fact that much has been learned about the pathology of PDAC in the last decades, many aspects are still to be unraveled. These include defining the cell of origin of PDAC, elucidating what triggers the development of the preneoplastic lesions, and determining what promotes progression of the preneoplastic lesions to full-blown PDAC.

With respects to the cell of origin, much progress has been made. Experiments targeting oncogenic *Kras* specifically to ductal cells showed that, despite the ductal appearance of PDAC and its precursor lesions, ductal cells might not be the cell type, from which PDAC predominantly arises [44]. In contrast, when oncogenic *Kras* was targeted to acinar cells, PanINs formed readily and were comparable to the ones obtained with whole-organ *Kras* activation [43, 45, 46]. Strikingly, PanINs developed more quickly and more abundantly when the mice were subjected to cerulein-induced pancreatitis [43, 47] and progressed to invasive PDAC in the context of either CP or *Trp53* deletion [43, 48].

It has thus been concluded that PanINs and PDAC arise predominantly from acinar cells via acinar-to-ductal metaplasia (ADM; [43, 44]).

Much less is known in the other two instances.

Nonetheless, Reactive Oxygen Species (ROS) and resulting oxidative stress have been implicated in virtually all PDAC etiologies:

ROS may be implicated in the pathogenesis of diabetes in at least three ways: (a) ROS may inhibit glycolysis and thus lead to hyperglycemia [49], (b) immune-cell derived ROS may destruct β -cells in type 1 diabetes [50], and (c) hyperglycemia-induced ROS may lead to β -cell dysfunction and insulin resistance in type 2 diabetes [51, 50].

Additionally, while the exact mechanisms of the premature pro-enzyme activation causal to AP are still largely unknown, one possible explanation suggests that increased levels of ROS increase intra-acinar calcium levels. Elevated intra-acinar calcium levels in turn cause fusion of different intracellular organelles and thereby create a milieu supportive of pro-enzyme activation, potentially via lysosomal cathepsin B-mediated or auto-activation of trypsinogen [52, 10].

Similarly, although the pathogenesis of CP remains largely elusive, four different lines of evidence suggest that ROS-derived oxidative stress might be involved (rev. in [53]). Firstly, CP patients display a marked increase in plasma lipid peroxidation (LPO) along with depletion in circulating antioxidants such as vitamins A, C, and E and serum thiol. Secondly, serum markers for oxidative stress correlate well with the severity of the disease. Thirdly, LPO is not only present in the plasma, but also in duodenal juice of pancreatitis patients

implicating that their oxidative stress originated in the pancreas. And finally, consistent with the clinical findings, oxidative stress can be observed in various experimental pancreatitis models and seems to be independent of the etiology of pancreatitis. In summary, these findings demonstrate a strong connection between pancreatic oxidative stress and CP. Furthermore, ROS are abundant in cigarette smoke (see II.2.2.2.2) and are excessively produced in obese individuals [54].

In addition, mutagenic ROS-derived oxidation products, such as malonyldialdehyde (MDA) from LPO (see II.2.3.1.1), DNA lesions (see II.2.3.1.2) or ROS themselves may initiate cancer through activation of oncogenes or inactivation of tumor suppressor genes [55, 56, 57, 58]. Therefore, it seems reasonable to speculate, that ROS-derived oxidative stress might play a role in the most initial phases of pancreatic neoplastic transformation.

Moreover, besides introducing further DNA mutations that might promote cancer progression [55], ROS cannot only render microenvironment permissive to migration and invasion, e.g. by activating the expression of matrix metalloproteinases (MMPs; [59, 60]), but also promote an invasive phenotype on the cellular level [59, 60, 61].

Finally, ROS can also promote cancers indirectly by inducing angiogenesis to establish sufficient nutrient supply for growth and vessels for dissemination [62] or by promoting inflammation, which potentiates cancers at all stages [63, 64, 65, 66, 59]. Consequently, ROS-derived oxidative stress might also be involved in PDAC progression.

2. Oxidants, Antioxidants and Oxidative Stress

2.1. Oxidants

All living organisms constantly produce oxidants e.g. during cellular metabolism (see II.2.2.2.1). Furthermore, biologically relevant oxidants also originate from exogenous factors, such as cigarette smoke, ionizing radiation, and heavy metal ions ([67, 68, 69]; see II.2.2.2.2).

Major biologically relevant oxidants include ROS, reactive nitrogen species (RNS), reactive sulfur species (RSS), and other unstable molecules formed through radical chain reactions initiated by members of the former three. ROS, RNS and RSS comprise both radical and non-radical derivatives of oxygen, nitrogen, and sulfur respectively [69, 53].

ROS are described in more detail in II.2.2. RNS predominantly consist of nitric oxide radicals ($\cdot\text{NO}$), peroxyxynitrite anions (ONOO^-), nitrogen dioxide radicals ($\cdot\text{NO}_2$), and other nitrates. In the cell, $\cdot\text{NO}$ is formed from arginine through the activity of nitric oxide synthases (NOS) [70, 71]. In addition, $\cdot\text{NO}$ is produced in the mitochondrial respiratory chain under hypoxic conditions [72]. It gives rise to ONOO^- by reacting with O_2^- (see II.2.2.1). The corresponding peroxyxynitric acid spontaneously decomposes to form the very reactive hydroxyl radical ($\cdot\text{OH}$; see II.2.2.1) and $\cdot\text{NO}_2$, which finally produces various nitrates [71, 70].

$\cdot\text{NO}$ is an important signaling molecule involved e.g. in vasodilation [73], neuronal synapse formation in the central nervous system (CNS; [74]), and host immune defense (rev. in [75]).

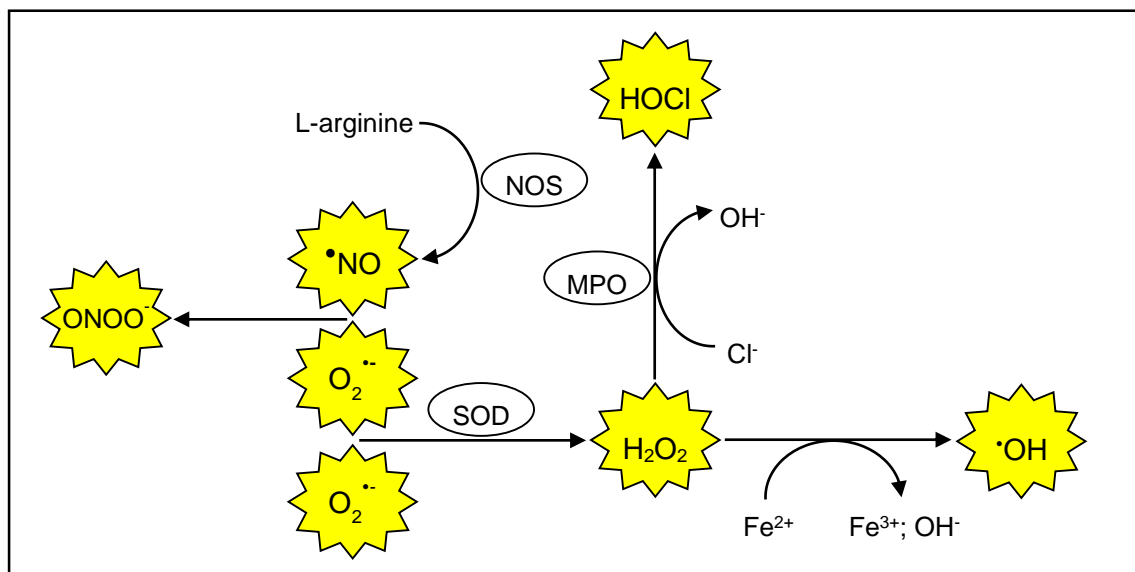
Most of these functions are mediated by binding to heme groups of guanyl cyclase-coupled receptors, thereby activating the enzyme and initiating the production of cGMP [76]. In contrast, other RNS, predominantly ONOO^- , are most recognized for conferring irreversible modifications, such as oxidation, nitration, and S-nitrosylation to proteins, lipids, and DNA [77, 78, 79]. These modifications have been implicated in many human diseases including neurodegenerative diseases and cancer [80, 81, 76].

Due to the well-documented role of the glutathione (GSH) system in detoxifying ROS (see II.2.4), sulfur compounds are generally considered to act as antioxidants (e.g. [82]). However, higher oxidation states of sulfur including sulfur radicals occur in biological systems that are likely to be also functionally relevant [83, 84].

2.2. Reactive Oxygen Species (ROS)

2.2.1. Types of ROS

ROS are the best reviewed types of oxidants. Most ROS represent intermediate redox stages of the most fundamental reaction of life of aerobic organisms: the reduction of molecular oxygen (O_2) to water [85, 67]. Major biologically relevant ROS comprise $\text{O}_2^{\cdot-}$, hydrogen peroxide (H_2O_2), $\cdot\text{OH}$, ONOO^- , and hypochlorous acid (HOCl ; [86]).



2.2.1.1. Superoxide ($\text{O}_2^{\cdot-}$)

$\text{O}_2^{\cdot-}$ is formed by the reduction of, i.e. by the transfer of one single electron, to O_2 . Due to its negative charge, $\text{O}_2^{\cdot-}$ supposedly cannot cross hydrophobic membranes (although anion channels may mediate transmembrane transport e.g. from the mitochondria to the cytosol

[87]). Nonetheless, its relatively long half-life permits diffusion within the cell which increases the number of potential targets. Furthermore, $O_2^{\cdot-}$ can rapidly react with some iron-sulfur clusters in proteins [88] and serve as a precursor for a series of other, more toxic oxidative species including H_2O_2 and $ONOO^{\cdot-}$ ([89]; see Figure II.3).

2.2.1.2. Hydrogen Peroxide (H_2O_2)

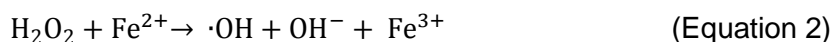
In addition to a number of enzymes that directly generate H_2O_2 (see II.2.2.2), $O_2^{\cdot-}$ is the primary source of cellular H_2O_2 . It is converted to H_2O_2 either through spontaneous dismutation or the action of superoxide dismutases (SODs; see II.2.4.1.1; [70]):



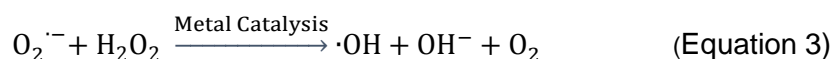
H_2O_2 is stable and has a relatively long half-life within the cell. As a small and uncharged molecule, it is permeable to membranes. It is a relatively weak oxidizing agent that is unable to directly oxidize DNA and lipids, however, it can inactivate some enzymes [88]. Nonetheless, H_2O_2 is cytotoxic and its cytotoxicity primarily occurs through the highly reactive $\cdot OH$ generated in metal-catalyzed reactions, like the Fenton reaction (see II.2.2.1.3).

2.2.1.3. Hydroxyl Radical ($\cdot OH$)

In the presence of ferrous ions, H_2O_2 can break down to form $\cdot OH$ by the Fenton reaction [88]:



The formation of $\cdot OH$ is enhanced when, at the same time, Fe^{3+} is recycled back to Fe^{2+} under consumption of $O_2^{\cdot-}$ according to the Haber-Weiss reaction [90]:



$\cdot OH$ radicals are highly reactive and have a strong oxidizing potential. They are potentially the most deleterious ROS present in biological systems and confer damage to virtually all biomolecules within the cell, however, with a half-life of less than one nanosecond, oxidative damage occurs solely in close vicinity of the site of their generation [88, 91]. Furthermore, their high reactivity does not allow for membrane passage. Owing to its very short half-life, the existence of the $\cdot OH$ radical in living organisms is difficult to be demonstrated directly, therefore, it is rather detected by the presence of its specific reaction products [89].

2.2.1.4. Peroxynitrite Anion ($ONOO^{\cdot-}$)

Although $ONOO^{\cdot-}$ is rather attributed to RNS than to ROS, it is described herein due to its high biological relevance. $ONOO^{\cdot-}$ is formed by reaction between $\cdot NO$ and $O_2^{\cdot-}$:



As this reaction occurs approximately three times faster than the dismutation of $O_2^{\cdot-}$ to H_2O_2 and even faster than the reaction of with heme groups, it is the primary reaction when both educts are present [89]. $ONOO^{\cdot-}$ (or its protonated form $ONOOH$) is highly reactive and a

strong oxidizing agent that can damage DNA and membranes, functionally alter proteins, and deplete the cell of thiols (rev. in [92]). Moreover, its relatively long half-life and its ability to cross membranes allow for multiple targets within the cell. In addition to its direct actions, it furthermore reduces bioavailability of $O_2^{\cdot-}$ and $\cdot NO$ and thereby interferes with their physiological roles.

2.2.1.5. Hypochlorous Acid (HOCl)

HOCl is produced from H_2O_2 and chloride ions, which abundantly occur in extracellular fluids, by myeloperoxidase activity in activated neutrophils according to Equation 5 [70]:



The active component of household bleach is a strong, oxidizing agent well recognized for its microbicidal function and an integral part of the innate immune defense [93]. However, in the same manner as fighting off infectious germs, HOCl can also harm the host. As a small and uncharged molecule it can readily cross cell membranes and oxidatively attack all cellular biomolecules. For instance, it can oxidize thiols [94], irreversibly inactivate important intracellular enzymes, including GAPDH [95] and caspases [96], and add chloride to the DNA bases [97].

2.2.1.6. Other ROS

Singlet oxygen (1O_2) is generated by electrical excitation of O_2 . Due to its large oxidation capacity, it has the potential to irreversibly damage DNA, proteins, or fatty acids. In theory, it can be generated by dismutation of $O_2^{\cdot-}$ in water, however, its biological relevance in mammals is not quite clear and it seems to have a far more important role in plants and phototrophic bacteria, where it is a byproduct of photosynthesis [88, 98, 99].

Furthermore, several carbon-centered secondary radical ROS exist in biological systems as the result of chain reactions of primary radical ROS. Such secondary radicals can donate electrons to O_2 , thereby generating peroxy radicals ($R-OO^{\cdot}$) that readily attack many targets within the cell and further propagate the chain reaction.

These chain reactions are usually terminated by reaction with other primary or secondary radicals, which can lead to the formation of cyclic peroxide ($R_1-O-O-R_2$) or hydroperoxides ($R-OOH$). Both compounds are precursors for a broad range of other reactive products that can confer damage to all cellular biomolecules ([100]; rev. in [101]).

2.2.2. Sources of ROS

As stated above, origins of ROS include both endogenous and exogenous sources.

2.2.2.1. Endogenous Sources of ROS

The primary source of cellular ROS lies in the cell's energy production machinery: the mitochondrion.

The electron transport chain (ETC) is the most important source of endogenous ROS [102]. The ETC, which is located in the inner mitochondrial membrane, consists of four multi-protein complexes with increasing redox potential: complex I (NADH dehydrogenase (ubiquinone)), complex II (succinate dehydrogenase), complex III (ubiquinol-cytochrome c

reductase), and complex IV (cytochrome c oxidase). Electron donors NADH or succinate provide electrons that are passed through complex I to complex IV of the ETC to the final electron acceptor, O_2 , thereby reducing O_2 to water. By the differences in redox potential of the electron acceptors, the flux of electrons provides the energy for ETC complexes I, III, and IV to pump H^+ ions from the mitochondrial matrix to the intermembrane space. This generates an H^+ electrochemical potential gradient and results in a net negative charge of the first and a net positive charge of the latter. The H^+ potential gradient, in turn, fuels the synthesis of ATP via the mitochondrial ATP synthase [103].

As electrons are transferred along the ETC, about 1 to 3 % of the electrons leak prematurely from complex I or III to O_2 giving rise to $O_2^{\cdot-}$ [104]. While complex I-derived $O_2^{\cdot-}$ (presumably originating from the iron-sulfur clusters located in the matrix-protruding hydrophilic arm) is exclusively released into the mitochondrial matrix, complex III-dependent $O_2^{\cdot-}$ (originating from the ubiquinol oxidation site located next to the intermembrane space) can be released to both sides of the inner mitochondrial membrane [105].

Besides the ETC, other major sources of mitochondrial ROS include p66^{Shc} protein and monoamine oxidase (MAO).

In mammals, three proteins are generated from the *SHC* gene locus: p52^{Shc}, p46^{Shc}, and p66^{Shc}. While cytosolic proteins p52^{Shc} and p46^{Shc} are implicated in Ras activation, p66^{Shc} most likely does not affect the Ras pathway [106]. Rather, redox enzyme p66^{Shc}, a fraction of which is located in the intermembrane space of the mitochondria, utilizes reducing equivalents of the ETC to reduce O_2 to H_2O_2 [107]. Interestingly, it is negatively correlated with aging, meaning that its knockout prolongs survival of transgenic mice by 30 % [106] and reduces the onset of metabolic and age-related diseases [108, 109, 110].

MAO is a flavoprotein that is ubiquitously expressed in higher eukaryotes and localized in the outer mitochondrial membrane. There are two isoforms of MAO, MAOA and MAOB that differ in substrate specificity and inhibitor sensitivity [111]. MAO catalyzes the oxidative deamination of neurotransmitters and biogenic amines with covalently bound FAD as its only cofactor, which is a quantitatively large source of H_2O_2 . Supported by the use of MAO inhibitors as a treatment for depression and its role in metabolizing neurotransmitters, MAO activity seems to be of particular importance in the brain [112]. Additionally, MAO-derived ROS have been implicated in pathological conditions of the heart [113, 114].

Additionally, considerable $O_2^{\cdot-}$ production takes place in phagocytic immune cells. Upon phagocytosis, NAD(P)H oxidase, an integral membrane protein of phagocytes including polymorphonuclear leukocytes, monocytes and macrophages is activated and translocates to the phagosomal membrane.

NAD(P)H oxidase then transfers electrons from NADPH to O_2 , thereby generating $O_2^{\cdot-}$. This process is accompanied by marked increase in oxygen consumption. It is therefore referred to as the respiratory burst. In the phagosomes, the $O_2^{\cdot-}$ is further processed to form other anti-microbial ROS including H_2O_2 , and $\cdot OH$. Finally, myeloperoxidase catalyzes the reaction of H_2O_2 and Cl^- to highly toxic HOCl [115].

Further $O_2^{\cdot-}$ -producing NAD(P)H oxidase systems have been found in lymphocytes [116], platelet cells [117] and mucus [118] and in non-inflammatory cells such as vascular smooth muscle cells [119], fibroblasts [120], and various tumor cells [121] as well as in other cellular compartments including endosomes and the endoplasmic reticulum [122, 123].

Consequently, in addition to their function in host defense, NAD(P)H oxidases also mediate cellular signaling (e.g. [122, 124]).

Moreover, xanthine dehydrogenase (XDH), a purin metabolizing enzyme, which is readily detected in various species (from bacteria to mammals) and tissues, produces considerable amounts of ROS. While catalyzing the two-step reaction from hypoxanthine to xanthine and further to urate, O_2 is first reduced to $O_2^{\cdot-}$ and then to H_2O_2 [125, 86].

Another endogenous source of ROS, predominantly for H_2O_2 , are microsomes and peroxisomes [126] with β -oxidation of fatty acids being the most important metabolic process for peroxisomal H_2O_2 production [127].

Furthermore, ROS, predominantly $O_2^{\cdot-}$ and H_2O_2 , are produced by the cytochrome P450 system. This system plays an important role in detoxifying many drugs and xenobiotics including amphetamines, ethanol, and nicotine as well as in steroid metabolism by a plethora of reduction, oxidation and hydrolysis reactions.

As these reactions are oxygen-dependent and require electron transfers similar to the ETC in the mitochondria, ROS can be produced due to a premature flux of electrons to oxygen [128].

In addition to the aforementioned enzymatic reactions, other enzymes can yield in ROS in conditions of inadequate substrate availability. For instance, nitric oxide synthase (NOS) also produces $O_2^{\cdot-}$ when levels of either its substrate L-arginine or its cofactor tetrahydropteridine are insufficient [129].

Finally, autoxidation processes of molecules like adrenalin, noradrenalin, dopamine, glyceraldehydes, FMNH₂, FADH₂ as well as thiol-containing molecules such as cysteine in the presence of O_2 provide non-enzymatic sources of $O_2^{\cdot-}$ [88].

2.2.2.2. Exogeneous Sources of ROS

Two of the most important environmental factors that lead to ROS formation in biological systems are ionizing radiation and heavy metal ions.

Ionizing radiation can directly form radicals that react with O_2 to form highly reactive peroxy radicals that can further react in many ways (see II.2.2.1.6, [130]). However, due to the high percentage of water in cells, more than 80 % of the energy of ionizing radiation results in the abstraction of electrons from water leading to the formation of several reactive species, such as $O_2^{\cdot-}$, H_2O_2 , and $\cdot OH$ radical [130]. Furthermore, ultraviolet A photons can mediate DNA oxidation via excitation of various photosensitive cellular components, such as porphyrins, NAD(P)H oxidase, and riboflavin. 8-hydroxyguanine (8-oxo-dG) is the major UVA-mediated DNA oxidation product [131].

Heavy metal ions, such as iron, copper, cadmium, lead, and arsenic, lead to ROS formation mostly by engaging in Fenton- and Haber-Weiss-type reactions producing highly reactive $\cdot OH$ (see II.2.2.1.3; [86]). In addition, heavy metal ions may also react with thiols, generating reactive sulfur species, and other cellular molecules or induce signaling processes all of which might, in turn promote the formation of ROS. Furthermore, replacing endogenous metal cofactors of antioxidant enzymes and thereby decreasing their activity, might be

another indirect way of how heavy metal ions cause an increase in ROS (rev. in [132] and [86]).

Further environmental sources of ROS include ozone exposure, environmental toxins, and air pollutants (rev. in [133]).

In addition to environmental factors, life style-related factors also lead to significant ROS production. The most important ones are cigarette smoking, alcohol consumption, and unhealthy/excess nutrition.

Cigarette smoke not only contains a variety of ROS itself (in addition to RNS and reactive organic compounds that can induce ROS; [134, 133]), but also triggers inflammatory processes that further contribute to ROS accumulation e.g. by the respiratory burst of neutrophils and macrophages [135, 133].

Excess alcohol consumption can have many detrimental consequences for the body [136]. Multiple lines of evidence suggest that at least some of these consequences depend on alcohol-induced ROS generation [137, 138, 139]. Alcohol can induce ROS in at least three ways: Firstly, during alcohol metabolism to acetate, two NADH molecules are generated per ethanol molecule. NADH on the other hand, enhances activity of the respiratory chain, thereby increasing O_2 consumption - and $O_2^{\cdot-}$ production (see II.2.2.2.1; [140]). Secondly, alcohol increases liver iron, possibly by increasing iron uptake from the gut [141]. Heavy metal ions like iron can engage in Fenton-like reactions and generate ROS (see II.2.2.1.3). Finally, alcohol can increase activity of cytochrome p450 [142, 143] and activate xanthine oxidase [140], which both produce ROS (see II.2.2.2.1). Further possibilities of how alcohol can lead to ROS production involve secondary or more downstream reactions of alcohol itself or its degradation products or inflammatory responses [140].

Diet-induced ROS production can occur in many ways [144]. For instance, heterocyclic amines, carcinogenic chemicals formed in red meat upon high temperature cooking, and N-nitrosamines, derived from common food preservatives, can, amongst other effects, both induce ROS-producing cytochrome P450 [144].

2.3. Biological Effects of ROS

2.3.1. ROS-Mediated Modifications of Biomolecules

In principle, all cellular molecules are possible targets of oxidative modifications by ROS. Among those, modifications of lipids, DNA, and proteins are best-characterized.

2.3.1.1. ROS-Mediated Modifications of Lipids

While, in principle, ROS can oxidize all cellular lipids, the cis double bonds of polyunsaturated fatty acids (PUFAs), major component of the lipid bilayer membranes around cells and their organelles, but also constituent of lipoproteins and low density lipoprotein (LDL), are specifically prone to oxidation by radical ROS.

In these instances, a process called lipid peroxidation (LPO) is primarily involved. In the first step of this process, carbon-centered lipid radicals are generated through hydrogen abstraction by radical ROS. Analogously as described for secondary radicals under II.2.2.1.6, these lipid radicals react with O_2 to generate highly reactive peroxy radicals [145, 146]. Afterwards, the position of the peroxy radical in the carbon chain of the PUFA

determines its fate. If the radical is situated at a terminal position, it is first reduced to hydroperoxide (by either another PUFA molecule, which propagates the chain reaction, or vitamin E) and then again to alkoxy radical, which can generate a large and complex variety of products including epoxides, further hydroperoxides, and carbonyl compounds, including cytotoxic 4-hydroxy-2-nonenal (4-HNE; [147, 146]). However, if the peroxy radical lays at an internal position, hydroperoxide formation competes with cyclization to a neighboring alkene bond, which produces an endocyclic peroxide with an adjacent carbon-centered radical. This new radical can either add again to O₂ generating another peroxy radical or undergo a second cyclization generating a bicyclic endoperoxide [148]. Via a prostaglandin-like intermediate, this product further reacts and finally generates isoprostanes and mutagenic MDA [149], two common biomarkers for LPO [146].

LPO has many effects in the cell and/or the body. On the membrane level, LPO leads to a destruction of the membrane bilayer. This involves (a) altered membrane fluidity, (b) increased permeability for constituents of cytosol or organelles [150], (c) release or inactivation of integral membrane proteins, such as receptors, transporters, or integral enzymes [151], and (d) covalent cross-linking of lipids and proteins ([152, 153]; rev. in [154]). Oxidized LDL, on the other hand, is an attractant for human macrophages, a property, which might be causal to the fat deposition in arterial walls observed at the in early stages of atherosclerosis [155].

In addition, the products of LPO, in particular 4-HNE and MDA, are cytotoxic and can readily react with and thereby damage other biomolecules, including DNA and proteins (see II.2.3.1.2 and II.2.3.1.3).

2.3.1.2. ROS-Mediated Modification of DNA

More than 100 DNA oxidation products have been identified to date [132], covering all components of the DNA molecule: the purine and pyrimidine bases and the deoxyribose backbone [156].

Both O₂^{•-} and H₂O₂ cannot react with DNA unless transition ions are present. This strongly indicates that they exhibit their DNA damaging effect merely via the [•]OH radical [157, 158, 159]. The oxidative damage conferred to DNA by the [•]OH radical are manifold. For instance, it can abstract hydrogen atoms from the deoxyribose backbone and, even more rapidly, add to the double bonds of the DNA bases [160].

Abstraction of hydrogen atoms from deoxyribose by [•]OH gives rise to sugar radicals that decay in various ways with two major consequences: (1) Abasic sites can emerge as the result of the release of purine and pyrimidine bases from the DNA. Such abasic sites not only inhibit DNA synthesis, but are also mutagenic as adenine is preferentially inserted opposite of the lesion, which produces a mutation if the lost base was anything other than thymine [156, 161]. (2) Single-strand DNA breaks (SSBs) can occur. While few individual SSBs can be repaired as the DNA is still held together by the other strand, double-strand DNA breaks (DSBs) caused by the attack of multiple [•]OH radicals and thus multiple SSBs in close proximity can have serious consequences including cell death [162, 156, 130, 163]. Various addition products of [•]OH to DNA base residues are described. For example, addition of [•]OH can add to the carbon atoms of the purine bases adenine and guanine creates radicals, which can, amongst others, be oxidized to form 8-oxo-dG or 8-hydroxyadenine respectively or undergo fragmentation of the imidazole ring.

In a normal human cell, the 8-oxo-dG mutation occurs approximately once every 10^5 guanine residues and is one of the most mutagenic DNA lesions [164]. By mispairing with an adenine instead of a cytosine, 8-oxo-dG can lead to a guanine to thymine conversion upon replication with an efficiency of 0.5 to 5 % per single guanine to 8-oxo-dG base mutation [165, 166]. Although, theoretically, the analogous adenine lesion could also mispair with guanine, the “correct” thymine base is largely preferred. Therefore, the 8-hydroxyadenine residue has only limited mutagenic potential [167]. The same holds true for ring-fragmented purines with the guanidine-derived variant possibly being even more mutagenic than 8-oxo-dG [168].

For pyrimidine bases, the most biologically relevant oxidative modifications result in glycol derivatives [169]. Thymine glycol is not mutagenic as it pairs with adenine like its unmodified counterpart, however, it can lethally block DNA replication [170]. Contrarily, cytosine glycol is not stable and decomposes quickly to 5-hydroxycytosine, 5-hydroxyuracil or uracil glycol, all of which are potentially mutagenic [169]. Up to 5 % of all cytosines in mammalian genomic DNA are present as the methylated derivative 5-methylcytosine. Remarkably, the primary product of oxidative attack to 5-methylcytosine is thymidine glycol [169].

In addition to the direct effects of $\cdot\text{OH}$, ROS might also trigger enzymatic DNA degradation. It is postulated that this is mediated by an apoptosis-like mechanism which involves an increase in intracellular free Ca^{2+} that activates Ca^{2+} -dependent DNA endonucleases [171].

Furthermore, MDA and 4-NHE, reactive products of LPO (see II.2.2.1.6), can both react with the DNA bases [146, 172], initiate chain reactions, and potentially lead to the formation of DNA/DNA or DNA/protein crosslinks [173].

As stated previously (see II.2.2.1.4 and II.2.2.1.5), ONOO^- and HOCl are also able to damage DNA: ONOO^- is reported to react with guanosine to form 8-oxo-dG and to introduce both SSBs and DSBs [79]. HOCl on the other hand, has been shown to introduce base modifications, mostly pyrimidine oxidation and chlorination of cytosine, as well as DSBs [174]. However, these effects have only been shown in *in vitro* systems or isolated cells and their biological relevance remains elusive. Nonetheless, the types and prevalences of the presented oxidative DNA lesions might strongly depend on the context in which they occur [174].

2.3.1.3. ROS-Mediated Modifications of Proteins

As for DNA, O_2^- , and H_2O_2 are not able to modify proteins unless transition metals are present. This again indicates that $\cdot\text{OH}$, which is produced in Fenton-like reactions, is the ROS mediating most of the ROS-dependent protein modifications. Consequently, proteins that bind metal ions, e.g. as a cofactor in their active sites, are more prone to ROS oxidative attack [88, 175, 176].

ROS-mediated protein modifications involve both the protein backbone as well as the amino acid side chains. On the level of the protein backbone, $\cdot\text{OH}$ radicals can abstract hydrogen atoms giving rise to a carbon-centered secondary radical. As described in section II.2.2.1.6, these secondary carbon-centered radicals can react with O_2 to form highly reactive peroxy radicals, which usually results in protein fragmentation. Thereby, generally, one of the released peptides is a carbonyl derivative with a ketone or aldehyde reactive moiety.

Alternatively, reaction with another carbon-centered secondary radical will result in protein-protein cross-linking [177].

ROS can oxidize a protein's residues either directly or indirectly via an increase in the ratio of oxidized to reduced GSH or thioredoxin (TXN; [178]). While in theory all amino acids residues in proteins are susceptible to oxidation, cysteine, methionine, arginine, glutamate, histidine, leucine, lysine, phenylalanine, proline, threonine, tryptophan, tyrosine, and valine are most vulnerable [179]. In particular the –SH group of cysteine and methionine can be readily, yet reversibly, oxidized to create intra- and intermolecular protein crosslinks via disulfide bonds. The disulfides can be converted back to sulfhydryls through disulfide exchange reactions with GSH or TXN catalyzed by thiol transferases [179].

Furthermore, methionine can be oxidized to methionine sulfoxide, which can be converted back by methionine sulfoxide reductase using TXN as electron donor [179]. Moreover, for both sulfhydryl groups, further oxidation to sulfinic, sulfonic acid or, in the presence of nitrogen, sulfenamide is possible [180].

In contrast, many other oxidative modifications of amino acids by ROS are not reversible. For example, oxidation of glutamate, aspartate, and proline can, like backbone oxidation, lead to protein fragmentation [181, 182].

Furthermore, ROS can directly oxidize Lysine, arginine, proline, and threonine side chains to generate carbonyl derivatives. Carbonyl moieties can also be formed after glycation of lysine amino residues with reducing carbohydrates or through addition reactions of histidine, cysteine or lysine side chains with unsaturated aldehydes formed during LPO, such as 4-HNE or MDA (see II.2.3.1.1; [183, 184]). Lysine amino groups can add to carbonyl groups generated in these processes or during protein fragmentation (see above) and create intra- and intermolecular protein crosslinks [184]. Protein crosslinks can also involve tyrosine residues due to oxidative bi-tyrosine formation [175].

Apart from $\cdot\text{OH}$ radicals, also ONOO^- and HOCl can modify proteins. Protein modifications by these two ROS include methionine oxidation to methionine sulfoxide ([185]; see above), nitration of tyrosine and tryptophan [186, 187], and chlorination of tyrosine side chains ([188]; rev. in [189]).

Susceptibility to ROS strongly varies between different proteins. For instance, misfolded proteins are far more prone to oxidative damage than intact proteins [190]. Physically, ROS-modifications range from protein fragmentation, intra- and intermolecular protein crosslinking, alterations of electrical charge, conformational changes to protein mis- or unfolding. Biologically, these modifications affect enzyme activity, membrane-receptor function, DNA-binding of transcription factors, and protein-complex assembly [191, 192, 193, 194] or – in the majority of cases – promote protein degradation. As oxidized proteins are usually less soluble and more sensitive to proteolysis, they are mostly cleared by proteasomal degradation [195]. The importance of proteasomal clearance is underscored by the fact that accumulation of oxidized proteins due to functional inhibition of the proteasome by misfolded SODs might be causally involved in the pathogenesis of amyotrophic lateral sclerosis [196]. However, some cross-linked proteins are not only resistant to proteasomal degradation, but also inhibit its proteolytic function [197].

2.3.2. Physiological Role of ROS

ROS exert vital roles in numerous physiological processes of the cell, tissue, or the entire organism.

On the cellular level, primarily, ROS acts as an intracellular signaling molecule [198]. Highly reactive ROS, such as $\cdot\text{OH}$, $\text{ONOO}\cdot$, and HOCl oxidize biomolecules mostly irreversibly and without preference or specificity, which is rather incompatible with regulated signaling functions. In contrast, the less reactive species, such as $\text{O}_2^{\cdot-}$ and H_2O_2 exert mainly reversible and more selective oxidative power, which is much more in keeping with cellular signaling [199]. Of the many ROS-mediated protein side chain modifications that might possess signaling capacities, those of cysteine modifications are best established [199] and possibly most important [180].

Two very prominent examples are (a) inactivation of protein tyrosine phosphatases (PTPs), such as PTPN1 [200] and PTPN6 [201] and (b) the activation of intracellular or membrane-associated protein tyrosine kinases (PTKs), such as SRC [202] and Janus kinases (JAKs; [203]), or insulin receptor kinases (IRK; [204]) and RET proto-oncogene [205] respectively, by oxidation of active-site cysteines (rev. in [201]). Example (a) is also thought to be involved in ROS-mediated activation of nuclear factor κB (NFKB), the first transcription factor shown to be ROS-regulated [206]: Activation of upstream kinases by cysteine oxidation promotes phosphorylation of inhibitory κB kinase (IKK) which releases NFKB and thereby allows it to translocate to the nucleus and activate target gene transcription [86].

As a third example, cysteine oxidation can also alter DNA-binding capacities of transcription factors. For instance, while cysteine oxidation reduces DNA-binding capacities of NFKB and activating protein-1 (AP-1; [207]), redox-active cysteine residues are essential for DNA-binding of TP53 [208].

In addition to primary ROS, also products of LPO have been shown to participate in cellular signaling processes. So, 4-HNE can readily add to histidine residues or other free amino groups of proteins and alter their activity. For example, 4-HNE addition to free amino groups of epidermal growth factor receptor (EGFR) activates the downstream pathway [209]. Moreover, addition to critical histidine residues of Jun N-terminal kinases (JNKs) promotes both their nuclear translocation and their activation [210].

The aforementioned ones represent only a small number of possible targets of signaling-active ROS. Consequently, there is a tremendous number of possible ROS-mediated cell fates, including induction (or reduction) of proliferation [124, 211], differentiation [212, 213], migration [214], senescence [215], autophagy [215, 216], and apoptosis. Of those, induction of apoptosis is the best-established one and many roads and mechanisms of how ROS lead to this cell fate have been described (rev. in [217, 218, 219]). They include for example activation of JNK as described above, which phosphorylates and thereby inhibits the anti-apoptotic function of BCL2 [220] or myeloid cell leukemia 1 (MCL1; [221]). Another possibility involves LPO of the cardiolipin, a highly unsaturated phospholipid that is found almost exclusively in the inner mitochondrial membrane mediating membrane association of cytochrome c. Upon oxidation, cardiolipin releases cytochrome c and mediates outer mitochondrial membrane permeabilization and subsequent release of pro-apoptotic factors, such as cytochrome c, into the cytoplasm, thereby triggering the intrinsic pathway of apoptosis [222].

While the diversity of cell fates sounds contradictory at first, it may simply support the notion that the specific cell fate strongly depends on types, levels, persistence, and subcellular

localization of ROS, type, state, and environment of the cell, and many more (e.g. [124, 211, 223]).

Furthermore, ROS do not only exert cell-autonomous functions, they also play crucial roles for organ-specific functions. For instance, thyroid hormone production critically depends on H_2O_2 as electron acceptor and specific NADPH oxidases are required to fuel this process with adequate amounts of this ROS [224].

In addition, ROS also participate in angiogenesis. Angiogenesis (i.e. the formation of new vessels from preexisting vasculature) is essential in many physiological and pathological processes including wound healing and embryonic development or tumor growth and cardiovascular and chronic inflammatory diseases, respectively [225]. At low doses, ROS (predominantly H_2O_2) promote angiogenesis e.g. by stimulating proliferation, migration, and adhesion of endothelial cells [226, 227, 228], or by inducing pro-angiogenic vascular endothelial growth factor (VEGF; [229, 230]). At high concentrations, however, ROS inhibit angiogenesis [228].

Finally, as implied in II.2.2.2.1, ROS also play an important role in host immune response e.g. in the course of the respiratory burst of phagocytotic cells, where ROS are deliberately produced to fight pathogenic germs. The importance of the respiratory burst is underscored by the chronic granulomatous disease, a hereditary defect of the NAD(P)H oxidase that results in disrupted $O_2^{\cdot-}$ formation and thus defective pathogen clearance capacity. Consequently, patients suffer from recurrent and life-threatening infections [115].

2.4. Antioxidants

To avoid oxidative damage while still allowing ROS to exert their physiological role in the cell, ROS need to be tightly balanced. To this end, aerobic organisms are equipped with numerous enzymatic and non-enzymatic antioxidants that apply different antioxidant strategies [68, 86, 132].

Three major antioxidant strategies involve (a) to convert ROS into less reactive molecules, (b) to scavenge ROS, and (c) to prevent the formation of the highly active ROS (e.g. $\cdot OH$) by reducing the availability of pro-oxidants (e.g. by chelating transition metals; [89]). While strategy (a) predominantly applies to antioxidant enzymes, strategies (b) and (c) mostly apply to non-enzymatic and dietary antioxidants.

2.4.1. Antioxidant Enzymes

Most important antioxidant enzymes that directly detoxify ROS are SOD, catalase (CAT), and glutathione peroxidase (GPX). Accessory antioxidant enzyme systems, on the other hand, predominantly support the first by recycling the required cofactors or by restoring the reduced state of cellular constituents like sulfur-containing proteins or PUFAs to maintain the cell's redox potential. Of the latter, TXN, glutaredoxin (GLRX), and peroxiredoxin (PRDX) systems are the most important ones [89, 132].

2.4.1.1. Superoxide Dismutase (SOD)

SODs (EC 1.15.1.1), whose function was first discovered in 1969 [231], catalyze the conversion of $O_2^{\cdot-}$ to H_2O_2 and O_2 (Equation 6). The fact that $O_2^{\cdot-}$ is the most frequently endogenously and exogenously produced ROS (see II.2.2.2), makes SODs the cell's first line of defense against ROS [232].



In mammals, three isoforms of SODs have been characterized that differ, amongst others, in their metal ion cofactor and subcellular location: SOD1, SOD2, and SOD3 [233, 232].

The transition metal ions in the active sites are critical for SOD function [233]. While highly homologous SOD1 and 3 both require copper and zinc as cofactors, SOD2, which is phylogenetically more distinct, utilizes manganese [233, 232].

SOD1 is most abundantly and ubiquitously expressed in the cytosol, however, yet to a lesser extent, it has also been found in nuclei, lysosomes, peroxisomes, and the mitochondrial intermembrane space [234, 235]. Whether it also localizes to the mitochondrial matrix, is still under debate ([236], rev. in [233]). Remarkably, mutations in the *SOD1* gene account for up to one fourth of familial cases of amyotrophic lateral sclerosis (ALS), a fatal neurodegenerative disease that affects the motor neurons in the spinal cord, brain stem, and cortex [237]. Accordingly, the *Sod1* mutant mouse is a famous model for ALS [238].

SOD3, is the most recently discovered and least characterized isoform. As it is the major SOD of extracellular fluids, such as plasma, lymph, and cerebrospinal fluid, it is also called extracellular SOD or EC-SOD [239, 240]. Its expression varies strongly between the cell types, tissues, and mammalian species and might be predominantly regulated by cytokines [241, 242, 243].

Expression of the third isoform, SOD2, which utilizes manganese as metal cofactor, is restricted to the mitochondrial matrix [244, 245]. SOD2 has the highest enzyme activity of all SOD isoforms [89] and can be regulated by cytokines like SOD3 [243], but also by numerous other stimuli and factors including ROS [246], manganese [247], and TP53 [248]. In addition, posttranscriptional, posttranslational, and epigenetic mechanisms can also regulate SOD2 (rev. in [249]).

Remarkably, of the SODs, SOD2 is the only isoform that is essential to aerobic life under physiological conditions [250, 251]. Consistent with this notion, mice lacking *Sod2* die around postnatal day 1 to 18 with dilated cardiomyopathy, neurodegeneration, and severe anemia [252, 253], whereas loss of *Sod1* or *Sod3* has little effect on survival ([254, 255]; rev. in [256]).

Heterozygous knockout, on the other hand, merely leads to a premature onset of age-related defects in the heart [257] and the liver [258] without affecting life expectancy in the mouse.

Numerous tissue-specific transgenic mice for *Sod2* have been characterized. Their phenotypes range from not detectable or very mild deficits, as described for liver [259, 260], mammary gland [261], and kidney [262] to severe and fatal defects, as described for embryonic neuronal progenitor cells [263] and heart muscle [264]. What is striking is the fact that even in those instances, when defects are merely detectable, *Sod2* deletion seems to sensitize these tissues to further injury [265, 266, 267]. Moreover, for neuronal *Sod2* knockout, a severe phenotype involving fatal spongiform neurodegeneration has been described, when *Sod2* is deleted already at the embryonic stage [263], whereas virtually no defects were detected, when *Sod2* was deleted postnatally [266].

2.4.1.2. Catalase (CAT)

CAT (EC 1.11.1.6) is widespread throughout the aerobic species. It catalyzes the breakdown of H_2O_2 into H_2O and O_2 ([268]; Equation 7) with a very high turnover rate [269]. In addition to this most renowned function, under conditions of low H_2O_2 , it can also act as a peroxidase, yet, with a much lower rate:



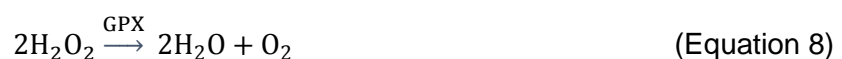
Mammalian CAT is a heme-containing enzyme and requires iron as essential cofactor [269]. In most mammals, including humans and mice, CAT localizes to peroxisomes. In erythrocytes, which do not have subcellular organelles, CAT is floating in the cytoplasm [88].

Acatlasemia, later described as a condition with less than 10 % of normal CAT activity in erythrocytes, has been described in humans already in 1948 [270, 271]. It is considered a mild syndrome presenting with oral gangrene and ulceration in less than 50 % of cases. It might further be associated with a higher risk of cardiovascular diseases [271].

Notably, targeted overexpression of *CAT* in mouse mitochondria significantly increased life span by approximately 20 %. In contrast, for peroxisomal (i.e. native) or nuclear overexpression only a very slight or no survival benefit was observed, respectively [272].

2.4.1.3. Glutathione Peroxidase (GPX)

Like CAT, GPX (EC 1.11.1.19), catalyzes the breakdown of H_2O_2 to H_2O and O_2 (Equation 8). In addition, it can also convert organic hydroperoxides, e.g. fatty acid hydroperoxides, to their respective alcohols (Equation 9). Moreover, compared with CAT, it has a much higher affinity for H_2O_2 , when H_2O_2 levels are low [88].



There are at least six GPX isoforms in humans that are transcribed from different genes and differ primarily in their subcellular and/or tissue location, accepted cofactor(s), and substrate specificity (rev. in [273, 274, 275, 276]).

GPX1 is expressed in the cytosol and mitochondria of cells of all tissues with particular high levels presented in erythrocytes, kidney, and liver. GPX2 is also cytosolic and has been detected predominantly in the gastrointestinal system. In contrast, GPX3 is an extracellular enzyme and highly abundant in plasma. GPX4 exists as a cytosolic, a mitochondrial, and a testis-specific variant. It is the only isoform that can, in addition to H₂O₂ and low molecular weight hydroperoxides, also reduce complex and/or esterified hydroperoxides, including oxidized or peroxidized membrane phospholipids, lipoproteins, or cholesterol esters, as they occur for example after LPO. GPX5, has been found in the epididymis of mouse, rat, pig, monkey and man. Finally, GPX6 is expressed in the olfactory epithelium and, potentially, also in the cochleae of mice with age-related hearing loss and in platelet trophoblasts infected with *Toxoplasma gondii* (rev. in [276]).

All human isoforms, except for GPX5, harbor a selenocysteine residue in their catalytic site that is critical for enzyme activity (rev. in [275]). In the course of reducing a hydroperoxide, GPX requires an additional cofactor as electron donor, which is, in turn, oxidized. While all isoforms accept GSH in this regard, GPX1 can also utilize γ -glutamylcysteine, when GSH is not available and GPX3 can also efficiently utilize TXN or GLRX [277].

In mice, of all *Gpx*, only cytosolic *Gpx4* whole body knockout was embryonically lethal [278, 279] indicating that *Gpx4* is the major antioxidant detoxifying H₂O₂ and counteracting LPO *in vivo* (rev. in [276]).

However, while not overtly affecting murine health per se, *Gpx1* knockout sensitized mice to oxidative stress [280] and *Gpx2* deletion aggravated both inflammation and tumor incidence in a chemically induced colon carcinogenesis model [281].

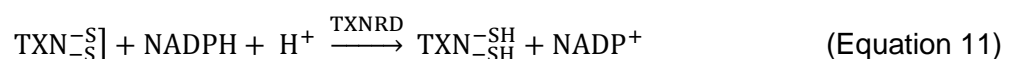
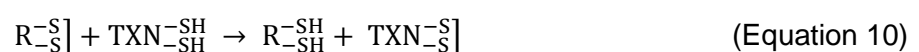
2.4.2. Accessory Antioxidant Enzyme Systems

The major accessory antioxidant enzyme systems, the TXN, the GLRX, and the PRDX system are reviewed in [282].

2.4.2.1. The Thioredoxin (TXN) System

The highly conserved TXN antioxidant system is composed of TXN and thioredoxin reductase (TXNRD; EC 1.8.1.9) and catalyzes the reduction of intra- and intermolecular disulfides and sulfenic acids to their respective sulfhydryl moieties. This reaction, which the TXN system fulfills much more efficiently than GSH or dithiothreitol (DTT), is not only important for reverting oxidative stress-related protein oxidation. Moreover, it is also an essential part of the operating mechanism of miscellaneous enzymes, including ribonucleotide reductase, the enzymes that reduces ribonucleotides to deoxyribonucleotides, which are required for DNA synthesis [283].

The reaction itself involves a two-step mechanism. First, TXN reduces the substrate becoming oxidized in turn (Equation 9), then TXNRD recycles TXN back to its reduced state at the expense of NADPH (Equation 10; [284]).



Two isoforms of TXN are of particular importance in mammals: TXN1 and TXN2. Both isoforms are ubiquitously expressed in human tissues, however, while TXN1, along with its corresponding reductase TXNRD1, presents largely in the cytosol, TXN2 and TXNRD2 reside in the mitochondria [284].

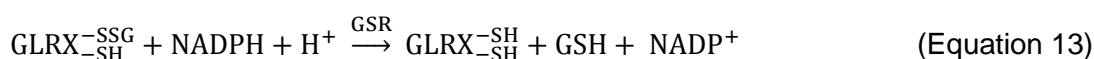
In biological systems, the TXN system has been implicated in a wide range of processes. Those include transcriptional regulation of gene expression, proliferation and apoptosis, and angiogenesis (rev. in [285, 286, 284]). In fact, the mammalian TXN system is particularly important for development, which is illustrated by the fact that total knockout of either *Txn1*, *Txn2*, *Txnrd1*, or *Txnrd2* is embryonically lethal in mice [287, 288, 289, 290, 291]. Moreover, TXN (most likely TXN1) and TXNRD (most likely TXNRD1) were found to be strongly overexpressed in a wide range of predominantly highly aggressive cancers, including tumors of the breast, thyroid, prostate, and melanomas [285, 292, 293].

2.4.2.2. The Glutaredoxin (GLRX) System

The GLRX antioxidant system, consist of GLRX and glutathione disulfide reductase (GSR). Like the TXN system, it catalyzes disulfide exchange reactions in a two-step mode, yet, the mechanisms are quite distinct. Thus, the only substrates for GLRX are glutathione-mixed disulfides (R-SSG) [284]. These compounds are readily formed since GSH is the most abundant non-protein thiol in cells [294].

In the first step of the reaction, the GLRX removes the GSH moiety from the substrate, becoming glutathionylated itself (Equation 12). In the second step, which is rate-limiting, GSR recycles GLRX and GSH using NADPH as reducing agent (Equation 13).

In contrast to the TXN system, where two cysteine residues participate in the first step of the reaction, in the GLRX system, only one cysteine is involved, which exists as a thiolate anion due to its extraordinary low pK_a [295]. Thus, the GLRX system reacts in a monothiolic, and the Txn system in a dithiolic manner [284].



In mammals, four GLRX isoforms have been identified: GLRX1, GLRX2, GLRX3, and GLRX5. Each isoform, except for GLRX5, which is restricted to the mitochondria, is present in various subcellular locations (rev. in [282]).

In mice, knockout of either *Glrx1*, *Glrx2*, or *Gsr* did not result in overt phenotypic changes [294, 296, 297].

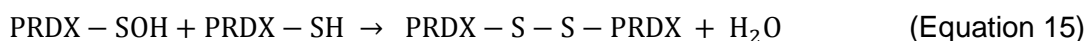
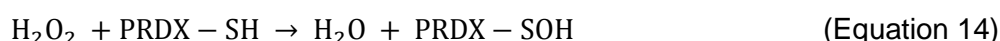
In contrast, *Glrx3* knockout mice did not survive beyond embryonic day 12.5 (E12.5), potentially due to a disturbed cell cycle progression [298].

For *Glrx5*, no data from knockout mice is available so far. However, knock-down zebrafish die between days 7 and 10 post fertilization due to defective hemoglobin synthesis [299]. Moreover, a quantitative defect in GLRX5 has been implicated with human sideroblast-like microcytic anemia [300].

2.4.2.3. The Peroxiredoxin (PRDX) System

PRDX are highly abundant peroxidases that can account for up to 1 % of soluble cellular proteins [301]. Similarly to the TXN and GLRX systems, the PRDX system reacts in a multistep manner. However, instead of disulfides, they reduce predominantly H_2O_2 . In the first step, PRDX reduces H_2O_2 to water. In the course, the N-terminal active site cysteine sulfhydryl group of Prx becomes oxidized to sulfenic acid (PRDX-SOH; Equation 14). In the second step, the previously formed sulfenic acid moiety is replaced by a disulfide bond to a non-active site cysteine sulfhydryl group of PRDX, thereby releasing another molecule of water (Equation 5). Of note, while most PRDX isoforms form intermolecular disulfides, some rather form intramolecular disulfides. In addition, further isoforms that lack the second cysteine are reduced by GSH.

Finally, disulfide PRDX is recycled by TXN in a reaction similar to Equation 10 (rev. in [302]).



Mammalian cells express six PRDX isoforms. PRDX1 is expressed predominantly in the cytosol, the nucleus, and the peroxisomes, but it was also detected in serum. PRDX2 binds to cell membranes and occurs in the cytosol and the nucleus. In contrast to the former, PRDX3 expression is restricted to the mitochondria. PRDX4 is expressed in the nucleus and in the endoplasmic reticulum. An N-terminal leader sequence suggests, it might be secreted. PRDX5 is located in cytosol, mitochondria, and peroxisomes. Finally, PRDX6 resides in the cytosol, vesicles, and lysosomes (rev. in [282]).

PRDX, while highly abundant, are much less efficient in H_2O_2 reduction than GPx or CAT. Their role in antioxidant defense has therefore been put into question [303].

Nonetheless, while being viable and hardly affected, knockout mice for all *Prdx* isoforms (i.e. *Prdx1-4* and *Prdx6*) present with increased sensitivity towards oxidative stress ([304, 305, 306, 307, 308]; rev. in [282]).

2.4.2.4. Other Accessory Antioxidant Enzymes

Glutathione transferases (GST), formerly called glutathione S-transferases, catalyze the nucleophilic attack of GSH on electrophilic carbon, nitrogen, or sulphur atoms of nonpolar inorganic and organic compounds [309]. Thereby, they play an important role in the detoxification of xenobiotics, including cancer chemotherapeutic like cisplatin (rev. in [310]), environmental toxins like arsenic [311], and food-borne carcinogens like heterocyclic amines [312]. In addition, they are able to recycle numerous ROS-derived oxidation products, such as the LPO products fatty acid hydroperoxide, acrolein, and 4-HNE, as well as oxidized DNA bases [313], which makes them part of the cellular antioxidant defense system.

There are three major families of GSTs: cytosolic (which is predominantly found in the cytosol), mitochondrial (or class κ , which is found in mitochondria and peroxisomes; [314]), and microsomal GST (which is associated to membranes and mostly involved in eicosanoid production and GSH metabolism; [315]).

Mammals possess seven classes of cytosolic GSTs, namely α -, μ -, π -, σ -, θ -, ω -, and ζ -GST that all act as soluble homo- or heterodimers (rev. in [316]). In addition to their catalytic

function, cytosolic GSTs can also bind and transport hydrophobic non-substrate ligands like heme, hormones, and xenobiotics [316]. Moreover, class μ - and π -GST bind and thereby inhibit ASK1 and MAPK8, respectively during non-stressed conditions, but release the kinases upon heat shock or oxidative stress, respectively [317, 318]. Finally, a class π GST physically interacts with PRDX6 and mediates reduction of the oxidized protein by glutathionylation to restore enzyme activity [319].

Human GST polymorphisms have been associated with cancer [320, 321, 322] and inflammatory conditions [323, 324].

Knockout mice for *Gsts* are mostly unaffected [325, 326, 327, 328, 329, 330, 331], however, at least some display increased sensitivity to stressors, including infection [325], xenobiotic stress [326, 327, 332], and oxidative stress. The latter is illustrated by a rise in LPO products in tissue and increased sensitivity towards paraquat [325]. Moreover, in response to *Gst* knockout, expression of other *Gst* classes or even other antioxidant enzymes is frequently increased [325, 329].

As many of the aforementioned enzymes and enzymatic systems require NADPH as a reducing equivalent, glucose-6-phosphate dehydrogenase (G6PD), the enzyme that generates NADPH in the first step of the pentose phosphate pathway, can also be considered an essential antioxidant.

The clinical presentation of human G6PD deficiency, the most common human enzyme defect, is in concert with this idea: While carriers live largely unaffected for most of their lives, any kind of treatment or environmental influence that triggers oxidative stress, e.g. certain drugs, infections or foods, can result in possibly fatal hemolysis (rev. in [333]).

Similarly, the GSH producing enzymes γ -glutamylcysteine synthetase and GSH synthetase (GSS) could also be considered accessory antioxidant enzymes due to the pivotal role of GSH in various antioxidant defense systems (II.2.4.3.1).

γ -glutamylcysteine synthetase is a heterodimeric enzyme composed of a catalytic subunit encoded by *GCLC* and a modifier subunit encoded by *GCLM*. Enzymatic activity is specifically inhibited by buthionine sulfoximine (BSO; [334]). In humans, γ -glutamylcysteine synthetase deficiency is a very rare autosomal recessive disorder characterized by hemolytic anemia, and, in some cases, by neurological symptoms. Only nine patients in seven families have been reported worldwide [335]. While *Gclc* knockout is embryonically lethal [336], *Gclm* knockout does not lead to an overt phenotype in the mouse, although GSH levels are markedly reduced [337].

Human GSS deficiency is a rare autosomal recessive disorder with about 40 cases reported worldwide [338]. It is characterized by hemolytic anemia, metabolic acidosis, 5-oxoprolinuria, progressive neurological symptoms and recurrent bacterial infections and fatal in about 25 % of cases. The disease may be managed, when diagnosed early by correction of acidosis and early supplementation with vitamin C and vitamin E [339].

2.4.3. Non-enzymatic Antioxidants

In addition to antioxidant enzymes, cells are equipped with numerous non-enzymatic antioxidants. These include dietary antioxidants, like the essential vitamins A, C, and E, as well as endogenously produced antioxidants, like GSH, uric acid, and bilirubin. Moreover, while some are lipophilic and act predominantly on membranes, fatty acids, and lipoproteins

(e.g. vitamin E, carotenoids, and vitamin A), others are hydrophilic and act predominantly in the aqueous intracellular or intra-organelle matrix, or in extracellular fluids (e.g. vitamin C).

2.4.3.1. Glutathione (GSH)

GSH is a tripeptide of glutamic acid, cysteine, and glycine (L-γ-glutamyl-L-cysteinyl-glycine). GSH synthesis via γ-glutamylcysteine synthetase and GSH synthetase takes place in virtually all cell types, yet, most GSH is produced by hepatocytes, secreted into bile and plasma [340] and consumed predominantly by kidney, lung, intestine [341], and probably pancreas (rev. in [342]).

While GSH is produced exclusively in the cytosol [343], it is also present in mitochondria [344] and the nucleus [343].

As stated above, GSH is the most abundant non-protein thiol in cells and together with its oxidized form, glutathione disulfide (GSSG), it is the major redox couple in animal cells. [345, 346]. As such, it is also the primary non-enzymatic antioxidant. This function is served in at least three ways: Firstly, GSH can directly and non-enzymatically scavenge a variety of electron accepting ROS, including $O_2^{\cdot-}$, $\cdot OH$, and hydroperoxyl radical, by donating a hydrogen atom and becoming oxidized to GSSG in turn [347]. Secondly, as mentioned earlier, it is a necessary cofactor of pivotal enzymatic antioxidants, including GPX, the GSR system, and GST (see II.2.4.1). Finally, GSH assists other non-enzymatic antioxidants, such as vitamins C and E by restoring their reduced, active state ([348, 349, 350]; see II.2.4.3.2).

Under non-stress conditions, the GSSG/GSH ratio is low (< 10 %; [351]), however, upon oxidative stress, GSSG can rise markedly, which can be measured minimal-/non-invasively in bile [352] and plasma [353]. Consequently, the GSSG/GSH ratio has been widely used as an indicator of oxidative stress [354, 355]. Moreover, a shifted GSSG/GSH ratio has been found in many human conditions and diseases, including diabetes [356], neurodegenerative diseases [357], and cancer [358].

2.4.3.2. Dietary Antioxidants

a. Vitamin E

Natural vitamin E comprises four tocopherols (α , β , γ , δ) and four tocotrienols (α , β , γ , δ) and occurs in all plant species [359]. Of the eight vitamin E compounds, α -tocopherol, is the most abundant form in nature and has the highest biological activity [360, 361].

As major lipid-soluble antioxidant [362, 363, 364], vitamin E scavenges peroxy radicals by donating electrons and thus terminates radical chain reactions in fatty cellular components, including membranes and lipoproteins. The vitamin E radicals that are generated in the process are recycled by vitamin C or GSH [365, 366, 367].

Clinically, human vitamin E deficiency manifests with progressive spinocerebellar dysfunction [368, 369, 370, 371, 372, 373, 374, 375, 376].

b. Carotenoids and Vitamin A

Carotenoids are a group of more than 500 intensely colored natural pigments [377] produced in plants, bacteria, fungi, and algae. They are lipid-soluble like vitamin E and responsible for many of the red, orange, and yellow hues of plant leaves, fruits, and flowers, as well as the colors of some birds, insects, fish, and crustaceans, which consumed

carotenoids in their diet. β -Carotene, the most prevalent carotenoid in nature [378], has first been isolated from carrot roots and is the eponym of the group (rev. in [379]).

Carotenoids are potent antioxidants, as their long chains of conjugated double bonds allow for delocalizing unpaired electrons. Consequently, carotenoids can scavenge many radical ROS, including $O_2^{\cdot-}$ [380], $\cdot OH$ [381, 382], and peroxy radicals [381, 383, 384]. As lipid-soluble compounds located predominantly in membranes and lipoproteins, they are effective in counteracting LPO [383, 382]. Moreover, some carotenoids (about 10 %; [385]), the so called provitamin A carotenoids, serve as precursors for vitamin A.

Consequently, vitamin A can be consumed either as plant-derived provitamin A carotenoids or animal-derived preformed vitamin A [386].

Vitamin A deficiency is still the major cause of preventable childhood blindness [387]. However, while vitamin A supplementation improves health and survival in vitamin A-deficient individuals [387, 388], excess vitamin A can be toxic and lead to gastrointestinal perturbances, increased intracranial pressure, and embryonic defects in pregnant women (rev. in [386]).

Moreover, although increased consumption of both carotenoids and vitamin A had been linked to a reduction in cancer risk, β -carotene and vitamin A supplementation increased the lung cancer incidence by more than 18 % and mortality by more than 8 % in two large-scale studies with more than 18,000 smoking individuals each [389, 390].

c. Vitamin C

In contrast to lipophilic vitamin E and carotenoids that act predominantly on lipids, fatty acids and lipoproteins, hydrophilic vitamin C is an antioxidant of the aqueous phase. It is highly abundant in plants and an essential dietary component in man and a few other higher species, such as apes, guinea pigs, and the flying mammals, which have lost L-gulonolactone oxidase, the enzyme that catalyzes the last step of vitamin C biosynthesis (rev. in [391]).

Vitamin C or ascorbic acid ($AscH_2$) is a difunctional ketolactone with two hydroxyl groups, which can readily be oxidized to generate ascorbate radical ($Asc^{\cdot-}$) and dehydroascorbic acid (DHA). Although radicalic, ascorbate radical is relatively unreactive due to mesomerism and two molecules can spontaneously disproportionate to give rise to ascorbate and DHA. DHA, on the other hand, can be regenerated by GSH [392, 393]. At physiological pH, however, the monoanion form ($AscH^-$) is the dominant form [394]. These properties allow vitamin C to directly detoxify many ROS, including $O_2^{\cdot-}$ [395, 396], H_2O_2 [396], and $\cdot OH$ [397]. Moreover, vitamin C recycles oxidized vitamin E and thus prevents LPO [365, 366, 367].

However, in spite of its role as an antioxidant, many of the symptoms of vitamin C deficiency, also called scurvy, are attributed rather to a role as a cofactor in collagen biosynthesis [398, 399]. Vitamin C supplementation on the other hand, yielded no adverse and only very minor positive effects [400, 401, 402].

d. Other Dietary Antioxidants

In addition to the aforementioned compounds, antioxidant capacities have been attributed to numerous other secondary plant metabolites, including polyphenols (predominantly flavonoids), tannins and lignans [403]. However, compared to the incredible wealth of substances in each of these groups, convincing *in vivo* data is scarce.

Although α -Lipoic acid (LA) or 1,2-dithiolane-3-pentanoic acid can be endogenously produced, it is also a dietary compound present in muscle meat, innards, and, to a lesser extent, in fruits and vegetables. Due to its hydrophobic carbohydrate chain and its hydrophilic functional groups, it is both, water- and fat-soluble [132]. LA is synthesized from octanoic acid by mitochondrial lipoic acid synthase particularly in heart, liver, and testis [404], but also readily absorbed from nutrition [405]. In addition to serving as an essential cofactor to several metabolic enzymes (rev. in [404]), together with its reduced counterpart dihydrolipoic acid (DHLA), LA is also an antioxidant. As such, LA and DHLA might not only directly scavenge ROS (e.g. $\cdot\text{OH}$ [406], HOCl [407, 408], and ONOO^- [409]) and regenerate other endogenous antioxidants (e.g. GSH, vitamin C and E; rev. in [410]), but also chelate redox-active metals to prevent $\cdot\text{OH}$ formation via the Fenton reaction [411, 412, 413]. However, convincing *in vivo* data is still missing (rev. in [405]).

2.4.3.3. Other Non-Enzymatic Antioxidants

Uric acid is a byproduct of purine metabolism in mammals. While in most mammals, uric acid is converted to allantoin and urea prior to excretion, humans and humanoid primates lack urate oxidase, the enzyme catalyzing the uric acid-to-allantoin conversion [414, 415]. In addition, humans have evolved two other mechanisms to further increase plasma uric acid levels: efficient absorption from nutritional purines and effective reabsorption (< 90 %) from the kidneys. Thus, plasma uric acid levels are 10 fold higher in humans compared with other, urate oxidase-proficient mammals, implying a role besides being a mere waste product [416]. In fact, uric acid might exert an important antioxidant function in humans as it scavenges peroxyxynitrate [417], HOCl (rev. in [418]), peroxy [419, 420], and $\cdot\text{OH}$ [416, 421]. Moreover, it can chelate iron ions and thus prevent $\cdot\text{OH}$ formation via the Fenton reaction [422] and potentially even regenerate peroxides [416] and oxidized DNA bases [419].

However, due to its poor solubility, excess uric acid may precipitate and form kidney stones [423] or cause gout [424, 425, 426, 427].

Bilirubin is a product of mammalian metabolism. In the first step of hemoprotein degradation, microsomal heme oxygenase (HMOX) converts hemoproteins like hemoglobin or cytochrome P-450 to hydrophilic biliverdin, which birds, amphibians, and reptiles directly excrete. However, in humans and other mammals, biliverdin reductase further reduces biliverdin to lipophilic and toxic bilirubin, which has to be further processed in energetically expensive conjugation reactions, before excretion is possible [428, 429]. If clearance is inadequate, bilirubin may accumulate and cause e.g. possibly fatal encephalopathy (kernicterus; [429]). The fact that mammals invest such efforts to produce a potentially dangerous compound might indicate an additional physiological function [428]. Indeed, bilirubin might be a potent antioxidant that readily scavenges peroxy radicals and thus prevents LPO [428, 430]. It has been postulated that the bilirubin antioxidant activity is exerted in a cyclic manner, where oxidants oxidize bilirubin to biliverdin, which is then regenerated by biliverdin reductase [429].

More indirect evidence comes from studies involving HMOX, the enzyme that catalyzes the first, rate-limiting step of hemoprotein catabolism, the degradation to biliverdin. Of the two isoforms, predominantly HMOX1 has been shown to be highly up-regulated upon various stimuli, including oxidative stress [431]. HMOX1 up-regulation, on the other hand, protects against oxidative stress [432, 433, 434] and might prevent fibrosis in pancreatic pathologies

[435]. These functions have, at least in part, been attributed to the generation of bilirubin [434].

Besides its role in the mitochondrial ETC, ubiquinone or coenzyme Q10 has also antioxidant properties. In fact, lipophilic ubiquinone might be more efficient in scavenging peroxy radicals in membranes and lipoproteins than vitamin E and regenerates oxidized α -tocopherol [436]. Moreover, in human studies, ubiquinone supplementation was shown to reduce oxidative stress and to induce expression of antioxidant enzymes [437, 438, 439].

2.5. Oxidative Stress

While physiological functions are mostly associated with low to moderate levels of ROS, high levels of ROS are predominantly harmful [440, 179, 198, 133]. High ROS levels occur, when excess ROS are produced and/or their production exceeds their elimination by antioxidants. This condition is called oxidative stress [218, 68].

During oxidative stress, oxidative damage conferred to the biomolecules of the cell (described in II.2.3.1) may no longer be repaired by general or specialized cellular repair mechanisms and therefore accumulates [441].

According to the “free radical theory of ageing” [442], accumulation of oxidative damage is causally involved in ageing, age-dependent decline, and the development of age-dependent pathologies [443, 444].

In addition, oxidative stress has been implicated in many other human diseases and conditions, such as neurological disorders [445, 446], cardiovascular diseases ([447], rev. in [448, 449, 450]), inflammatory conditions including pancreatitis [451, 53, 452, 453], and cancer, including PDAC ([57, 454, 455]; see also II.1.3).

3. Aims of the Study

Alterations in mitochondrial respiration, the major source of endogenously produced ROS (see II.2.2.2.1), have long been considered a key event in carcinogenesis [456]. Compatibly, evidence for an involvement of ROS in cancer, and particularly PDAC, is striking (see II.1.3). Given the substantial capacity of mitochondria in generating ROS, and the prominent position of SODs in detoxifying ROS (see II.2.4.1.1), a role of *SOD2*, which is the mitochondrial (and the only essential isoform of SODs; see II.2.4.1.1), in cancer seems likely and has been under extensive investigation – yet, with contradictory results.

SOD2 has long been considered a tumor suppressor, as many different cancer cells, including human melanoma, rat glioma, and human oral squamous carcinoma cells, expressed only low levels of *SOD2*. In addition, *SOD2* overexpression in these cells reduced growth and malignancy *in vitro* and in xenograft mouse models [457, 458, 459].

Moreover, SOD2 expression in human breast and prostate carcinoma was significantly lower compared with normal tissue [457, 460].

In concert with these data, life-long reduction in *Sod2* levels leads to an increase in oxidative DNA damage and a 100 % increase in overall tumor incidence in mice [461].

In contrast, other studies report increased levels of SOD2 in various, especially high-grade human tumors, including gastric [462], pulmonary [463], and ovarian cancers [464], and an increase in SOD2 has been associated with poor prognosis [465].

Similarly, a thymine/cytosine single nucleotide polymorphism (SNP) in the mitochondrial targeting sequence of *SOD2* resulting in a valine to alanine conversion at position 16 of the amino acid chain (Val16Ala) and enhanced enzyme activity [466], is associated with an increased risk for breast [467], ovarian [468] and prostate cancer [469, 470], but a decreased risk for lung [471, 470] and bladder cancer [472]. Other studies, however, failed to confirm an association between this SNP and cancer [473, 474, 475].

The association between SOD2 and cancer might therefore differ strongly between the tissues. As the pancreas contains relatively high levels of SOD2 [241], a link between pancreatic cancer and SOD2 seems particularly plausible. However, pancreas-specific data is scarce and similarly contradictory.

Using human PDAC cell lines, similar results were obtained as reported for other cancer cell lines (see above). Generally, the employed cell lines were uniformly low in SOD2 and enforced SOD2 expression reduced growth and malignant properties both *in vitro* and in xenograft mouse models [476, 477, 478, 479].

With respects to the aforementioned Val16Ala SNP, the alanine allele was associated with a significantly decreased risk for pancreatic cancer in one [480], a slightly but not significantly increased risk in another [481], and a significant increased risk in a third study [482].

Another SNP, a guanine/adenine dimorphism in position 1221 of the gene sequence (1221 G>A), on the other hand, is associated with a significant increase in pancreatic cancer risk for the adenine over the guanine allele carriers for those consuming low amounts of dietary vitamin E, but a significant decrease for those consuming high amounts of vitamin E. However, while this SNP lies in the regulatory region of the *SOD2* genetic sequence, its functional impact is yet to be unraveled [481].

Organ-specific transgenic mouse models could provide a valuable tool to clarify the role of *Sod2* in the pancreas – and specifically in pancreatic carcinogenesis. While organ-specific data from transgenic mouse models is available for numerous tissues (see II.2.4.1.1), no such reports exist for the pancreas. Furthermore, tissue-specific *Sod2* knockout has never been investigated in a mouse model of a solid tumor.

The present thesis aims to assess the role of *Sod2* in the pancreas, by characterizing a pancreas-specific knockout mouse. It further investigates whether *Sod2* influences pancreatic carcinogenesis by combining pancreas-specific *Sod2* deletion with a well-characterized pancreas-specific tumor-promoting mutation of the *Kras* oncogene in the mouse ([28]; see also II.1.3). In a third step, the effects of pancreas-specific *Sod2* deletion

are studied in an even faster and more stringent PDAC mouse model combining activation of oncogenic *Kras* with deletion of the tumor suppressor *Trp53* [32].

Thus, this study not only allows for gaining new insight into the involvement of ROS and oxidative stress in pancreatic development, tissue preservation and cancer biology, but also for speculating on whether pancreatic cancer patients might benefit from antioxidant supplementation.

III. Material and Methods

For company details see Table Appendix.2.

Chemicals, Buffers and Solutions

1.1. Standard Chemicals

Table III.1: Standard chemicals.

Chemical	Article Number	Brand/Company
2-propanol (for analysis)	1.09634.1000	Merck
acetic acid, glacial	1.00063.1000	Merck
calcium chloride (CaCl ₂)	C3881	Sigma-Aldrich
ethanol, absolute (for analysis)	1.00983.1000	Merck
ethylenediaminetetraacetic acid (EDTA)	CN06.3	Carl Roth
glycerol	3783.1	Carl Roth
glycine	50046-1KG	Sigma-Aldrich
H ₂ O ₂	1.08597.1000	Merck
methanol	8045	J.T. Baker
Nonidet® P40 Substitute (NP-40)	74385-1L	Sigma-Aldrich
PBS Dulbecco	L182-50	Merck
sodium chloride (NaCl)	S3014-1KG	Sigma-Aldrich
sodium deoxycholate	30970-100G	Sigma-Aldrich
sodium dodecyl sulfate (SDS)	CN30.3	Carl Roth
sodium hydroxide (NaOH)	6771.1	Carl Roth
Titriplex® III	108421	Merck
TRIS	5429.2	Carl Roth
TRIS-hydrochloride (TRIS-HCl)	9090.3	Carl Roth
Triton® X-100	T9282-100ML	Sigma-Aldrich
Tween® 20	9127.1	Carl Roth

1.2. Standard Buffers and Solutions

PBS: PBS Dulbecco diluted in deionized water according to the manufacturer's instructions and stored at room temperature.

TBS: 0.02 M TRIS-HCl, 0.137 M NaCl, pH 7.6 in deionized water. Solution was kept refrigerated.

TBS-T: 0.1 % (v/v) Tween® 20 in TBS. Solution was kept refrigerated.

2. Mice

2.1. Transgenic Mouse Strains

Ptf1a-Cre^{ex1}, *Kras^{+/LSL-G12D}*, *Trp53^{fl/fl}*, and *Sod2^{fl/fl}* strains have been described previously [483, 28, 484, 257] and were backcrossed to a C57BL/6J background. All mice used in this study were obtained by crossbreeding of the aforementioned strains. Age-matched littermates with no *Kras^{+/LSL-G12D}* mutation and either no *Ptf1a-Cre^{ex1}* mutation or no other mutations were used as wild-type (wt) controls.

The following genotypes and abbreviations were used:

<i>Ptf1a-Cre^{ex1}</i> ; <i>Sod2^{fl/fl}</i>	<i>Sod2^{ΔPanc/ΔPanc}</i>
<i>Ptf1a-Cre^{ex1}</i> ; <i>Kras^{+/LSL-G12D}</i>	<i>Kras^{+/G12D}</i>
<i>Ptf1a-Cre^{ex1}</i> ; <i>Kras^{+/LSL-G12D}</i> ; <i>Sod2^{fl/fl}</i>	<i>Kras^{+/G12D}</i> ; <i>Sod2^{ΔPanc/ΔPanc}</i>
<i>Ptf1a-Cre^{ex1}</i> ; <i>Kras^{+/LSL-G12D}</i> ; <i>Trp53^{fl/fl}</i>	<i>Kras^{+/G12D}</i> ; <i>p53^{+/ΔPanc}</i>
<i>Ptf1a-Cre^{ex1}</i> ; <i>Kras^{+/LSL-G12D}</i> ; <i>Trp53^{fl/fl}</i> ; <i>Sod2^{fl/fl}</i>	<i>Kras^{+/G12D}</i> ; <i>p53^{+/ΔPanc}</i> ; <i>Sod2^{ΔPanc/ΔPanc}</i>
<i>Ptf1a-Cre^{ex1}</i> ; <i>Kras^{+/LSL-G12D}</i> ; <i>Trp53^{fl/fl}</i>	<i>Kras^{+/G12D}</i> ; <i>p53^{ΔPanc/ΔPanc}</i>
<i>Ptf1a-Cre^{ex1}</i> ; <i>Kras^{+/LSL-G12D}</i> ; <i>Trp53^{fl/fl}</i> ; <i>Sod2^{fl/fl}</i>	<i>Kras^{+/G12D}</i> ; <i>p53^{ΔPanc/ΔPanc}</i> ; <i>Sod2^{ΔPanc/ΔPanc}</i>

2.2. Mouse Husbandry

All mice were kept at the animal facilities of the Klinikum rechts der Isar University Hospital of the Technische Universität München under specific pathogen free (SPF) conditions according to the recommendations of the Federation of European Laboratory Animal Science Associations (FELASA) and sentinel mice were examined for hygiene monitoring every three month. The mice were free of all tested pathogens except for *Helicobacter spp.* The animals were housed in groups of up to six in Sealsafe NEXT Blue Line cages (#1145T, Scanbur) at 20 to 24 °C, 50 to 60 % humidity, and a 12h/12 h light/dark cycle. Sterile filtered water was given *ad libitum*. All mice were kept on a standard diet (#Forti, Altromin Spezialfutter) unless indicated otherwise.

Breedings were started at six weeks for male and eight weeks for female mice, respectively. Mice were weaned and ear marked with an ear puncher at three weeks in age. Genotyping was performed as described in III.4.1.1.1 and III.4.1.2 using either tail tips or punched out tissue from ear marking.

All animal experiments were conducted in accordance with German Federal Animal Protection Laws and approved by the Institutional Animal Care and Use Committee of the Technische Universität München, Munich, Germany.

2.3. High Fat Diet (HFD) Feeding Experiments

As HFD, mice received fat-enriched chow (#S5745-E712, ssniff Spezialdiäten) containing 20 % (w/w) crude fat (compared with 5 % (w/w) crude fat in standard diet) for indicated periods. Mice were monitored for weight and wellbeing every week.

2.4. Intraperitoneal Glucose Tolerance Test (IP-GTT)

IP-GTT was performed as recommended by [485] and [486]. A CONTOUR® XT (Bayer Vital) glucose measurement device together with CONTOUR® NEXT sensors (#8884487, Bayer Vital) was used for blood glucose measurements.

Briefly, 12 weeks-old mice were morning fasted for 6 h. After measuring body weights, initial fasting blood glucose levels were determined with a drop of blood received from the tail veins after small needle puncture. After blood withdrawal, tails were compressed to avoid hematoma.

Next, mice were intraperitoneally injected with 2 g glucose/kg bodyweight using 20 % (w/v) glucose solution (#2349480, AlleMan Pharma) and blood glucose levels were determined as before in the indicated intervals.

After IP-GTT, mice were returned to standard husbandry conditions (see above) and monitored for wellbeing for at least two consecutive days.

2.5. Analysis of Stool Samples

2.5.1. Collection of Stool Samples

Stool samples were taken after spontaneous defecation during handling, transferred to sterile Eppendorf tubes, and stored at -20 °C until analysis.

2.5.2. Assay for Total Proteases in Stool

Assay for total stool proteases was performed according to [487] and [488]. Briefly, stool samples of 10-20 mg were weighted, suspended in 1 ml Resuspension buffer, and centrifuged at 20,000 relative centrifugal force (rcf) and 4 °C for 10 min.

Standards were prepared using serial dilutions of Sequencing Grade Modified Trypsin (V5111, Promega). Therefore, trypsin was diluted at 2 U/μl in the provided buffer, incubated at 30 °C for 15 min for maximum activity and serially diluted in Resuspension buffer to 25, 12.5, 6.25, 3.125, 1.5625, and 0.78125 U/100 μl.

100 μl of stool suspension supernatant or standard were mixed with 25 μl Reaction buffer and incubated for 1 h at 37 °C. Then, reaction was stopped with 250 μl of 8 % (w/v) TCA (diluted from 100 % (w/v) TCA). After centrifugation at 9,600 rcf and room temperature for 5 min, absorption was measured in triplicates at 405 nm in a MULTISKAN FC plate reader (ThermoFisher).

The standard curve was obtained by third order polynomial regression of standard optical density plotted against the respective standard trypsin activity. Protease activity was expressed as units/mg (U/mg) feces.

Resuspension buffer: 0.5 M NaCl, 0.1 M CaCl₂, 0.1 % (w/v) Triton X-100 in deionized water. Prepared freshly.

Reaction buffer: 3 % (w/v) Azo-Casein (11610-5G, Sigma) in 50 mM TRIS-HCl, pH 8.5; filter sterilized (0.2 μm). Prepared freshly.

100 % (w/v) TCA: 100 % (w/v) trichloroacetic acid (T9159-100G, Sigma-Aldrich) in deionized water. Prepared freshly.

2.5.3. Assay for Total Lipases in Stool

Stool samples were suspended and centrifuged as described for total proteases assay (III.2.5.2). Thereafter, supernatant was analyzed for lipases in a Cobas® 8000 Modular Analyzer (Roche Diagnostics).

2.6. Tissue Harvesting and Preparation of Formalin-Fixed, Paraffin-Embedded (FFPE) Tissue Blocks

Mice were taken for analyses either at indicated time points (7 days, 4 weeks, 12 weeks, or 24 weeks) or upon notable signs of illness. The latter included tumor-associated symptoms including abdominal enlargement, cachexia, and pain, but also other, non-tumor-related symptoms including hind limb paralysis (or other neurological deficits), hydrocephaly, and skin lesions.

At the day of analysis, mice were injected intraperitoneally at 50 mg/g (or 10 µl/g) body weight with 5-Bromo-2-deoxyuridine (BrdU) working solution.

2 h after BrdU injection, mice were anesthetized with isoflurane (798-932, cp-pharma) and sacrificed by cervical dislocation.

The pancreas was quickly resected, transferred to a sterile petri dish and weighted.

Approximately 1 mm³ samples were taken for DNA, RNA, and protein isolation from at least two distinctive sites, respectively. Protein samples were snap-frozen in liquid nitrogen.

RNA samples were suspended in RLT Lysis buffer (1015762, Qiagen) supplemented with 10 % (v/v) 2-Mercaptoethanol (4227.3, Carl Roth), crushed with a SilentCrusher M (Heidolph) until no visible tissue pieces were present and snap-frozen in liquid nitrogen.

DNA was extracted using the DNeasy® Blood & Tissue Kit (69504, Qiagen) according to the manufacturer's instructions (see also III.4.1.1.1). Until extraction (see III.4.3.1), protein samples were stored in liquid nitrogen and RNA samples at -80 °C. DNA was stored at -20 °C.

Parts of the lung, liver, the upper duodenum, and the spleen were resected and, together with the remaining pancreatic tissue, fixed in 4 % (w/v) paraformaldehyde at 4 °C overnight. The next day, organs were dehydrated with increasing concentrations of ethanol, xylol and paraffin in a S300 tissue processing unit (Leica). Finally, organs were embedded in liquid paraffin and stored at room temperature.

4 % paraformaldehyde: 16 % (w/v) paraformaldehyde solution (#15710, EMS) diluted in PBS. Prepared freshly.

BrdU stock solution: 50 mg/µl BrdU (B5002-5G, Sigma-Aldrich) dissolved in deionized water by alkalization with 10 M sodium hydroxide (NaOH). Stored in single-use aliquots at -20 °C.

BrdU working solution: 1:10 dilution of BrdU stock solution in sterile 0.9 % (w/v) sodium chloride (NaCl; 6697366.00.00, B. Braun). Stored at -20 °C.

2.7. Histological Analyses

For histological analyses, generally, 2 µm paraffin sections were cut from the FFPE tissue blocks on a MICROM HM 355S microtome (ThermoFisher) and mounted on

SUPERFROST® PLUS microscope slides (ThermoFisher). After air drying overnight at room temperature, slides were either subjected to a staining protocol as described below or stored in lightproof slide boxes at room temperature.

2.7.1. Hemalaun-Eosin (H&E) Staining

H&E staining was used for basic evaluation of tissue histology. First, paraffin sections were deparaffinized by incubation in Roti-Histol (6640.4, Carl Roth) twice for 5 min each. Then, the slides were rehydrated in decreasing concentrations of ethanol in demineralized water, namely, 100 %, 96 %; 70 %, and 0 % (v/v), twice for 3 min per concentration.

Subsequently, basophilic tissue structures were stained in Mayer's hemalaun solution (1.09249.2500, Merck) for 3 min and blued under running tap water for 10 min. Acidophilic tissue structures were then counterstained in eosin (2C-140, Waldeck) for 3.5 min.

After staining, slides were dehydrated by incubation in 96 % (v/v) ethanol and isopropanol for 25 sec each. Finally, slides were cleared in Roti-Histol (6640.4, Carl Roth) twice for 2.5 min each, mounted in pertex embedding medium (41-4012-00, Medite) and sheeted with coverslips (MENZEL-Gläser, e.g. BB024032A1, ThermoFisher).

2.7.2. Masson's Trichrome Staining

As indication for fibrosis, collagen deposition was visualized by Masson's Trichrome staining. After deparaffinization and rehydration was performed as described for H&E staining (III.2.7.1), paraffin slides were fixed in Bouin's solution (HT10132-1L, Sigma-Aldrich) overnight at room temperature. Then, slides were washed for 10 min under running tap water to remove the yellow color. Thereafter, nuclei were stained with Weigert's iron hematoxylin solution (HT1079-1SET, Sigma-Aldrich) for 10 min. Residual staining solution was removed by washing under running tap water for 5 min. After a rinse in demineralized water, cytoplasm was stained in Biebrich scarlet-acid fuchsin solution for 5 min. Slides were rinsed again in demineralized water. Then, collagen was discolored by incubation in phosphotungstic/phosphomolybdic acid solution and immediately stained in aniline blue solution for 5 min. Biebrich scarlet-acid fuchsin, phosphotungstic/phosphomolybdic acid, and aniline blue solution were all components of the Accustain Trichrome Stain (Masson) kit (HT15-1KT, Sigma-Aldrich). Afterwards, slides were washed for 2 min in 1 % (v/v) acetic acid solution in demineralized water, rinsed in demineralized water and dehydrated in increasing concentrations of ethanol in demineralized water, namely, 70 %, 96 %, and 100 % (v/v), twice each, for 10 sec per concentration. Finally, slides were cleared in Roti-Histol (6640.4, Carl Roth) twice for 2.5 min each, mounted in pertex embedding medium (41-4012-00, Medite) and sheeted with coverslips (MENZEL-Gläser, e.g. BB024032A1, ThermoFisher).

2.7.3. Immunohistochemistry

For specific antigen detection, paraffin tissue slides were subjected to immunohistochemistry. Incubation steps were performed either in a humidified chamber with the tissues encircled with an ImmEdge pen (H-4000, Vector) or with the Shandon Sequenza Immunostaining system (ThermoFisher).

Some conditions were dependent on the primary antibody. For each primary antibody, these conditions are listed in Table III.2.

First, paraffin slides were deparaffinized and rehydrated as described for H&E staining (III.2.7.1). Then, antigen unmasking was performed depending on the primary antibody either with Antigen Unmasking solution (standard or high pH; H3300 or H3301, Vector) diluted according to the manufacturer's protocol or with 10 mM sodium citrate buffer, pH 6.0. Slides were boiled either in a standard microwave at 300 W for 10 min or in a pressure cooker. After letting slides cool for 30 min at room temperature, endogenous peroxidases were blocked in 3 % (w/v) H₂O₂ (see Table III.2) for 30 min at room temperature. Slides were washed three times in buffer solution according to the primary antibody. Thereafter, unspecific antibody binding was blocked in blocking solution as specified in Table III.2 for 1 h at room temperature. Target antigens were detected by incubation in primary antibody solution either overnight at 4 °C or for 1 to 2 h at room temperature (see Table III.2). After washing three times in buffer solution, primary antibody was detected by incubation in a 1:500 solution of the respective secondary antibody in blocking solution. For all primary antibodies, except for insulin (Ins2), signal was amplified with the Vectastain ABC Kit (PK-6100, Vector) in the respective buffer according to the manufacturer's protocol. Slides were washed three times in deionized water. Next, signal was detected with the DAB Peroxidase Substrate Kit (SK-4100, Vector; brown color) for 1 to 4 min at room temperature according to the manufacturer's protocol and slides were washed for 5 min in deionized water. Tissues were counterstained by quickly dipping slides into hematoxylin solution (1.05175.2500, Merck) and subsequent blueing under running tap water for 5 min. Finally, slides were dehydrated, cleared and mounted as described for Masson's trichrome staining (III.2.7.2).

Table III.2: Antibodies and conditions for immunohistochemistry.

Primary Antibody	Antigen Unmasking	Buffer	Blocking Solution	Primary Antibody Conditions	Secondary Antibody	Time of DAB Devel.
Amy1 (A8273, Sigma-Aldrich)	Antigen Unmasking solution, high pH; microwave	PBS	10 % (v/v) Normal Goat Serum in PBS	1:1000 dilution in blocking solution; 1 h at room temp.	anti-rabbit, made in goat (BA-1000, Vector)	2 min
Ck19 (TROMA-III, Developmental Studies Hybridoma Bank)	Antigen Unmasking solution, standard pH; microwave	PBS	5 % (v/v) Normal Rabbit Serum in PBS	1:300 dilution in blocking solution; overnight at 4 °C	anti-rat, made in rabbit (BA-4000, Vector)	2 min
Ins2 (A0564, Dako)	Antigen Unmasking solution, standard pH; microwave	PBS	5 % (v/v) Normal Goat Serum in PBS	1:100 dilution in blocking solution; overnight at 4 °C	anti-guinea pig, made in goat (A7289, Sigma-Aldrich)	1.5 min
BrdU (MCA2060, AbD Serotec)	Antigen Unmasking solution, standard pH; microwave	PBS	5 % (v/v) Normal Rabbit Serum in PBS	1:250 dilution in blocking solution; 2 h at room temp.	anti-rat, made in rabbit (BA-4000, Vector)	2 min

cleaved Casp3 (#9661L, Cell Signaling)	10 mM sodium citrate buffer, pH 6.0; pressure cooker (100 °C, 20 min)	TBS-T	5 % (v/v) Normal Goat Serum in TBS-T	1:200 dilution in Antibody Diluent; overnight at 4 °C	anti-rabbit, made in goat (BA-1000, Vector)	1.5 min
Esr1 (06-935, Merck)	no antigen unmasking	TBS-T	5 % (v/v) Normal Goat Serum in TBS-T	1:200 dilution in blocking solution; overnight at 4 °C	anti-rabbit, made in goat (BA-1000, Vector)	1.5 min
Trp53 (NCL-p53-CM5p, Leica)	10 mM sodium citrate buffer, pH 6.0; pressure cooker (120 °C, 1 min)	TBS	5 % (v/v) Normal Goat Serum in TBS*	1:500 dilution in blocking solution; 1 h at room temp.	anti-rabbit, made in goat (BA-1000, Vector)	3-4 min

*The Avidin/Biotin Blocking Kit (SP-2001, Vector) was incorporated according to the manufacturer's instructions.

Normal Goat Serum: X0907, Dako.
 Normal Rabbit Serum: X0902, Dako.
 Antibody Diluent: SignalStain® Ab Diluent, #8112S, Cell Signaling.

2.7.4. Immunofluorescence

Immunofluorescence was performed for co-localization studies on murine paraffin slides and murine primary pancreatic acini.

2.7.4.1. Immunofluorescence of Paraffin Tissue Slides

All incubation steps were performed in a humidified chamber with the tissues encircled with the ImmEdge pen (H-4000, Vector). First, paraffin slides were deparaffinized and rehydrated as described for H&E staining (III.2.7.1). Then, antigen unmasking was performed with 10 mM sodium citrate buffer in a pressure cooker (100 °C, 20 min). After letting slides cool for 30 min at room temperature, tissue was permeabilized in 100 % (v/v) methanol for 10 min at -20 °C. Slides were washed three times with PBS and unspecific antibody binding was blocked in Blocking buffer 1 (see below) for 1 h at room temperature. Subsequently, slides were incubated in a 1:100 (v/v) dilution of anti-SDHB primary antibody (ab14714, abcam) in Blocking buffer 1 overnight at 4 °C. The next day, slides were washed three times in PBS and unspecific antibody binding was blocked in Blocking buffer 2. Then, tissues were incubated in a 1:250 (v/v) dilution of anti-Sod2 primary antibody (ADI-SOD-110-F, ENZO) in Blocking buffer 2 for 8 h at 4 °C. Slides were washed again three times in PBS and incubated in a 1:500 (v/v) dilution of both Alexa Fluor 568 goat anti-rabbit IgG (H+L; A11036, Life Technologies) and Alexa Fluor 488 goat anti-rat IgG (H+L; A11006, Life Technologies) in Blocking buffer 2. After washing slides three times in PBS, nuclei were counterstained in 5 µg/ml Hoechst 33342 in PBS (see below) for 15 min at room temperature. Slides were washed again three times in PBS, mounted with ProLong Gold antifade reagent (P36930, Invitrogen), sheeted with coverslips (MENZEL-Gläser, e.g. BB024032A1, ThermoFisher), and sealed with nail polish. Slides were kept refrigerated and images were acquired within less than 1 week.

Blocking buffer 1: 1 % (w/v) BSA (A4503-100G, Sigma), 10 % (v/v) Normal Goat Serum (X0907, Dako), 0.1 % (v/v) Tween® 20 in PBS. Prepared freshly.

Blocking buffer 2: 10 % (v/v) Normal Goat Serum (X0907, Dako), 0.1 % (v/v) Triton® X-100 in PBS. Prepared freshly.

Hoechst 33342: For a stock solution, 1 mg/ml bisBenzimide H33342 trihydrochloride (B2261-25MG, Sigma) was dissolved in deionized water, aliquoted and stored at -20 °C long-term or at 4 °C for up to 6 months. Stock solution was diluted just prior to use.

2.7.4.2. Immunofluorescence of Primary Pancreatic Acini

Primary acini were stained in collagen disks in 48 well plates (see III.3.2.1) for pancreatic α -amylase (Amy1) and cytokeratin-19 (Ck19) expression. Stainings were performed at least in triplicates and controls with either no Amy1, no Ck19, or no secondary antibody were incorporated in duplicates.

After getting 48 well plates from refrigeration, collagen disks were washed once with room temperature PBS. Then, acini were permeabilized in PBT twice for 5 min at room temperature and unspecific antibody binding was blocked in 10 % (v/v) Normal Goat Serum (X0907, Dako) for 1 h at room temperature. Then, collagen disks were incubated in a 1:300 (v/v) dilution of primary Amy1 antibody (A8273, Sigma-Aldrich) in PBTB overnight at 4 °C. The next day, collagen disks were washed three times in PBS and once in PBT and incubated in a 1:100 (v/v) dilution of primary Ck19 antibody (TROMA-III, Developmental Studies Hybridoma Bank) in PBTB overnight at 4 °C. Thereafter, acini were washed again three times in PBS and once in PBT and incubated in a 1:500 (v/v) dilution of both Alexa Fluor 568 goat anti-rabbit IgG (H+L; A11036, Life Technologies) and Alexa Fluor 488 goat anti-rat IgG (H+L; A11006, Life Technologies) in PBTB overnight at 4 °C. Then collagen disks were washed again three times in PBS and once in PBT and nuclei were counterstained in 5 μ g/ml Hoechst 33342 in PBT (see III.2.7.4.1) for 10 min at room temperature. Finally, collagen disks were washed three times in PBS, transferred to SUPERFROST® PLUS microscope slides (ThermoFisher) and mounted in ProLong Gold antifade reagent as described for paraffin tissue slides (III.2.7.4.1). Slides were kept refrigerated and images were acquired within less than 1 week.

PBT: 0.1 % (v/v) Triton X-100 (T9282-100ML, Sigma) in PBS. Prepared freshly.

PBTB: 0.2 % (w/v) BSA in PBT. Prepared freshly.

2.7.5. Image Acquisition and Preparation

Bright field images were taken with an Axio Imager A1 microscope (Carl Zeiss). Used objectives were 5x, 10x, and 20x EC Plan-Neofluar (420330-9900, 420340-9900, or 420350-9900, Carl Zeiss).

Whole slides were scanned with MIRAX DESK (H&E stainings; Carl Zeiss) or an Aperio ScanScope CS2 (Masson's trichrome stainings; Leica; 20x magnification) slide scanning device. Overview images with embedded local magnification image sections were prepared

with the GIMP 2.8.10 for Windows (GNU Image Manipulation Program, Free Software Foundation Inc.).

Fluorescent images were taken with a TCS SP5 confocal microscope (Leica). A 40x oil immersion objective was used to acquire images as a z-stack covering the total object depth in a sequential scan for each channel. In the Results section, fluorescent images are depicted as the maximum intensity over the z-stack for each channel. These, as well as the overlay images were prepared with the Fiji Software [489].

All images were saved as TIFF files or in the original format and image panels were prepared with the FigureJ plugin for Fiji [489, 490]. If necessary for better visualization, brightness and contrast were linearly adjusted.

2.7.6. Image Analysis

Whole slide scans of H&E stainings were analyzed using the Pannoramic Viewer Software (Carl Zeiss). Pancreatic integrity was evaluated by determining the percentage of intact (=neither dysplastic nor anaplastic) to total tissue for all the pancreatic tissue on the slide (minimum 12 mm²). Similarly, preneoplastic lesions were graded according to [491] and quantified for all the pancreatic tissue on the slide.

Whole slide scans of Masson's trichrome stainings were analyzed using the AxioVision Software (Carl Zeiss). Collagen deposition was analyzed by Dr. Henrik Einwächter by determining the percentage of blue stained to total tissue for all the pancreatic tissue on the slide. For both H&E and Masson's trichrome staining, one slide per animal was analyzed. Immunohistochemistry stainings were analyzed using the AxioVision Software (Carl Zeiss). For Amy1, Ck19, and cleaved Casp3, the positive-to-total tissue ratio was determined, for BrdU positive-to-total nuclei were quantified in at least three high power fields of vision (10x magnification).

3. Cell Isolation and Culture

3.1. Equipment and Supplies

All cells were handled in a Herasafe class II Hera Safe biological safety cabinet (ThermoFisher) and incubated in a humidified HeracellTM 240 incubator (ThermoFisher) at 37 °C and 5 % CO₂. To avoid contamination, sterilized deionized water used in the incubator was supplemented with Incuwater-CleanTM (A5219,0100, Applichem) and incubator was cleaned with Incubator-CleanTM BC (A5230,1000, Applichem) biweekly. Plasma treated cell culture plates and vented cap flasks were purchased from Corning, sterile, single packed pipettes from Greiner Bio-One. For pipetting volumes of less than 1 ml, SafeSeal-Tips[®] professional (Biozym), for removal of supernatants, autoclaved single-use glass Pasteur pipettes (Brand) were used.

3.2. Murine Primary Acini

3.2.1. Isolation of Murine Primary Acini

Murine primary acini were isolated from 4-6 weeks-old mice. First, mice were sacrificed as described in III.2.6. Then, the pancreas was quickly resected and transferred to a sterile cell culture dish containing sterile PBS. In the biological safety cabinet, the pancreas was washed twice more in sterile petri dishes containing sterile PBS and transferred to another sterile cell culture dish containing 5 ml of sterile-filtered (0.2 μm) Solution 2. Solution 2 was collected with a sterile syringe and injected into the pancreas with a sterile needle (Sterican® Gr. 1, 4657519, B. Braun). This step was repeated once more, thereafter, the pancreas was cut into small pieces using sterile surgical scissors. Then, the suspension was incubated in the cell culture incubator. After 10 min of incubation, the tissue suspension together with 10 ml of Solution 1, which was used to flush the petri dish, was transferred to a sterile 50 ml-Falcon tube and centrifuged. The supernatant was removed and the pellet suspended in 5 ml of new Solution 2. Then, the suspension was transferred to a sterile cell culture dish and incubated for another 10 min in the cell culture incubator. Subsequently, the suspension was passed through a 100 μm nylon mesh (08-771-19, Corning) into another sterile 50 ml-Falcon tube. The nylon mesh was flushed with 10 ml of Solution 1, which was also collected in the Falcon tube. After another centrifugation step, the supernatant was removed and the pellet was washed in 20 ml of Solution 1 and centrifuged again at 300 rcf and 18 °C for 5 min. The supernatant was removed and the cells suspended in 2-3 ml of acinar cell medium supplemented with 30 % (v/v) fetal bovine serum (FBS; 10499044, Life Technologies). The suspension was transferred to a sterile cell culture dish and placed in the cell culture incubator for recovery. In the meantime, the anticipated culture plates were coated with Collagen solution 1 and placed in the cell culture incubator for 30 min to allow solidification of collagen. After 30 to 60 min of recovery, the cell suspension was transferred to a sterile 15 ml-Falcon tube, centrifuged, and the supernatant was removed. Then, the cell pellet was suspended in 1-3 ml of acinar cell medium (depending on the pellet size), mixed with Collagen solution 2, plated into collagen-coated culture plates and placed in the cell culture incubator for 30 min for solidification. Thereafter, the acinar cell suspension/Collagen solution 2 mixture was covered with another layer of Collagen solution 1 and placed again in the cell culture incubator for 30 min for solidification. Finally, the collagen disks were covered with sterile-filtered (0.2 μm) acinar cell medium and cultivated under standard cell culture conditions (see III.3.1). Medium was first replaced after 24 h, then every 48 h.

All centrifugation steps were performed at 300 rcf and 18 °C for 5 min.

PBS:	14190-169, Life Technologies.
Solution 1:	0.1 % (w/v) BSA (A4503-100G, Sigma-Aldrich) 0.02 % (w/v) Trypsin Inhibitor (from soybean; T9008-5ML, Sigma-Aldrich) in McCoy's 5A Medium (M8403, Sigma-Aldrich). Prepared freshly.
Solution 2:	1.2 mg/ml Collagenase from <i>Clostridium histolyticum</i> , Type VIII (C2139-100MG, Sigma-Aldrich) in Solution 1. Prepared freshly.

Acinar cell medium:	0.1 % (w/v) BSA (A4503-100G, Sigma-Aldrich)
	0.1 % (v/v) FBS (10499-044, Life Technologies)
	0.01 % (w/v) Trypsin Inhibitor (from soybean; T9008-5ML, Sigma-Aldrich)
	1 x Insulin-Trans-Sel-G (41400045, Life Technologies)
	50 µg/ml Bovine Pituitary Extract (13022814, Life Technologies)
	10 mM HEPES (15630-080, Life Technologies)
	0.26 % (w/v) NaHCO ₃ (1.06329.0500, Merck)
	in Waymouth's MB 752/1 Medium (31220023, Life Technologies). Prepared freshly.
Collagen solution 1:	2.5 mg/ml Rat Tail Collagen Type I (354236, Corning)
	0.01 % (w/v) NaOH
	in PBS. Prepared freshly.
Collagen solution 2:	2.5 mg/ml Rat Tail Collagen Type I (354236, Corning)
	0.01 % (w/v) NaOH
	in acinar cell medium minus volume of cell suspension. Prepared freshly.

3.2.2. Analysis of Murine Primary Acini

3.2.2.1. Quantification of Transdifferentiation of Acinar Explants

Acinar-to-ductal transdifferentiation of *Kras*^{G12D/+} and *Kras*^{G12D/+}; *Sod2*^{ΔPanc/ΔPanc} acini was quantified after two days of culture in collagen gels in at least 10 wells of a 48 well cell culture plate. Therefore, wells were examined in an inverted light microscope and transdifferentiated and total acinar colonies were quantified in at least three high power fields of vision for each well.

3.2.2.2. Viability of Murine Primary Acini

Viability of murine primary acini was assessed in triplicates in cell culture medium supernatants after the indicated days of culture in collagen disks with the Cytotoxicity Detection Kit (LDH; 11644793001, Roche) according to the manufacturer's instructions. Fresh acinar cell medium served as negative, frozen acinar cells lysed in 2 % (v/v) Triton[®] X-100 in acinar cell medium as positive control. Absorbance was measured at 450 nm in a MULTISKAN FC plate reader (ThermoFisher).

3.2.2.3. Immunofluorescence of Murine Primary Acini

Immunofluorescence on collagen-embedded acinar explants was performed after 0, 2, and 3 days of culture for *Kras*^{G12D/+} and *Kras*^{G12D/+}; *Sod2*^{ΔPanc/ΔPanc} acini as described in III.2.7.4.2.

3.2.2.4. Isolation of Protein from Murine Primary Acini

For immunoblot analysis, protein was isolated from acinar cell explants seeded into 12 well cell culture plates. Therefore, medium was removed and acinar cell-containing collagen disks were washed with PBS. Then, at least two volumes of sterile-filtered (0.2 µm) Solution 2 (see III.3.2.1) were added to each well, the collagen disks dislodged from the plates and the contents of each well were transferred into a sterile 15 ml-Falcon tube each. The tubes were incubated for 10 min in the cell culture incubator, the collagenase reaction was stopped with at least two volumes of Solution 1 (see III.3.2.1) and the tubes were centrifuged. Thereafter, the supernatant was removed and new Solution 2 was added to the

tubes. After another incubation step of 10 min, collagenase reaction was stopped with at least two volumes of Solution 1 and the tubes were centrifuged again. These steps were repeated until no collagen gel was visible anymore. Then, the pellet was washed twice in ice-cold PBS, transferred to a 1.5 ml-Eppendorf tube and the supernatant was completely removed. Protein was isolated either subsequently or after storage of pellets at -80 °C as described in III.3.2.2.4.

3.2.2.5. Analysis of ROS in Murine Primary Acini

For analysis of ROS, primary acini were not seeded into collagen gel, but analyzed directly after isolation as described in III.4.4.1.

3.3. Murine PDAC Cell Lines

3.3.1. Isolation and Maintenance of Murine PDAC Cell Lines

3.3.1.1. Isolation and Maintenance of Murine PDAC Cell Lines from Tumor Tissue

The tumor-bearing mouse was sacrificed and the pancreas resected as described in III.2.6. When PDAC was macroscopically evident, an at least 5 mm³ piece was cut from the tumor, immediately placed in a new sterile petri dish and kept at room temperature until tissue harvesting as described in III.2.6 was completed.

Then, the tumor piece was washed three times in sterile PBS and placed in a new sterile petri dish. Afterwards, the tumor piece was cut into small pieces using sterile scalpels (2975#23, GF Health Products), suspended in sterile standard cell culture medium (see below) and transferred to a sterile T25 cell culture flask. The cell culture flask was incubated overnight in the cell culture incubator (see III.3.1). The next day, medium was replaced with fresh standard cell culture medium and the flask returned to the cell culture incubator. Medium was replaced twice a week and cells grown to confluence. At confluence, medium was removed. Cells were washed with sterile PBS, detached from the flask with trypsin, transferred to a sterile T75 cell culture flask, provided with new standard cell culture medium, and again, cultivated to confluence. At confluence, cells were detached again as described before and passaged to a T175 cell culture flask and two 3 cm cell culture plates. At confluence, the 3 cm cell culture plates were washed twice with sterile PBS and stored at -20 °C until DNA and protein isolation for genotype verification. The confluent T175 cell culture flask was taken for freezing cells as a stock for long-term storage. Therefore, cells were harvested as described before, transferred to a 25 ml Falcon tube and centrifuged for 5 min at 300 rcf at room temperature. Subsequently, supernatant was removed and the cell pellet suspended in sterile-filtered (0.2 µm) freezing medium (see below). Cell suspension was immediately partitioned in three cryo tubes (72.380, Sarstedt) and transferred to -80 °C. After 24 h, tubes were transferred to liquid nitrogen and stored infinitely.

PBS: 14190-169, Life Technologies.

Trypsin: 25300-096, Life Technologies.

Standard cell culture medium: 1 % (v/v) FBS (10499-044, Life Technologies)
 1 x MEM NEAA (11140-068, Life Technologies)
 1 x Pen Strep (15140-163, Life Technologies)
 in L-glutamine- and glucose-containing DMEM (41965-062, Life Technologies). Medium was kept refrigerated.

Freezing medium: 10 % (v/v) DMSO (D5879-100ML, Sigma-Aldrich)
 in FBS (10499-044, Life Technologies). Kept refrigerated.

3.3.1.2. Isolation of Murine PDAC Cancer Cell Lines from Ascites

The tumor-bearing mouse was sacrificed as described under III.2.6. Thereafter, the abdominal wall was opened leaving the peritoneum intact to verify presence of malignant ascites. Ascites fluid was taken with a sterile syringe, suspended in sterile standard cell culture medium (see III.3.3.1.1), transferred to a sterile T25 cell culture flask and passaged until freezing and DNA and protein isolation as described for PDAC cell lines (see III.3.3.1.1).

3.3.2. Culture of Murine PDAC Cell Lines

When genotype had been verified by PCR and immunoblot (see below) and cells were required for an experiment, cancer cell lines isolated from PDAC or ascites (see above) were thawed. Therefore, cryo vials were removed from liquid nitrogen, thawed in a 37 °C water bath and quickly suspended into pre-warmed standard culture medium. Cell suspension was transferred to a T75 cell culture flask and cultivated in the cell culture incubator. Medium was replaced after 24 h. At confluence, two to three times a week, cells were split at a 1:5 to 1:20 ratio according to the respective growth characteristics as previously described (see III.3.3.1.1).

3.3.3. Treatment of Murine PDAC Cell Lines

After at least two passages, cells were taken for experiments. For treatments, cells were seeded into black/clear bottom 96 well assay plates and allowed to attach overnight. The next day, standard medium was replaced with sterile Glucose or Galactose medium or rotenone or SIN-1 in Glucose or Galactose medium (see below) and plates were returned to the incubator. After 24 h, ATP production was determined using the CellTiter-Glo® Luminescent Cell Viability Assay (G7570, Promega) according to the manufacturer's instructions.

To avoid serum-specific side effects, for all experiments with Galactose medium, Glucose medium was used as control medium.

Glucose medium: 2 mg/ml BSA (A4503-100G, Sigma-Aldrich)
 1 mM Sodium Pyruvate (11360-039, Life Technologies)
 1 x Pen Strep (15140-163, Life Technologies)
 4.5 g/l Glucose (04164543, B. Braun)
 1 mM HEPES (15630-080, Life Technologies)
 in L-glutamine-containing, glucose-free DMEM (11966-025, Life Technologies). Prepared freshly.

Galactose medium:	2 mg/ml BSA (A4503-100G, Sigma-Aldrich) 1 mM Sodium Pyruvate (11360-039, Life Technologies) 1 x Pen Strep (15140-163, Life Technologies) 10 mM Galactose (G5388-100G, Sigma-Aldrich) 1 mM HEPES (15630-080, Life Technologies) in L-glutamine-containing, glucose-free DMEM (11966-025, Life Technologies). Prepared freshly.
Rotenone treatment:	5 μ m Rotenone (R8875-1G, Sigma-Aldrich) in the indicated cell culture medium. Prepared freshly.
SIN-1 treatment:	500 μ m SIN-1 Chloride (82220, Cayman Chemicals) in the indicated cell culture medium. Prepared freshly.

3.3.4. Mycoplasma Testing

Mycoplasma testing was performed with cells in culture at least every three weeks by direct PCR according to [492]. Briefly, 0.5-1 ml of medium of at least three days of consecutive culture was transferred from the cell culture vessel to a sterile Eppendorf tube and centrifuged at 200 rcf for 1 min. The supernatant was transferred to a new sterile tube and used as a template for mycoplasma detection PCR (see III.4.1.2).

4. *Molecular Biological Methods*

4.1. DNA-based Methods

4.1.1. DNA Isolation

4.1.1.1. DNA Isolation from Murine Tissues

High quality DNA (e.g. for mitochondrial DNA damage qPCR; see III.4.1.3) was extracted from murine pancreas using the DNeasy[®] Blood & Tissue Kit (69504, Qiagen) with RNaseA digestion according to the manufacturer's instruction and stored at -20 °C in a laboratory freezer until analysis.

For genotyping of the genetically modified mice, crude DNA was extracted from tail tips or punched out tissue from ear marking. Extraction was performed with 200 μ l of DirectPCR-Tail Lysis Reagent (31-102-T, Peqlab) supplemented with 10 μ l of Proteinase K (03115828001, Roche Diagnostics) according to the manufacturer's instructions.

4.1.1.2. DNA Isolation from Murine PDAC Cell Lines

PDAC cell lines grown in 12 well cell culture plates were washed twice with room temperature PBS (see III.3.3.1.1). Thereafter, 600 μ l of Lysis buffer was added to each well. The cells were detached with a Cell Scraper S (99002, TPP) and the contents of each well were transferred each to an Eppendorf tube. 30 μ l of Proteinase K (03115828001, Roche Diagnostics) was added and samples were incubated at 55 °C in a Thermomixer[®] compact (Eppendorf) for at least 2 h. Then, DNA was precipitated by addition of 0.1 vol of 3 M sodium

acetate, pH 7.5 and 2.5 vol ethanol, absolute for 20 min at -20 °C. Subsequently, DNA was pelleted by centrifugation at 20,000 rcf and 4 °C for 5 min. After washing the pellet in 2 ml of 70 % (v/v) ethanol, ethanol was allowed to evaporate by air drying the pellet for 20-30 min at room temperature. Finally, the pellet was suspended in 150 µl of PCR-grade water, incubated at 37 °C in a Thermomixer® compact (Eppendorf) to allow full solubilization and stored at -20 °C.

Lysis buffer: 5 mM TRIS (stock solution: 1 M, pH 7.5)
 50 mM NaCl (stock solution: 5 M)
 5 mM EDTA (stock solution: 0.5 M, pH 8.0)
 0.25 % (w/v) SDS
 in deionized water. Stored at room temperature.

4.1.2. Polymerase Chain Reaction (PCR)

PCR was predominantly performed for genotyping of genetically modified mice, sexing and mycoplasma detection.

For all PCRs, the ReadyMix™ REDTaq® PCR Reaction Mix with MgCl₂ (R2648, Sigma) was used according to the manufacturer's protocol in a 12 µl-volume containing 5 pmol of both forward and reverse primer. For genotyping and sexing, 0.5 µl of tail DNA, for mycoplasma detection, 0.25 µl of medium supernatant was used as template. If DNA from PDAC cell lines or pancreas was amplified, 10 to 50 ng of template was added to the reaction.

Primers were obtained from Eurofins Genomics as High Purity Salt Free (HPSF) purified lyophilisates, suspended at 100 mM in 1 x TE buffer according to the manufacturer's instructions and stored at -20 °C. Further primer dilutions were done in PCR-grade water. All primer sequences and amplicon sizes can be found in Table III.3.

PCRs were run either in a T100™ Thermal Cycler (Biorad) or a Mastercycler (Eppendorf). An annealing temperature of 58 °C was used and elongation time was 1 min for amplicons smaller than 1 kilobase and 1.5 min for amplicons larger than 1 kilobase.

Table III.3: Sequences and amplicon sizes of primers used in PCR.

Target	Purpose	Primer Sequences	Amplicon Size
<i>Cre</i>	GT	1. 5'-ACCAGCCAGCTATCAACTCG-3' 2. 5'-TTACATTGGTCCAGCCACC-3' 3. 5'-CTAGGCCACAGAATTGAAAGATCT-3' 4. 5'-GTAGGTGGAAATTCTAGCATCATCC-3'	324 bp (all), 199 bp (<i>Cre</i>)
<i>Ptf1a-Cre^{ex1}</i>	GT	1. 5'-GTCCAATTTACTGACCGTACACCAA-3' 2. 5'-CCTCGAAGGCGTCGTTGATGGACTGCA-3'	1155 bp
<i>Sod2^{fl}</i>	GT	1. 5'-GAGGGGCATCTAGTGGAGAA-3' 2. 5'-CCAGATCTGCAATTTCCAAAA-3'	180 bp (wt, <i>Sod2^{ΔΔ}</i>), 250 bp (<i>Sod2^{fl}</i>)
<i>Kras^{+/+}</i>	GT	1. 5'-CGCAGACTGTAGAGCAGCG-3' ¹ 2. 5'-GTCGACAAGCTCATGCGGG-3' ¹	507 bp (wt)
<i>Kras^{LSL-G12D}</i>	GT	1. 5'-CGCAGACTGTAGAGCAGCG-3' ¹ 2. 5'-CCATGGCTTGAGTAAGTCTGC-3' ¹	600 bp
<i>Trp53^{fl}</i>	GT	1. 5'-CACAAAAACAGGTTAAACCCA-3' ² 2. 5'-AGCACATAGGAGGCAGAGAC-3'	250 bp (wt), 300 bp (<i>Trp53^{fl}</i>)
<i>Trp53^{ΔΔ}</i>	GT	1. 5'-CACAAAAACAGGTTAAACCCA-3' ² 2. 5'-GAAGACAGAAAAGGGGAGGG-3' ² 3. 5'-CTAGGCCACAGAATTGAAAGATCT-3'	324 bp (all), 612 bp (<i>Trp53^{ΔΔ}</i>)

		4. 5'-GTAGGTGGAAATTCTAGCATCATCC-3'	
<i>Jarid1</i>	SEX	1. 5'-CTGAAGCTTTTGGCTTTGAG-3' ³ 2. 5'-CCACTGCCAAATTCTTTGG-3' ³	302 and 331 bp (m), 331 bp (f)
<i>Mycoplasma</i>	MYC	1. 5'-TGCACCATCTGTCACTCTGTAAACCTC-3' ⁴ 2. 5'-GGGAGCAAACAGGATTAGATACCCT-3' ⁴	270 bp

¹Primer sequences are taken from [493].

²Primer sequences are taken from [484].

³Primer sequences are taken from [494].

⁴Primer sequences are taken from [492].

GT=genotyping, SEX=sexing, MYC=mycoplasma detection, wt=wild type, bp=base pairs, m=male, f=female.

TE buffer: Tris-EDTA buffer 100 x Concentrate (T9285-100ML, Sigma) diluted to 1 x with PCR-grade water. Stored at room temperature.

4.1.3. Mitochondrial DNA Damage Quantitative PCR (qPCR) and Copy Number Assay

DNA damage qPCR is based on the principle that many kinds of DNA lesions impair DNA polymerase. Therefore, if different samples are amplified under identical conditions, DNA with fewer lesions will amplify more efficiently than DNA with more lesions. Such differences in efficiency depend on amplicon length and can be detected reliably for DNA stretches of about 1 kilobase in quantitative PCR [102].

To assess mitochondrial DNA damage, primers ("Long") were designed to three distinctive regions in the mitochondrial DNA (Mt), namely region A, B, and C. To normalize for mitochondrial copy number, for each mitochondrial DNA region a second primer set ("Short") was used (see Table III.4). Primers were obtained from Eurofins Genomics as High Purity Salt Free (HPSF) purified lyophilisates, suspended at 100 mM in 1 x TE buffer according to the manufacturer's instructions and stored at -20 °C in a laboratory freezer.

Template DNA was isolated from murine tissues or PDAC cell lines as described in III.4.1.1, measured in a NanoDrop 2000 (ThermoFisher) and diluted to 2 ng/μl in PCR-grade water. Primer efficiencies were determined with a mix of all analyzed samples starting at a concentration about 10 x higher than the samples and serial 1:10, 1:100 and 1:1000 dilutions.

Quantitative PCR was performed using the LightCycler® 480 SYBR Green I Master (04887352001, Roche Diagnostics) in a 10 μl-volume containing 2.5 pmol of both forward and reverse primer and 5 ng DNA. A LightCycler® 480 (Roche Diagnostics) was used.

The PCR program consisted of an initial denaturation (95 °C, 10 min), 45 cycles of denaturation (95 °C, 10 sec), annealing (52 °C, 10 sec), and elongation (72 °C, 50 sec (Long) or 10 sec (Short)) with single acquisition, and a melt analysis consisting of 65 to 97 °C temperature gradient at a ramp rate of 0.11 °C/s with acquisition every 5 °C. Melt analysis confirmed the presence of one specific PCR product for all primer sets.

Differences in PCR efficiencies were determined for each mitochondrial DNA region with the ΔΔCP method [495] according to Equation 16.

$$R = \frac{E_{\text{Short}}^{(\text{Mean CP}_{\text{Controls}} - \text{CP}_{\text{Sample}})_{\text{Short}}}}{E_{\text{Long}}^{(\text{Mean CP}_{\text{Controls}} - \text{CP}_{\text{Sample}})_{\text{Long}}}} \quad (\text{Equation 16})$$

with E=primer efficiency and CP=Crossing Point.

For murine tissues wild type tissues, for PDAC cell lines $\text{Kras}^{\text{G12D/+}}$ PDAC cell line DNAs served as controls.

Assuming a Poisson distribution, DNA damage can be expressed as number of lesions per a specific number of base pairs [102]. This was performed according to Equation 17.

$$\text{Lesion per 10 kb DNA} = R \times \frac{10000 \text{ bp}}{\text{Amplicon Size}_{\text{Long}} [\text{bp}]} \quad (\text{Equation 17})$$

For final assessment of mitochondrial damage, values for all three mitochondrial DNA regions were utilized.

Validity of the method was confirmed with H_2O_2 -treated PDAC cell lines and a linear correlation between H_2O_2 concentration and DNA damage could be demonstrated (data not shown).

To exclude that differences in mitochondrial copy numbers interfere with the DNA damage qPCR assay, mitochondrial copy number was determined according to Equations 16 and 17 by replacing the “Long” primer set values with values obtained in a “Short” PCR program with a primer set specific to cyclophilin A (*Cypa*), which amplifies a short stretch of nuclear DNA. Then, all values obtained for mitochondrial DNA damage were normalized to their corresponding number of mitochondria.

All primer sequences and their respective efficiencies and amplicon sizes are listed in Table III.4.

Table III.4: Sequences, amplicon sizes and efficiencies of primers used in Mitochondrial DNA Damage Quantitative PCR (qPCR) and Copy Number Assay

Target	Primer Sequences	Amplicon Size	Primer Efficiency
<i>Cypa</i>	1. 5'-ATGGTCAACCCACCGTG-3' 2. 5'-TTCTGCTGTCTTTGGAACCTTGTC-3'	99 bp	1.893
Mt_A_Short	1. 5'-CCGTGAACCAAACTCTAATCA-3' 2. 5'-CATTTCAGTGCTTTGCTTTG-3'	89 bp	1.916
Mt_B_Short	1. 5'-TTCTATGGCCAATGCTCTGA-3' 2. 5'-CAATGGGCATAAAGCTATGG-3'	55 bp	1.945
Mt_C_Short	1. 5'-TGATGGTACGGACGAACAGA-3' 2. 5'-GATGTCTCCGATGCGGTTAT-3'	72 bp	1.960
Mt_A_Long	1. 5'-TCTGGTCTTGTAACCTGAAATGA-3' 2. 5'-GCATTTTCAGTGCTTTGCTTT-3'	1029 bp	1.795
Mt_B_Long	1. 5'-TCTATGGCCAATGCTCTGAA-3' 2. 5'-GCATGAGTTTGGTGGGTCAT-3'	1040 bp	2.029
Mt_C_Long	1. 5'-CAACGCGGCAAACCTAACC-3' 2. 5'-AGGCCTATAAGTGAATTAGATTGT-3'	980 bp	1.626

4.1.4. Agarose Gel Electrophoresis

PCR products were detected by ethidium bromide-based agarose gel electrophoresis using the Sub-Cell[®] horizontal electrophoresis system (Bio-Rad).

Agarose gels were prepared at 2 % (w/v) in 1 x TAE buffer and contained 5 µg/ml ethidium bromide (2218.2, Carl Roth). For each sample, 10 µl of PCR product was loaded into the gel pockets. DNA Ladder-Mix (25-2040, Peqlab) was used as a marker according to the manufacturer's instructions. Gels were run at constant voltages (90-150 V depending on gel length) until fragment sizes were clearly distinguishable and photographed with a Gel Doc[™] XR system (Bio-Rad) and the Quantity One software (version 4.5.2 (Basic), Bio-Rad). Images were exported as TIFF files and analyzed with the Fiji Software [489].

TAE buffer: 40 mM TRIS
 2 mM Titriplex[®] III
 20 mM acetic acid, glacial
 in deionized water. Stored at room temperature.

4.2. RNA-based Methods

4.2.1. RNA Isolation from Murine Pancreas

RNA isolation from murine pancreas was performed with 200-300 µl of RLT buffer-shredded tissue (see III.2.6) with the Maxwell[®] 16 LEV simplyRNA Tissue Kit (AS1280, Promega) in the Maxwell[®] 16 Instrument (Promega) according to the manufacturer's instructions. Thereafter, samples were eluted in 30 µl PCR-grade water and RNA concentration and quality was assessed in a NanoDrop 2000 (ThermoFisher). RNA was stored at -80 °C until used in reverse transcription.

4.2.2. Reverse Transcription-Polymerase Chain Reaction (RT-PCR)

4.2.2.1. Reverse Transcription

For reverse transcription of pancreas RNA, the SuperScript II Reverse Transcriptase system (18064-014, Life Technologies) was used with Random Primers (C1181, Promega) and at least 250 ng of RNA of acceptable quality ($A_{260/280} = 2.0 \pm 0.2$ and $A_{260/230} = 2.2 \pm 0.3$) according to the manufacturer's instructions.

4.2.2.2. Quantitative PCR (qPCR)

Quantitative PCR was performed using the LightCycler[®] 480 SYBR Green I Master (04887352001, Roche Diagnostics) in a 10 µl-volume containing 2.5 pmol of both forward and reverse primer and 2.5 µl of a 1:40 dilution of cDNA. A LightCycler[®] 480 (Roche Diagnostics) was used.

Primers were obtained from Eurofins Genomics as High Purity Salt Free (HPSF) purified lyophilisates, suspended at 100 µM in 1 x TE buffer according to the manufacturer's instructions and stored at -20 °C in a laboratory freezer.

Primer efficiencies were determined with a mix of all analyzed samples starting at a concentration about 10 x higher than the samples and serial 1:10, 1:100 and 1:1000 dilutions.

The PCR program consisted of an initial denaturation (95 °C, 10 min), 45 cycles of denaturation (95 °C, 20 sec), annealing (52 °C, 30 sec), and elongation (72 °C, 25 sec) with single acquisition, and a melt analysis consisting of 65 to 97 °C temperature gradient at a ramp rate of 0.11 °C/s with acquisition every 5 °C. Melt analysis confirmed the presence of one specific PCR product for all primer sets.

Quantification was performed relative to *Cypa* mRNA expression with the LightCycler® 480 software (version 1.5.0.39, Roche Diagnostics) as 2nd Derivative Max type analysis with an All-To-Mean pairing rule.

All primer sequences and their respective efficiencies and amplicon sizes are listed in Table III.5.

Table III.5: Sequences, amplicon sizes and efficiencies of primers used in RT-PCR.

Target	Primer Sequences	Exon Spanning?	Amplicon Size	Primer Efficiency
<i>Cypa</i>	1. 5'-ATGGTCAACCCACCGTG-3' 2. 5'-TTCTGCTGTCTTTGGAACCTTGTC-3'	no	99 bp	1.992
<i>Sod2</i>	1. 5'-ACACATTAACGCGCAGATCA-3' 2. 5'-ATATGTCCCCACCATTGAA-3'	yes	172 bp	1.790
<i>Sod1</i>	1. 5'-CGGTGAACCAGTTGTGTTGT-3' 2. 5'-CAGGTCTCCAACATGCCTCT-3'	yes	180 bp	1.794
<i>Cat</i>	1. 5'-AGCGACCAGATGAAGCAGTG-3' 2. 5'-TCCGCTCTCTGTCAAAGTGTG-3'	yes	181 bp	1.631
<i>Gpx1</i>	1. 5'-GTTCCGACACCAGGAGAATG-3' 2. 5'-CATTCCGCAGGAAGGTAAG-3'	yes	155 bp	1.738
<i>Gpx4</i>	1. 5'-AGTACAGGGGTTTCGTGTGC-3' 2. 5'-GGCTGCAAACCTCTTGATTT-3'	yes	195 bp	1.703
<i>Txnrd2</i>	1. 5'-GGAGCCCTGGAATATGGAAT-3' 2. 5'-GCGCATCATGACAGTGGTAT-3'	yes	262 bp	1.871
<i>Hmox1</i>	1. 5'-GCCACCAAGGAGGTACACAT-3' 2. 5'-GCTTGTTGCGCTCTATCTCC-3'	yes	155 bp	1.814
<i>Amy1</i>	1. 5'-TGGTCAATGGTCAGCCTTTTTC-3' 2. 5'-CACAGTATGTGCCAGCAGGAAG-3'	yes	153 bp	2.015
<i>Ck19</i>	1. 5'-ACCCTCCCGAGATTACAACC-3' 2. 5'-CAAGGCGTGTCTGTCTCAA-3'	yes	140 bp	1.849
<i>Braf</i>	1. 5'-TGATGCGCTGTCTTCGAAAT-3' 2. 5'-GCCAGGCTCAAATCAAACACT-3'	no	92 bp	2.134
<i>Esr1</i>	1. 5'-CCTCCCGCCTTCTACAGGT-3' 2. 5'-CACACGGCACAGTAGCGAG-3'	yes	128 bp	2.065
<i>Esr2</i>	1. 5'-CTGTGCCTTCTCACAAGGA-3' 2. 5'-TGCTCCAAGGTAGGATGGAC-3'	no	129 bp	2.150
<i>Tyms</i>	1. 5'-GGAAGGGTGTGTTTGGAGGAGT-3' 2. 5'-GCTGTCCAGAAAATCTCGGGA-3'	yes	119 bp	1.968
<i>Ada</i>	1. 5'-ACCCGCATTCAACAAACCCA-3' 2. 5'-AGGGCGATGCCTCTCTTCT-3'	yes	102 bp	2.065
<i>Rara</i>	1. 5'-TTCTTTCCCCTATGCTGGGT-3' 2. 5'-GGGAGGGCTGGGTACTATCTC-3'	yes	150 bp	1.853
<i>Cdc25a</i>	1. 5'-ACAGCAGTCTACAGAGAATGGG-3' 2. 5'-GATGAGGTGAAAGGTGTCTTGG-3'	yes	203 bp	2.022
<i>Pak1</i>	1. 5'-GGTGCTTCAGGCACAGTGTA-3' 2. 5'-TCCCTCATGACCAGGATCTC-3'	yes	128 bp	2.241
<i>Ddr2</i>	1. 5'-GTGTGGGCCTTTGGGGTGA CTCT-3'	yes	214 bp	2.279

	2. 5'-ATGGCCGGTGCTTGGTTTCTCTTC-3'			
<i>Sfn</i>	1. 5'-GTGTGTGCGACACCGTACT-3' 2. 5'-CTCGGCTAGGTAGCGGTAG-3'	no	119 bp	2.050
<i>Cdkn1a</i>	1. 5'-AGATCCACAGCGATATCCAGAC-3' 2. 5'-ACCGAAGAGACAACGGCACACT-3'	yes	101 bp	2.017
<i>Gadd45b</i>	1. 5'-CCGAAAGGATGGACACGGTG-3' 2. 5'-TTATCGGGGTCTACGTTGAGC-3'	yes	101 bp	1.855
<i>Puma</i>	1. 5'-ACGACCTCAACGCGCAGTACG-3' 2. 5'-GAGGAGTCCCATGAAGAGATTG-3'	yes	101 bp	1.959
<i>Bax</i>	1. 5'-CAGGATGCGTCCACCAAGAA-3' 2. 5'-AGTCCGTGCCACGTCAGCA-3'	yes	106 bp	2.055
<i>Noxa</i>	1. 5'-TCGCAAAAGAGCAGGATGAG-3' 2. 5'-CACTTTGTCTCCAATCCTCCG-3'	yes	96 bp	1.765

4.3. Protein-based Methods

4.3.1. Protein Isolation from Murine Tissues, PDAC Cell Lines and Primary Pancreatic Acini

Frozen tissue pieces (see III.2.6) were weighted and crushed in 20 μ l of ice-cold Supplemented RIPA buffer per mg tissue with a SilentCrusher M (Heidolph) until no visible tissue pieces were present.

PDAC cell lines plated in 12 well cell culture plates were washed twice in ice-cold PBS and lysed on ice with 200 μ l of ice-cold Supplemented RIPA buffer for 5 min. Thereafter, cells were detached with a Cell Scraper S (99002, TPP) and the contents of each well were transferred each to an Eppendorf tube.

Pelleted primary pancreatic acini (see III.3.2.2.4) were suspended in 100 μ l of Supplemented RIPA buffer and cells were lysed on ice for 5 min.

Following lysis in Supplemented RIPA buffer, all three sample types were sonicated once at 35 % for 10 sec with a SONOPULS HD 2070 homogenizer (Bandelin electronic) and centrifuged at 20,000 rcf and 4 °C for 15 min to separate debris. Supernatants were transferred to sterile 1.5 ml Eppendorf tubes and kept on ice for further analysis.

For long-term storage, lysates were snap frozen and kept in liquid nitrogen.

RIPA buffer: 50 mM TRIS-HCl (stock solution: 1 M, pH 7.5)
 150 mM NaCl (stock solution: 5 M)
 1 % (v/v) NP-40
 0.5 % (w/v) sodium deoxycholate
 0.1 % (w/v) SDS
 in deionized water. Kept refrigerated.

Supplemented RIPA buffer: 10 % (v/v) glycerol
 1 Tablet/7 ml cOMplete Protease Inhibitor Cocktail Tablets
 (04693132001, Roche Diagnostics)
 1 Tablet/10 ml PhosSTOP Phosphatase Inhibitor Cocktail Tablets
 (04906837001, Roche Diagnostics)
 in RIPA buffer. Prepared freshly.

4.3.2. Immunoblot Analysis

For immunoblot analysis, first, protein concentration of lysates prepared as explained in III.4.3.1 was measured with the Pierce[®] BCA Protein Assay Kit (#23225, ThermoFisher) according to the manufacturer's instructions.

For each immunoblot analysis, lysates were adjusted to equal concentrations with Supplemented RIPA buffer (see III.3.3.1). Then, 1/5 volume of 6 x SDS Sample buffer was added to each sample and samples were denatured for 5 min at 95 °C in a Thermomixer[®] compact (Eppendorf).

SDS-polyacrylamide gel electrophoreses (SDS-PAGE) gel casting and running as well as protein transfer was performed with the mini-PROTEAN Tetra Cell system (Bio-Rad). Percentage of polyacrylamide was chosen according to target protein size. Equal amounts of protein lysates were loaded into the pockets of each gel. The Fermentas Spectra[™] Multicolor Broad Range Protein Ladder (11862124, ThermoFisher) was used as marker. Gels were run first at 100 V until the dye front reached the stacking/separation gel border and at 200 V for the rest of the gel.

After SDS-PAGE, proteins were transferred onto a Protran BA83 or BA85 Nitrocellulose Blotting Membrane (10402495 or 10401197, GE Healthcare) depending on the target protein size for 110 min at 100 V.

Then, membranes were washed briefly in TBS-T and blocked in 5 % (w/v) blocking agent (see Table III.6) in TBS-T for one hour at room temperature. Subsequently, membranes were incubated in target gene specific primary antibody diluted in blocking solution as specified in Table III.6 at 4 °C overnight.

The next day, membranes were washed once for 15 min and three times for 5 min in TBS-T. To detect primary antibodies, membranes were next incubated in a 1:5000 dilution of secondary antibody matching the organism that the respective primary antibody was made in, anti-rabbit, anti-mouse, or anti-rat (NA934-1ML, NA931-1ML, or NA935, GE Healthcare; see Table III.6). Thereafter, membranes were washed again once for 15 min and three times for 5 min in TBS-T.

Hrp-conjugated secondary antibodies were detected on Amersham Hyperfilm ECL autoradiography films (28-9068-37, GE Healthcare) with Amersham ECL Western Blotting Detection Reagent (RPN2106, GE Healthcare) or, for low-abundance proteins, SuperSignal West Femto Maximum Sensitivity Substrate (PI34095, ThermoFisher) as substrates in a Hyperprocessor SRX-101A (Konica minolta).

Developed autoradiography films were digitalized with a flatbed scanner and analyzed with the Fiji Software [489]. Erk1/2 served as loading control and for normalization of protein expression.

Table III.6: Primary antibodies, target protein sizes and conditions used for immunoblot analysis.

Primary Antibody	Order Number, Brand/Company	Target Protein Size	Blocking Agent	Primary Antibody Dilution	Secondary Antibody
Erk1/2	sc-93 and -154, Santa Cruz	42 and 44 kDa	Milk	1:2000	anti-rabbit
Sod2	ADI-SOD-111-F, ENZO	25 kDa	Milk	1:1000	anti-rabbit
Hmox1	ADI-OSA-111-F, ENZO	32 kDa	Milk	1:1000	anti-mouse
Amy1	A8273, Sigma-Aldrich	58 kDa	Milk	1:1000	anti-rabbit
Ck19	TROMA-III, Developmental Studies Hybridoma Bank	44 kDa	Milk	1:1000	anti-rat

p-p38	#4631, Cell Signaling	43 kDa	BSA	1:1000	anti-rabbit
p38	#9212, Cell Signaling	43 kDa	BSA	1:1000	anti-rabbit
Esr1	sc-542, Santa Cruz ¹ or 06-935, Merck ¹	66 kDa	Milk	1:1000	anti-rabbit
Esr2	sc-8974, Santa Cruz	58 kDa	Milk	1:1000	anti-rabbit
Trp53	NCL-p53-CM5p, Leica	53 kDa	Milk	1:1000	anti-rabbit

¹Both antibodies gave highly similar results.

6 x SDS Sample buffer: 7 ml/10 ml Stacking Gel buffer
 30 % (v/v) glycerol
 10 % (w/v) SDS
 0.012 % (w/v) bromophenol blue (B0126-25G, Sigma-Aldrich)
 0.6 M DTT (D9163-5G, Sigma-Aldrich)
 in deionized water. Stored at -80 °C in single-use aliquots.

4 x Separation Gel buffer: 1 M TRIS-HCl, 0.4 % (w/v) SDS, pH 8.8. Buffer was kept refrigerated.

Separation Gel: 10-12 % (w/v) polyacrylamide (Rotiphorese® Gel 30, 3029.2, Carl Roth)
 6 µl/1 ml APS (A3678-26G, Sigma-Aldrich; stock solution: 10 % (w/v))
 2.4 µl/1 ml TEMED (T9281-100ML, Sigma-Aldrich)
 1/4 vol Separation Gel buffer
 in deionized water. Prepared freshly.

4 x Stacking Gel buffer: 0.5 M TrisHCl, 0.4 % (w/v) SDS, pH 6.8. Buffer was kept refrigerated.

Stacking Gel: 4 % (w/v) polyacrylamide (Rotiphorese® Gel 30, 3029.2, Carl Roth)
 10 µl/1 ml APS (A3678-26G, Sigma-Aldrich; stock solution: 10 % (w/v))
 2 µl/1 ml TEMED (T9281-100ML, Sigma-Aldrich)
 1/4 vol Stacking Gel buffer
 in deionized water. Prepared freshly.

5 x SDS-PAGE buffer: 0.125 M TRIS
 0.96 M glycine
 0.5 % (w/v) SDS
 in deionized water. Buffer was kept refrigerated.

10 x Transfer buffer: 0.25 M TRIS
 1.38 M glycine
 in deionized water. Buffer was kept refrigerated.

1 x Transfer buffer: 20 % (v/v) methanol
 1/10 vol 10 x Transfer buffer
 in deionized water. Prepared freshly.

4.3.3. Ras Activity Assay

Ras activity was assessed with the Ras Activation Assay Kit (17-218, Merck). At least 3/4 of the total pancreas of 4 weeks-old mice was crushed in 700 µl of 1 x MLB with a SilentCrusher M (Heidolph) until no visible tissue pieces were present. Samples were

centrifuged at 20,000 rcf and 4 °C for 15 min to separate debris. Supernatants were transferred to sterile 1.5 ml Eppendorf tubes and kept on ice for further analysis. For long-term storage, lysates were snap frozen and kept in liquid nitrogen.

Protein concentration of lysates was measured with the Pierce[®] BCA Protein Assay Kit (#23225, ThermoFisher) according to the manufacturer's instructions and lysates were adjusted to equal concentrations with 1 x MLB.

In a fraction of each lysate (500 μ l), active GTP-bound Ras was pulled-down and eluted according to the instructions provided with the Ras Activation Assay Kit.

Thereafter, both pulled-down GTP-Ras and crude lysate (25 μ l) of each sample were supplemented with 6 x SDS Sample buffer (see III.4.3.2) to create a 1 x SDS Sample buffer solution and denatured for 5 min at 95 °C in a Thermomixer[®] compact (Eppendorf). Then, 0.5 vol of both pulled-down GTP-Ras and crude lysate were loaded into the pockets of an 11 % (w/v) SDS-PAGE gel and immunoblot was performed as described in the instructions provided with the Ras Activation Assay Kit with the equipment described in III.4.3.2.

Ras protein was detected and digitalized as described in III.4.3.2. GTP-Ras:Pan-Ras ratio was determined for each sample through densitometry of the respective signals obtained for the pulled-down vs. the crude lysates using the Fiji Software [489].

1 x MLB: 10 % (v/v) glycerol
 1 Tablet/7 ml cComplete Protease Inhibitor Cocktail Tablets
 (04693132001, Roche Diagnostics)
 1 Tablet/10 ml PhosSTOP Phosphatase Inhibitor Cocktail Tablets
 (04906837001, Roche Diagnostics)
 1/5 vol 5 x MLB (provided with the Ras Activation Assay Kit (17-218, Merck)
 in deionized water. Prepared freshly.

4.4. Oxidative Stress Methods

4.4.1. Carboxy-H₂DCFDA and MitoSOX Plate Assay

Cytosolic ROS and mitochondrial O₂^{•-} were detected in primary pancreatic acini and PDAC cell lines through Carboxy-H₂DCFDA and MitoSOX Plate Assay.

Acini were loaded with either 10 μ M Carboxy-H₂DCFDA (C400, Life Technologies) or 5 μ M MitoSOX (M36008, Life Technologies) for 30 min in the incubator after the last washing step in Solution 1 (see III.3.2.1). Subsequently, acini were centrifuged, washed once in PBS and suspended in PBS. Fluorescence was measured in triplicates in black/clear bottom 96 well assay plates at excitation/emission 485/520 nm (Carboxy-H₂DCFDA) or 530/590 nm (MitoSOX) in a FLUOstar OPTIMA microplate reader (Bmg Labtech).

PDAC cell lines were seeded into black/clear bottom 96 well assay plates at 1000 cells/well 24 hours prior to analysis. Then, cells were loaded with Carboxy-H₂DCFDA and MitoSOX in Glucose medium (see II.3.3.3) as described for primary acinar explants. After loading, cells were washed once in PBS, covered with 100 μ l of PBS and fluorescence was measured at least in triplicates as described for primary acinar cells.

For normalization, for each sample cell number was determined using the CellTiter-Glo[®] Luminescent Cell Viability Assay (G7571, Promega) according to the manufacturer's instructions.

4.4.2. Spin Trap and Electron Spin Resonance (ESR) Spectrometry

In murine pancreatic tissue, ROS were analyzed by Spin Trap and ESR Spectrometry. These analyses were conducted by our collaborators Pirkko Koelle and Priv. Doz. Dr. med. Peter Kuhlencordt of the Department of Vascular Medicine, Medizinische Klinik und Poliklinik IV, Klinikum der Ludwig-Maximilians-Universität München, Munich, Germany.

5. *Statistical Analysis*

Statistical analysis was performed using the GraphPad Prism version 6.00 for Windows (GraphPad Software) with the test mentioned in the figure legend for each experiment. P-values of less than 0.05 were considered significant.

IV. Results

1. Characterization of the Pancreas-Specific *Sod2* Knockout Mouse

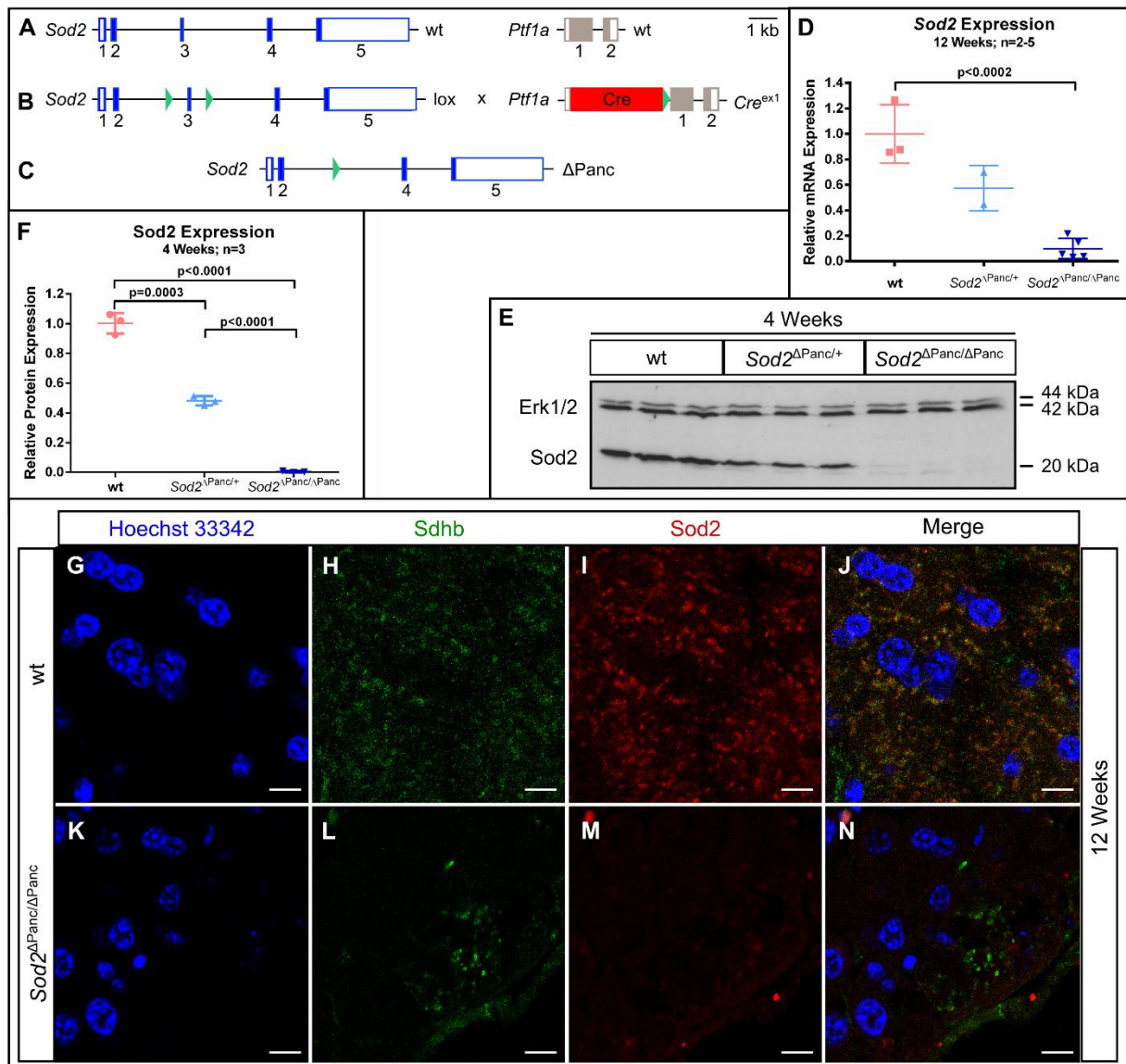


Figure IV.1: *Sod2*-loss is confirmed in pancreata of *Sod2*^{ΔPanc/ΔPanc} mice on RNA and protein level. (A-C) Gene loci for pancreas-specific *Sod2* deletion. *Sod2*^{fl/fl} mice were bred to *Ptf1a*-*Cre*^{ex1} mice (B) to generate the *Sod2*^{ΔPanc/ΔPanc} mice (C).

(D) Relative expression of *Sod2* mRNA in whole pancreas lysates of 12 weeks-old wt and *Sod2*^{ΔPanc/ΔPanc} mice determined by RT-PCR. Data are normalized to *Cypa* mRNA expression.

(E) Immunoblot analysis of *Sod2* in whole pancreas lysates of 4 weeks-old wt, *Sod2*^{ΔPanc/+}, and *Sod2*^{ΔPanc/ΔPanc} mice (n=3). Erk1/2 served as loading control.

(F) Quantification of *Sod2* protein expression by densitometry of immunoblot (E). Data were normalized to Erk1/2 expression.

(G-N) Representative immunofluorescence stainings of succinate dehydrogenase complex, subunit B, iron sulfur (I_p; Sdhb; (H and L)) as mitochondrial marker and *Sod2* (I and M) in pancreata of 12 weeks-old wt (G-J) and *Sod2*^{ΔPanc/ΔPanc} mice (K-N). Nuclei are stained with Hoechst 33342 (G and K). All three channels are merged in (J and N). Scale bars equal 7.5 μm.

Data in (D) and (F) are expressed as mean fold change compared with wt mice ± SD (n≥3); statistical analysis was performed using unpaired, two-tailed Student's *t*-test.

Sod2^{ΔPanc/ΔPanc} mice were generated by breeding *Sod2*^{fl/fl} mice [257] to *Ptf1a-Cre*^{ex1} mice ([483]; Figure IV.1A-C). Pancreas-specific *Sod2* knockout was confirmed on the level of RNA (Figure IV.1D) and protein (Figure IV.1E-F). Additionally, *Sod2*-deletion was demonstrated by loss of co-localization with the mitochondrial marker succinate dehydrogenase complex, subunit B, iron sulfur (Ip; *Sdhb*; Figure IV.1G-N). Heterozygous *Sod2*^{ΔPanc/+} mice had about half the *Sod2* mRNA and protein levels as the wt mice (Figure IV.1A-D).

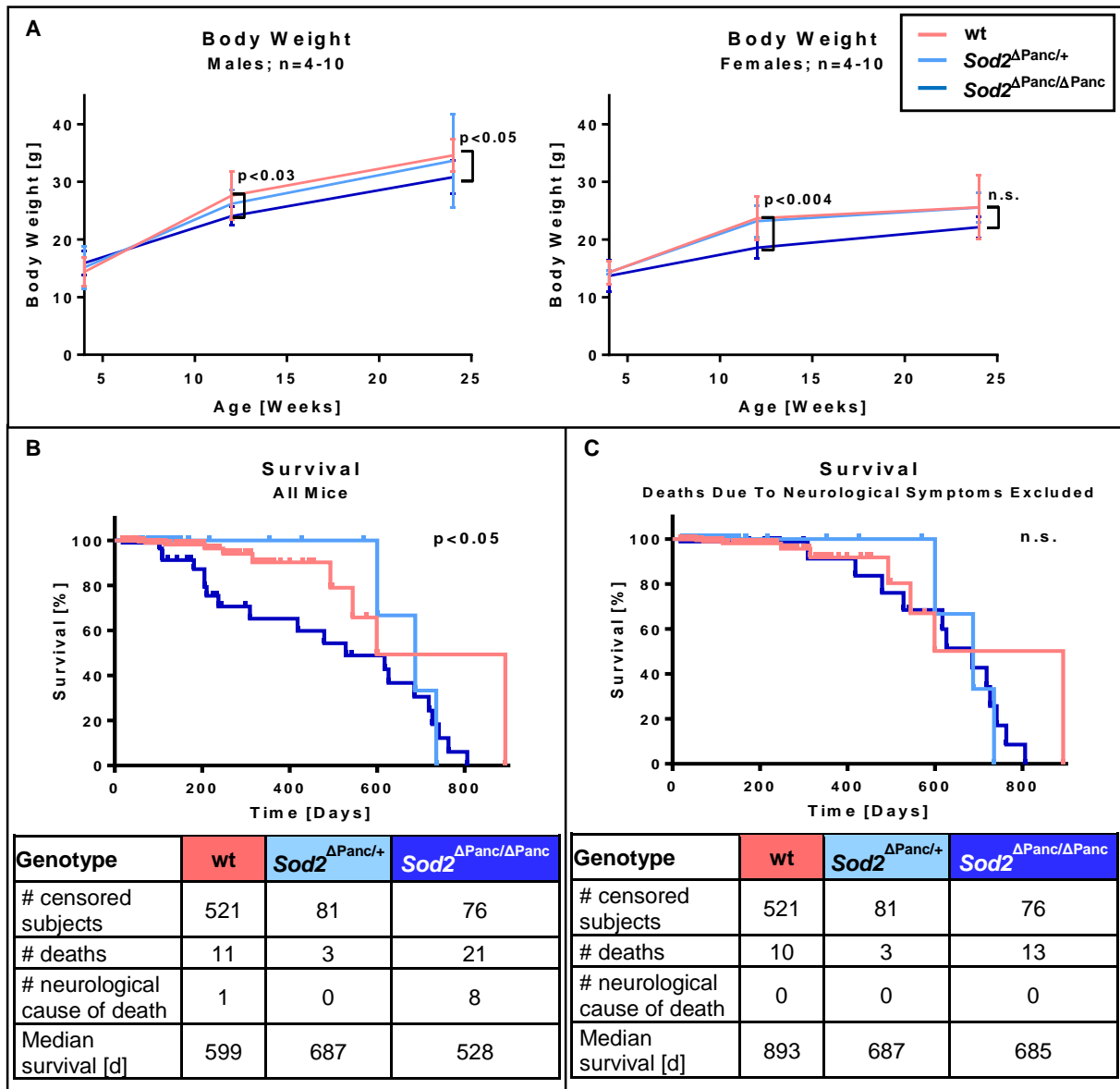


Figure IV.2: Body weights and survival are reduced in *Sod2* knockout compared with wt mice.

(A) Body weights of male (left) and female (right) wt, *Sod2*^{ΔPanc/+} and *Sod2*^{ΔPanc/ΔPanc} mice at 4, 12, and 24 weeks. Data are expressed as means ± SD (n≥3).

(B) Kaplan-Meier analysis of wt, *Sod2*^{ΔPanc/+} and *Sod2*^{ΔPanc/ΔPanc} mice.

(C) Kaplan-Meier analysis of wt, *Sod2*^{ΔPanc/+} and *Sod2*^{ΔPanc/ΔPanc} mice excluding all deaths that occurred due to neurological symptoms. Neurological symptoms included hind limb paralysis, circling, and balance disturbances.

Statistical analysis in (A) was performed using unpaired, two-tailed Student's *t*-test. In (B) and (C) log-rank (Mantel-Cox) test was used.

Upon basic evaluation, most young (12 weeks) and middle-aged (24 weeks) *Sod2*^{ΔPanc/ΔPanc} mice did not display overt phenotypic anomalies unless that their body weights were slightly reduced compared with wt mice (Figure IV.2A).

Surprisingly, about one third of all *Sod2*^{ΔPanc/ΔPanc}, but none of the *Sod2*^{ΔPanc/+} or wt animals, developed neurological symptoms including balance disturbances, hind limb paralysis, and circling that required euthanization between day 72 to 545. As a result, survival data of *Sod2*^{ΔPanc/ΔPanc} mice was significantly reduced compared with wt mice (Figure IV.2B).

As this phenotype was most likely due to undesirable CNS- and not pancreas-specific *Sod2* deletion (owing to CNS-specific *Ptf1a* expression; see V.1.6.), mice that had succumbed owing to neurological symptoms were excluded from survival analysis in the following. Having excluded these individuals, survival times of *Sod2*^{ΔPanc/ΔPanc} animals differed no longer from wt mice (Figure IV.2C).

Next, pancreata of *Sod2*^{ΔPanc/ΔPanc} mice were examined. Comparing basic histology by H&E staining, *Sod2*^{ΔPanc/ΔPanc} pancreata were indistinguishable from wt pancreata (Figure IV.3A-D). Moreover, like wt, *Sod2*^{ΔPanc/ΔPanc} pancreata displayed the expected expression patterns of three markers for the three major pancreatic cell types: α-amylase (*Amy1*; acinar cells; Figure IV.3E-H), cytokeratin 19 (*Ck19*; ductal cells; Figure IV.3I-L), and insulin (*Ins2*; endocrine β-cells; Figure IV.3M-P).

Function of *Sod2*^{ΔPanc/ΔPanc} pancreata was assessed for both the endocrine and the exocrine compartment. Basal glucose levels and IP-GTT strongly suggested that *Sod2* deletion leaves endocrine pancreatic function fully intact (Figure IV.4A-B). Of note, male *Sod2*^{ΔPanc/ΔPanc} and wt mice had higher basal, but a lower overall increase in blood glucose levels after glucose injection than female *Sod2*^{ΔPanc/ΔPanc} and wt mice.

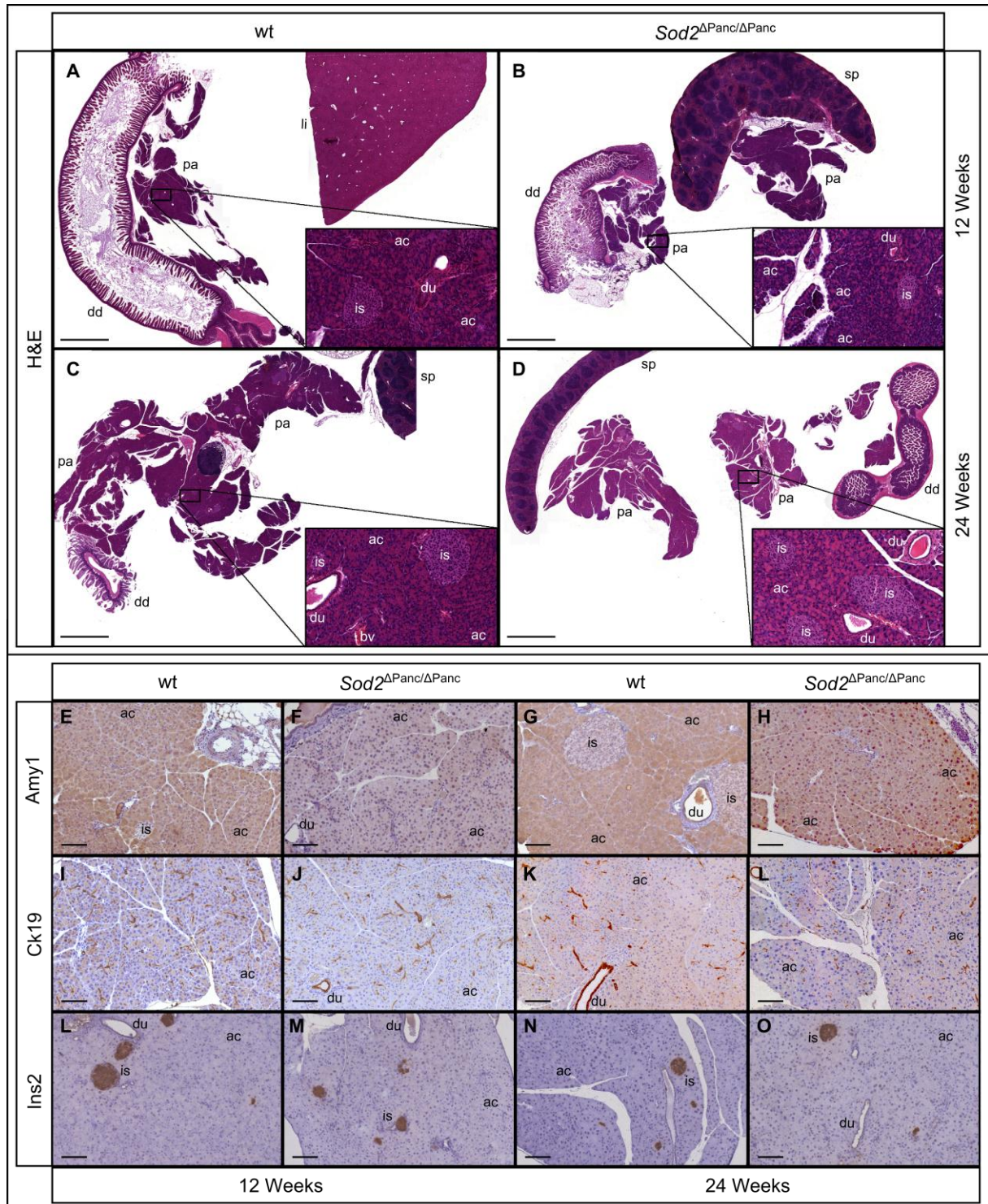


Figure IV.3: Histomorphologically, *Sod2* knockout are indistinguishable from wt pancreata.

(A-D) Representative H&E stainings of wt (A and C) and *Sod2* knockout (B and D) pancreata (pa) and control tissues (duodenum (dd), liver (li), and spleen (sp)) at 12 (A and B) and 24 weeks (C and D). Scale bars equal 2000 μ m. Embedded image sections represent 10 x magnifications of indicated areas of the pancreata.

(E-P) Representative immunohistochemistry stainings for Amy1 (E-H), Ck19 (I-L), and Ins2 (M-P) of wt (E, I, M, G, K, and O) and *Sod2* knockout (F, J, N, H, L, and P) pancreata at 12 (E, F, I, J, M, and N) and 24 weeks (G, H, K, L, O, and P). Scale bars equal 200 μ m.

ac=acini, is=islet of Langerhans, du=duct, bv=blood vessel.

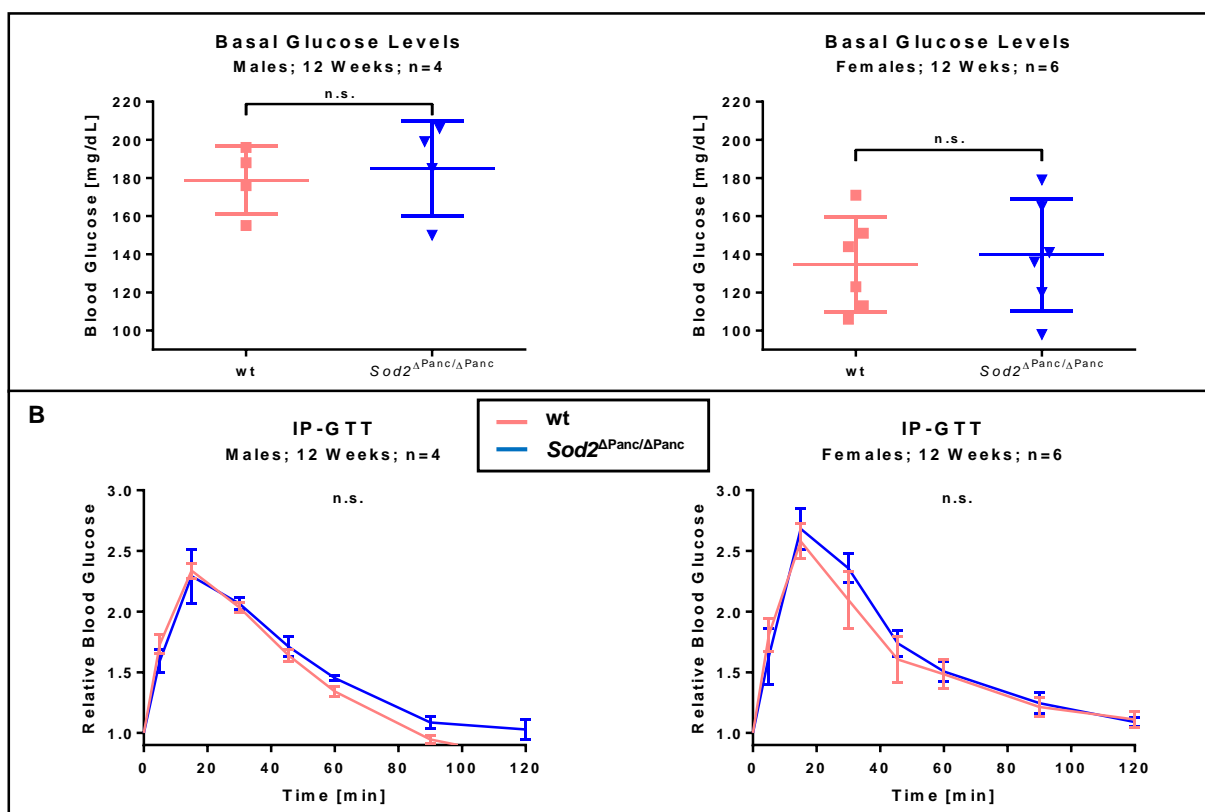


Figure IV.4: Endocrine function of $Sod2$ knockout is not different from wt pancreata.

(A) Basal blood glucose levels of male (left) and female (right) wt and $Sod2^{\Delta Panc/\Delta Panc}$ mice after a 6-hour morning fast at 12 weeks.

(B) IP-GTT of male (left) and female (right) mice after a 6-hour morning fast at 12 weeks. Data were normalized to basal glucose levels (0 min; (A)).

Data are expressed as means \pm SD (n \geq 4). Statistical analysis in (A) was performed using unpaired, two-tailed Student's *t*-test. In (B) Wilcoxon test was used.

The slightly reduced body weight of $Sod2^{\Delta Panc/\Delta Panc}$ compared with wt mice indicated that $Sod2$ deletion might have elicited mild pancreatic exocrine insufficiency. To further assess exocrine function, body weight gain was investigated in more detail by feeding mice with HFD (20 instead of 5 % crude fat) for six weeks and weighting them every week. As a control, age-matched mice kept on standard diet were weighted simultaneously (Figure IV.5A). While this analysis confirmed the weight difference observed between $Sod2^{\Delta Panc/\Delta Panc}$ and wt mice on standard diet, surprisingly, female mice gained less weight on fat-enriched, than on standard diet. However, the difference in weight gain observed with the standard diet manifested also for the fat-enriched chow. In contrast, males might have gained more weight on HFD than on standard diet, while the HFD might have abolished the weight difference observed for standard diet-fed $Sod2^{\Delta Panc/\Delta Panc}$ and wt mice (Figure IV.5A). In concert, when these mice were sacrificed at the age of 12 weeks after six weeks on HFD, female $Sod2^{\Delta Panc/\Delta Panc}$ mice had deposited significantly less fat in their livers than female wt mice, while there was no significant difference between male $Sod2^{\Delta Panc/\Delta Panc}$ and wt animals (Figure IV.5B-F).

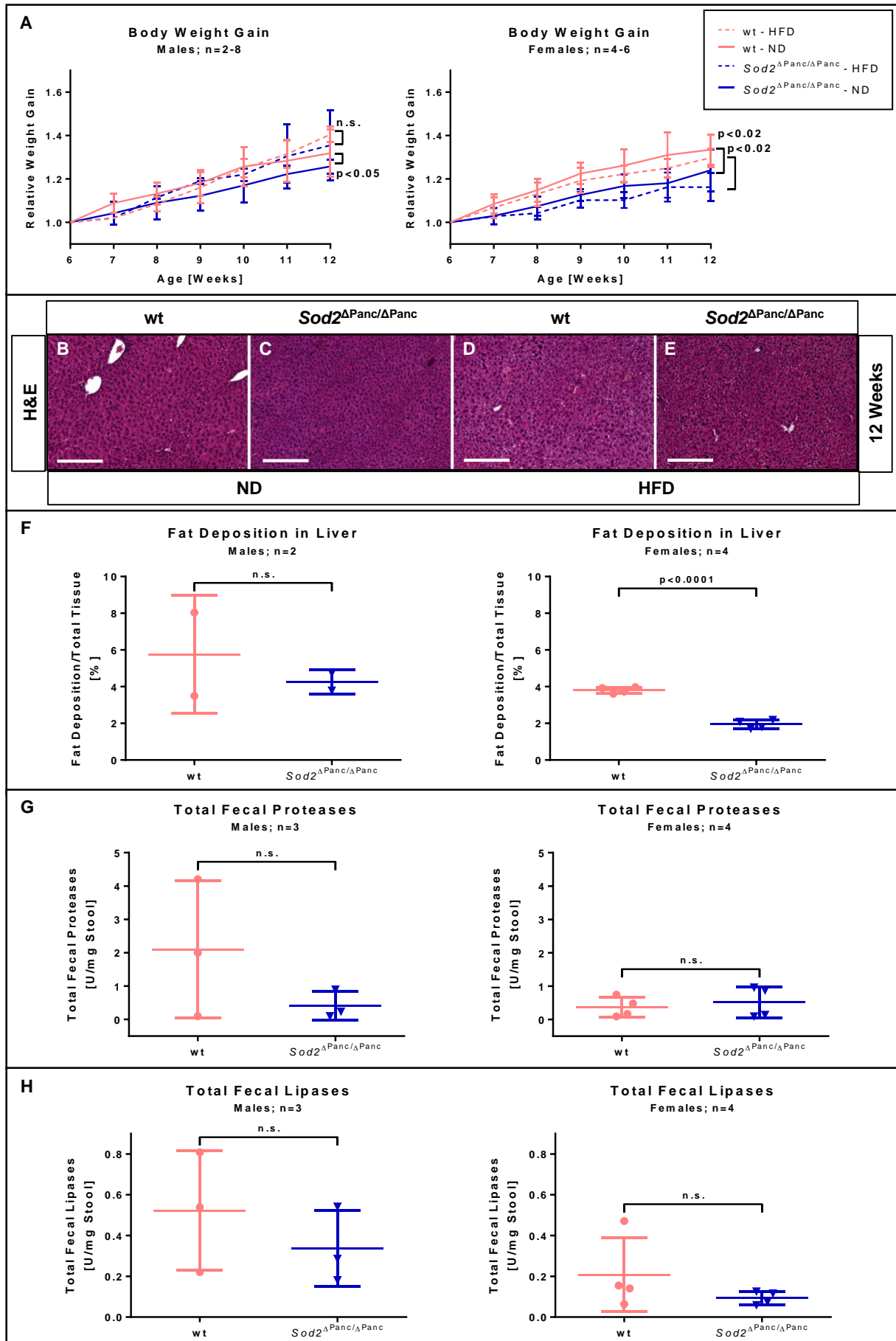


Figure IV.5: Exocrine function of female *Sod2* knockout might be slightly reduced compared with female wt pancreata.

Figure IV.5: Exocrine function of female *Sod2* knockout might be slightly reduced compared with female wt pancreata - continued.

(A) Weight gain during 6 weeks on standard (ND) and HFD in male (left) and female (right) wt and *Sod2* knockout mice. HFD and weight gain observations were started at 6 weeks; final weight observations were taken at 12 weeks.

(B-E) Representative H&E stainings of livers of 12 weeks-old wt (B and D) and *Sod2*^{ΔPanc/ΔPanc} (C and E) mice on ND (B and C) or after 6 weeks on HFD (D and E). Scale bars equal 200 μm.

(F) Quantification of fat deposition in livers of 12 weeks-old male (left) and female (right) wt and *Sod2*^{ΔPanc/ΔPanc} mice after 6 weeks on HFD.

(G) Quantification of total stool proteases in 12 weeks-old male (left) and female (right) wt and *Sod2*^{ΔPanc/ΔPanc} mice after 1 week on HFD. (H) Quantification of total stool lipases in 12 weeks-old male (left) and female (right) wt and *Sod2*^{ΔPanc/ΔPanc} mice after 1 week on HFD.

Data in (A), (F), and (G) are expressed as means ± SD (n≥2). Statistical analysis in (A) was performed using Wilcoxon test. In (F), (G), and (H), unpaired, two-tailed Student's *t*-test was used.

Despite these findings, however, there was no significant difference in levels of fecal proteases or lipases for neither the female nor the male *Sod2*^{ΔPanc/ΔPanc} compared with wt mice after one week of HFD (Figure IV.5G-H).

As *Sod2* is an antioxidant gene, *Sod2*^{ΔPanc/ΔPanc} and wt pancreata were next assessed for oxidative stress. To this end, ROS were measured by spin trap and ESR spectrometry in whole pancreas lysates (Figure IV.6C). Additionally, fluorescent probes Carboxy-H₂DCFDA and MitoSOX were used to analyze primary pancreatic acini for cytosolic ROS or mitochondrial O₂^{•-}, respectively (Figure IV.6A-B). While, with the fluorescent probes, there was a slight increase in ROS levels, spin trap and ESR spectrometry did not uncover a difference in ROS levels. Moreover, as *Sod2* specifically detoxifies mitochondrial O₂^{•-} which cannot cross biological membranes, DNA damage qPCR was applied to assess mitochondrial oxidative DNA damage. Yet, *Sod2*^{ΔPanc/ΔPanc} pancreata did not display increased levels of mitochondrial DNA damage (Figure IV.6D) while mitochondrial copy numbers were identical (data not shown).

To exclude that other antioxidants compensated for *Sod2*-loss, mRNA levels of five other key antioxidant enzymes were measured in *Sod2*^{ΔPanc/ΔPanc} and wt pancreata, including *superoxide dismutase 1 (Sod1)*, *catalase (Cat)*, *glutathione peroxidase 1 (Gpx1)*, and *glutathione peroxidase 4 (Gpx4)*, and *thioredoxin reductase 2 (Txnrd2)*; (Figure IV.6E-J). None of these antioxidants was significantly increased in the *Sod2* knockout animals. On the contrary, significant reduction of *Gpx4* was noted in the *Sod2* knockout compared with wt animals.

Furthermore, mRNA and protein levels of *heme oxygenase-1 (Hmox1)*, a key marker of oxidative stress, were similarly not increased in *Sod2*^{ΔPanc/ΔPanc} compared with wt pancreata (Figure IV.6J-L).

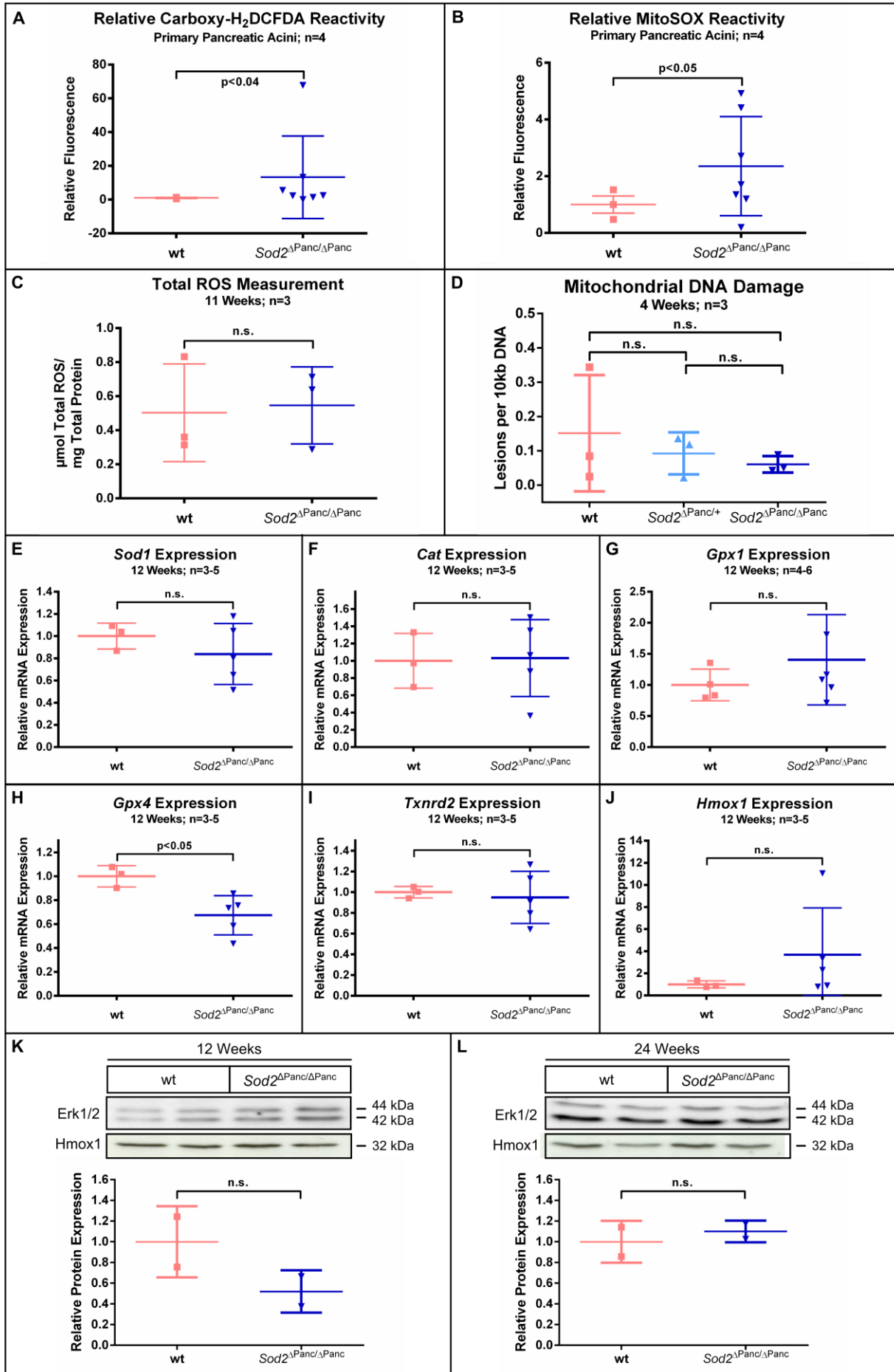

 Figure IV.6: ROS are mildly increased in *Sod2* knockout pancreata.

Figure IV.6: ROS are mildly increased in *Sod2* knockout pancreata - continued.

(A) Relative Carboxy-H₂DCFDA reactivity of wt and *Sod2*^{ΔPanc/ΔPanc} primary pancreatic acini. Fluorescence was measured at excitation/emission=485 nm/520 nm and normalized to unstained primary acini. Wt acini served as calibrator.

(B) Relative MitoSOX reactivity of wt and *Sod2*^{ΔPanc/ΔPanc} primary pancreatic acini. Fluorescence was measured at excitation/emission=530 nm/590 nm and normalized to unstained primary acini. Wt acini served as calibrator.

(C) Quantification of total ROS in whole pancreas lysates of 11 weeks-old wt and *Sod2*^{ΔPanc/ΔPanc} mice by Spin Trap and ESR Spectrometry.

(D) Mitochondrial DNA damage in whole pancreas lysates of 4 weeks-old wt, *Sod2*^{ΔPanc/+}, and *Sod2*^{ΔPanc/ΔPanc} mice analyzed by qPCR-DNA damage assay.

(E-J) Relative mRNA expression of *superoxide dismutase 1* (*Sod1*; E), *catalase* (*Cat*; F), *glutathione peroxidase 1* (*Gpx1*; G), *glutathione peroxidase 4* (*Gpx4*; H), *thioredoxin reductase 2* (*Txnrd2*; I), and *heme oxygenase-1* (*Hmox1*; J) in whole pancreas lysates of 12 weeks-old wt and *Sod2*^{ΔPanc/ΔPanc} mice analyzed by RT-PCR. Data were normalized to *Cypa* mRNA expression.

(K-L) Western blot analyses of Hmox1 expression (top) in whole pancreas lysates of 12 (K) and 24 weeks-old (L) wt and *Sod2*^{ΔPanc/ΔPanc} mice and their respective quantifications by densitometry (bottom). Erk1/2 served as loading control and for normalization of densitometry data.

In (A-D), data are expressed as means ± SD (n≥3). In (E-L), data are expressed as mean fold change compared with wt mice ± SD (n≥3). Statistical analysis in (A-L) was performed using unpaired, two-tailed Student's *t*-test.

To investigate whether *Sod2* regulates pancreatic cell fate, proliferation and apoptosis were assessed by BrdU incorporation or cleaved Casp3 expression quantification in the *Sod2*^{ΔPanc/ΔPanc} and wt pancreata. Notably, there was no significant difference in neither proliferation nor apoptosis comparing *Sod2*^{ΔPanc/ΔPanc} and wt pancreata (Figure IV.7).

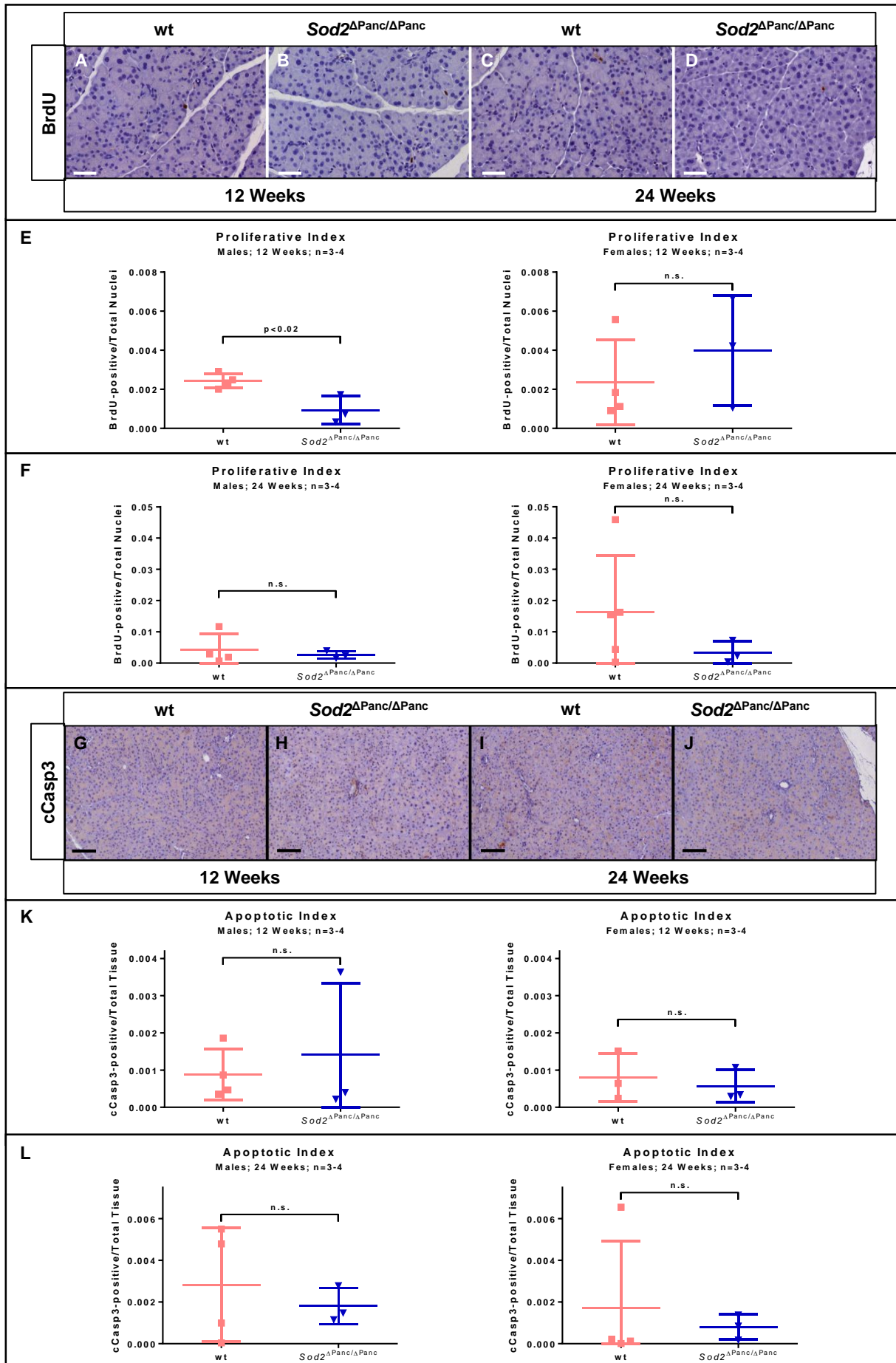


Figure IV.7: Proliferation and apoptosis are not affected by pancreas-specific *Sod2* knockout.

Figure IV.7: Proliferation and apoptosis are not affected by pancreas-specific *Sod2* knockout - continued.

(A-D) Representative BrdU immunohistochemistry stainings of pancreata of 12 (A and B) and 24 weeks-old (C and D) wt (A and C) and *Sod2*^{ΔPanc/ΔPanc} (B and D) mice. Scale bars equal 50 μm.

(E-F) Quantification of BrdU incorporation in pancreata of 12 (E) and 24 weeks-old (F) male (left) and female (right) wt and *Sod2*^{ΔPanc/ΔPanc} mice. (G-J) Representative cleaved Casp3 (cCasp3) immunohistochemistry stainings of pancreata of 12 (G and H) and 24 weeks-old (I and J) wt (G and I) and *Sod2*^{ΔPanc/ΔPanc} (H and J) mice. Scale bars equal 25 μm.

(K-L) Quantification of cCasp3 immunohistochemistry in pancreata of 12 (K) and 24 weeks-old (L) male (left) and female (right) wt and *Sod2*^{ΔPanc/ΔPanc} mice.

In (E-F) and (K-L), data are expressed as means ± SD (n≥3) and statistical analysis was performed using unpaired, two-tailed Student's *t*-test.

2. Role of *Sod2* in Pancreatic Cancer

2.1. Role of *Sod2* in *Kras*^{G12D}-Mediated PDAC

To assess the role of *Sod2* in pancreatic cancer, the effects of *Sod2* deletion were investigated in the context of the *Kras*^{G12D}-driven PDAC model.

Basic phenotyping revealed that, similar to the mice without *Kras* mutation, body weights of *Kras*^{G12D/+}; *Sod2*^{ΔPanc/ΔPanc} mice were significantly lower compared with *Kras*^{G12D/+} mice (Figure IV.8A).

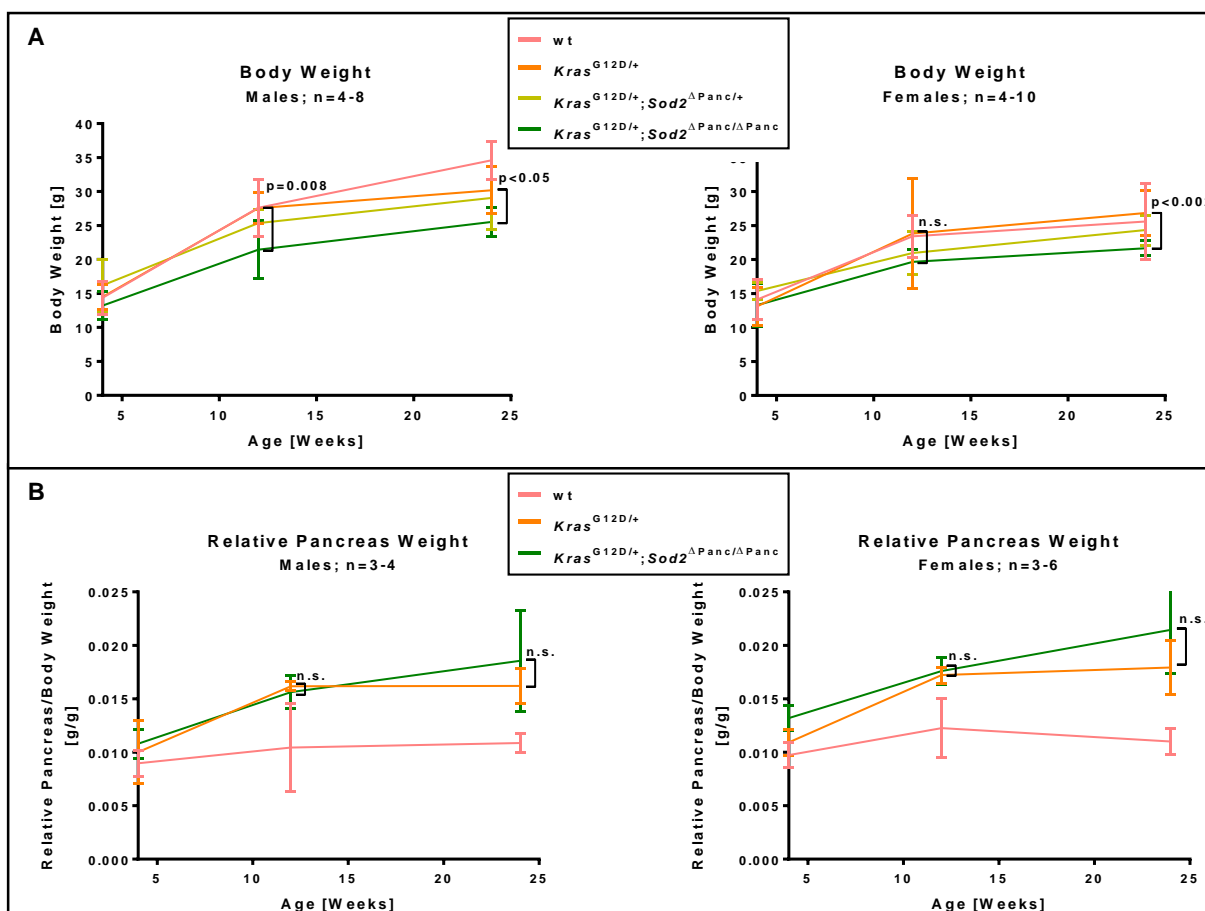


Figure IV.8: Body weights are reduced in *Kras*^{G12D/+}; *Sod2*^{ΔPanc/ΔPanc} compared with *Kras*^{G12D/+} mice.

Figure IV.8: Body weights are reduced in $Kras^{G12D/+};Sod2^{\Delta Panc/\Delta Panc}$ compared with $Kras^{G12D/+}$ mice - continued.

(A) Body weights of male (left) and female (right) $Kras^{G12D/+}$ and $Kras^{G12D/+};Sod2^{\Delta Panc/\Delta Panc}$ mice at 4, 12, and 24 weeks.

(B) Relative pancreas/body weights of male (left) and female (right) $Kras^{G12D/+}$ and $Kras^{G12D/+};Sod2^{\Delta Panc/\Delta Panc}$ mice at 4, 12, and 24 weeks.

All data are expressed as means \pm SD ($n \geq 3$). Statistical analyses comparing $Kras^{G12D/+}$ with $Kras^{G12D/+};Sod2^{\Delta Panc/\Delta Panc}$ animals were performed using unpaired, two-tailed Student's *t*-test.

Interestingly, at the age of 24 weeks, there was a non-significant trend towards an increased relative pancreatic weight in both male and female $Kras^{G12D/+};Sod2^{\Delta Panc/\Delta Panc}$ compared with $Kras^{G12D/+}$ mice (Figure IV.8B).

As for the mice without *Kras* mutation, about one third of all $Kras^{G12D/+};Sod2^{\Delta Panc/\Delta Panc}$ animals developed neurological symptoms that required euthanization, while none of the $Kras^{G12D/+}$ or $Kras^{G12D/+};Sod2^{\Delta Panc/+}$ animals were affected (Figure IV.9A-B). Again, these animals were excluded from survival analysis.

On basic survival analysis, *Sod2* deletion did not affect survival times of $Kras^{G12D/+}$ mice (Figure IV.9A-B). Yet remarkably, tumor free survival was significantly prolonged in the female $Kras^{G12D/+};Sod2^{\Delta Panc/\Delta Panc}$ over the female $Kras^{G12D/+}$ animals (Figure IV.9D), while for male mice, no such benefit could be detected (Figure IV.9C).

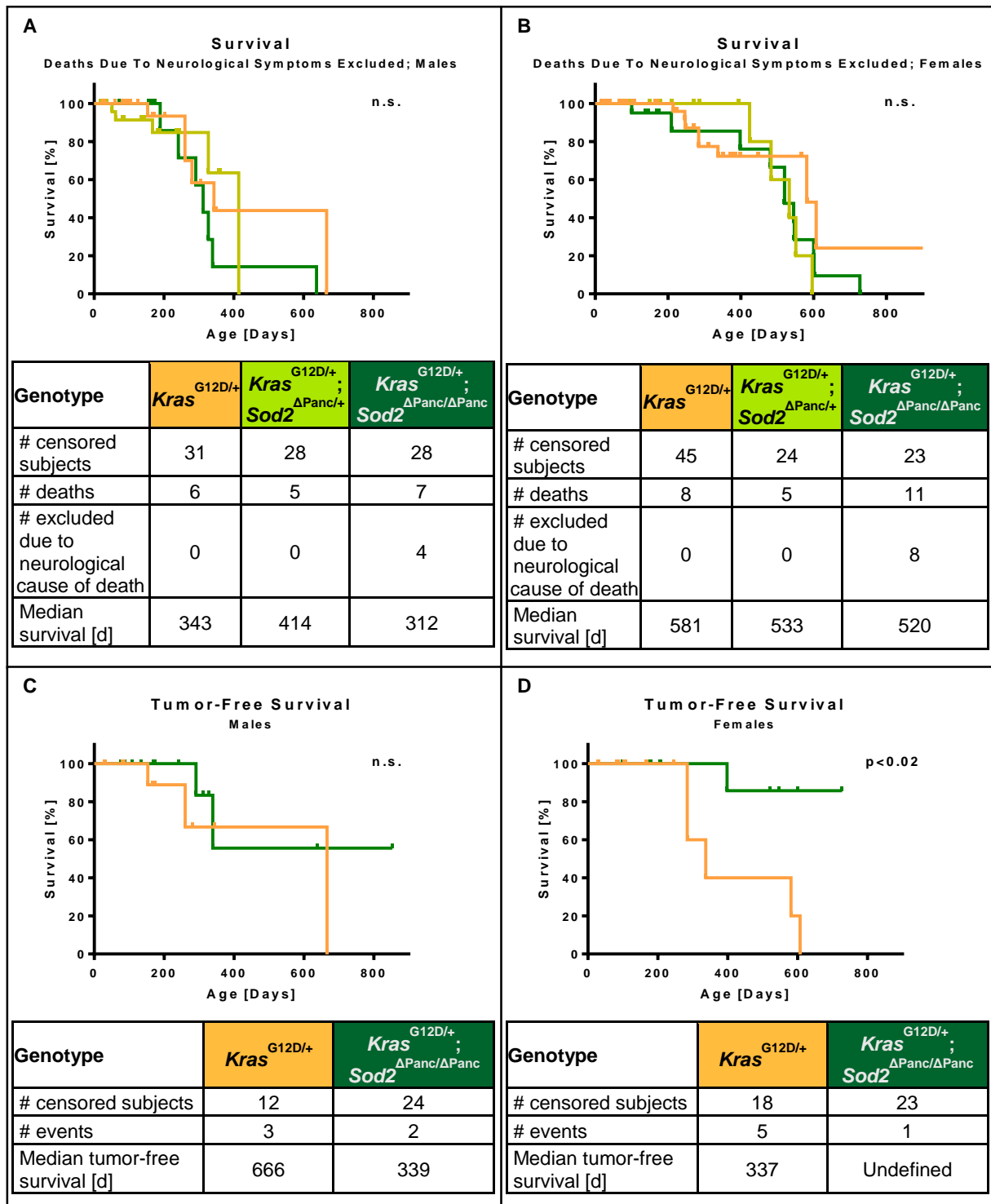


Figure IV.9: *Sod2* knockout prolongs tumor-free, but not overall survival in female *Kras*^{G12D/+} mice.

(A-B) Kaplan-Meier analysis of male (A) and female (B) *Kras*^{G12D/+}, *Kras*^{G12D/+};*Sod2*^{ΔPanc/+}, and *Kras*^{G12D/+};*Sod2*^{ΔPanc/ΔPanc} mice excluding all deaths that occurred due to neurological symptoms.

(C-D) Kaplan-Meier analysis of male (C) and female (D) *Kras*^{G12D/+} and *Kras*^{G12D/+};*Sod2*^{ΔPanc/ΔPanc} mice.

Microscopically evident PDACs at necropsy were considered positive, PDAC absence as negative events. All mice of (A) and (B) with available histology were included in the analyses.

Statistical analysis was performed using log-rank (Mantel-Cox) test.

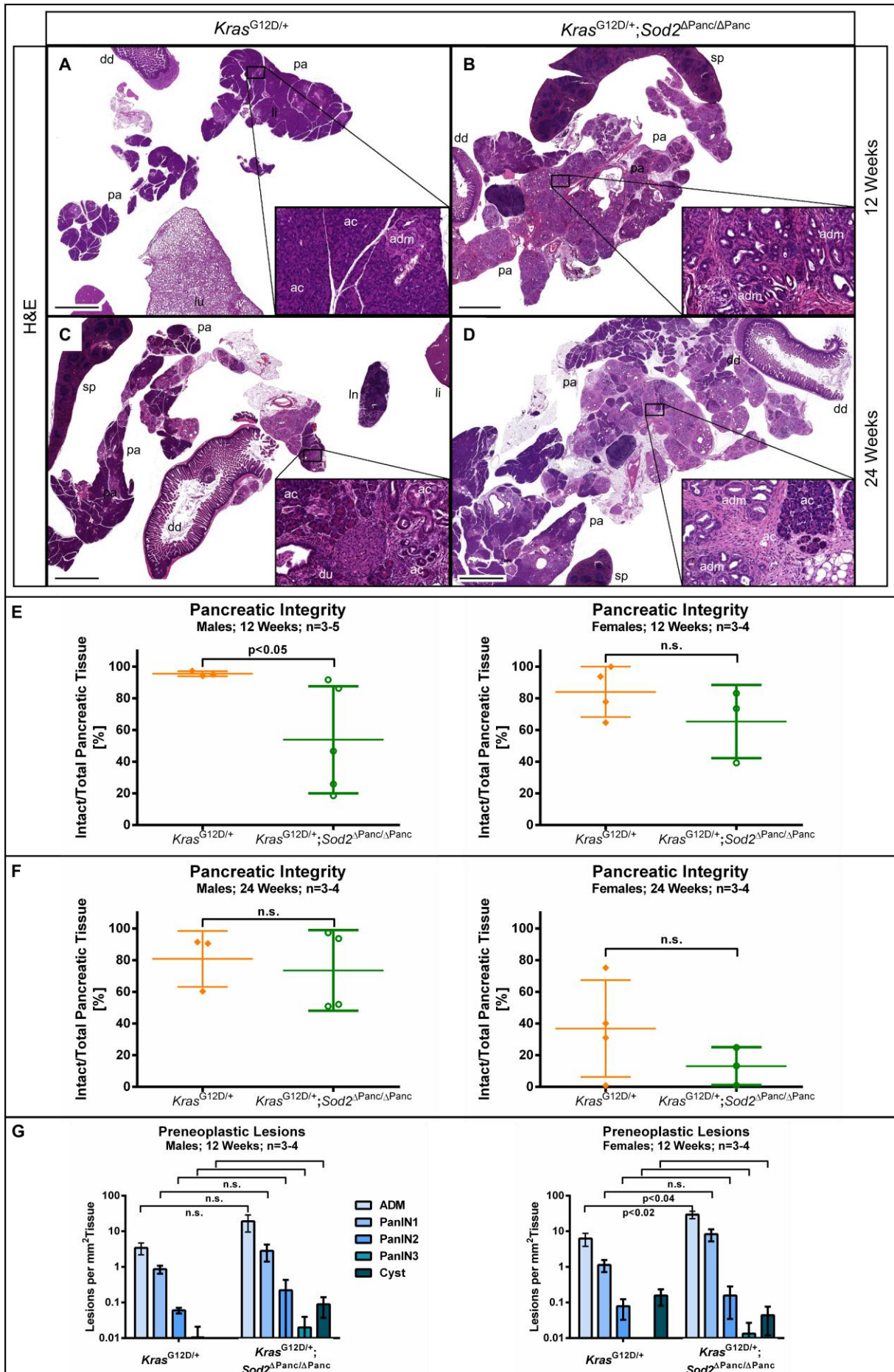


Figure IV.10: There is a partly significant trend towards less intact pancreatic tissue and a higher number of PanIN lesions comparing *Kras*^{G12D/+};*Sod2*^{ΔPanc/ΔPanc} with *Kras*^{G12D/+} mice.

Figure IV.10: There is a partly significant trend towards less intact pancreatic tissue and a higher number of PanIN lesions comparing $Kras^{G12D/+};Sod2^{\Delta Panc/\Delta Panc}$ with $Kras^{G12D/+}$ mice - continued.

(A-D) Representative H&E stainings of $Kras^{G12D/+}$ (A and C) and $Kras^{G12D/+};Sod2$ knockout (B and D) pancreata (pa) and control tissues (duodenum (dd), liver (li), lung (lu), spleen (sp), and lymph node (ln)) at 12 (A and B) and 24 weeks (C and D). Scale bars equal 2000 μ m. Embedded image sections represent 10x magnifications of indicated areas of the pancreata. ac=acini, is=islet of Langerhans, du=duct, bv=blood vessel, adm=acinar-to-ductal metaplasia (including PanIN lesions), dys=dysplasia.

(E-F) Quantification of the percentage of intact (i.e. not meta- or dysplastic) pancreatic tissue of male (left) and female (right) 12 (E) and 24 weeks-old (F) $Kras^{G12D/+}$ and $Kras^{G12D/+};Sod2^{\Delta Panc/\Delta Panc}$ mice in relation to total tissue area.

(G) Quantification and grading of preneoplastic lesions (ADMs, PanINs, and cysts) in male (left) and female (right) 12 weeks-old $Kras^{G12D/+}$ and $Kras^{G12D/+};Sod2^{\Delta Panc/\Delta Panc}$ mouse pancreata in relation to total tissue area in mm^2 .

Data in (E-G) are expressed as means \pm SD ($n \geq 3$); statistical analysis was performed using unpaired, two-tailed Student's *t*-test.

Analyzing histomorphology, integrity of $Kras^{G12D/+};Sod2^{\Delta Panc/\Delta Panc}$ pancreata seemed slightly reduced (statistically significant only in 12 weeks-old males) compared with the $Kras^{G12D/+}$ pancreata (Figure IV.10A-F). In addition, there were slightly more preneoplastic lesions in the $Kras^{G12D/+};Sod2^{\Delta Panc/\Delta Panc}$ than in the $Kras^{G12D/+}$ pancreata (Figure IV.10G).

Moreover, *Sod2* deletion might have slightly increased collagen deposition in male $Kras^{G12D/+};Sod2^{\Delta Panc/\Delta Panc}$ pancreata (Figure IV.11).

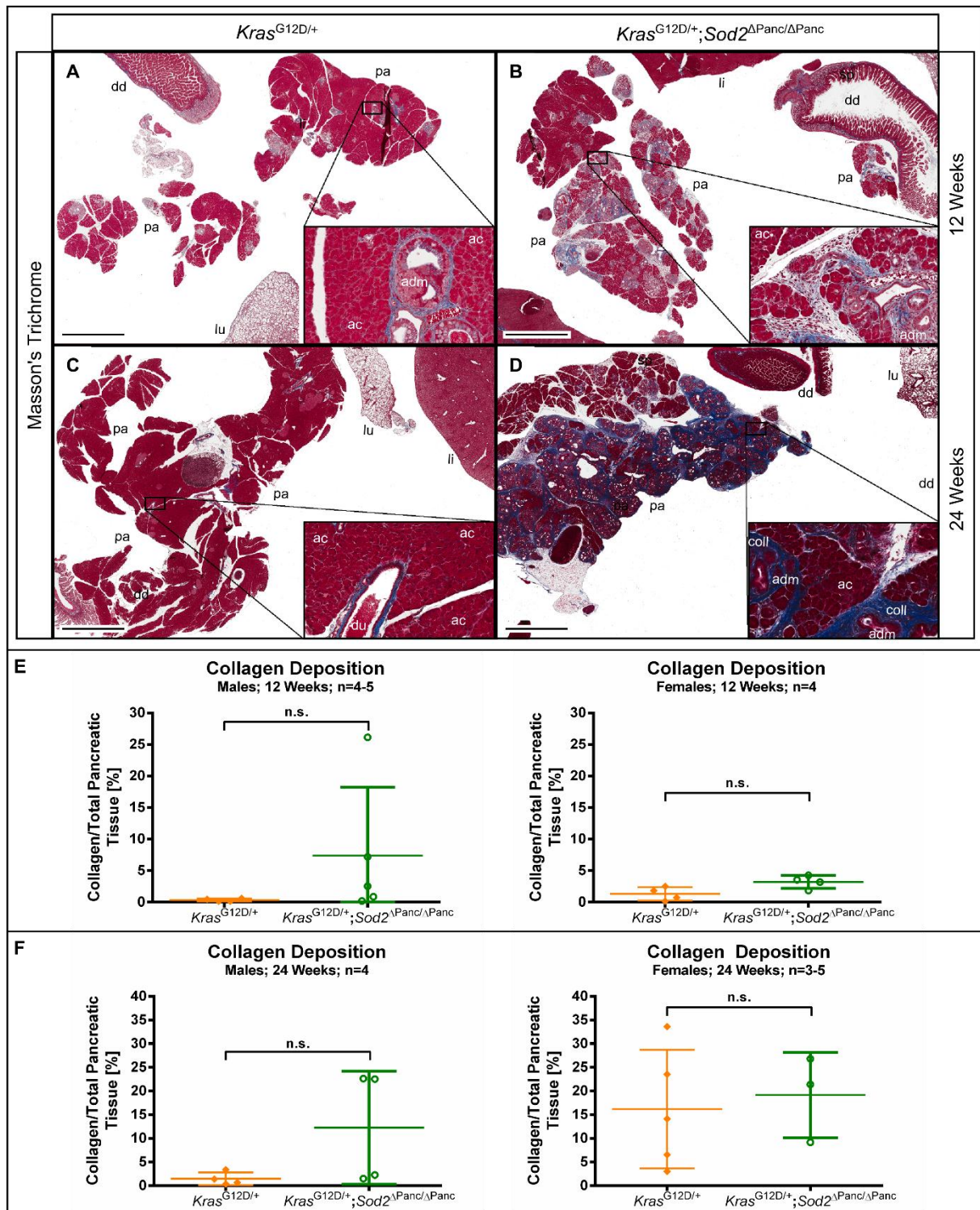


Figure IV.11: Male $Kras^{G12D/+}; Sod2^{\Delta Panc/\Delta Panc}$ deposit slightly, but not significantly more collagen than male $Kras^{G12D/+}$ pancreata.

(A-D) Representative Masson's Trichrome stainings of $Kras^{G12D/+}$ (A and C) and $Kras^{G12D/+}; Sod2$ knockout (B and D) pancreata (pa) and control tissues (duodenum (dd), liver (li), lung (lu), spleen (sp), and lymph node (ln)) at 12 (A and B) and 24 weeks (C and D). Scale bars equal 2000 μm . Embedded image sections represent 10x magnifications of indicated areas of the pancreata, du=duct, adm=acinar-to-ductal metaplasia (including PanIN lesions), coll=collagen.

(E-F) Quantification of the percentage of collagen deposition in pancreatic tissue of male (left) and female (right) 12 (E) and 24 weeks-old (F) $Kras^{G12D/+}$ and $Kras^{G12D/+}; Sod2^{\Delta Panc/\Delta Panc}$ mice in relation to total tissue. Analysis of slides was done by Dr. Henrik Einwächter. Data are expressed as means \pm SD ($n \geq 3$); statistical analysis was performed using unpaired, two-tailed Student's *t*-test.

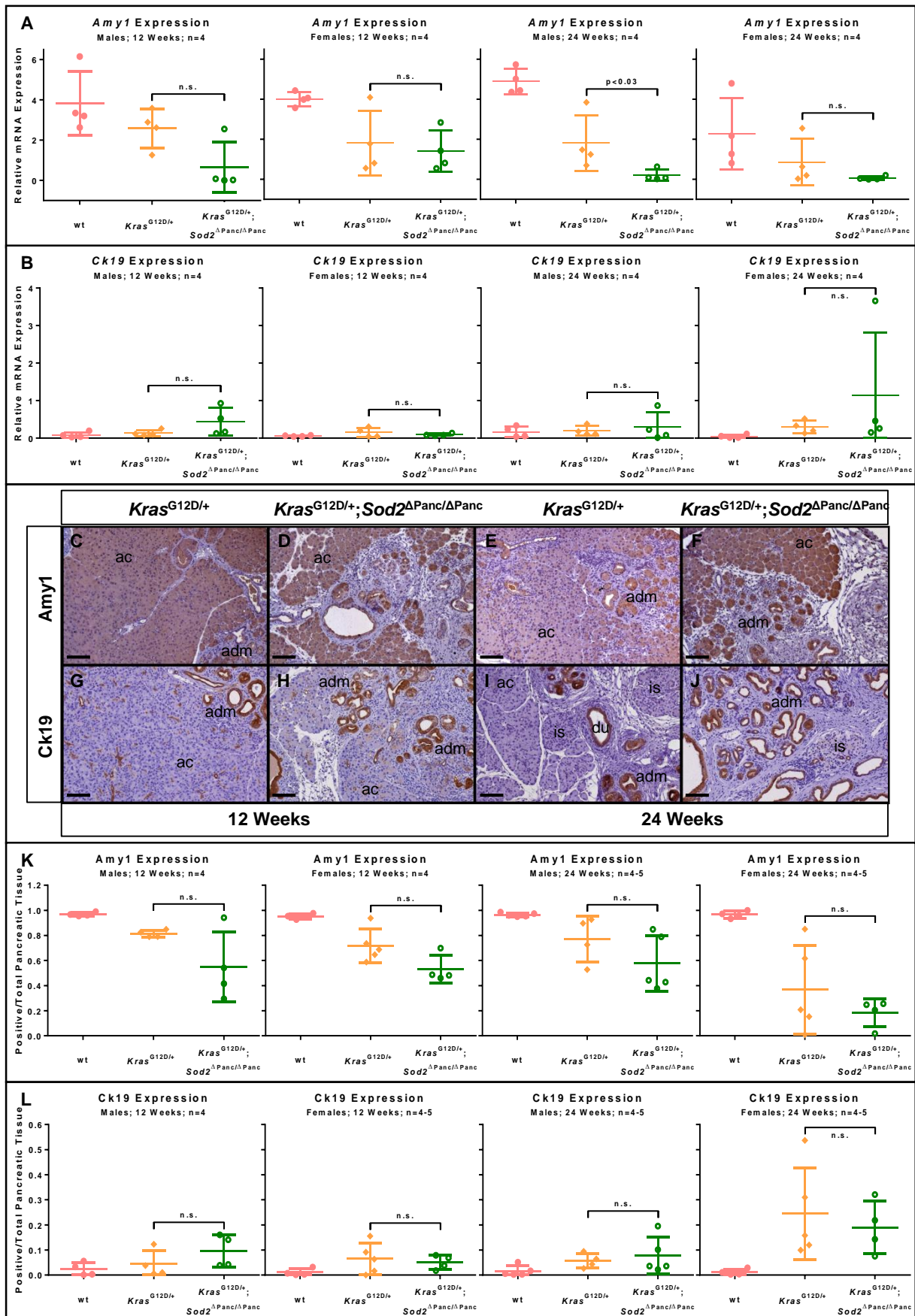


Figure IV.12: *Kras*^{G12D/+}; *Sod2*^{ΔPanc/ΔPanc} might express less *Amy1* and more *Ck19* than *Kras*^{G12D/+} pancreata.

Figure IV.12: *Kras*^{G12D/+};*Sod2*^{ΔPanc/ΔPanc} might express less *Amy1* and more *Ck19* than *Kras*^{G12D/+} pancreata - continued.

(A-B) Relative expression of *Amy1* (A) and *Ck19* (B) mRNA in whole pancreas lysates of 12 and 24 weeks-old *Kras*^{G12D/+} and *Kras*^{G12D/+};*Sod2*^{ΔPanc/ΔPanc} mice determined by RT-PCR. Data are normalized to *Cypa* mRNA expression.

(C-J) Representative *Amy1* (C-F) and *Ck19* (G-J) immunohistochemistry stainings of pancreata of 12 (C-D and G-H) and 24 weeks-old (E-F and I-J) *Kras*^{G12D/+} (C, E, G, I) and *Kras*^{G12D/+};*Sod2*^{ΔPanc/ΔPanc} (D, F, H, J) mice. Scale bars equal 100 μm. ac=acini, is=islet of Langerhans, adm=acinar-to-ductal metaplasia (including PanIN lesions).

(K-L) Quantification of positive *Amy1* (K) and *Ck19* (L) immunohistochemistry in relation to total pancreatic tissue of 12 and 24 weeks-old male and female *Kras*^{G12D/+} and *Kras*^{G12D/+};*Sod2*^{ΔPanc/ΔPanc} mice.

In (A-B) and (K-L), data are expressed as means ± SD (n≥3) and statistical analysis was performed using unpaired, two-tailed Student's *t*-test.

To investigate ADM, one of the key initiatory events in PDAC development, expression of an acinar (*Amy1*) and a ductal marker (*Ck19*) was assessed on the level of RNA (RT-PCR) and protein (immunohistochemistry). Although significant difference was only seen in one instance, there was a tendency towards lower expression of the acinar and a higher expression of the ductal marker in the *Kras*^{G12D/+};*Sod2*^{ΔPanc/ΔPanc} than in the *Kras*^{G12D/+} pancreata (Figure IV.12) indicating an increased rate of ADM.

For a further investigation of a possible role of *Sod2* in ADM, primary acinar cells were isolated from *Kras*^{G12D/+};*Sod2*^{ΔPanc/ΔPanc} and *Kras*^{G12D/+} mice, submitted to 3D culture in collagen gels and analyzed for *in vitro* ADM.

Notably, *Kras*^{G12D/+};*Sod2*^{ΔPanc/ΔPanc} primary acinar explants transdifferentiated significantly faster than *Kras*^{G12D/+} counterparts (Figure IV.13).

The next set of experiments aimed to determine whether oxidative stress could account for the phenotypic differences between the *Kras*^{G12D/+};*Sod2*^{ΔPanc/ΔPanc} and the *Kras*^{G12D/+} mice (prolonged tumor latency in females and accelerated ADM). Therefore, pancreata were analyzed for mitochondrial DNA damage (Figure IV.14A-B) and PDAC cell lines for Carboxy-H₂DCFDA (Figure IV.14C) and MitoSOX (Figure IV.14D) reactivity.

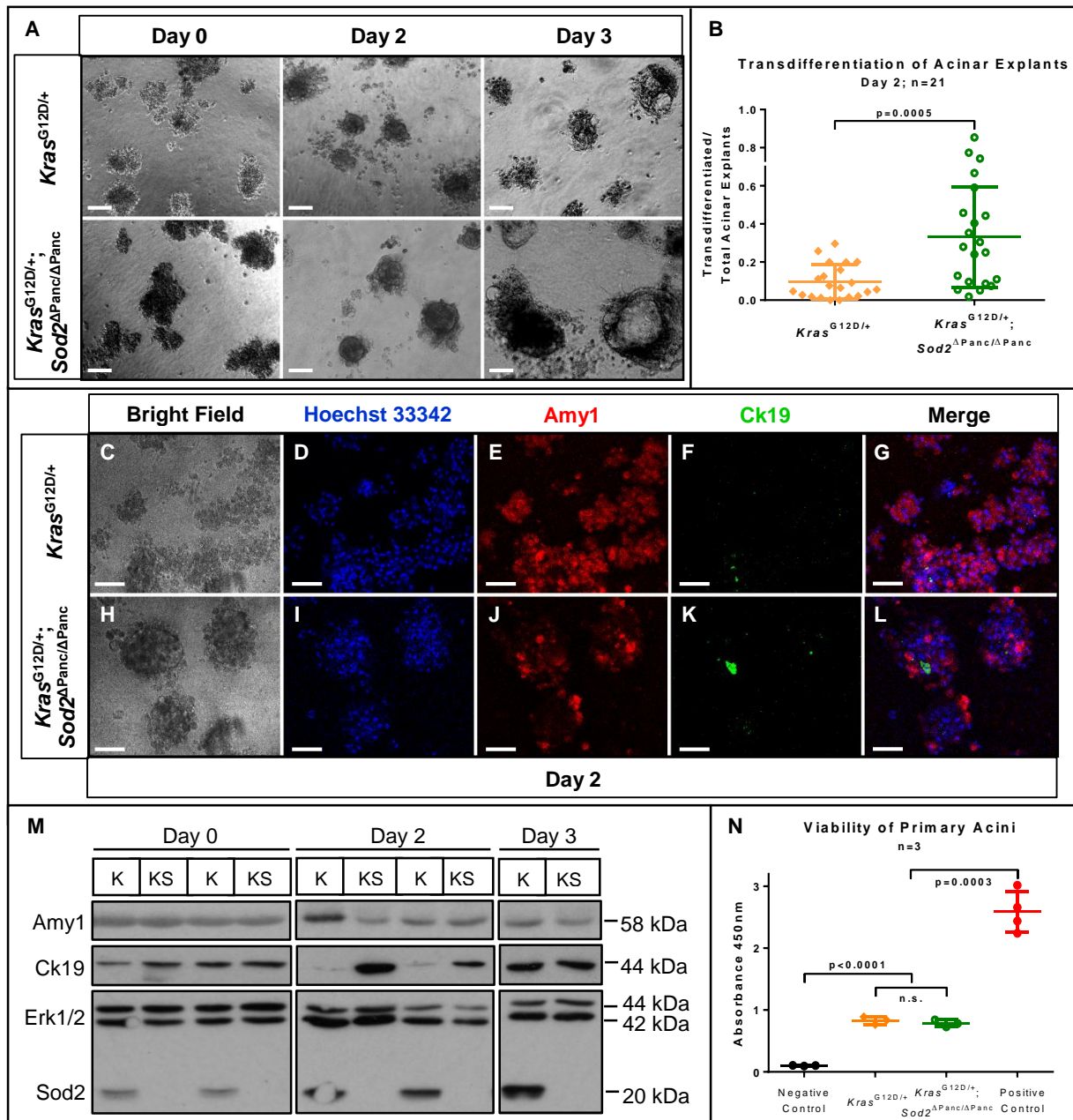


Figure IV.13: *Kras*^{G12D/+}; *Sod2*^{ΔPanc/ΔPanc} acinar explant transdifferentiate faster than *Kras*^{G12D/+} acinar explants.

(A) Representative images of acinar explants of *Kras*^{G12D/+} and *Kras*^{G12D/+}; *Sod2*^{ΔPanc/ΔPanc} mice at day 0 (=day of isolation), and day 2 and 3 after isolation. Scale bars equal 100 μ m.

(B) Quantification of transdifferentiated in relation to total number of acinar explants of *Kras*^{G12D/+} and *Kras*^{G12D/+}; *Sod2*^{ΔPanc/ΔPanc} mice. Acinar explants were prepared from two mice per genotype and seeded into 10-11 wells of 48 well plates per mouse. For each well, at least three high power fields of vision were counted on day 2 after isolation.

(C-L) Representative immunofluorescence stainings for Amy1 (E, J) and Ck19 (F, K) in acinar explants of *Kras*^{G12D/+} and *Kras*^{G12D/+}; *Sod2*^{ΔPanc/ΔPanc} mice at day 2 after isolation. Nuclei are visualized using Hoechst 33342 stain (D, I), all fluorescence channels are merged in (G) and (L); respective bright field images are given in (C) and (H). Scale bars equal 60 μ m.

(M) Immunoblot analysis of Amy1, Ck19, and Sod2 in lysates of acinar explants from *Kras*^{G12D/+} (K) and *Kras*^{G12D/+}; *Sod2*^{ΔPanc/ΔPanc} (KS) mice at day 0, 2 and 3 after isolation. Erk1/2 and Sod2 detection served as loading control or for genotype verification, respectively.

(N) Viability of acinar explants of *Kras*^{G12D/+} and *Kras*^{G12D/+}; *Sod2*^{ΔPanc/ΔPanc} mice determined by LDH assay of medium supernatants at day 2 after isolation. negative control=culture medium, positive control=acinar cell lysates.

In (B) and (N), data are expressed as means \pm SD (n \geq 3) and statistical analysis was performed using unpaired, two-tailed Student's *t*-test.

Determined by Carboxy-H₂DCFDA and MitoSOX, ROS were slightly increased comparing two *Kras*^{G12D/+}; *Sod2*^{ΔPanc/ΔPanc} with two *Kras*^{G12D/+} PDAC cell lines, while a third *Kras*^{G12D/+} PDAC cell line had comparable ROS marker fluorescence levels as the two *Kras*^{G12D/+}; *Sod2*^{ΔPanc/ΔPanc} cell lines (Figure IV.14C-D).

As for the *Kras*-wt animals, there was no increase in mitochondrial DNA damage and no difference in mitochondrial copy number in the *Kras*^{G12D/+}; *Sod2*^{ΔPanc/ΔPanc} compared with the *Kras*^{G12D/+} pancreata or PDAC cell lines (Figure IV.14A-B).

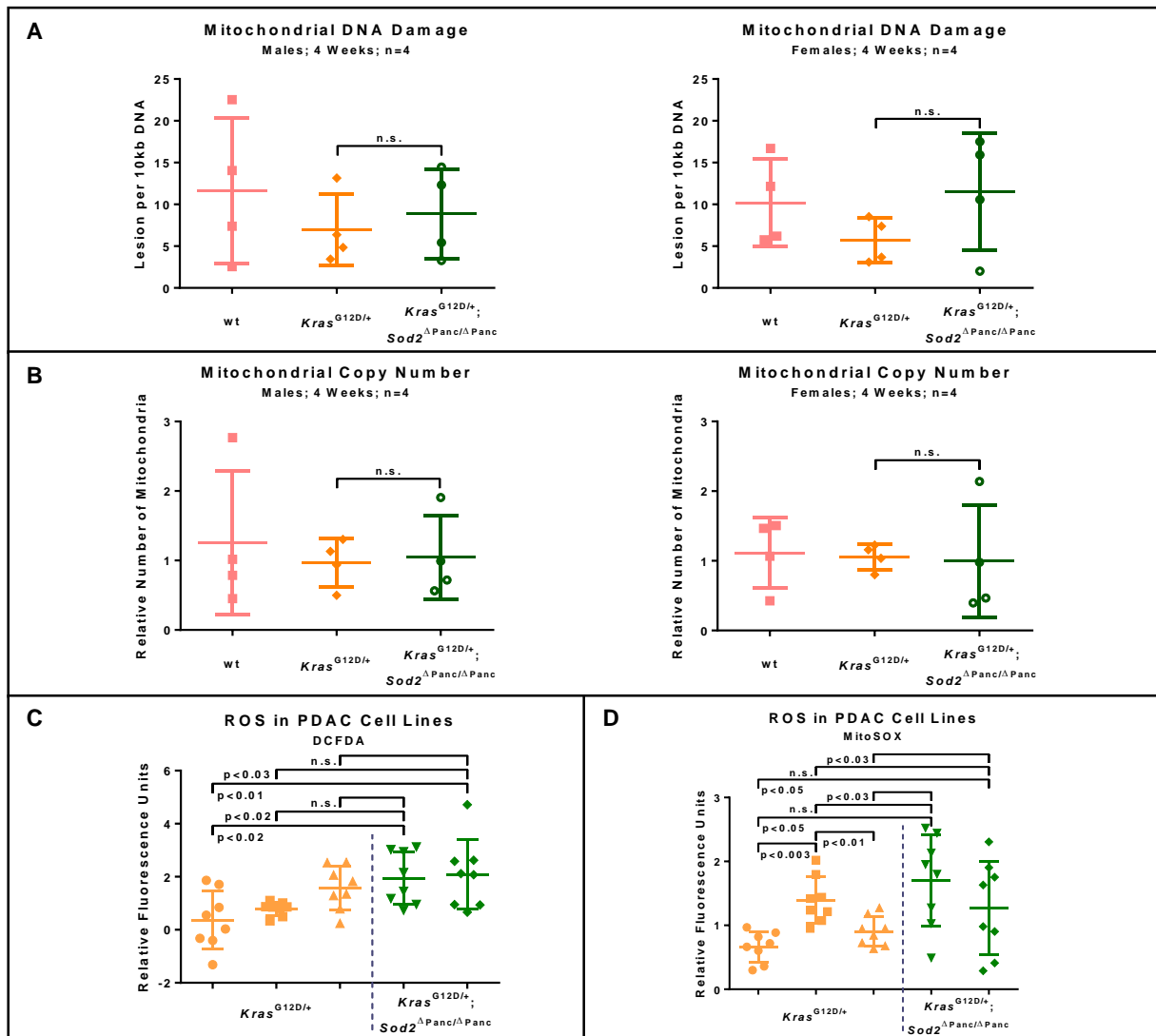


Figure IV.14: Concomitant *Sod2* knockout slightly increases ROS in *Kras*^{G12D/+} pancreata.

(A) Mitochondrial DNA damage analysis in whole pancreas lysates of 4 weeks-old male (left) and female (right) wt, *Kras*^{G12D/+}, and *Kras*^{G12D/+}; *Sod2*^{ΔPanc/ΔPanc} mice determined by qPCR-DNA damage assay.

(B) Mitochondrial copy number in whole pancreas lysates of 4 weeks-old male (left) and female (right) wt, *Kras*^{G12D/+}, and *Kras*^{G12D/+}; *Sod2*^{ΔPanc/ΔPanc} mice determined as control for qPCR-DNA damage assay.

(C) Relative Carboxy-H₂DCFDA reactivity of *Kras*^{G12D/+} and *Kras*^{G12D/+}; *Sod2*^{ΔPanc/ΔPanc} PDAC cell lines.

(D) Relative MitoSOX reactivity of *Kras*^{G12D/+} and *Kras*^{G12D/+}; *Sod2*^{ΔPanc/ΔPanc} PDAC cell lines. In (C-D), each bar represents one cell line. Cell lines of the same genotypes were plotted in one color. Numbers of cell lines were: *Kras*^{G12D/+}: 3, *Kras*^{G12D/+}; *Sod2*^{ΔPanc/ΔPanc}: 2. Data were obtained in 8 independent experiments.

In (A-D), data are expressed as means ± SD (n≥4); statistical analysis was performed using unpaired, two-tailed Student's *t*-test.

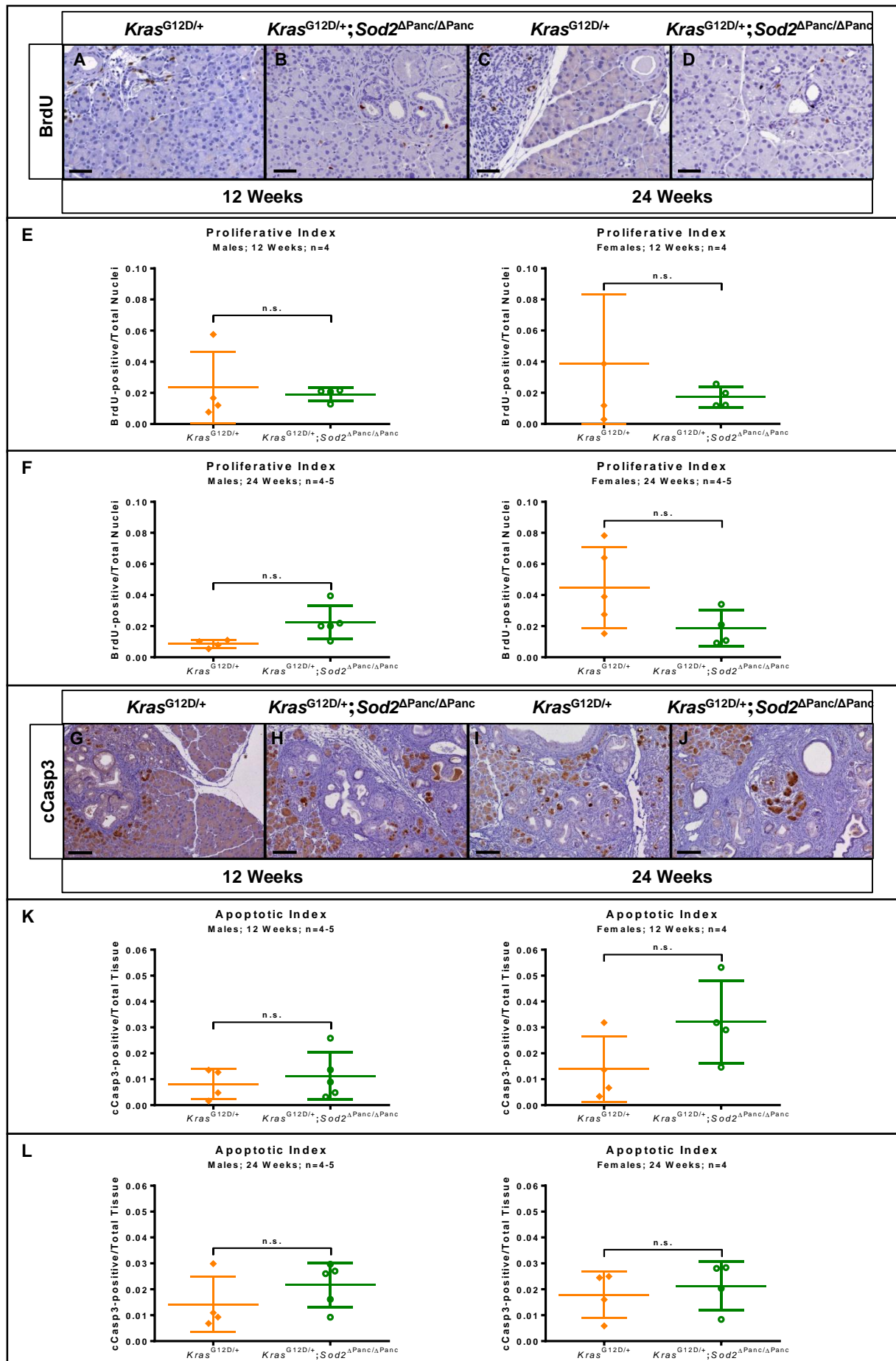


Figure IV.15: *Sod2* knockout might reduce proliferation and increase apoptosis in *Kras*^{G12D/+} pancreata.

Figure IV.15: *Sod2* knockout might reduce proliferation and increase apoptosis in *Kras*^{G12D/+} pancreata - continued.

(A-D) Representative BrdU immunohistochemistry stainings of 12 (A and B) and 24 weeks-old (C and D) *Kras*^{G12D/+} (A and C) and *Kras*^{G12D/+}; *Sod2* knockout (B and D) pancreata. Scale bars equal 50 μ m.

(E-F) Quantification of BrdU incorporation in pancreata of 12 (E) and 24 weeks-old (F) male (left) and female (right) *Kras*^{G12D/+} and *Kras*^{G12D/+}; *Sod2* ^{Δ Panc/ Δ Panc} mice.

(G-J) Representative cleaved Casp3 (cCasp3) immunohistochemistry stainings of pancreata of 12 (G and H) and 24 weeks-old (I and J) *Kras*^{G12D/+} (G and I) and *Kras*^{G12D/+}; *Sod2* ^{Δ Panc/ Δ Panc} (H and J) mice. Scale bars equal 25 μ m.

(K-L) Quantification of cCasp3 immunohistochemistry in pancreata of 12 (K) and 24 weeks-old (L) male (left) and female (right) *Kras*^{G12D/+} and *Kras*^{G12D/+}; *Sod2* ^{Δ Panc/ Δ Panc} mice.

In (E-F) and (K-L), data are expressed as means \pm SD ($n \geq 3$) and statistical analysis was performed using unpaired, two-tailed Student's *t*-test.

To investigate whether *Sod2* deletion with concomitant *Kras* activation affects cell fate, proliferation and apoptosis was assessed in the *Kras*^{G12D/+}; *Sod2* ^{Δ Panc/ Δ Panc} and the *Kras*^{G12D/+} pancreata. Although neither proliferation nor apoptosis significantly differed between the two genotypes, there was a trend towards reduced proliferation and increased apoptosis for the *Kras*^{G12D/+}; *Sod2* ^{Δ Panc/ Δ Panc} over the *Kras*^{G12D/+} pancreata (Figure IV.15A-L).

As ROS may affect Ras signaling and Ras-dependent carcinogenesis, potentially via p38 [57], we next investigated Ras and p38 activation in *Kras*^{G12D/+}; *Sod2* ^{Δ Panc/ Δ Panc} and *Kras*^{G12D/+} pancreata. While Ras signaling was slightly, but not significantly reduced in the *Kras*^{G12D/+}; *Sod2* ^{Δ Panc/ Δ Panc} compared with the *Kras*^{G12D/+} pancreata (Figure IV.16A-B), there was virtually no difference in p38 activity between the genotypes (Figure IV.16C-D).

The possibility that *Sod2* deletion might reduce Ras signaling in the *Kras*^{G12D/+} background was further investigated by analyzing mRNA expression of the direct *Kras* target B-Raf proto-oncogene, serine/threonine kinase (*Braf*, [496]). However, *Braf* expression was not altered in male, and might even be increased in female *Kras*^{G12D/+}; *Sod2* ^{Δ Panc/ Δ Panc} compared with the *Kras*^{G12D/+} pancreata (Figure IV.16E).

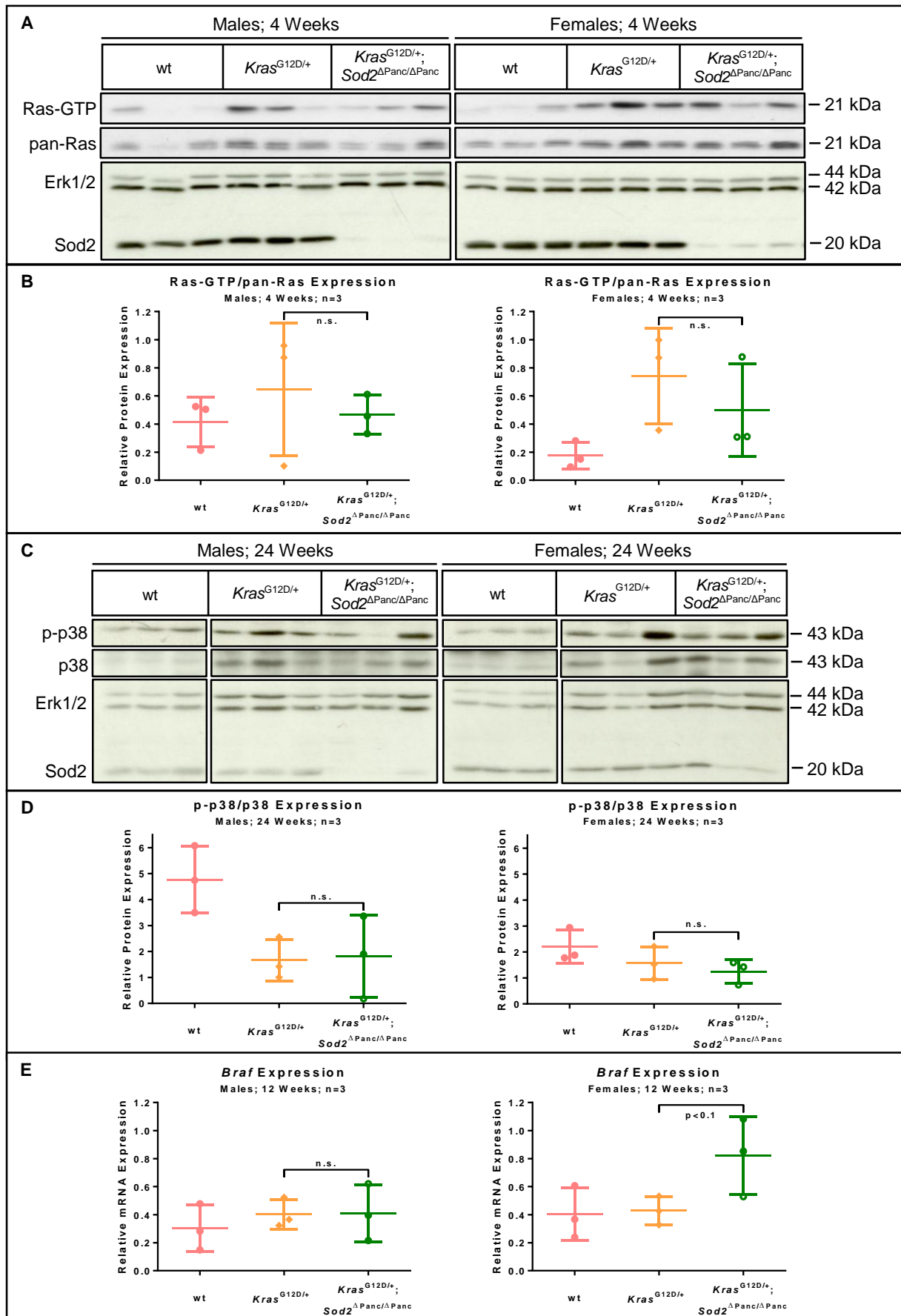


Figure IV. 16: *Sod2* knockout might reduce Ras activity in *Kras*^{G12D/+} mice.

Figure IV.16: Sod2 knockout might reduce Ras activity in *Kras*^{G12D/+} mice - continued.

(A) Ras activation analysis in whole pancreas lysates of 4 weeks-old male (left) and female (right) *Kras*^{G12D/+} and *Kras*^{G12D/+};*Sod2*^{ΔPanc/ΔPanc} mice. Immunoblot detection with an anti-Ras antibody recognizing H-, K-, and Nras was performed after pull-down with Raf-1 RBD agarose conjugate for Ras-GTP (=active Ras) and with crude lysates for pan-Ras detection. Erk1/2 and Sod2 detection serves as loading control or for genotype verification, respectively.

(B) Quantification of Ras activation by densitometry of the Ras-GTP in relation to the pan-Ras signal in immunoblots (A).

(C) Immunoblot detection of p38 and phospho-p38 (Thr180/Tyr182; p-p38) in whole pancreas lysates of 24 weeks-old male (left) and female (right) *Kras*^{G12D/+} and *Kras*^{G12D/+};*Sod2*^{ΔPanc/ΔPanc} mice. Erk1/2 and Sod2 detection serves as loading control or for genotype verification, respectively.

(D) Quantification of p38 activation by densitometry of the p-p38 in relation to the p38 signal in immunoblots (C).

(E) Relative expression of *B-Raf proto-oncogene, serine/threonine kinase (Braf)* mRNA in whole pancreas lysates of 12 weeks-old male (left) and female (right) *Kras*^{G12D/+} and *Kras*^{G12D/+};*Sod2*^{ΔPanc/ΔPanc} mice determined by RT-PCR. Data were normalized to *Cypa* mRNA expression.

In (B) and (D-E), data are expressed as means ± SD (n=3) and statistical analysis was performed using unpaired, two-tailed Student's *t*-test.

As shown earlier, pancreas-specific *Sod2* deletion might confer a gender-specific increase in tumor latency to the female, but not the male *Kras*^{G12D/+} mice (Figure IV.9C-D). Differential sex hormone signaling might be involved in mediating this benefit. To test this hypothesis, I next thoroughly investigated estrogen receptor signaling. While *Esr1* mRNA expression might be reduced in 4 and 12 weeks-old male and female *Kras*^{G12D/+};*Sod2*^{ΔPanc/ΔPanc} compared with the *Kras*^{G12D/+} pancreata (Figure IV.17aA-B), no difference could be detected in 24 weeks-old male and female mice (Figure IV.17aC). Notably, protein expression of *Esr1* was markedly decreased in all *Kras*^{G12D/+};*Sod2*^{ΔPanc/ΔPanc} compared with the *Kras*^{G12D/+} pancreata (Figure IV.17aE-F). In immunohistochemistry, *Esr1* expression seemed to shift from cytosolic expression in intact acinar cells to nuclear expression in precancerous lesions in male and female mice of both genotypes (Figure IV.17aD).

No obvious differences in expression of *Esr2* expression could be detected on the level of RNA and protein (Figure IV.17aG-I).

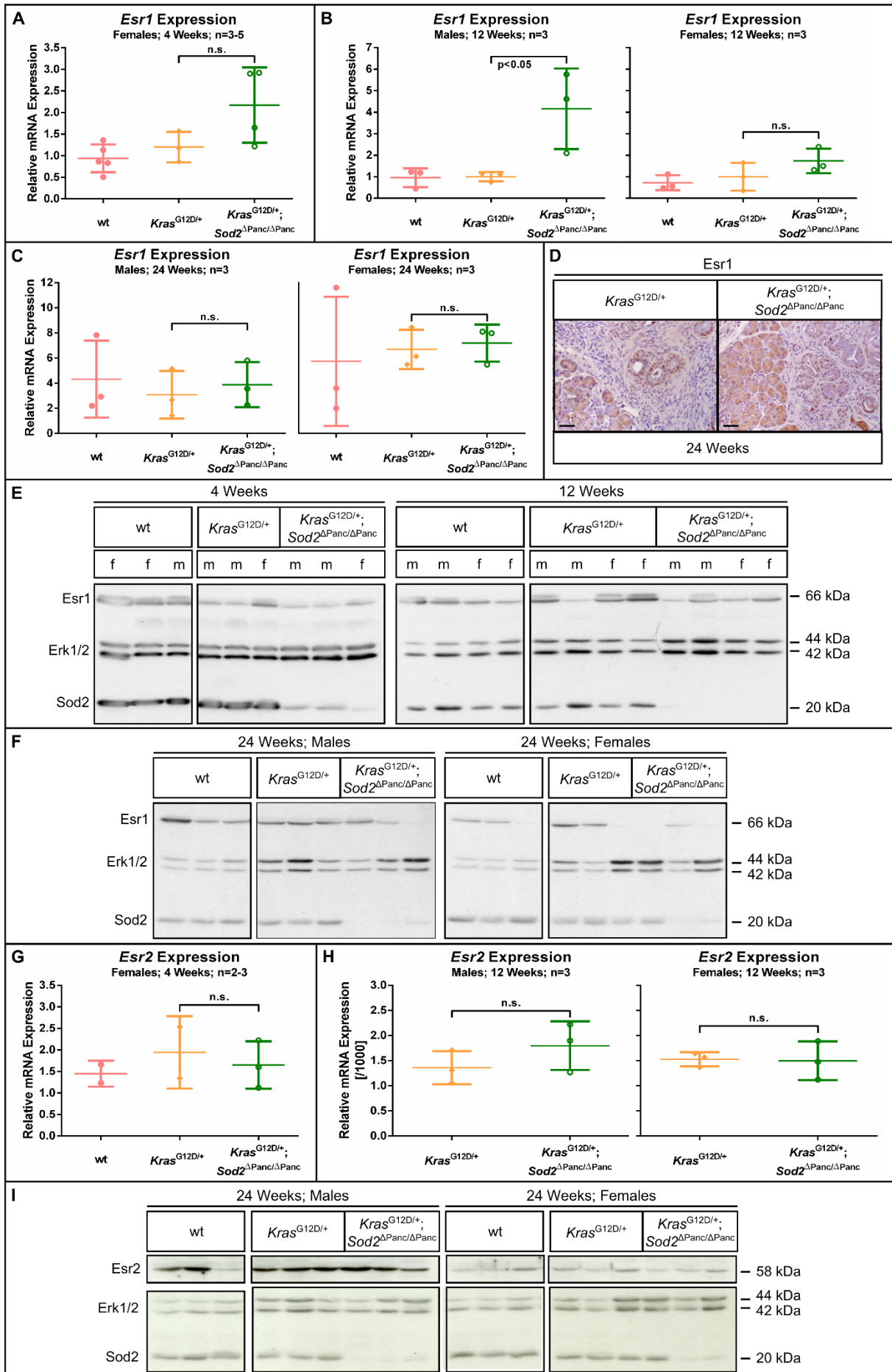

 Figure IV.17a: *Esr1*, but not *Esr2* signaling might be altered by *Sod2* knockout in *Kras*^{G12D/+} mice.

Figure IV.17a: *Esr1*, but not *Esr2* signaling might be altered by *Sod2* knockout in *Kras*^{G12D/+} mice - continued.

(A) Relative mRNA expression of *Esr1* in whole pancreas lysates of 4 weeks-old female wt, *Kras*^{G12D/+}, and *Kras*^{G12D/+};*Sod2*^{ΔPanc/ΔPanc} mice determined by RT-PCR.

(B-C) Relative mRNA expression of *Esr1* in whole pancreas lysates of 12 (B) and 24 weeks-old (C) male (left) and female (right) wt, *Kras*^{G12D/+}, and *Kras*^{G12D/+};*Sod2*^{ΔPanc/ΔPanc} mice determined by RT-PCR.

(D) Representative *Esr1* immunohistochemistry stainings of 24 weeks-old *Kras*^{G12D/+} (left) and *Kras*^{G12D/+};*Sod2* knockout (right) pancreata. Scale bars equal 20 μm. (E-F) Immunoblot detection of *Esr1* in whole pancreas lysates of 4, 12 (E), and 24 weeks-old (F) male and female wt, *Kras*^{G12D/+}, and *Kras*^{G12D/+};*Sod2*^{ΔPanc/ΔPanc} mice. Erk1/2 and *Sod2* detection serves as loading control or for genotype verification, respectively.

(G) Relative mRNA expression of *Esr2* in whole pancreas lysates of 4 weeks-old female wt, *Kras*^{G12D/+}, and *Kras*^{G12D/+};*Sod2*^{ΔPanc/ΔPanc} mice determined by RT-PCR.

(H) Relative mRNA expression of *Esr2* in whole pancreas lysates of 12 weeks-old male (left) and female (right) wt, *Kras*^{G12D/+}, and *Kras*^{G12D/+};*Sod2*^{ΔPanc/ΔPanc} mice determined by RT-PCR.

(I) Immunoblot detection of *Esr2* in whole pancreas lysates of 24 weeks-old male (left) and female (right) wt, *Kras*^{G12D/+}, and *Kras*^{G12D/+};*Sod2*^{ΔPanc/ΔPanc} mice. Erk1/2 and *Sod2* detection serves as loading control or for genotype verification, respectively.

In (A-C) and (G-H), data are normalized to *Cypa* mRNA expression and expressed as means ± SD (n≥2). Statistical analysis was performed using unpaired, two-tailed Student's *t*-test.

To further investigate whether *Esr1* signaling could be involved in the prolonged tumor latency of female *Kras*^{G12D/+};*Sod2*^{ΔPanc/ΔPanc} mice, I determined mRNA expression levels of six postulated *Esr1* targets: *thymidylate synthase (Tyms)*, *adenosine deaminase (Ada)*, *retinoic acid receptor α (Rara)*, *cell division cycle 25A, p21 protein (Cdc42/Rac)-activated kinase 1 (Cdc25a)*, and *discoidin domain receptor tyrosine kinase 2 (Ddr2)*. Of these six targets, none were statistically significantly differentially regulated between *Kras*^{G12D/+};*Sod2*^{ΔPanc/ΔPanc} and *Kras*^{G12D/+} pancreata (Figure IV.17b).

Borderline significance was observed for *Tyms*, *Rara*, and *Cdc25a* in male (Figure IV.17bA, C, and E) as well as for *Ddr2* in female *Kras*^{G12D/+};*Sod2*^{ΔPanc/ΔPanc} (Figure IV.17bF) compared with male or female *Kras*^{G12D/+} mice, respectively.

Inactivation of tumor suppressor *TP53* occurs in 60 % of human pancreatic cancers and appears to be involved in the late stages of carcinogenesis [497]. To test whether sustained Trp53 signaling might increase tumor latency in female *Kras*^{G12D/+};*Sod2*^{ΔPanc/ΔPanc} mice, mRNA expression levels of six different Trp53 target genes were tested in the *Kras*^{G12D/+} and the *Kras*^{G12D/+};*Sod2*^{ΔPanc/ΔPanc} pancreata (Figure IV.18). Of these six targets, however, only *cyclin-dependent kinase inhibitor 1A (Cdkn1a)* was significantly downregulated in female *Kras*^{G12D/+};*Sod2*^{ΔPanc/ΔPanc} compared with female *Kras*^{G12D/+} pancreata (Figure IV.18B). For all other targets and genotypes, not even borderline significance was detected.

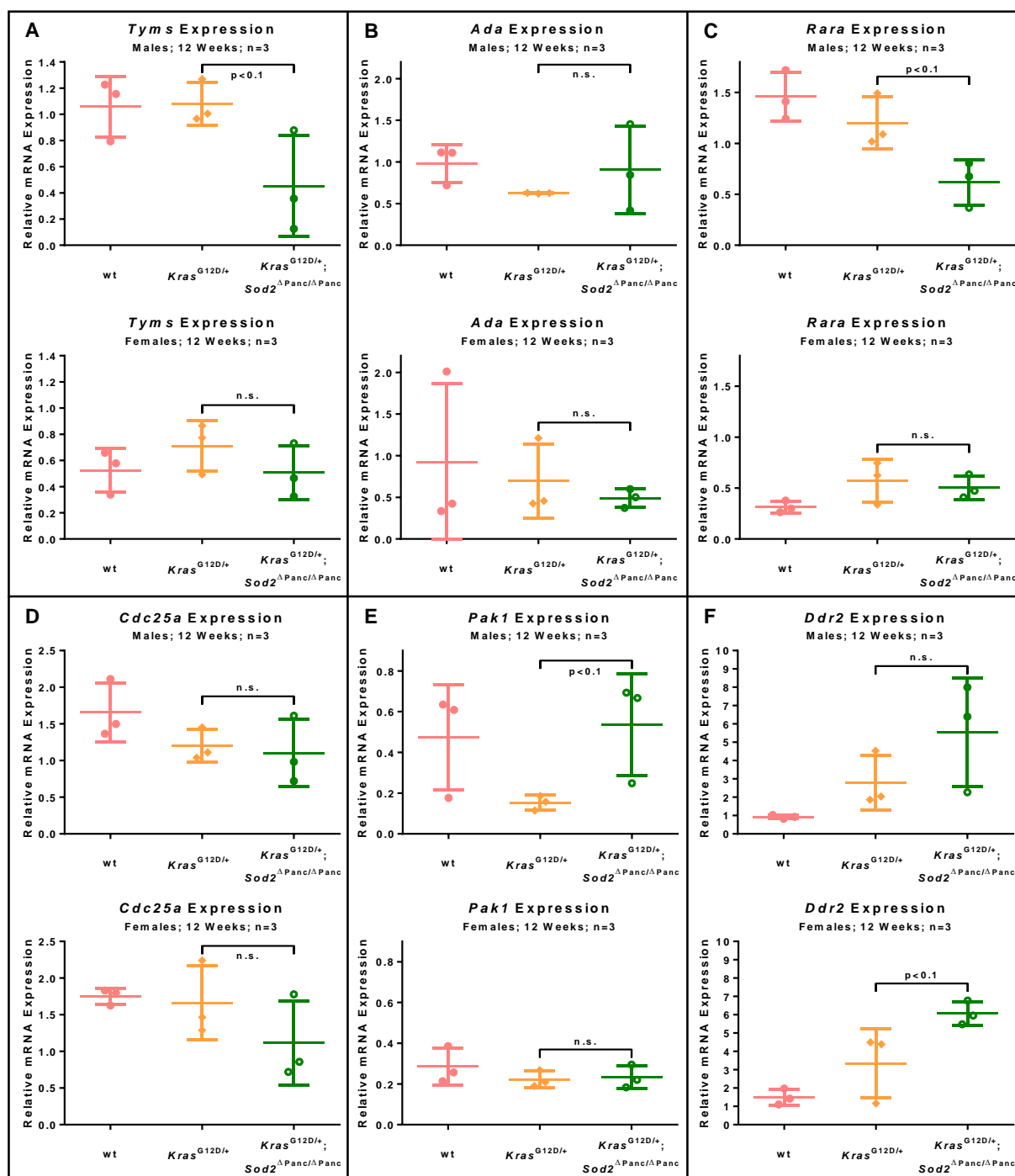


Figure IV.17b: Expression of several potential *Esr1* target genes is altered by *Sod2* knockout in *Kras*^{G12D/+} mice.

(A-F) Relative mRNA expression of potential *Esr1* target genes in whole pancreas lysates of 12 weeks-old male (top) and female (bottom) wt, *Kras*^{G12D/+}, and *Kras*^{G12D/+}; *Sod2*^{ΔPanc/ΔPanc} mice determined by RT-PCR. Potential target genes are taken from [498] or found through microarray analyses. See Table Appendix.1 for gene symbols and names.

Data are normalized to *Cypa* mRNA expression and expressed as means \pm SD (n=3). Statistical analysis was performed using unpaired, two-tailed Student's *t*-test.

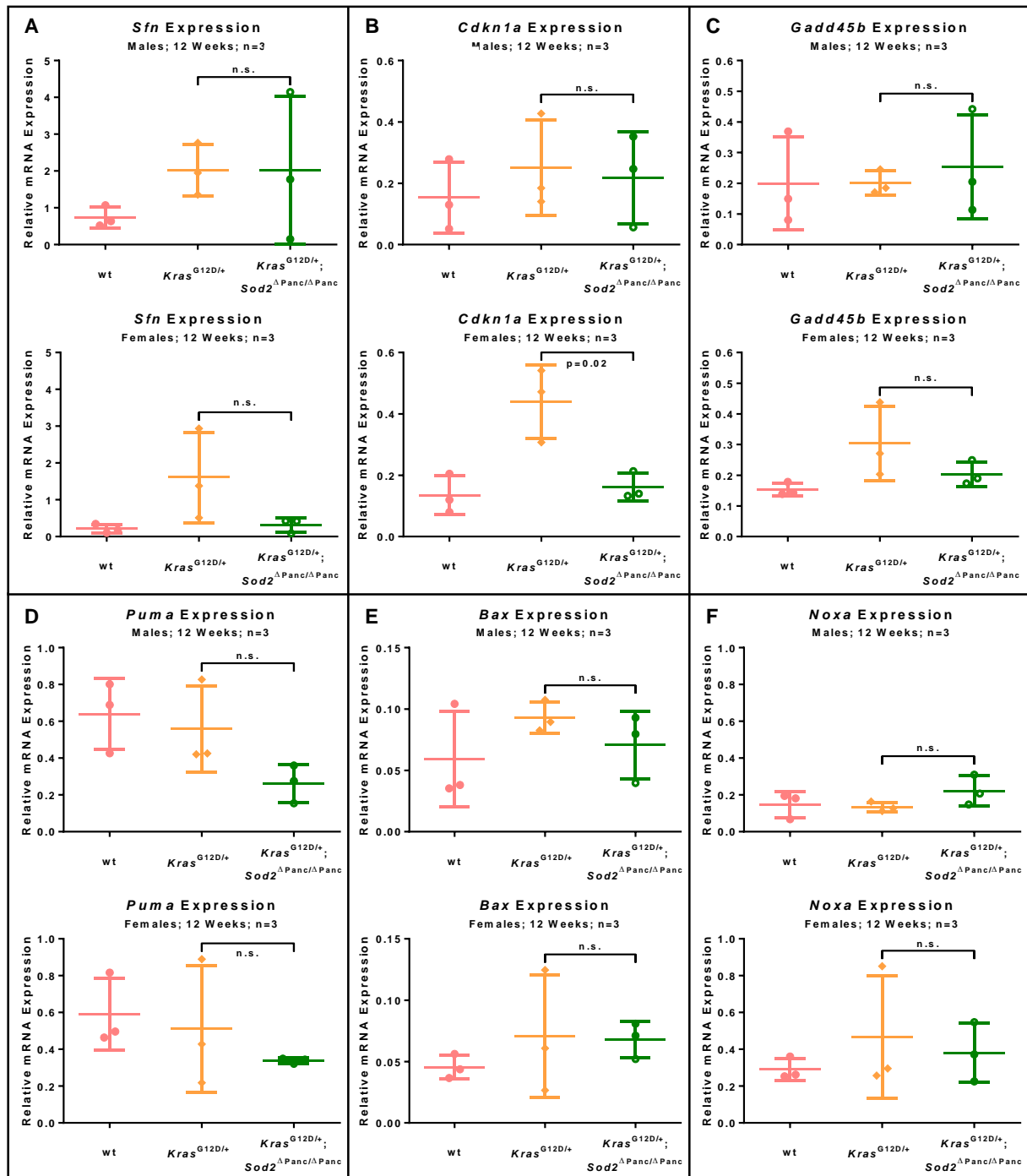


Figure IV.18: Trp53 target gene expression is probably unaffected by *Sod2* knockout in *Kras*^{G12D/+} mice.

(A-F) Relative mRNA expression of Trp53 target genes in whole pancreas lysates of 12 weeks-old male (top) and female (bottom) wt, *Kras*^{G12D/+}, and *Kras*^{G12D/+}; *Sod2*^{ΔPanc/ΔPanc} mice determined by RT-PCR. See Table Appendix.1 for gene symbols and names.

Data are normalized to *Cypa* mRNA expression and expressed as means ± SD (n=3). Statistical analysis was performed using unpaired, two-tailed Student's *t*-test.

2.2. Role of *Sod2* in *Trp53*^Δ;*Kras*^{G12D}-Mediated PDAC

To further elaborate on the role of *Sod2* in PDAC, the effects of *Sod2* deletion were also studied in a faster, more stringent PDAC mouse model combining pancreas-specific *Kras* activation with pancreas-specific *Trp53* deletion.

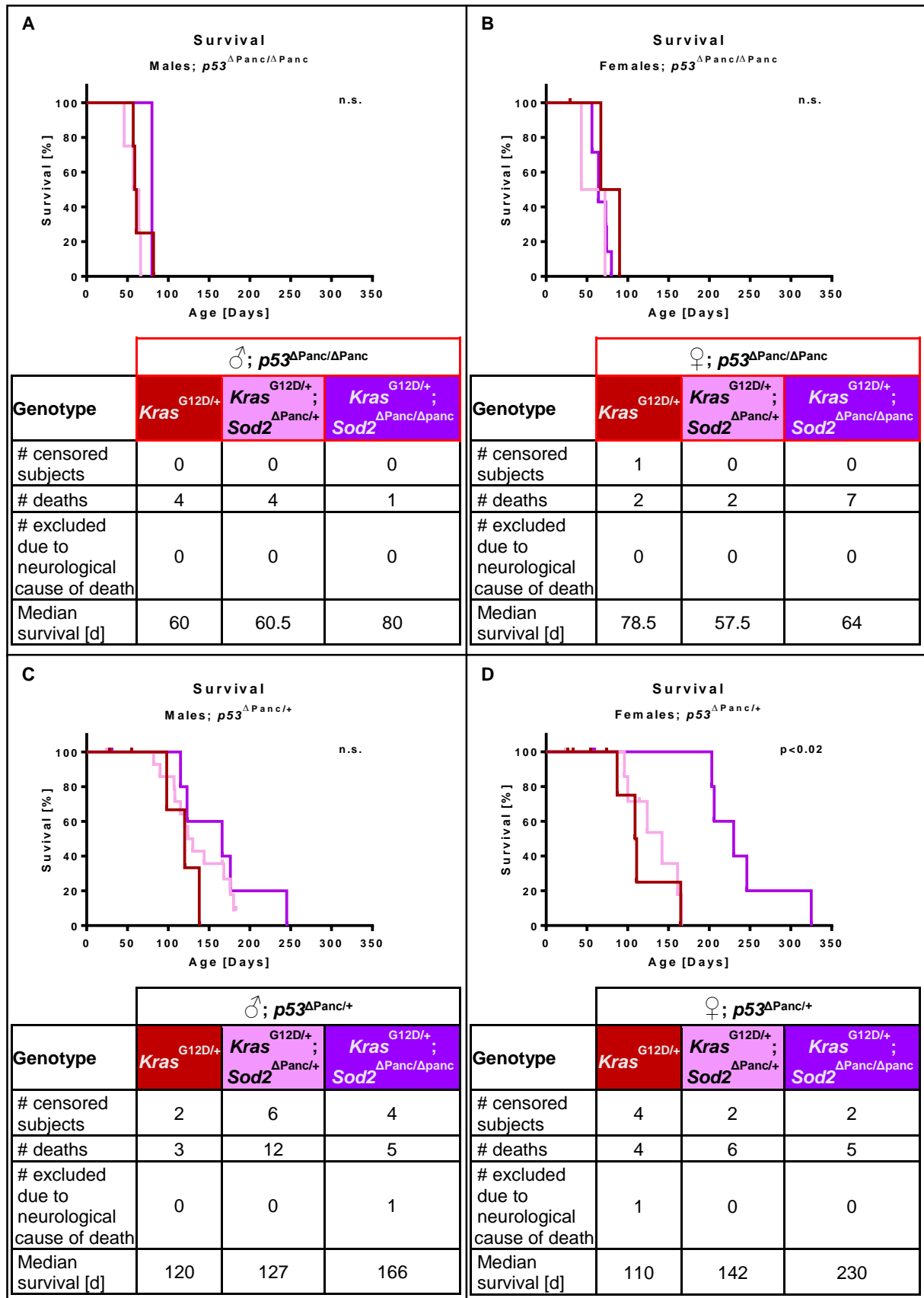


Figure IV.19: Pancreas-specific *Sod2* knockout significantly prolongs survival in female *p53*^{ΔPanc/+};*Kras*^{G12D/+}, but not *p53*^{ΔPanc/Panc};*Kras*^{G12D/+} mice.

Figure IV.19: Pancreas-specific *Sod2* knockout significantly prolongs survival in female $p53^{\Delta\text{Panc}/+};Kras^{G12D/+}$, but not $p53^{\Delta\text{Panc}/\text{Panc}};Kras^{G12D/+}$ mice - continued.

(A-B) Kaplan-Meier analysis of male (A) and female (B) $p53^{\Delta\text{Panc}/\Delta\text{Panc}};Kras^{G12D/+}$, $p53^{\Delta\text{Panc}/\Delta\text{Panc}};Kras^{G12D/+};Sod2^{\Delta\text{Panc}/+}$, and $p53^{\Delta\text{Panc}/\Delta\text{Panc}};Kras^{G12D/+};Sod2^{\Delta\text{Panc}/\Delta\text{Panc}}$ mice.

(C-D) Kaplan-Meier analysis of male (C) and female (D) $p53^{\Delta\text{Panc}/+};Kras^{G12D/+}$, $p53^{\Delta\text{Panc}/+};Kras^{G12D/+};Sod2^{\Delta\text{Panc}/+}$, and $p53^{\Delta\text{Panc}/+};Kras^{G12D/+};Sod2^{\Delta\text{Panc}/\Delta\text{Panc}}$ mice. Two deaths that might have occurred due to neurological symptoms were excluded from analysis. Statistical analysis was performed using log-rank (Mantel-Cox) test.

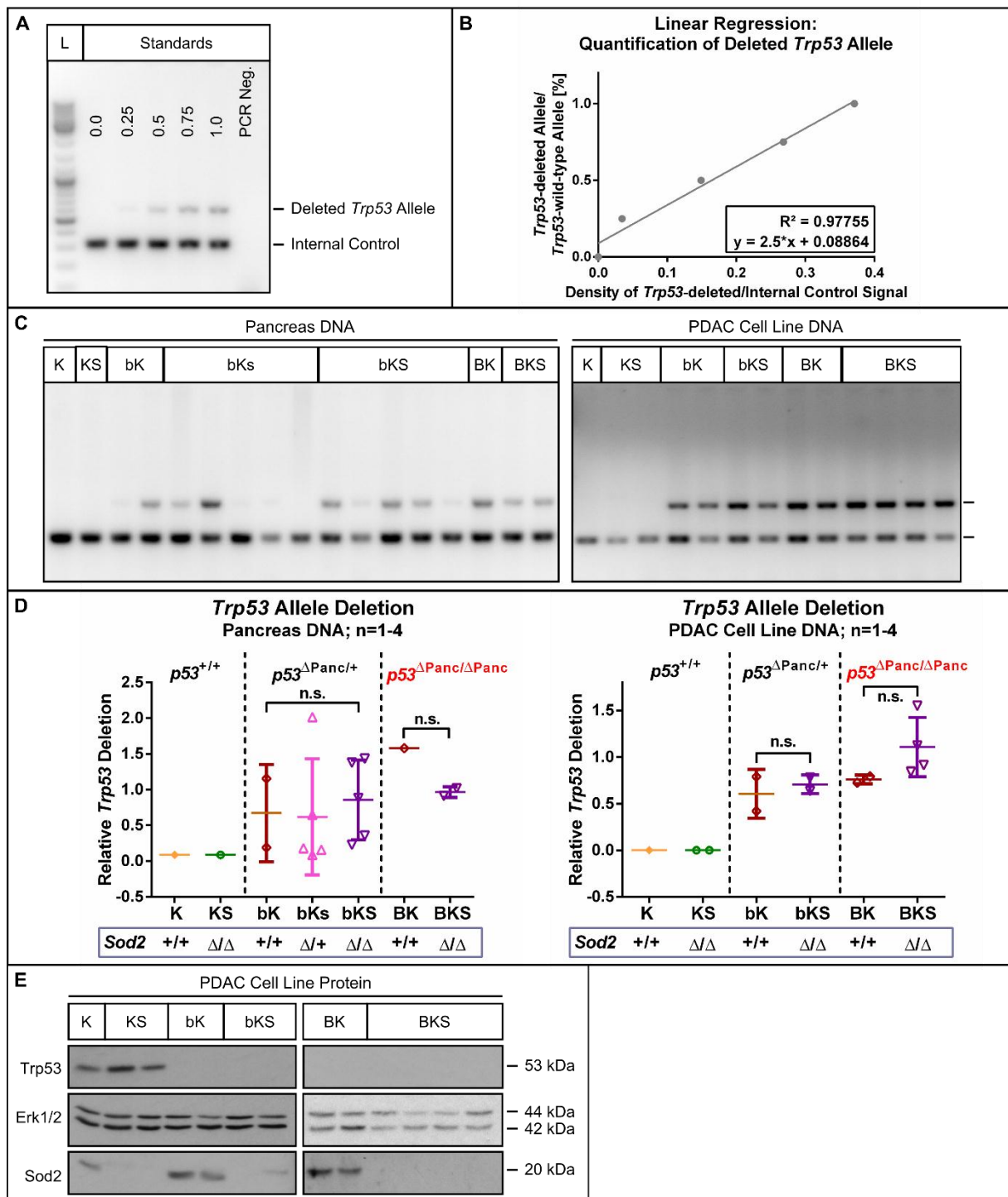


Figure IV.20: *Sod2* deletion does not prevent loss of the second *Trp53* allele in $p53^{\Delta\text{Panc}/+};Kras^{G12D/+}$ derived PDAC or PDAC cell lines.

Figure IV.20: *Sod2* deletion does not prevent loss of the second *Trp53* allele in $p53^{\Delta\text{Panc}/+};Kras^{G12D/+}$ derived PDAC or PDAC cell lines - continued.

(A) Agarose gel of a semi-quantitative PCR of a serial dilution of *Trp53*-wt with *Trp53*^{ΔΔ} DNA derived from pancreata of $Kras^{G12D/+}$, and $Kras^{G12D/+};Sod2^{\Delta\text{Panc}/\Delta\text{Panc}}$ or $p53^{\Delta\text{Panc}/\Delta\text{Panc}};Kras^{G12D/+}$ and $p53^{\Delta\text{Panc}/\Delta\text{Panc}};Kras^{G12D/+};Sod2^{\Delta\text{Panc}/\Delta\text{Panc}}$ mice, respectively. Numbers represent ratio of *Trp53*^{ΔΔ} to *Trp53*-wt DNA. The upper signals show amplicons of a primer set specific to the deleted *Trp53* allele, the lower ones, which are used as an internal PCR control, those of a primer set specific to the murine interleukin 2 locus. L=DNA ladder as marker.

(B) Linear regression of the signal ratios of the deleted *Trp53* allele to the internal control as determined by densitometry of the agarose gel (A) plotted against the respective ratio of *Trp53*^{ΔΔ} to *Trp53*-wt DNA. The regression equation is used for quantification in (D).

(C) Agarose gel of a semi-quantitative PCR of pancreas DNA (left) or PDAC cell line DNA (right) derived from $Kras^{G12D/+}$ (K), $Kras^{G12D/+};Sod2^{\Delta\text{Panc}/\Delta\text{Panc}}$ (KS), $p53^{\Delta\text{Panc}/+};Kras^{G12D/+}$ (bK), $p53^{\Delta\text{Panc}/+};Kras^{G12D/+};Sod2^{\Delta\text{Panc}/+}$ (bKs), $p53^{\Delta\text{Panc}/+};Kras^{G12D/+};Sod2^{\Delta\text{Panc}/\Delta\text{Panc}}$ (bKS), $p53^{\Delta\text{Panc}/\Delta\text{Panc}};Kras^{G12D/+}$ (BK), and $p53^{\Delta\text{Panc}/\Delta\text{Panc}};Kras^{G12D/+};Sod2^{\Delta\text{Panc}/\Delta\text{Panc}}$ (BKS) mice. Primer sets were the ones specified in (A). Each lane represents one animal/cell line.

(D) Quantification of the deleted *Trp53* allele by densitometry of agarose gels (C) and application of the regression equation determined in (B). Data are expressed as means ± SD (for n≥2) and statistical analysis was performed using unpaired, two-tailed Student's *t*-test.

(E) Immunoblot analysis of Trp53, Erk1/2 (loading control) and Sod2 in lysates of PDAC cell lines derived from $Kras^{G12D/+}$ (K), $Kras^{G12D/+};Sod2^{\Delta\text{Panc}/\Delta\text{Panc}}$ (KS), $p53^{\Delta\text{Panc}/+};Kras^{G12D/+}$ (bK), $p53^{\Delta\text{Panc}/+};Kras^{G12D/+};Sod2^{\Delta\text{Panc}/\Delta\text{Panc}}$ (bKS), $p53^{\Delta\text{Panc}/\Delta\text{Panc}};Kras^{G12D/+}$ (BK), and $p53^{\Delta\text{Panc}/\Delta\text{Panc}};Kras^{G12D/+};Sod2^{\Delta\text{Panc}/\Delta\text{Panc}}$ (BKS) mice. The Trp53 signal could not be detected in either the $p53^{\Delta\text{Panc}/+}$ or the $p53^{\Delta\text{Panc}/\Delta\text{Panc}}$ lysates. Each lane represents one cell line. Erk1/2 and Sod2 detection was performed as loading control or for genotype verification, respectively.

In female $p53^{\Delta\text{Panc}/+};Kras^{G12D/+}$ mice, which harbor one intact *Trp53* allele, concomitant *Sod2* deletion significantly prolonged survival (Figure IV.19D). In contrast, neither male $p53^{\Delta\text{Panc}/+};Kras^{G12D/+}$ mice nor $p53^{\Delta\text{Panc}/\Delta\text{Panc}};Kras^{G12D/+}$ mice of either gender benefited from *Sod2* deletion with respects to survival (Figure IV.19A-C).

To test the possibility that *Sod2* deletion prevents loss of the second *Trp53* allele and thus hinders tumor formation, the occurrence of the deleted *Trp53* allele was quantified in both PDAC samples and PDAC cell lines derived from the different mutant mouse strains. Generally, *Trp53* loss seemed to be less abundant in the samples with wt *Trp53* ($Kras^{G12D/+}$ and $Kras^{G12D/+};Sod2^{\Delta\text{Panc}/\Delta\text{Panc}}$ samples) and more abundant in the samples with *Trp53* total knockout ($p53^{\Delta\text{Panc}/\Delta\text{Panc}};Kras^{G12D/+}$ and $p53^{\Delta\text{Panc}/\Delta\text{Panc}};Kras^{G12D/+};Sod2^{\Delta\text{Panc}/\Delta\text{Panc}}$) compared with those with *Trp53* heterozygous knockout ($p53^{\Delta\text{Panc}/+};Kras^{G12D/+}$ and $p53^{\Delta\text{Panc}/+};Kras^{G12D/+};Sod2^{\Delta\text{Panc}/\Delta\text{Panc}}$), which indicates that the method is valid. However, comparing *Sod2*-proficient with *Sod2*-deficient genotypes, *Trp53*-loss seemed to occur equally frequent (Figure IV.20A-D). Moreover, *Trp53* protein product could not be detected in either of the $p53^{\Delta\text{Panc}/\Delta\text{Panc}};Kras^{G12D/+}$ and $p53^{\Delta\text{Panc}/+};Kras^{G12D/+}$ tumor samples or cell lines by immunoblot (Figure IV.20E).

Another possible explanation for the survival benefit of female $p53^{\Delta\text{Panc}/+};Kras^{G12D/+};Sod2^{\Delta\text{Panc}/\Delta\text{Panc}}$ over female $p53^{\Delta\text{Panc}/+};Kras^{G12D/+}$ could be that signaling from the remaining *Trp53* allele is increased, when *Sod2* is lost. To examine this option, Trp53-specific immunohistochemistry was performed on tissues of naturally succumbed individuals of the different mutant mouse strains and scored 0, 1, or 2 for no, weak, or strong

Trp53-positivity, respectively in PDAC, metastases of PDAC and non-tumor pancreatic tissue (Figure IV.21A).

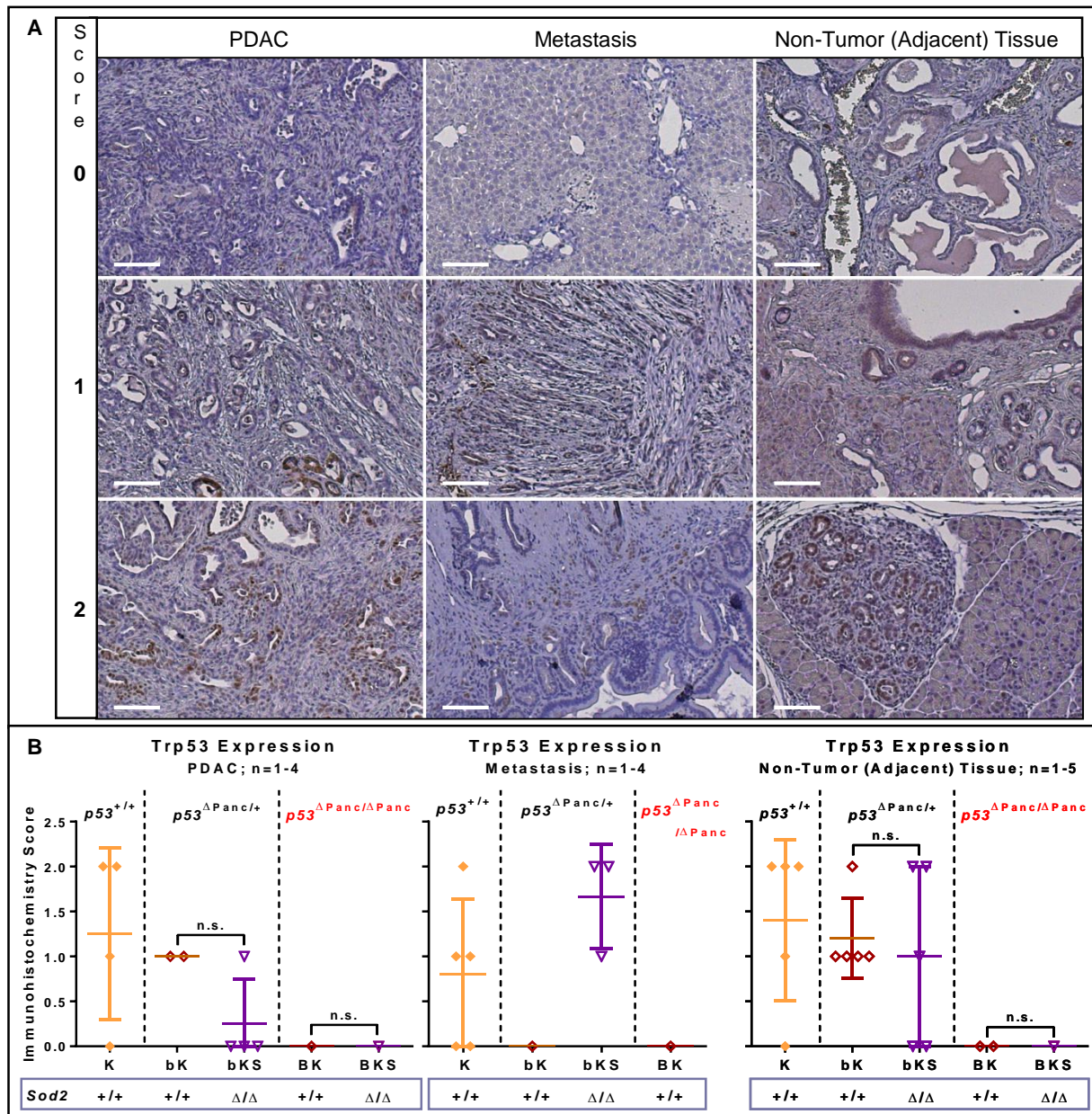


Figure IV.21: *Sod2* deletion does not increase expression of the remaining *Trp53* allele in $p53^{\Delta Panc/+}; Kras^{G12D/+}$ derived PDAC.

(A) Representative immunohistochemistry stainings for Trp53 in tissues (PDAC (left), liver or duodenal metastasis (middle), and non-tumor or tumor-adjacent pancreatic tissue (right)) from $Kras^{G12D/+}$ (K), $Kras^{G12D/+}; Sod2^{\Delta Panc/\Delta Panc}$ (KS), $p53^{\Delta Panc/+}; Kras^{G12D/+}$ (bK), $p53^{\Delta Panc/+}; Kras^{G12D/+}; Sod2^{\Delta Panc/\Delta Panc}$ (bKS), $p53^{\Delta Panc/\Delta Panc}; Kras^{G12D/+}$ (BK), or $p53^{\Delta Panc/\Delta Panc}; Kras^{G12D/+}; Sod2^{\Delta Panc/\Delta Panc}$ (BKS) mice. Respective immunohistochemistry scores from 0 (=no positive staining) to 2 (=strong positive staining) are indicated on the left. Scale bars equal 100 μ m.

(B) Analysis of immunohistochemistry. For each genotype, immunohistochemistry scores are plotted for PDAC (left; each data point represents one individual with apparent PDAC), metastasis (middle; each data point represents one metastasis; for one individual several distinctive sites of metastasis (liver, lung, or duodenum) might be included) or non-tumor pancreatic tissues (right; each data point represents one individual). Data are expressed as means \pm SD for $n \geq 2$; statistical analysis was performed using unpaired, two-tailed Student's *t*-test. No statistical analysis could be performed for metastases, as metastasis could be detected in only one of the $p53^{\Delta Panc/+}; Kras^{G12D/+}$ tissues.

While Trp53 protein expression was completely absent in all *Trp53* total knockout samples ($p53^{\Delta\text{Panc}/\Delta\text{Panc}};Kras^{G12D/+}$ and $p53^{\Delta\text{Panc}/\Delta\text{Panc}};Kras^{G12D/+};Sod2^{\Delta\text{Panc}/\Delta\text{Panc}}$ mice), *Trp53*-proficient $Kras^{G12D/+}$ mice had, overall, the highest Trp53 expression scores for PDAC and non-PDAC pancreatic tissue (Figure IV.21B). However, in PDAC metastases, $p53^{\Delta\text{Panc}/+};Kras^{G12D/+};Sod2^{\Delta\text{Panc}/\Delta\text{Panc}}$ mice might have had an even higher Trp53 expression score than the $Kras^{G12D/+}$ mice.

In neither PDAC nor non-PDAC pancreatic tissue, significant differences in Trp53 protein expression could be detected, when comparing *Sod2*-proficient with *Sod2*-deficient genotypes. For metastasis, statistical significance could not be assessed, as only one of the $p53^{\Delta\text{Panc}/+};Kras^{G12D/+}$ mice had had metastasis (Figure IV.21B).

To assess mitochondrial function, $Kras^{G12D/+}$ and $Kras^{G12D/+};Sod2^{\Delta\text{Panc}/\Delta\text{Panc}}$ PDAC cell lines, were treated with mitochondrial inhibitor rotenone followed by measuring ATP content. Thereby, it became apparent that cell lines were insensitive towards rotenone, when left in standard cell culture medium (data not shown). The same was observed, when cell lines were treated with rotenone in serum-free, glucose-containing medium (=Glucose medium; Figure IV.22A) or serum-containing, glucose-free, galactose-containing medium (data not shown). In contrast, when treated in serum-free, glucose-free, galactose-containing medium (=Galactose medium), cells were highly sensitive towards rotenone (Figure IV.22A).

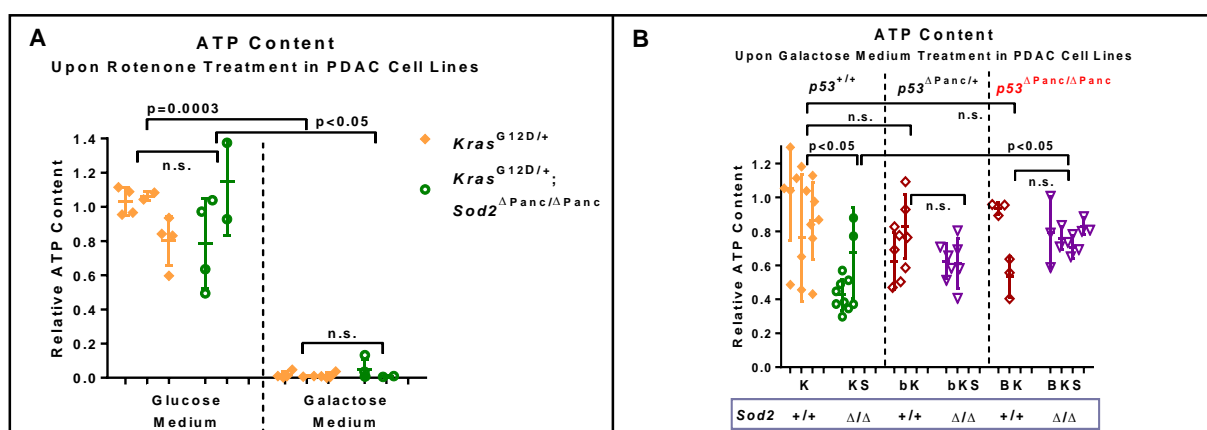


Figure IV. 22: *Sod2* deletion might reduce mitochondrial function in $Kras^{G12D/+}$, but not in $p53^{\Delta\text{Panc}/+};Kras^{G12D/+}$ and $p53^{\Delta\text{Panc}/\Delta\text{Panc}};Kras^{G12D/+}$ PDAC cell lines.

(A) Relative ATP content after 24 hour-treatment with mitochondrial inhibitor rotenone (5 μM) under serum-free conditions determined by CellTiter GLO assay. Data are normalized to vehicle control (0.5 % vol/vol DMSO). Glucose medium=serum-free standard medium, Galactose medium=serum-free standard medium, where glucose has been replaced by galactose (see III.3.3.3). Each bar represents one cell line. Cell lines of the same genotypes were plotted in the same color. Numbers of cell lines are: $Kras^{G12D/+}$: 3, $Kras^{G12D/+};Sod2^{\Delta\text{Panc}/\Delta\text{Panc}}$: 2.

(B) Relative ATP content after 24 hour-treatment with Galactose medium. Each bar represents one cell line. Cell lines of the same genotypes were plotted in the same color. Numbers of cell lines are: $Kras^{G12D/+}$ (K): 3, $Kras^{G12D/+};Sod2^{\Delta\text{Panc}/\Delta\text{Panc}}$ (KS): 2, $p53^{\Delta\text{Panc}/+};Kras^{G12D/+}$ (bK): 2, $p53^{\Delta\text{Panc}/+};Kras^{G12D/+};Sod2^{\Delta\text{Panc}/\Delta\text{Panc}}$ (bKS): 2, $p53^{\Delta\text{Panc}/\Delta\text{Panc}};Kras^{G12D/+}$ (BK): 2, and $p53^{\Delta\text{Panc}/\Delta\text{Panc}};Kras^{G12D/+};Sod2^{\Delta\text{Panc}/\Delta\text{Panc}}$ (BKS): 4. Data are normalized to ATP content after 24 hour-treatment with Glucose medium.

Data are expressed as means \pm SD (≥ 3 independent experiments) and statistical analysis was performed using unpaired, two-tailed Student's *t*-test.

These results may indicate that mitochondria, the main source of endogenously produced ROS and site of the Sod2 activity, might only be of functional importance for PDAC cell lines under very specific cell culture conditions provided e.g. by the herein presented Galactose medium. For this reason, for all further experiments with PDAC cell lines, Galactose medium was used.

Comparing ATP content of PDAC cell lines, the $Kras^{G12D/+};Sod2^{\Delta Panc/\Delta Panc}$ PDAC cell lines, but not the $Kras^{G12D/+}$ PDAC cell lines contained significantly less ATP in Galactose medium than in Glucose medium (Figure IV.22B). Interestingly, in the $p53^{\Delta Panc/+};Kras^{G12D/+}$ and the $p53^{\Delta Panc/\Delta Panc};Kras^{G12D/+}$ backgrounds, *Sod2* deletion did not increase sensitivity to Galactose medium. Moreover, *Sod2*-proficient $p53^{\Delta Panc/+};Kras^{G12D/+}$ and $p53^{\Delta Panc/\Delta Panc};Kras^{G12D/+}$ PDAC cell lines were slightly (but not significantly) more sensitive to Galactose medium than *Sod2*-proficient $Kras^{G12D/+}$ PDAC cell lines, whereas *Sod2*-deficient $p53^{\Delta Panc/+};Kras^{G12D/+}$ and the $p53^{\Delta Panc/\Delta Panc};Kras^{G12D/+}$ PDAC cell lines were significantly less sensitive to Galactose medium than the *Sod2*-deficient $Kras^{G12D/+}$ PDAC cell line (Figure IV.22B). In conclusion, both *Sod2*- and *Trp53*-loss might reduce mitochondrial activity. In addition, *Trp53* status might also relativize reduced mitochondrial activity and vulnerability secondary to *Sod2*-deficiency.

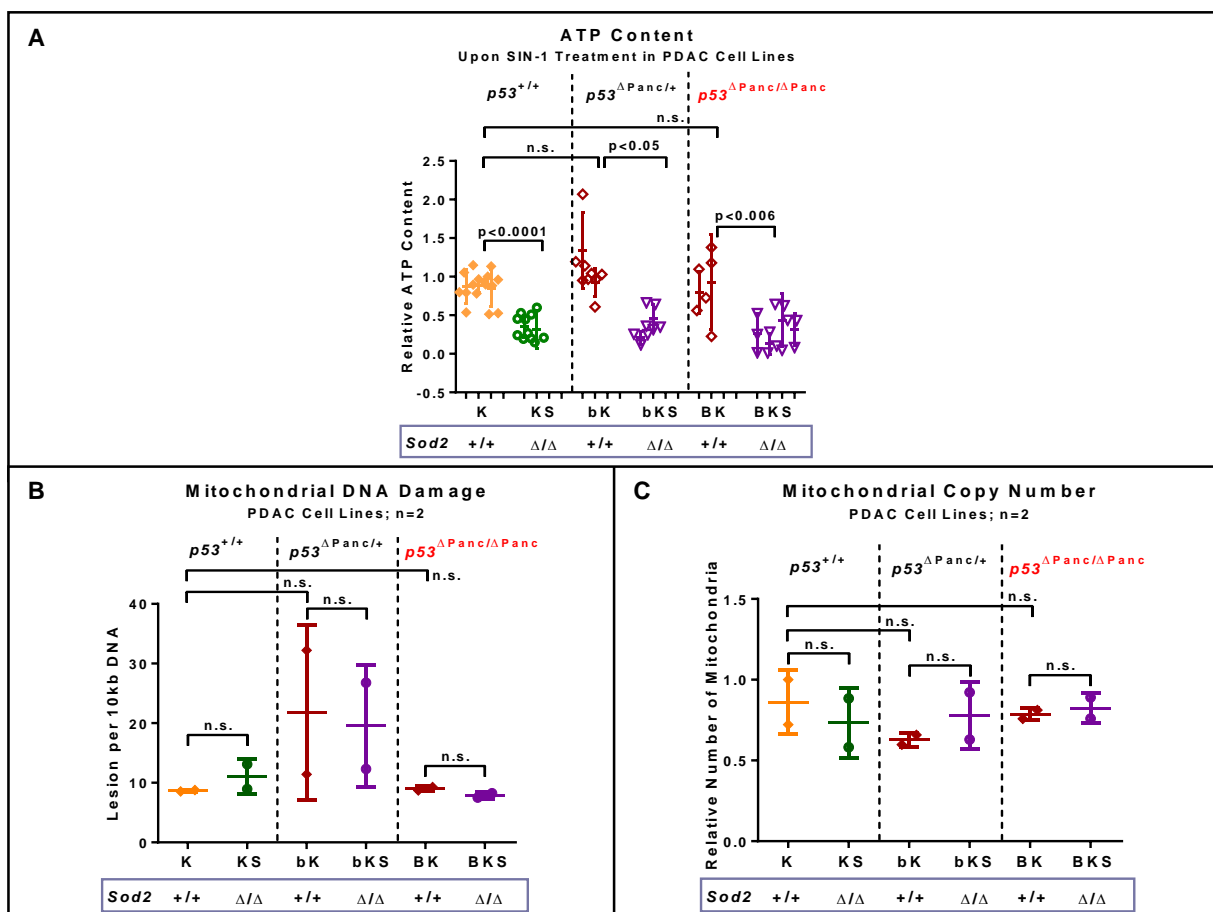


Figure IV. 23: *Sod2* deletion increases sensitivity of $Kras^{G12D/+}$, $p53^{\Delta Panc/+};Kras^{G12D/+}$, and $p53^{\Delta Panc/\Delta Panc};Kras^{G12D/+}$ PDAC cell lines to SIN-1 but does not alter mitochondrial DNA damage or copy number.

Figure IV.23: *Sod2* deletion increases sensitivity of *Kras*^{G12D/+}, *p53*^{ΔPanc/+}; *Kras*^{G12D/+}, and *p53*^{ΔPanc/ΔPanc}; *Kras*^{G12D/+} PDAC cell lines to SIN-1 but does not alter mitochondrial DNA damage or copy number - continued.

(A) Relative ATP content after 24 hour-treatment with O₂^{•-} and *NO source SIN-1 (500 μM) in galactose medium (=serum-free standard medium, where glucose has been replaced by galactose (see III.3.3.3)) determined by CellTiter GLO assay. Each bar represents one cell line. Cell lines of the same genotypes were plotted in the same color. Numbers of cell lines are: *Kras*^{G12D/+} (K): 3, *Kras*^{G12D/+}; *Sod2*^{ΔPanc/ΔPanc} (KS): 2, *p53*^{ΔPanc/+}; *Kras*^{G12D/+} (bK): 2, *p53*^{ΔPanc/+}; *Kras*^{G12D/+}; *Sod2*^{ΔPanc/ΔPanc} (bKS): 2, *p53*^{ΔPanc/ΔPanc}; *Kras*^{G12D/+} (BK): 2, and *p53*^{ΔPanc/ΔPanc}; *Kras*^{G12D/+}; *Sod2*^{ΔPanc/ΔPanc} (BKS): 4. Data are normalized to galactose medium and expressed as means ± SD (≥3 independent experiments). Statistical analysis was performed using unpaired, two-tailed Student's *t*-test.

(B) Mitochondrial DNA damage analysis in lysates of PDAC cell lines determined by qPCR-DNA damage assay.

(C) Mitochondrial copy number in lysates of PDAC cell lines determined by qPCR-DNA damage assay.

In (B) and (C), for each genotype, two different cell lines were analyzed. Statistical analysis was performed using unpaired, two-tailed Student's *t*-test.

To determine sensitivity of PDAC cell lines to oxidative stress, cell lines were treated with SIN-1, which produces O₂^{•-} and *NO, and ATP content was measured (Figure IV.23A).

Remarkably, all *Sod2*-deficient cell lines were more sensitive to SIN-1 treatment as their *Sod2*-proficient counterparts (Figure IV.23A).

Notably, with no further treatment, there were no differences in mitochondrial DNA damage or copy number for any of the analyzed PDAC cell lines (Figure IV.23B-C).

V. Discussion

1. Characterization of the Pancreas-Specific *Sod2* Knockout Mouse

SODs are the cells' first line of defense against ROS, however, in the mouse, of all three *Sods*, only *Sod2* knockout results in drastic phenotypic abnormalities, which lead to early postnatal death [252, 253, 257, 254, 255].

Similarly severe phenotypes were so far only obtained for the knockouts of three other key antioxidant enzymes or enzyme systems, namely, cytosolic *Gpx4* [278, 279], *Glrx3* [298], and the enzymes of the TXN antioxidant system, *Txn1*, *Txn2*, *Txnrd1*, or *Txnrd2* [287, 288, 289, 290, 291]. However, all these mice died already at the embryonic stage, which hindered a clear identification of pathologic conditions at death.

For *Sod2* knockout mice, on the other hand, besides dilated cardiomyopathy, symptoms included accumulation of fat in liver and skeletal muscle, metabolic acidosis, ketosis, and stark growth retardation indicative of defective food metabolism [252, 253, 499, 257]. As the pancreas is essentially involved in fat, protein and carbohydrate digestion [2] and expresses relatively high levels of *SOD2* [241], it seemed reasonable, that a pancreas-related defect might be involved in the phenotype of the *Sod2* knockout mouse. Therefore, to test this hypothesis, in the first part of the present study, the effects of pancreas-specific *Sod2* deletion have been studied.

In the *Sod2*^{ΔPanc/ΔPanc} mice, *Sod2* loss was convincingly confirmed in the pancreas on the level of RNA and protein, whereas the heterozygous *Sod2*^{ΔPanc/+} mice expressed about 50 % of the *Sod2* protein compared with the wt controls.

1.1. Effects of *Sod2* Deletion on Pancreatic Development and Function

In the murine pancreas, in the absence of other genetic or non-genetic manipulations, *Sod2* deletion did not lead to overt phenotypic aberrations. *Sod2*^{ΔPanc/ΔPanc} (and *Sod2*^{ΔPanc/+}) mice were viable, fertile, and bred at the expected Mendelian ratios (data not shown). Moreover, excluding from analysis progressive neurological deficits that presented in about one third of the *Sod2*^{ΔPanc/ΔPanc} mice and will be discussed in detail in section V.1.6, the *Sod2*^{ΔPanc/ΔPanc} mice lived without obvious abnormalities to full life expectancy, similar to what has been described in four studies of liver-specific [259, 500, 263, 260], and one study of kidney-specific *Sod2* deletion [262].

As observed for one of the liver- [500] and the kidney-specific *Sod2* knockout [262], the pancreas-specific *Sod2* knockout mice weighed significantly less than the wt controls.

In the *Sod2*^{ΔPanc/ΔPanc} pancreata, no obvious morphological anomalies were detected and both the endocrine and exocrine compartment appeared completely normal.

Moreover, endocrine function of *Sod2*^{ΔPanc/ΔPanc} pancreata, as assessed by IP-GTT, was indistinguishable from wt pancreata.

As a side note, the finding that male mice of both genotypes displayed higher fasting, but a lower rise in blood glucose levels upon glucose injection than female mice indicates a gender-specific difference in glucose homeostasis.

In contrast to endocrine function, there is some indication of a mild reduction in exocrine pancreatic function, as evidenced by reduced weight gain and increased liver fat deposition, predominantly in female *Sod2*^{ΔPanc/ΔPanc} compared with female wt mice. Yet, this difference is not reflected in fecal protease- or lipase-activity. Unfortunately, the HFD (15 % more fat than standard diet) used in this study did not result in an increase in weight gain compared with the standard diet. Thus, to unequivocally determine whether *Sod2* deletion results in mild exocrine pancreatic insufficiency, a diet with a higher fat content than the diet used in this study might evoke a more pronounced effect. Additionally, analysis of pancreatic juices instead of feces might serve to more directly assess exocrine pancreatic function. Notably, the fat-enriched chow seemed to abolish the differences in weight gain observed between the standard diet-fed male *Sod2*^{ΔPanc/ΔPanc} and the standard diet-fed male wt mice.

While the question whether pancreas-specific *Sod2* deletion reduces pancreatic exocrine function could not be fully clarified within the present study, disturbed lipid metabolism has also been observed in the whole body *Sod2* knockout mice [252, 253, 257]. Reduced pancreatic exocrine function might, at least in part, contribute to these phenotypic characteristics.

While *Sod2* was found to be crucial to normal tissue development and/or function in brain [263] and heart [264], the main sites affected in whole body *Sod2* knockout mice [252, 253, 499, 257], from this study, I conclude that *Sod2* is fully dispensable for pancreatic physiological development and function in the mouse. The same has been reported for kidney- [262], as well as postnatal mammary gland- [261] and liver-specific [259, 263, 260] *Sod2* deletion.

1.1.1. Influence of the Genetic Background on *Sod2* Deletion

For the whole body *Sod2* knockout mice, phenotypic characteristics strongly depended on the genetic background [501, 257, 502] and most severe phenotypes were commonly described for the C57BL/6J background. As the pancreas-specific *Sod2* knockout mice of the present study were backcrossed to C57BL/6J mice for several generations, the possibility that the lack of a pancreatic phenotype might be explained by a too heterogeneous genetic background should be considerably low, yet not neglectable.

1.2. Loss of *Sod2* and Oxidative Stress

Whether *Sod2*-loss causes an increase in oxidative stress in tissues, is controversially reported in literature: Markers of oxidative stress were found to be increased in many *Sod2* deletion models, including the whole body homozygous [502] and heterozygous [258, 503, 461, 504], as well as several cell/tissue-specific (e.g. gastric parietal cells [265], T lymphocytes [505] and skeletal muscle [267, 506]) *Sod2* knockout mice.

In contrast, other studies indicate that the common paradigm that *Sod2*-loss causes oxidative stress by increasing cellular O₂^{•-} might be an oversimplification. For example, in three studies of murine postnatal liver-specific *Sod2* knockout, authors were unable to

detect signs of increased oxidative stress secondary to *Sod2* deletion [259, 263, 260]. In addition, while observing an increase in $O_2^{\cdot-}$ levels in a subset of *Sod2*-deficient motor neurons, other markers of oxidative stress were not increased in this subset, while other *Sod2*-deficient motor neurons not even displayed elevated levels of $O_2^{\cdot-}$ [266]. Moreover, increased oxidative stress was observed in many tissues of whole body *Sod2* knockout mice, but neither in the cerebellum [501] nor in the liver [507]. Consequently, different cell types or tissues might respond differently to *Sod2*-loss and some might not develop oxidative stress.

Carboxy- H_2DCFDA and MitoSOX are two common probes for directly detecting intracellular ROS or mitochondrial $O_2^{\cdot-}$, respectively [508, 509] and have been applied for ROS detection for example in *Sod2*-deficient T cells [505], motor neurons [266], and liver cells [500]. As application of these probes in tissues is questionable because comparable results critically depend on equal intracellular probe concentration [510], I used these probes only in isolated primary acinar cells or PDAC cell lines. In the present study, ROS were found to be mildly increased as determined by Carboxy- H_2DCFDA and MitoSOX reactivity, but not, when analyzed by ESR spectrometry. A possible reason for this discrepancy may be that, while ESR spectrometry is a highly reliable analytical technique for direct measurement of free radicals, it is relatively insensitive and requires micromolar levels of steady-state free radicals [355]. Thus, in the *Sod2* ^{Δ Panc/ Δ Panc} pancreata, ROS concentrations might have been below the detection limit of ESR spectrometry.

In addition to directly demonstrating their presence, ROS, and more importantly, increases in ROS levels can also be detected indirectly by an increase in ROS-specific oxidation products, or, in other words, the presence of oxidative stress. In this regard, researchers commonly assess occurrence of LPO products (MDA, 4-HNE, and isoprostanes), oxidative protein modifications (e.g. protein carbonyls or tyrosine nitrates), or oxidative DNA modifications (e.g. 8-oxo-dG; [355]).

Yet, reliable analysis of either oxidation product requires stable and readily detectable levels of the analyzed compounds/modifications. This might be problematic, predominantly in *ex vivo* samples, as e.g. oxidatively damaged proteins are rapidly removed by proteases [355]. Moreover, reliable detection of many of the commonly assessed substances often requires HPLC or GC-MS analysis [355]. Besides, MDA, whose detection is also possible by UV/vis spectrometry of thiobarbituric acid-reactive substances (TBARS; [355]), is, firstly, only a minor product of LPO and, secondly, readily metabolized. Potentially, for these reasons, in my hands, in a TBARS assay performed according to [511] with whole pancreas lysates of *Sod2* ^{Δ Panc/ Δ Panc} and wt mice, MDA concentration was always below the detection limits, even when the entire tissue was used (data not shown). Finally, the 8-oxo-dG modification, the most commonly analyzed oxidative DNA modification, represents only 10 % of DNA base modifications conferred by $\cdot OH$ [512] and is efficiently removed from the DNA by specialized and general repair mechanisms (e.g. rev. in [513]).

For these reasons, I chose a more general strategy and assessed mitochondrial DNA damage by DNA damage qPCR assay. The strengths of this approach are at least three-fold. Firstly, the assay is very sensitive as it involves analyzing a broad spectrum of DNA modifications rather than a specific one [102]. Secondly, it requires only a few nanograms of DNA (in contrast to the TBARS assay, which might require more than one entire pancreas; [102]; see above). Thirdly, analyzing mitochondrial DNA damage

specifically might be a robust approach to assess oxidative stress, as mitochondrial DNA is considered highly vulnerable to ROS-mediated lesions e.g. due to its close spatial proximity to the mitochondrial ETC, the major site of endogenous ROS production [102]. Evidence for a high susceptibility of mitochondrial DNA to oxidative damage comes from many *in vitro* and *in vivo* studies (e.g. [514, 515, 516, 517, 518]). Furthermore, the third point might especially apply to the *Sod2*^{ΔPanc/ΔPanc} mouse, as *Sod2* is a mitochondrial enzyme, and its knockout should increase mitochondrial O₂^{•-}, which cannot cross biological membranes. Therefore, analyzing mitochondrial DNA should reduce background, in particular with the model system of the present study.

As shown for whole body heterozygous *Sod2* knockout mice [519], I also expected a rise in oxidative stress predominantly in the mitochondria.

However, an increase in mitochondrial DNA damage was detectable neither in the *Sod2*^{ΔPanc/ΔPanc} compared with wt pancreata nor in the *Sod2*-deficient compared with *Sod2*-proficient PDAC cell lines.

Oxidative stress has been linked to alterations in mitochondrial copy numbers ([520, 521]; rev. in [522]). The DNA damage qPCR assay also allowed to assess mitochondrial DNA copy number by quantifying mitochondrial to nuclear DNA. Yet, I detected no differences in mitochondrial DNA copy numbers comparing *Sod2*^{ΔPanc/ΔPanc} with wt pancreata or *Sod2*-deficient with *Sod2*-proficient PDAC cell lines. While the use of a column-based DNA extraction kit together with RNase digestion for the pancreatic tissues may have reduced mitochondrial DNA yield [523], neither columns and nor RNase digestion were implemented in the DNA extraction from the PDAC cell lines. Nonetheless, mitochondrial DNA copy numbers were slightly lower in the PDAC cell lines compared with the tissue samples. Thus, I concluded that the DNA extraction method, did not, at least not drastically, affect mitochondrial DNA copy number determination.

To exclude that other antioxidants compensated for *Sod2* loss in the pancreas, I tested expression of six other key antioxidant enzymes. While in the hepatocytes of liver-specific *Sod2* knockout mice several antioxidant enzymes, including *Sod1*, *Txnrd2*, and *Hmox1* were significantly up-regulated by at least two-fold [260], in the *Sod2*^{ΔPanc/ΔPanc} pancreata, the only significant divergence was a significant down-regulation of *Gpx4*, the only essential isoform of *Gpx* [278, 279, 524]. Yet, *Gpx4* was decreased by no more than 50 %, which did not lead to an overt phenotype in the mouse [278, 279].

Similarly, Parajuli and colleagues also reported no alterations in *Sod1* expression in the kidneys of their kidney-specific *Sod2* knockout mice [262].

As none of the six antioxidant enzymes was significantly up-regulated in the *Sod2*^{ΔPanc/ΔPanc} pancreata, I concluded that *Sod2*-loss is probably not compensated by one specific or a combination of other antioxidant enzymes. Yet, it is possible that other, non-enzymatic antioxidants (e.g. GSH or vitamin C) compensated for *Sod2*-loss.

While there is a multiplicity of assays for detecting ROS and oxidative stress, none of them is flawless (rev. in [355]). Although Carboxy-H₂DCFDA and MitoSOX indicated a slight increase in ROS, I noted neither an increase in ROS, when determined by ESR spectrometry nor in mitochondrial DNA damage. All these findings as well as the very mild pancreas-specific phenotype in all of the *Sod2*-deficient mouse strains of the present study may suggest that ROS induction by *Sod2* deletion may not be high enough to lead to

deleterious oxidative stress, possibly, because untreated pancreatic mitochondria do not produce significant amounts of $O_2^{\cdot-}$.

Some evidence that this hypothesis might be true, also comes from the observation, that, in all of the *Sod2*-deficient PDAC cell lines, basal ATP levels were similar to their *Sod2*-proficient counterparts, but dropped drastically, upon treatment with the $O_2^{\cdot-}$ - and \cdot NO-generating drug SIN-1. This indicates that, although not producing deleterious ROS levels themselves, *Sod2*-deficient pancreatic mitochondria are highly vulnerable to increased ROS levels. Similar findings have also been obtained for several mice deficient of other antioxidant enzymes, including the *Gpx1*, *Prdx1-4*, or *Prdx6* whole body knockout mice, which did not display overt phenotypic abnormalities, but were highly sensitized to oxidative stress.

It will be of great interest to investigate whether this effect also translates into the *in vivo* situation of the *Sod2* ^{Δ Panc/ Δ Panc} mouse lines. In fact, treating the mice with a ROS- or oxidative stress-inducing agent (e.g. SIN-1 or paraquat) and determining whether this treatment increases oxidative stress (and potentially also impairs mitochondrial and tissue function) to a greater extent in the *Sod2* ^{Δ Panc/ Δ Panc} than in the control mice might provide a valid strategy to further test the hypothesis.

Another possible explanation for absence of increased mitochondrial DNA damage in the *Sod2*-deficient pancreata may also be that due to the absence of *Sod2*, mitochondrial $O_2^{\cdot-}$ may no longer be converted to other, more deleterious ROS, such as H_2O_2 or \cdot OH, which are thought to be most responsible for oxidative damage [89]. Thus, a potential increase in relatively harmless $O_2^{\cdot-}$ may actually not lead to a detectable increase in oxidative stress.

1.3. Loss of *Sod2* and Cell Fate Determination

ROS are known to regulate both proliferation and apoptosis and increased apoptosis has been reported in the whole body *Sod2* heterozygous knockout mouse [258, 257] as well as several cell type- or organ-specific *Sod2* knockout mice (e.g. gastric parietal cells [265], thymocytes [505], and liver [500]).

In contrast, the *Sod2*-deficient pancreata only presented with a minimal, non-significant reduction in proliferation and a minimal, non-significant increase in apoptosis with concomitant activation of oncogenic *Kras*. This is, however, not too surprising, as the *Sod2*-deficient *Sod2* ^{Δ Panc/ Δ Panc} and *Kras*^{G12D/+},*Sod2* ^{Δ Panc/ Δ Panc} pancreata were barely distinguishable from the respective *Sod2*-proficient pancreata and, as discussed in V.1.2., there was only a slight increase in ROS, but probably not in oxidative stress levels. Similarly, no difference in apoptosis was found in the case of the postnatal liver-specific [259] and heart muscle-specific [264] *Sod2* knockout. Moreover, even in lymphomas, which developed at higher rates in whole body heterozygous *Sod2* knockout mice, proliferation rates were equal comparing the whole body heterozygous *Sod2* knockout with wt mouse cancers [461]. In most studies that demonstrated increased apoptosis in *Sod2* knockout mice, apoptosis has been attributed to increased oxidative stress. As I did not detect increased oxidative stress in the pancreas-specific *Sod2* knockout animals, analyzing

apoptosis after challenging the mice with increased oxidative stress (e.g. by treating mice with SIN-1 or paraquat) could be topic of further studies.

1.4. Loss of *Sod2* and Mitochondrial Function

Several studies report aberrant mitochondrial morphology secondary to *Sod2* knockout [253, 501, 257], some additionally provide a more detailed analysis of mitochondrial function. Whenever mitochondrial function was assessed in homozygous whole body or cell type-/tissue-specific *Sod2* knockout mice, authors consistently report a dramatic decrease in complex II activity associated with a marked reduction in Sdhb protein levels [252, 507, 525, 502, 264, 506, 260]. Notably, in all these reports, these alterations were attributed to a proven increase in ROS and/or oxidative stress levels.

I did not investigate mitochondrial morphology or function, but I was unable to demonstrate presence of increased oxidative stress in the *Sod2*-deficient pancreata or cells. The fact that the drastic decline in ATP content upon SIN-1 treatment of PDAC cell lines was only present under conditions that demanded mitochondrial activity indicates that *Sod2*-loss with concomitant oxidative stress dramatically reduces mitochondrial function.

Thus, it appears feasible to perform a more thorough analysis of mitochondrial function in the *Sod2*-deficient mice, especially after additional induction of oxidative stress.

1.5. Effects of Heterozygous Pancreas-Specific *Sod2* Deletion

No significant differences were noted for heterozygous *Sod2* ^{Δ Panc/+} mice compared with their *Sod2*-wt counterparts. Therefore, in many instances, the respective data are not shown to achieve better visualization in the graphs of the present study. The lack of an overt phenotype of the *Sod2* ^{Δ Panc/+} mice is, however, not too surprising, as even for the whole body *Sod2* ^{Δ +/+} mutant mice, phenotypes were not peculiar. For example, body weight, food consumption, and fecundity did not differ between whole body *Sod2* ^{Δ +/+} mutant and wt mice [461, 257]. Instead, the only observed differences were ultrastructural, but not functional alterations [257], increased oxidative stress as evidenced by increased oxidative DNA damage particularly late in life (> 1.25 years; [461]), LPO [257], and tyrosine nitration of proteins [257], increased rate of apoptosis [258, 257], and a premature onset of age-related decline in mitochondrial function [258, 526]. Moreover, a 100 % increase in cancer was observed, which, however, did not affect life span [461]. But in none of these studies, pancreas-specific alterations were studied.

Now, considering the already weak overall phenotypic alterations between the *Sod2* ^{Δ Panc/ Δ Panc} strains and their respective *Sod2*-proficient control mice in this study, it seems reasonable to conclude that if there was a dose-dependent effect of *Sod2* deletion, this effect would be very hard to detect. Potential approaches may include assessing mitochondrial function and oxidative stress, possibly at ages older than 24 weeks.

1.6. The Neurological Phenotype Observed with *Ptf1a-Cre*^{ex1}-Mediated *Sod2* Deletion

Cre/LoxP-mediated mutagenesis provides a valuable tool for tissue- and/or cell type-specific mutagenesis in mouse models. However, when the *Cre* driver gene is not only

expressed in the tissue/cell type of interest, phenotypes may arise that are not linked to a genetic manipulation of the tissue/cell type of interest, but rather to an undesirable manipulation of other tissues and/or cell types that the driver and thus the Cre gene becomes expressed at any time point in development or postnatal life [527].

For pancreas-specific mutagenesis, two Cre driver lines are commonly used: *Ptf1a-Cre^{ex1}* and *Pdx1-Cre* [28, 527].

Ptf1a-Cre^{ex1} shows wide-spread, pancreas-specific expression and allows for efficient recombination of floxed alleles throughout the pancreatic lineages [528]. Therefore, it has been used for pancreas-specific recombination in this study. However, besides pancreas-specific recombination, *Ptf1a-Cre^{ex1}*-mediated recombination of floxed alleles has also been reported for the retina [483] and the cerebellum [529]. Moreover, prominent *Ptf1a* expression has also been detected in an area of the neural tube of the mouse embryo that will later develop into the cerebellum, the medulla oblongata and the spinal cord [529, 530]. No obvious signs of visual impairment became apparent in neither of the *Ptf1a-Cre^{ex1}*-driven *Sod2*-deficient mouse strains of the present study, although Sandbach and colleagues described ocular pathology in the whole body *Sod2* knockout mouse [531]. Yet, I did not analyze the eyes of the animals sufficiently to exclude retinal involvement.

About one third of the *Sod2*-deficient animals (*Sod2^{ΔPanc/ΔPanc}* and *Kras^{G12D/+};Sod2^{ΔPanc/ΔPanc}*) developed neurological symptoms requiring euthanization between day 72 to 545 after birth. *p53^{ΔPanc/ΔPanc};Kras^{G12D/+};Sod2^{ΔPanc/ΔPanc}* and *p53^{ΔPanc/+};Kras^{G12D/+};Sod2^{ΔPanc/ΔPanc}* mice, which died between postnatal day 56 to 80 or 94 to 325, respectively, in most instances, probably succumbed too early to pancreas-related symptoms to have evolved this CNS pathology. Thus, I concluded that *Sod2* might play an important role in the CNS.

This conclusion is well in line with a study, in which whole body *Sod2* knockout mice were treated with the *Sod2* mimetic MnTBAP [499]. In this study, MnTBAP prevented early postnatal death (day 3 to 13) due to dilated cardiomyopathy and strongly reduced liver lipid accumulation in the mutant mice. But, as MnTBAP does not cross the blood-brain barrier, the mutant mice lived to develop CNS-related deficits, which are strikingly similar to the ones observed in the present study and included progressive hind limb ataxia and tremors leading to death around day 16 [499].

Similarly, in another study using a different whole body *Sod2* knockout mouse line, which survived up to three weeks, in addition to a marked growth reduction, *Sod2^{Δ/Δ}* mice exhibited severe and progressive neurological abnormalities. Those included limb weakness and circling behavior, which I also observed commonly in the *Sod2^{ΔPanc/ΔPanc}* mice [253].

Moreover, the CNS-related defects observed in the *Sod2^{ΔPanc/ΔPanc}* mice also remarkably resembled the phenotypic characteristics of *Sod1* mutant mice, one of the most widely used mouse models for ALS [238]. In these mice, inactive *Sod1* protein may aberrantly localize and subsequently aggregate in the mitochondrial matrix, which elicits motor neuron degeneration [236]. A similar mechanism may also take place in the CNS of the *Sod2^{ΔPanc/ΔPanc}* mice.

Additionally, replacement of one allele of *Ptf1a* with the *Ptf1a-Cre^{ex1}* allele and a possibly resulting haploinsufficiency might at least predispose the mice to further CNS injury, as Saborowski and colleagues also observed neurological deficits in about 10 % of their *Ptf1a-Cre^{ex1}* mice, which still had two functional *Sod2* alleles [532]. Moreover, within a number of *Ptf1a-Cre^{ex1};Trp53^{LSL-R172H/+}* mutant mouse strains in our laboratory, all *Ptf1a-Cre^{ex1};Trp53^{LSL-R172H/+}* mutant individuals succumbed also early (day 54 to 499) due

to very similar neurological deficits as observed in the $Sod2^{\Delta\text{Panc}/\Delta\text{Panc}}$ mice, irrespective of their $Sod2$ status (data not shown).

$Pdx1-Cre$, which displays rather dispersed expression in the pancreas, mediates recombination, apart from the pancreas, in duodenum, antral stomach, bile duct, hypothalamus and inner ear (rev. in [527]). Consequently, when used for driving the $Kras^{G12D}$ -mutation, transgenic mice frequently developed intestinal metaplasia and mucocutaneous papillomas, and, occasionally, duodenal hyperplasia [28].

To avoid the neurological symptoms observed in the $Ptf1a-Cre^{ex1};Sod2^{fl/fl}$ and $Ptf1a-Cre^{ex1};Kras^{+/LSL-G12D};Sod2^{fl/fl}$ mice, I also started breeding $Pdx1-Cre;Sod2^{fl/fl}$ and $Pdx1-Cre;Kras^{G12D/+};Sod2^{\Delta\text{Panc}/\Delta\text{Panc}}$ strains. However, as previously reported, $Pdx1-Cre$ animals developed cutaneous papillomas and bloody anal prolapses at high frequencies (data not shown, [28]), which also required premature euthanization. For this reason, the $Pdx1-Cre;Sod2^{fl/fl}$ and $Pdx1-Cre;Kras^{G12D/+};Sod2^{\Delta\text{Panc}/\Delta\text{Panc}}$ breedings were soon discontinued.

Recently, three more Cre driver lines have been developed for pancreas-directed mutagenesis that are thought to be more tissue specific: $Cpa1-Cre^{ER}$ [533], $Hnf1b-Cre^{ER}$ [534], and $Sox9-Cre^{ER}$ [44]. Yet, while these drivers might be useful in circumventing the pancreas-unrelated side effects observed with the $Ptf1a-Cre^{ex1}$ and $Pdx1-Cre$ driver lines, all of the three novel drivers require carefully timed tamoxifen induction to achieve pancreas-wide recombination, which may have two potential drawbacks. First, tamoxifen-induced recombination is not always efficient and might require multiple doses of tamoxifen or might occur weeks after tamoxifen administration [535, 527]. Second, as the benefits observed with $Sod2$ deletion are gender specific (increased tumor latency for the female $Kras^{G12D/+};Sod2^{\Delta\text{Panc}/\Delta\text{Panc}}$ mice and prolonged survival for the female $p53^{\Delta\text{Panc}/+};Kras^{G12D/+};Sod2^{\Delta\text{Panc}/\Delta\text{Panc}}$ mice) and tamoxifen is an estrogen analogon, which may exert both agonist and antagonist function on estrogen receptor signaling [536], tamoxifen might interfere with the $Sod2^{\Delta\text{Panc}/\Delta\text{Panc}}$ phenotype and thus preclude the study. Therefore, to thoroughly study the effects of pancreas-specific $Sod2$ deletion without off-target or drug-induced interferences, novel non-inducible, highly pancreas-specific Cre driver lines might be required.

2. Role of $Sod2$ in Pancreatic Cancer

Many *in vitro* and xenograft studies have indicated that $SOD2$ might be a classical tumor suppressor gene (e.g. [457, 476, 477]; refer also to II.3).

In concert with these findings, in the present study, there was a non-significant trend towards reduced tissue integrity, a higher number of preneoplastic lesions, and enhanced fibrosis in the pancreata of the 12 and 24 weeks-old $Kras^{G12D/+};Sod2^{\Delta\text{Panc}/\Delta\text{Panc}}$ mice in relation to pancreata of age-matched $Kras^{G12D/+}$ mice. Furthermore, ADM, one of the key events in pancreatic carcinogenesis [43, 44], was partly significantly increased *in vivo* and significantly accelerated *in vitro*. Lastly, the slightly increased relative pancreatic weight of $Kras^{G12D/+};Sod2^{\Delta\text{Panc}/\Delta\text{Panc}}$ at 24 weeks may also be indicative of hyperplasia.

Interestingly, *Kras*^{G12D/+};*Sod2*^{ΔPanc/ΔPanc} mice did not succumb earlier than *Kras*^{G12D/+} mice, in fact, female *Kras*^{G12D/+};*Sod2*^{ΔPanc/ΔPanc} mice developed significantly less pancreatic tumors than female *Kras*^{G12D/+} mice and had mostly died due to age-related defects. I thus concluded that, while *Sod2*-loss seems to promote pancreatic metaplasia and formation of early preneoplastic lesions on the one hand, it may provide protection at the later stages of pancreatic tumor formation on the other hand.

A similar, yet not this striking observation was made by van Remmen and colleagues, who observed a 100 % increase in overall tumor incidence, but unshortened survival times in their heterozygous whole body *Sod2* knockout mice. They concluded that *Sod2* deletion only accelerates the earliest stages of cancer development [461].

Moreover, the data of the present study are well in line with the findings obtained in a chemical-induced skin cancer mouse model: After cancer induction, *Sod2* protein levels and enzyme activity were significantly decreased in treated skin areas and consecutively formed benign papilloma. In contrast, *Sod2* levels were significantly increased at the later stage of tumorigenesis (i.e. squamous cell carcinoma). The authors reasoned that early tumor formation might create oxidative stress and that *Sod2* might be required to allow late-stage cancer cells to survive under these conditions [537]. More recently, *Sod2* deletion was shown to significantly attenuate cancer formation in a *Trp53* knockout-driven mouse model of thymic and splenic lymphoma [538].

With the chemical-induced murine skin cancer model, Zhao and colleagues observed that *Sod2* deletion significantly increased proliferation and apoptosis [503]. An increase in neoplastic cell apoptosis could explain the unshortened life span of the *Kras*^{G12D/+};*Sod2*^{ΔPanc/ΔPanc} mice and the increased tumor latency of the female *Kras*^{G12D/+};*Sod2*^{ΔPanc/ΔPanc} mice. However, as described in V.1.3, at 12 and 24 weeks, proliferation was only mildly and not significantly reduced and apoptosis was similarly increased.

2.1. Influence of *Sod2* Status on Ras Signaling in *Kras*^{G12D} Pancreata

Increased Ras activity levels are sufficient for initiating pancreatic cancer [48], a process which critically depends on mitochondrial ROS [454, 57]. Thus, I next assessed Ras activity, as well as p38 activity and *Braf* expression, two Ras downstream targets, in the pancreata of *Kras*^{G12D/+};*Sod2*^{ΔPanc/ΔPanc} and *Kras*^{G12D/+} mice. None of these factors was significantly altered, which indicates that *Sod2* deletion might not alter Ras activity and/or signaling. Yet, to fully exclude that the *Sod2* status affects Ras signaling, more detailed analyses are required. This would include not only to extend the analyses to other Ras downstream effectors (e.g. Erk1/2 activity), but also to investigate each factor for each of the herein examined (and potentially also at a later) time point.

2.2. Influence of *Sod2* Status on Trp53 Signaling in *Kras*^{G12D} Pancreata

Oncogenic *Kras*^{G12D} has been identified as the major driver in PDAC development, but progression of premalignant lesions to PDAC critically requires inactivation of tumor suppressor *Trp53* [539]. To determine whether *Sod2*-deletion affects Trp53 signaling and thus potentially prevents progression of precancerous lesions to PDAC in the *Kras*^{G12D/+}

mouse, I examined expression of six Trp53 target genes in the pancreata of 12 weeks-old mice. Yet, of the six target genes, only *Cdkn1a* was significantly downregulated in female *Kras*^{G12D/+};*Sod2*^{ΔPanc/ΔPanc} compared with female *Kras*^{G12D/+} mice. This is highly surprising, as *Cdkn1a* has been identified as the major Trp53 target gene responsible for mediating Trp53-dependent growth arrest [539]. Consequently, one would expect increased rather than decreased *Cdkn1a* mRNA levels in the female *Kras*^{G12D/+};*Sod2*^{ΔPanc/ΔPanc} compared with female *Kras*^{G12D/+} mice. A possible explanation could be that *Trp53*-inactivation is a late event in pancreatic carcinogenesis [497]. Therefore, the 12 weeks-time point might have been too early as for the Trp53-dependent growth arrest to be effective. In fact, maybe in the initial stages of pancreatic carcinogenesis, when *Sod2*-loss is still tumor promoting, Trp53 signaling might be lower, but in the late stages, when *Sod2*-loss becomes protective, Trp53 signaling and thus *Cdkn1a* expression increase more prominently in the female *Kras*^{G12D/+};*Sod2*^{ΔPanc/ΔPanc} than in the female *Kras*^{G12D/+} pancreata. Thus, the Trp53/*Cdkn1a* signaling cascade might still be an effector of *Sod2*-loss.

2.3. Gender-Specific Effect of *Sod2* Deletion in Pancreatic Carcinogenesis

It is a well-known fact that in many species, including humans, females live longer than males. A possible explanation includes that female body cells produce less ROS and contain higher amounts of enzymatic and non-enzymatic antioxidants. Both factors may prevent aging according to the mitochondrial theory of aging (rev. in [540]).

In addition to increased longevity, females have also been found to have lower susceptibility to various types of cancer, including pancreatic cancer. (rev. in [541, 542]). Besides differences in lifestyle and environmental exposure, several other factors are thought to mediate this gender disparity, including genetic and epigenetic differences, microchimerism, and sex hormones [542]. Among the sex hormones, estrogens, which might not only have antioxidant properties themselves, but might also induce expression of antioxidant genes (rev. in [540]), are likely candidates.

In concert with this idea, various studies have indicated that estrogen might protect from pancreatic cancer [543, 544, 545, 546]. Moreover, in a study with Fischer rats, estrogen significantly inhibited pancreatic carcinogenesis in a chemically induced pancreatic cancer model [547]. Besides, tamoxifen, which is considered a competitive inhibitor of estrogen receptors, might increase PDAC survival in postmenopausal women (rev. in [541]).

In the present study, female *Kras*^{G12D/+} mice were only protected from pancreatic cancer, when *Sod2* was deleted. This may mean that, in the *Kras*^{G12D}-driven pancreatic cancer model, the beneficial effects of estrogen signaling require absence of the *Sod2* protein. Notably, sex hormones are known to regulate mitochondrial function, and conversely, mitochondria are known to be critically involved in sex hormone biosynthesis (rev. in [548]). Additionally, both *Esr1* and *Esr2* may localize to mitochondria (rev. in [548]) and were readily detected in PDAC cell lines [549]. Therefore, I thoroughly tested expression of *Esr1* and *Esr2* in the pancreata of the *Kras*^{G12D/+};*Sod2*^{ΔPanc/ΔPanc} and *Kras*^{G12D/+} mice. Interestingly, while *Esr2* expression seemed to be, if at all, only mildly differentially regulated between the different genotypes, *Esr1* mRNA seemed to be increased predominantly in young (4 weeks) and young adult (12 weeks) mice, but not in middle-aged (24 weeks)

Kras^{G12D/+}; *Sod2*^{ΔPanc/ΔPanc} compared with *Kras*^{G12D/+} mice. In contrast, *Esr1* protein levels were markedly reduced in all age groups, but most prominently in middle-aged *Kras*^{G12D/+}; *Sod2*^{ΔPanc/ΔPanc} compared with *Kras*^{G12D/+} mice. As *Esr1* protein degradation accompanies transcriptional activation of estrogen target genes [550, 551], reduced *Esr1* protein levels may indicate active estrogen/*Esr1* signaling. Moreover, the shift from cytosolic to nuclear localization observed for *Esr1* in normal acinar tissue or precancerous lesions respectively, provides an indication that estrogen signaling may play a role in pancreatic cancer development.

To test whether estrogen/*Esr1* signaling might be differentially active in the *Kras*^{G12D/+}; *Sod2*^{ΔPanc/ΔPanc} compared with the *Kras*^{G12D/+} pancreata, I next tested expression of six presumptive *Esr1* target genes.

For none of these genes, expression differed significantly between the two genotypes, potentially due to the small sample size of three animals per genotype and gender. However, both *Tyms* and *Rara*, genes that are reported to be upregulated by *Esr1* [552, 553], were, in fact downregulated in male and unaltered in female *Kras*^{G12D/+}; *Sod2*^{ΔPanc/ΔPanc} compared with *Kras*^{G12D/+} pancreata. A clear trend was also discernable for *Ddr2*, which might be upregulated in male and female *Kras*^{G12D/+}; *Sod2*^{ΔPanc/ΔPanc} compared with *Kras*^{G12D/+} pancreata. Remarkably, Dr. Henrik Einwächter identified *Ddr2* as a gene, which might be downregulated *Esr1*-dependently in microarray analyses (unpublished data).

Thus, *Esr1* target gene expression data suggest that, if *Esr1* signaling plays a role in mediating the effects of *Sod2*-loss in the pancreas of the *Kras*^{G12D} mouse model, it might attribute to reduced estrogen responsiveness rather than to increased *Esr1* signaling.

A potential mechanisms of how *Esr1* signaling may be implicated in mediating the gender-specific benefit in the pancreatic cancer mouse models of the present study involves co-regulatory activity with the transcription factor forkhead box A1 (*Foxa1*): *Esr1*/*Foxa1* co-signaling was found to mediate gender-specific protection of female mice from experimentally induced hepatocellular carcinoma (HCC; [554]).

Additionally, Naugler and colleagues, who also studied the phenomenon of female protection from HCC, found that enhanced *Esr1* signaling protected mice from experimentally induced HCC by reducing interleukin 6 (*Il6*) expression [555].

Both of these possibilities have not been assessed in the present study and will be subject of further studies in our laboratory.

Importantly, *Nfkb*, which is regulated by ROS (see II.2.3.2), is also known to down-regulate *Il6* [556]. Dependence of cancer protection on a certain permissive level of ROS, potentially via *Nfkb* regulation, may provide an explanation for why, in the present study, female *Kras*^{G12D/+} mice were only protected from pancreatic cancer, when *Sod2* was deleted.

Noteworthy, another study in our laboratory has recently recapitulated the observation that the absence of an antioxidant enzyme (in this case *Txnrd2*) protects female, but not (or to a lesser extent) male mice from PDAC (unpublished results). Therefore, if *Esr1* signaling is not involved in mediating the beneficial effects of antioxidant enzyme inactivation, some other gender-specific factor should be.

2.4. *Trp53*-Dependency of the Gender-Specific Benefit of *Sod2* Deletion in Pancreatic Cancer

In the beginning of the present study, all analyses (i.e. integrity of tissue, numbers of preneoplastic lesions, deposition of collagen, prevalence of and proneness to ADM) indicated that *Sod2*-loss accelerated *Kras*^{G12D}-dependent pancreatic carcinogenesis in the mouse and that *Sod2* might be a classical tumor suppressor gene, as previously anticipated (see V.2.1). Therefore, I focused my further analyses mainly on two age time points, namely 12 (young adulthood) and 24 weeks (young middle-aged), when *Kras*^{G12D/+} mice usually already present with all stages of premalignant lesions, but no full-blown cancer, yet [28]. But later in the study, when the protective effect of *Sod2*-deletion became apparent, examination of later time points, when *Kras*^{G12D/+} mice usually already developed tumors seemed highly required.

However, as *Kras*^{G12D/+} mice generally develop pancreatic cancer only with long latency and at low penetrance [557], choosing an appropriate time point is not easy. Moreover, pronounced fat deposition in the pancreata of aged mice may complicate pancreas-specific analyses (personal observation).

Therefore, I sought to reexamine the effects of pancreatic *Sod2* deletion in a faster and more stringent PDAC model, which combines pancreas-specific oncogenic *Kras* activation with *Trp53* inactivation [32].

Strikingly, *Sod2* deletion significantly prolonged survival of the female *p53*^{ΔPanc/+};*Kras*^{G12D/+} mice. A similar, but less pronounced and not significant trend was also observed for the male *p53*^{ΔPanc/+};*Kras*^{G12D/+} mice. These findings not only underpin the previous observations that *Sod2*-loss does not accelerate, but rather protect female mice from PDAC formation, but also further argue against a role of *Sod2* as a classical tumor suppressor gene.

Even more surprisingly, *Sod2* deletion did not affect survival of male or female *p53*^{ΔPanc/Panc};*Kras*^{G12D/+} mice. This strongly indicated that, in the pancreas, the beneficial effect of *Sod2* deletion critically depends on the presence of at least one functional allele of *Trp53*.

As in the *p53*^{ΔPanc/+};*Kras*^{G12D/+} mouse, PDAC development always involves loss of the remaining intact allele of *Trp53* [32], a possible explanation for the inhibitory effect of *Sod2*-deletion might involve prevention of the loss of the second *Trp53* allele. Alternatively, *Sod2*-loss could increase signaling from the remaining *Trp53* allele. Both possibilities were tested in the tumors of the *p53*^{ΔPanc/+};*Kras*^{G12D/+} mutant mice and PDAC cell lines derived from these mice. Yet, neither loss of heterozygosity, nor immunohistochemistry analysis of *Trp53* revealed any differences between the *p53*^{ΔPanc/+};*Kras*^{G12D/+};*Sod2*^{ΔPanc/ΔPanc} and the *p53*^{ΔPanc/+};*Kras*^{G12D/+} samples. Nonetheless, both possibilities cannot be fully excluded, as *Sod2*-deficient animals developed tumors much later in life than the *Sod2*-proficient animals. These analyses will therefore have to be repeated in age-matched mice.

Notably, several studies provide evidence that *Sod2* protects from *Trp53*-mediated apoptosis [558, 559, 560]. Thus, a third possibility of how *Sod2*-deletion protects from PDAC might be that late stage premalignant, *Sod2*-proficient cells are protected from

Trp53-mediated cell death and can progress to cancer, whereas *Sod2*-deficient cells are arrested by Trp53. This option may be investigated by analyzing pancreata of age-matched animals at the late stage of tumorigenesis for proliferation, apoptosis, and, potentially, also for senescence.

All the other possible explanations that have already been discussed for the *Kras*^{G12D} model (see V.2.1.) can also not be rejected. Investigating these processes also in the *p53*^{ΔPanc/+};*Kras*^{G12D/+} model may help to clarify whether they are involved in the protective effect of *Sod2* deletion on pancreatic tumorigenesis. Nonetheless, due to the fact that *Sod2* deletion is significantly beneficial only in female *Trp53*-proficient animals strongly suggests that Trp53-dependent processes, as well as female gender-specific properties are critically involved.

2.5. Possible Implications for Human Disease

ROS and other oxidants can inflict oxidative damage that may foster cancer. For this reason and supported by several *in vitro* and preclinical studies, dietary antioxidants were long considered potent anticancer drugs (e.g. [561, 58]; rev. in [367, 562, 563, 564]).

However, while some prospective human clinical trials confirmed this idea, others failed to detect a beneficial effect of dietary antioxidants, in contrast, some even suggested that dietary antioxidant have adverse effects with respects to cancer incidence and/or survival [565, 402, 389, 566, 567].

In line with potential cancer-promoting properties of antioxidants, a very recent preclinical study reported that antioxidant supplementation significantly increased tumor progression and reduced survival in transgenic murine lung cancer model [564].

The present study rather suggests a dual-faced mode of action for antioxidants in cancer: Antioxidants may hinder the early, but promote the late phases of carcinogenesis and thus reduce cancer survival. A similar conclusion has also been drawn by Dhar and colleagues from the results of their study with a chemically induced skin cancer mouse model [537].

A two-edged character of antioxidants could explain, why researchers made partly contradictory observations. Human clinical trials may serve to illustrate the implications of this theory: Within a study population that has low predisposition to cancer, antioxidants may prevent the formation of precancerous lesions. In contrast, within a study population that already has an increased risk of developing cancer, which could mean that precancerous lesions may already be present in a substantial part of the study population, the late-stage cancer-promoting properties of the antioxidants may allow these lesions to progress to full-blown cancer.

In concert with this theory, in a large clinical trial with smokers, lung cancer mortality was significantly increased upon antioxidant supplementation [389].

Moreover, the present study may indicate that women might be even more at risk of the potentially adverse effects of antioxidant supplementation than men.

In any case, in concert with a recently published commentary by Chandel and Tuveson, [568], the herein presented results plead, that careful consideration should be taken when supplementing cancer patients with antioxidants.

Finally, as suggested by Pani and colleagues [569], some additional thought should be given to the question, whether *Sod2* might serve as a novel target in treating pancreatic cancer in women. A first step to answering this question may lie in preclinical studies investigating the effects of *Sod2* inhibitors in different mouse models of pancreatic cancer.

VI. Conclusions

Superoxide dismutases are a class of antioxidant enzymes that convert superoxide to hydrogen peroxide. Thereof, mitochondrial *Sod2* is the only essential isoform as *Sod2* knockout mice succumb early after birth. To my best knowledge, the present thesis represents the first study describing the effects of pancreas-specific *Sod2* knockout in the mouse. It convincingly shows that *Sod2* is fully dispensable to physiological pancreatic development and function.

Oxidants, predominantly reactive oxygen species have been implicated in human cancers, specifically in pancreatic ductal adenocarcinoma (PDAC), one of the deadliest types of cancers. Therefore, in the second part of the present thesis, the effects of pancreas-specific *Sod2* deletion on pancreatic carcinogenesis were assessed, firstly in the context of the relatively mild *Kras*^{G12D}, then in the context of the faster and more stringent *Kras*^{G12D}; *Trp53*^A tumor model mouse.

The present study shows for the first time that compound pancreas-specific *Sod2* knockout mice develop and live completely unaffected. More importantly, it also provides strong evidence that *Sod2* deletion provides gender-specific protection from PDAC in the late, but not in the early stages of tumorigenesis.

These findings might be clinically relevant, as antioxidant supplementation was shown to be ineffective, if not even harmful in treating human cancers. The present study supports these findings. In addition, it indicates that gender-specific differences may have a role in the correlation between antioxidants and cancer and that these differences may be implicated in cancer progression and survival.

VII. References

- 1 Cruickshank, A.H. and Benbow, E.W. (1995) *Pathology of the Pancreas*, Springer London, London.
- 2 Rovasio, R.A. (2010) Development and Structure of the Pancreas, in *Pancreatic cancer* (eds J. Neoptolemos, R. Urrutia, J.L. Abbruzzese, M.W. Büchler), Springer, New York, London, pp. 27-38.
- 3 Kaul, K., Tarr, J.M., Ahmad, S.I., Kohner, E.M., Chibber, R. (2013) Introduction to Diabetes Mellitus, in *Diabetes: An old disease, a new insight* (ed S.I. Ahmad), Springer New York, New York, Austin, Tex., pp. 1-11.
- 4 Andralojc, K.M., Mercalli, A., Nowak, K.W., Albarello, L., Calcagno, R., Luzi, L., Bonifacio, E., Doglioni, C., Piemonti, L. (2009) Ghrelin-producing epsilon cells in the developing and adult human pancreas. *Diabetologia*, **52** (3), 486-493.
- 5 Arnes, L., Hill, J.T., Gross, S., Magnuson, M.A., Sussel, L. (2012) Ghrelin expression in the mouse pancreas defines a unique multipotent progenitor population. *PLoS One*, **7** (12), e52026.
- 6 Ginter, E. and Simko, V. (2013) Global Prevalence and Future of Diabetes Mellitus, in *Diabetes: An old disease, a new insight* (ed S.I. Ahmad), Springer New York, New York, Austin, Tex., pp. 35-41.
- 7 Maraschin, J.d.F. (2013) Classification of Diabetes, in *Diabetes: An old disease, a new insight* (ed S.I. Ahmad), Springer New York, New York, Austin, Tex., pp. 12-19.
- 8 Nagar, A.B. and Gorelick, F.S. (2005) Epidemiology and Pathophysiology of Acute Pancreatitis, in *Pancreatitis and its complications* (ed C.E. Forsmark), Humana Press, Totowa, N.J, pp. 3-15.
- 9 De Dios, I. (2010) Inflammatory role of the acinar cells during acute pancreatitis. *World J Gastrointest Pharmacol Ther*, **1** (1), 15-20.
- 10 Ulrich, C.D. (2005) Other Causes of Acute Pancreatitis, in *Pancreatitis and its complications* (ed C.E. Forsmark), Humana Press, Totowa, N.J, pp. 51-61.
- 11 Whitcomb, D.C. (2005) Risk, Etiology, and Pathophysiology of Chronic Pancreatitis, in *Pancreatitis and its complications* (ed C.E. Forsmark), Humana Press, Totowa, N.J, pp. 149-169.
- 12 Jupp, J., Fine, D., Johnson, C.D. (2010) The epidemiology and socioeconomic impact of chronic pancreatitis. *Best Pract Res Clin Gastroenterol*, **24** (3), 219-231.
- 13 Lowenfels, A.B., Maisonneuve, P., Cavallini, G., Ammann, R.W., Lankisch, P.G., Andersen, J.R., Dimagno, E.P., Andren-Sandberg, A., Domellof, L. (1993) Pancreatitis and the risk of pancreatic cancer. international pancreatitis study group. *N Engl J Med*, **328** (20), 1433-1437.
- 14 American Cancer Society (2013) Cancer facts & figures 2013. *Atlanta: American Cancer Society*.
- 15 Volmar, K.E., Routbort, M.J., Jones, C.K., Xie, H.B. (2004) Primary pancreatic lymphoma evaluated by fine-needle aspiration: findings in 14 cases. *Am J Clin Pathol*, **121** (6), 898-903.
- 16 Brown, P.C., Hart, M.J., White, T.T. (1987) Pancreatic lymphoma, diagnosis and management. *Int J Pancreatol*, **2** (2), 93-99.
- 17 Adsay, N.V., Andea, A., Basturk, O., Kilinc, N., Nassar, H., Cheng, J.D. (2004) Secondary tumors of the pancreas: an analysis of a surgical and autopsy database and review of the literature. *Virchows Arch*, **444** (6), 527-535.
- 18 Mulkeen, A.-L., Yoo, P.-S., Cha, C. (2006) Less common neoplasms of the pancreas. *World J Gastroenterol*, **12** (20), 3180-3185.
- 19 Hezel, A.F., Kimmelman, A.C., Stanger, B.Z., Bardeesy, N., Depinho, R.A. (2006) Genetics and biology of pancreatic ductal adenocarcinoma. *Genes Dev*, **20** (10), 1218-1249.
- 20 Hruban, R.H., Takaori, K., Klimstra, D.S., Adsay, N.V., Albores-Saavedra, J., Biankin, A.V., Biankin, S.A., Compton, C., Fukushima, N., Furukawa, T., Goggins, M., Kato, Y., Kloppel, G., Longnecker, D.S., Luttges, J., Maitra, A., Offerhaus, G.J.A., Shimizu, M., Yonezawa, S. (2004) An illustrated consensus on the classification of pancreatic intraepithelial neoplasia and intraductal papillary mucinous neoplasms. *Am J Surg Pathol*, **28** (8), 977-987.
- 21 Koorstra, J.-B.M., Feldmann, G., Habbe, N., Maitra, A. (2008) Morphogenesis of pancreatic cancer: role of pancreatic intraepithelial neoplasia (PanINs). *Langenbecks Arch Surg*, **393** (4), 561-570.
- 22 Papavramidis, T. and Papavramidis, S. (2005) Solid pseudopapillary tumors of the pancreas: review of 718 patients reported in English literature. *J Am Coll Surg*, **200** (6), 965-972.

- 23 Holen, K.D., Klimstra, D.S., Hummer, A., Gonen, M., Conlon, K., Brennan, M., Saltz, L.B. (2002) Clinical characteristics and outcomes from an institutional series of acinar cell carcinoma of the pancreas and related tumors. *J Clin Oncol*, **20** (24), 4673-4678.
- 24 Brown, H.A., Dotto, J., Robert, M., Salem, R.R. (2005) Squamous cell carcinoma of the pancreas. *J Clin Gastroenterol*, **39** (10), 915-919.
- 25 Klimstra, D.S., Wenig, B.M., Adair, C.F., Heffess, C.S. (1995) Pancreatoblastoma. A clinicopathologic study and review of the literature. *Am J Surg Pathol*, **19** (12), 1371-1389.
- 26 Kyriazi, M.A., Arkadopoulos, N., Stafyla, V.K., Yiallourou, A.I., Dafnios, N., Theodosopoulos, T., Kairi-Vassilatou, E., Smyrniotis, V. (2009) Mixed acinar-endocrine carcinoma of the pancreas: a case report and review of the literature. *Cases J*, **2**, 6481.
- 27 Stelow, E.B., Shaco-Levy, R., Bao, F., Garcia, J., Klimstra, D.S. (2010) Pancreatic acinar cell carcinomas with prominent ductal differentiation: Mixed acinar ductal carcinoma and mixed acinar endocrine ductal carcinoma. *Am J Surg Pathol*, **34** (4), 510-518.
- 28 Hingorani, S.R., Petricoin, E.F., Maitra, A., Rajapakse, V., King, C., Jacobetz, M.A., Ross, S., Conrads, T.P., Veenstra, T.D., Hitt, B.A., Kawaguchi, Y., Johann, D., Liotta, L.A., Crawford, H.C., Putt, M.E., Jacks, T., Wright, C.V., Hruban, R.H., Lowy, A.M., Tuveson, D.A. (2003) Preinvasive and invasive ductal pancreatic cancer and its early detection in the mouse. *Cancer Cell*, **4** (6), 437-450.
- 29 Hruban, R.H., Goggins, M., Parsons, J., Kern, S.E. (2000) Progression model for pancreatic cancer. *Clin Cancer Res*, **6** (8), 2969-2972.
- 30 Aguirre, A.J., Bardeesy, N., Sinha, M., Lopez, L., Tuveson, D.A., Horner, J., Redston, M.S., Depinho, R.A. (2003) Activated Kras and Ink4a/Arf deficiency cooperate to produce metastatic pancreatic ductal adenocarcinoma. *Genes Dev*, **17** (24), 3112-3126.
- 31 Hingorani, S.R., Wang, L., Multani, A.S., Combs, C., Deramaudt, T.B., Hruban, R.H., Rustgi, A.K., Chang, S., Tuveson, D.A. (2005) Trp53R172H and KrasG12D cooperate to promote chromosomal instability and widely metastatic pancreatic ductal adenocarcinoma in mice. *Cancer Cell*, **7** (5), 469-483.
- 32 Bardeesy, N., Aguirre, A.J., Chu, G.C., Cheng, K.-H., Lopez, L.V., Hezel, A.F., Feng, B., Brennan, C., Weissleder, R., Mahmood, U., Hanahan, D., Redston, M.S., Chin, L., Depinho, R.A. (2006) Both p16(Ink4a) and the p19(Arf)-p53 pathway constrain progression of pancreatic adenocarcinoma in the mouse. *Proc Natl Acad Sci U S A*, **103** (15), 5947-5952.
- 33 Izeradjene, K., Combs, C., Best, M., Gopinathan, A., Wagner, A., Grady, W.M., Deng, C.-X., Hruban, R.H., Adsay, N.V., Tuveson, D.A., Hingorani, S.R. (2007) Kras(G12D) and Smad4/Dpc4 haploinsufficiency cooperate to induce mucinous cystic neoplasms and invasive adenocarcinoma of the pancreas. *Cancer Cell*, **11** (3), 229-243.
- 34 Davies, C.C., Harvey, E., McMahon, R.F.T., Finegan, K.G., Connor, F., Davis, R.J., Tuveson, D.A., Tournier, C. (2014) Impaired JNK signaling cooperates with KrasG12D expression to accelerate pancreatic ductal adenocarcinoma. *Cancer Res*.
- 35 Distler, M., Aust, D., Weitz, J., Pilarsky, C., Grutzmann, R. (2014) Precursor lesions for sporadic pancreatic cancer: PanIN, IPMN, and MCN. *Biomed Res Int*, **2014**, 474905.
- 36 Ottenhof, N.A., Milne, A.N., Morsink, F.H., Drillenburger, P., Ten, K.F.J., Maitra, A., Offerhaus, G.J. (2009) Pancreatic intraepithelial neoplasia and pancreatic tumorigenesis: of mice and men. *Arch Pathol Lab Med*, **133** (3), 375-381.
- 37 Pylayeva-Gupta, Y., Grabocka, E., Bar-Sagi, D. (2011) RAS oncogenes: weaving a tumorigenic web. *Nat Rev Cancer*, **11** (11), 761-774.
- 38 Maitra, A., Adsay, N.V., Argani, P., Iacobuzio-Donahue, C., Marzo, A. de, Cameron, J.L., Yeo, C.J., Hruban, R.H. (2003) Multicomponent analysis of the pancreatic adenocarcinoma progression model using a pancreatic intraepithelial neoplasia tissue microarray. *Mod Pathol*, **16** (9), 902-912.
- 39 Iovanna, J., Mallmann, M.C., Gonçalves, A., Turrini, O., Dagorn, J.-C. (2012) Current Knowledge on Pancreatic Cancer. *Front. Oncol.*, **2**.
- 40 Iacobuzio-Donahue, C.A. (2012) Genetic evolution of pancreatic cancer: lessons learnt from the pancreatic cancer genome sequencing project. *Gut*, **61** (7), 1085-1094.
- 41 Murtaugh, L.C. (2013) Pathogenesis of Pancreatic Cancer: Lessons from Animal Models. *Toxicol Pathol*.
- 42 Morton, J.P., Jamieson, N.B., Karim, S.A., Athineos, D., Ridgway, R.A., Nixon, C., McKay, C.J., Carter, R., Brunton, V.G., Frame, M.C., Ashworth, A., Oien, K.A., Evans, T.R., Sansom, O.J. (2010) LKB1 haploinsufficiency cooperates with Kras to promote pancreatic cancer through suppression of p21-dependent growth arrest. *Gastroenterology*, **139** (2), 586-97, 597.e1-6.

- 43 Guerra, C., Schuhmacher, A.J., Canamero, M., Grippo, P.J., Verdaguer, L., Perez-Gallego, L., Dubus, P., Sandgren, E.P., Barbacid, M. (2007) Chronic pancreatitis is essential for induction of pancreatic ductal adenocarcinoma by K-Ras oncogenes in adult mice. *Cancer Cell*, **11** (3), 291-302.
- 44 Kopp, J.L., Figura, G. von, Mayes, E., Liu, F.-F., Dubois, C.L., Morris, J.P., 4th., Pan, F.C., Akiyama, H., Wright, C.V.E., Jensen, K., Hebrok, M., Sander, M. (2012) Identification of Sox9-dependent acinar-to-ductal reprogramming as the principal mechanism for initiation of pancreatic ductal adenocarcinoma. *Cancer Cell*, **22** (6), 737-750.
- 45 De La O, J.-P., Emerson, L.L., Goodman, J.L., Froebe, S.C., Illum, B.E., Curtis, A.B., Murtaugh, L.C. (2008) Notch and Kras reprogram pancreatic acinar cells to ductal intraepithelial neoplasia. *Proc Natl Acad Sci U S A*, **105** (48), 18907-18912.
- 46 Habbe, N., Shi, G., Meguid, R.A., Fendrich, V., Esni, F., Chen, H., Feldmann, G., Stoffers, D.A., Konieczny, S.F., Leach, S.D., Maitra, A. (2008) Spontaneous induction of murine pancreatic intraepithelial neoplasia (mPanIN) by acinar cell targeting of oncogenic Kras in adult mice. *Proc Natl Acad Sci U S A*, **105** (48), 18913-18918.
- 47 Morris, J.P., 4th., Cano, D.A., Sekine, S., Wang, S.C., Hebrok, M. (2010) Beta-catenin blocks Kras-dependent reprogramming of acini into pancreatic cancer precursor lesions in mice. *J Clin Invest*, **120** (2), 508-520.
- 48 Ji, B., Tsou, L., Wang, H., Gaiser, S., Chang, D.Z., Daniluk, J., Bi, Y., Grote, T., Longnecker, D.S., Logsdon, C.D. (2009) Ras activity levels control the development of pancreatic diseases. *Gastroenterology*, **137** (3), 1072-82, 1082.e1-6.
- 49 Yan, L.-J. (2014) Pathogenesis of Chronic Hyperglycemia: From Reductive Stress to Oxidative Stress. *J Diabetes Res*, **2014**, 137919.
- 50 Kaneto, H., Katakami, N., Kawamori, D., Miyatsuka, T., Sakamoto, K., Matsuoka, T.-A., Matsuhisa, M., Yamasaki, Y. (2007) Involvement of oxidative stress in the pathogenesis of diabetes. *Antioxid Redox Signal*, **9** (3), 355-366.
- 51 Ihara, Y., Toyokuni, S., Uchida, K., Odaka, H., Tanaka, T., Ikeda, H., Hiai, H., Seino, Y., Yamada, Y. (1999) Hyperglycemia causes oxidative stress in pancreatic beta-cells of GK rats, a model of type 2 diabetes. *Diabetes*, **48** (4), 927-932.
- 52 Gonzalez, A., Schmid, A., Salido, G.M., Camello, P.J., Pariente, J.A. (2002) XOD-catalyzed ROS generation mobilizes calcium from intracellular stores in mouse pancreatic acinar cells. *Cell Signal*, **14** (2), 153-159.
- 53 Leung, P.S. and Chan, Y.C. (2009) Role of oxidative stress in pancreatic inflammation. *Antioxid Redox Signal*, **11** (1), 135-165.
- 54 Furukawa, S., Fujita, T., Shimabukuro, M., Iwaki, M., Yamada, Y., Nakajima, Y., Nakayama, O., Makishima, M., Matsuda, M., Shimomura, I. (2004) Increased oxidative stress in obesity and its impact on metabolic syndrome. *J Clin Invest*, **114** (12), 1752-1761.
- 55 Guyton, K.Z. and Kensler, T.W. (1993) Oxidative mechanisms in carcinogenesis. *Br Med Bull*, **49** (3), 523-544.
- 56 Bandy, B. and Davison, A.J. (1990) Mitochondrial mutations may increase oxidative stress: implications for carcinogenesis and aging? *Free Radic Biol Med*, **8** (6), 523-539.
- 57 Kobayashi, Y., Qi, X., Chen, G. (2012) MK2 regulates Ras oncogenesis through stimulating ROS production. *Genes Cancer*, **3** (7-8), 521-530.
- 58 Sablina, A.A., Budanov, A.V., Ilyinskaya, G.V., Agapova, L.S., Kravchenko, J.E., Chumakov, P.M. (2005) The antioxidant function of the p53 tumor suppressor. *Nat Med*, **11** (12), 1306-1313.
- 59 Mori, K., Shibamura, M., Nose, K. (2004) Invasive potential induced under long-term oxidative stress in mammary epithelial cells. *Cancer Res*, **64** (20), 7464-7472.
- 60 Connor, K.M., Hempel, N., Nelson, K.K., Dabiri, G., Gamarra, A., Belarmino, J., van de Water, L., Mian, B.M., Melendez, J.A. (2007) Manganese superoxide dismutase enhances the invasive and migratory activity of tumor cells. *Cancer Res*, **67** (21), 10260-10267.
- 61 Ishikawa, K., Takenaga, K., Akimoto, M., Koshikawa, N., Yamaguchi, A., Imanishi, H., Nakada, K., Honma, Y., Hayashi, J.-I. (2008) ROS-generating mitochondrial DNA mutations can regulate tumor cell metastasis. *Science*, **320** (5876), 661-664.
- 62 Folkman, J. (1971) Tumor angiogenesis: therapeutic implications. *N Engl J Med*, **285** (21), 1182-1186.
- 63 Erez, N., Truitt, M., Olson, P., Arron, S.T., Hanahan, D. (2010) Cancer-associated fibroblasts are activated in incipient neoplasia to orchestrate tumor-promoting inflammation in an NF-kappaB-dependent manner. *Cancer Cell*, **17** (2), 135-147.

- 64 Visser, K.E. de, Korets, L.V., Coussens, L.M. (2005) De novo carcinogenesis promoted by chronic inflammation is B lymphocyte dependent. *Cancer Cell*, **7** (5), 411-423.
- 65 Karin, M. and Greten, F.R. (2005) NF-kappaB: linking inflammation and immunity to cancer development and progression. *Nat Rev Immunol*, **5** (10), 749-759.
- 66 Mantovani, A., Allavena, P., Sica, A., Balkwill, F. (2008) Cancer-related inflammation. *Nature*, **454** (7203), 436-444.
- 67 Sies, H. (1997) Oxidative stress: oxidants and antioxidants. *Exp Physiol*, **82** (2), 291-295.
- 68 Durackova, Z. (2010) Some current insights into oxidative stress. *Physiol Res*, **59** (4), 459-469.
- 69 Malorni, W., Campesi, I., Straface, E., Vella, S., Franconi, F. (2007) Redox features of the cell: a gender perspective. *Antioxid Redox Signal*, **9** (11), 1779-1801.
- 70 Bergendi, L., Benes, L., Durackova, Z., Ferencik, M. (1999) Chemistry, physiology and pathology of free radicals. *Life Sci*, **65**, 1865-1874.
- 71 Pryor, W.A., Houk, K.N., Foote, C.S., Fukuto, J.M., Ignarro, L.J., Squadrito, G.L., Davies, K.J.A. (2006) Free radical biology and medicine: it's a gas, man! *Am J Physiol Regul Integr Comp Physiol*, **291** (3), R491-511.
- 72 Castello, P.R., David, P.S., McClure, T., Crook, Z., Poyton, R.O. (2006) Mitochondrial cytochrome oxidase produces nitric oxide under hypoxic conditions: implications for oxygen sensing and hypoxic signaling in eukaryotes. *Cell Metab*, **3** (4), 277-287.
- 73 Evgenov, O.V., Pacher, P., Schmidt, P.M., Hasko, G., Schmidt, H.H.H.W., Stasch, J.-P. (2006) NO-independent stimulators and activators of soluble guanylate cyclase: discovery and therapeutic potential. *Nat Rev Drug Discov*, **5** (9), 755-768.
- 74 Moreno-Lopez, B. and Gonzalez-Forero, D. (2006) Nitric oxide and synaptic dynamics in the adult brain: physiopathological aspects. *Rev Neurosci*, **17** (3), 309-357.
- 75 Groote, M.A. de and Fang, F.C. (1995) NO inhibitions: antimicrobial properties of nitric oxide. *Clin Infect Dis*, **21 Suppl 2**, S162-5.
- 76 Blaise, G.A., Gauvin, D., Gangal, M., Authier, S. (2005) Nitric oxide, cell signaling and cell death. *Toxicology*, **208** (2), 177-192.
- 77 Sanctis, F. de, Sandri, S., Ferrarini, G., Pagliarello, I., Sartoris, S., Ugel, S., Marigo, I., Molon, B., Bronte, V. (2014) The Emerging Immunological Role of Post-Translational Modifications by Reactive Nitrogen Species in Cancer Microenvironment. *Front Immunol*, **5**, 69.
- 78 Radi, R., Beckman, J.S., Bush, K.M., Freeman, B.A. (1991) Peroxynitrite-induced membrane lipid peroxidation: the cytotoxic potential of superoxide and nitric oxide. *Arch Biochem Biophys*, **288** (2), 481-487.
- 79 Inoue, S. and Kawanishi, S. (1995) Oxidative DNA damage induced by simultaneous generation of nitric oxide and superoxide. *FEBS Lett*, **371** (1), 86-88.
- 80 Calabrese, V., Cornelius, C., Rizzarelli, E., Owen, J.B., Dinkova-Kostova, A.T., Butterfield, D.A. (2009) Nitric oxide in cell survival: a janus molecule. *Antioxid Redox Signal*, **11** (11), 2717-2739.
- 81 Aranda, E., Lopez-Pedreira, C., La Haba-Rodriguez, J.R. de, Rodriguez-Ariza, A. (2012) Nitric oxide and cancer: the emerging role of S-nitrosylation. *Curr Mol Med*, **12** (1), 50-67.
- 82 Zhang, H. and Forman, H.J. (2012) Glutathione synthesis and its role in redox signaling. *Semin Cell Dev Biol*, **23** (7), 722-728.
- 83 Brannan, R.G. (2010) Reactive sulfur species act as prooxidants in liposomal and skeletal muscle model systems. *J Agric Food Chem*, **58** (6), 3767-3771.
- 84 Giles, G.I., Tasker, K.M., Jacob, C. (2002) Oxidation of biological thiols by highly reactive disulfide-S-oxides. *Gen Physiol Biophys*, **21** (1), 65-72.
- 85 Juranek, I., Nikitovic, D., Kouretas, D., Wallace Hayes, A., Tsatsakis, A.M. (2013) Biological importance of reactive oxygen species in relation to difficulties of treating pathologies involving oxidative stress by exogenous antioxidants. *Food Chem Toxicol*.
- 86 Birben, E., Sahiner, U.M., Sackesen, C., Erzurum, S., Kalayci, O. (2012) Oxidative stress and antioxidant defense. *World Allergy Organ J*, **5** (1), 9-19.
- 87 Brady, N.R., Hamacher-Brady, A., Westerhoff, H.V., Gottlieb, R.A. (2006) A wave of reactive oxygen species (ROS)-induced ROS release in a sea of excitable mitochondria. *Antioxid Redox Signal*, **8** (9-10), 1651-1665.
- 88 Halliwell, B. and Gutteridge, J.M. (eds) (1989) *Free radicals in biology and medicine*, 2nd edn, Clarendon Pr., Oxford.
- 89 Powers, S.K. and Jackson, M.J. (2008) Exercise-induced oxidative stress: cellular mechanisms and impact on muscle force production. *Physiol Rev*, **88** (4), 1243-1276.

- 90 Mello Filho, A.C. and Meneghini, R. (1984) In vivo formation of single-strand breaks in DNA by hydrogen peroxide is mediated by the Haber-Weiss reaction. *Biochim Biophys Acta*, **781** (1-2), 56-63.
- 91 Bergamini, C.M., Gambetti, S., Dondi, A., Cervellati, C. (2004) Oxygen, reactive oxygen species and tissue damage. *Curr Pharm Des*, **10** (14), 1611-1626.
- 92 Murphy, M.P., Packer, M.A., Scarlett, J.L., Martin, S.W. (1998) Peroxynitrite: a biologically significant oxidant. *Gen Pharmacol*, **31** (2), 179-186.
- 93 Pullar, J.M., Vissers, M.C., Winterbourn, C.C. (2000) Living with a killer: the effects of hypochlorous acid on mammalian cells. *IUBMB Life*, **50** (4-5), 259-266.
- 94 Folkes, L.K., Candeias, L.P., Wardman, P. (1995) Kinetics and mechanisms of hypochlorous acid reactions. *Arch Biochem Biophys*, **323** (1), 120-126.
- 95 Pullar, J.M., Winterbourn, C.C., Vissers, M.C. (1999) Loss of GSH and thiol enzymes in endothelial cells exposed to sublethal concentrations of hypochlorous acid. *Am J Physiol*, **277** (4 Pt 2), H1505-12.
- 96 Whiteman, M., Rose, P., Siau, J.L., Cheung, N.S., Tan, G.S., Halliwell, B., Armstrong, J.S. (2005) Hypochlorous acid-mediated mitochondrial dysfunction and apoptosis in human hepatoma HepG2 and human fetal liver cells: role of mitochondrial permeability transition. *Free Radic Biol Med*, **38** (12), 1571-1584.
- 97 Whiteman, M., Jenner, A., Halliwell, B. (1997) Hypochlorous acid-induced base modifications in isolated calf thymus DNA. *Chem Res Toxicol*, **10** (11), 1240-1246.
- 98 Triantaphylides, C., Krischke, M., Hoeberichts, F.A., Ksas, B., Gresser, G., Havaux, M., van Breusegem, F., Mueller, M.J. (2008) Singlet oxygen is the major reactive oxygen species involved in photooxidative damage to plants. *Plant Physiol*, **148** (2), 960-968.
- 99 Nam, T.-W., Ziegelhoffer, E.C., Lemke, R.A.S., Donohue, T.J. (2013) Proteins needed to activate a transcriptional response to the reactive oxygen species singlet oxygen. *MBio*, **4** (1), e00541-12.
- 100 Negre-Salvayre, A., Coatrieux, C., Ingueneau, C., Salvayre, R. (2008) Advanced lipid peroxidation end products in oxidative damage to proteins. Potential role in diseases and therapeutic prospects for the inhibitors. *Br J Pharmacol*, **153** (1), 6-20.
- 101 Valko, M., Izakovic, M., Mazur, M., Rhodes, C.J., Telser, J. (2004) Role of oxygen radicals in DNA damage and cancer incidence. *Mol Cell Biochem*, **266** (1-2), 37-56.
- 102 Santos, J.H., Meyer, J.N., Mandavilli, B.S., van Houten, B. (2006) Quantitative PCR-based measurement of nuclear and mitochondrial DNA damage and repair in mammalian cells. *Methods Mol Biol*, **314**, 183-199.
- 103 Navarro, A. and Boveris, A. (2007) The mitochondrial energy transduction system and the aging process. *Am J Physiol Cell Physiol*, **292** (2), C670-86.
- 104 Valko, M., Leibfritz, D., Moncol, J., Cronin, M., Mazur, M., Telser, J. (2007) Free radicals and antioxidants in normal physiological functions and human disease. *Int J Biochem Cell Biol*, **39** (1), 44-84.
- 105 Muller, F.L., Liu, Y., van Remmen, H. (2004) Complex III releases superoxide to both sides of the inner mitochondrial membrane. *J Biol Chem*, **279** (47), 49064-49073.
- 106 Migliaccio, E., Giorgio, M., Mele, S., Pelicci, G., Reboldi, P., Pandolfi, P.P., Lanfrancone, L., Pelicci, P.G. (1999) The p66shc adaptor protein controls oxidative stress response and life span in mammals. *Nature*, **402** (6759), 309-313.
- 107 Giorgio, M., Migliaccio, E., Orsini, F., Paolucci, D., Moroni, M., Contursi, C., Pelliccia, G., Luzi, L., Minucci, S., Marcaccio, M., Pinton, P., Rizzuto, R., Bernardi, P., Paolucci, F., Pelicci, P.G. (2005) Electron transfer between cytochrome c and p66Shc generates reactive oxygen species that trigger mitochondrial apoptosis. *Cell*, **122** (2), 221-233.
- 108 Menini, S., Amadio, L., Oddi, G., Ricci, C., Pesce, C., Pugliese, F., Giorgio, M., Migliaccio, E., Pelicci, P., Iacobini, C., Pugliese, G. (2006) Deletion of p66Shc longevity gene protects against experimental diabetic glomerulopathy by preventing diabetes-induced oxidative stress. *Diabetes*, **55** (6), 1642-1650.
- 109 Napoli, C., Martin-Padura, I., Nigris, F. de, Giorgio, M., Mansueto, G., Somma, P., Condorelli, M., Sica, G., Rosa, G. de, Pelicci, P. (2003) Deletion of the p66Shc longevity gene reduces systemic and tissue oxidative stress, vascular cell apoptosis, and early atherogenesis in mice fed a high-fat diet. *Proc Natl Acad Sci U S A*, **100** (4), 2112-2116.
- 110 Rota, M., LeCapitaine, N., Hosoda, T., Boni, A., Angelis, A. de, Padin-Iruegas, M.E., Esposito, G., Vitale, S., Urbanek, K., Casarsa, C., Giorgio, M., Luscher, T.F., Pelicci, P.G., Anversa, P.,

- Leri, A., Kajstura, J. (2006) Diabetes promotes cardiac stem cell aging and heart failure, which are prevented by deletion of the p66shc gene. *Circ Res*, **99** (1), 42-52.
- 111 Edmondson, D.E., Mattevi, A., Binda, C., Li, M., Hubalek, F. (2004) Structure and mechanism of monoamine oxidase. *Curr Med Chem*, **11** (15), 1983-1993.
- 112 Hauptmann, N., Grimsby, J., Shih, J.C., Cadenas, E. (1996) The metabolism of tyramine by monoamine oxidase A/B causes oxidative damage to mitochondrial DNA. *Arch Biochem Biophys*, **335** (2), 295-304.
- 113 Maurel, A., Hernandez, C., Kunduzova, O., Bompard, G., Cambon, C., Parini, A., Frances, B. (2003) Age-dependent increase in hydrogen peroxide production by cardiac monoamine oxidase A in rats. *Am J Physiol Heart Circ Physiol*, **284** (4), H1460-7.
- 114 Bianchi, P., Kunduzova, O., Masini, E., Cambon, C., Bani, D., Raimondi, L., Seguelas, M.-H., Nistri, S., Colucci, W., Leducq, N., Parini, A. (2005) Oxidative stress by monoamine oxidase mediates receptor-independent cardiomyocyte apoptosis by serotonin and postischemic myocardial injury. *Circulation*, **112** (21), 3297-3305.
- 115 Minakami, R. and Sumimoto, H. (2006) Phagocytosis-coupled activation of the superoxide-producing phagocyte oxidase, a member of the NADPH oxidase (nox) family. *Int J Hematol*, **84** (3), 193-198.
- 116 Roder, J.C., Helfand, S.L., Werkmeister, J., McGarry, R., Beaumont, T.J., Duwe, A. (1982) Oxygen intermediates are triggered early in the cytolytic pathway of human NK cells. *Nature*, **298** (5874), 569-572.
- 117 Krotz, F., Sohn, H.Y., Gloc, T., Zahler, S., Riexinger, T., Schiele, T.M., Becker, B.F., Theisen, K., Klaus, V., Pohl, U. (2002) NAD(P)H oxidase-dependent platelet superoxide anion release increases platelet recruitment. *Blood*, **100** (3), 917-924.
- 118 Proctor, P., Kirkpatrick, D., McGinness, J. (1977) A superoxide-producing system in the conjunctival mucus thread. *Invest Ophthalmol Vis Sci*, **16** (8), 762-765.
- 119 Griendling, K.K., Minieri, C.A., Ollerenshaw, J.D., Alexander, R.W. (1994) Angiotensin II stimulates NADH and NADPH oxidase activity in cultured vascular smooth muscle cells. *Circ Res*, **74** (6), 1141-1148.
- 120 Meier, B., Cross, A.R., Hancock, J.T., Kaup, F.J., Jones, O.T. (1991) Identification of a superoxide-generating NADPH oxidase system in human fibroblasts. *Biochem J*, **275** (Pt 1), 241-245.
- 121 Sztatowski, T.P. and Nathan, C.F. (1991) Production of large amounts of hydrogen peroxide by human tumor cells. *Cancer Res*, **51** (3), 794-798.
- 122 Li, Q., Harraz, M.M., Zhou, W., Zhang, L.N., Ding, W., Zhang, Y., Eggleston, T., Yeaman, C., Banfi, B., Engelhardt, J.F. (2006) Nox2 and Rac1 regulate H₂O₂-dependent recruitment of TRAF6 to endosomal interleukin-1 receptor complexes. *Mol Cell Biol*, **26** (1), 140-154.
- 123 van Buul, J.D., Fernandez-Borja, M., Anthony, E.C., Hordijk, P.L. (2005) Expression and localization of NOX2 and NOX4 in primary human endothelial cells. *Antioxid Redox Signal*, **7** (3-4), 308-317.
- 124 Dong-Yun, S., Yu-Ru, D., Shan-Lin, L., Ya-Dong, Z., Lian, W. (2003) Redox stress regulates cell proliferation and apoptosis of human hepatoma through Akt protein phosphorylation. *FEBS Lett*, **542** (1-3), 60-64.
- 125 Harrison, R. (2002) Structure and function of xanthine oxidoreductase: where are we now? *Free Radic Biol Med*, **33** (6), 774-797.
- 126 Boveris, A., Oshino, N., Chance, B. (1972) The cellular production of hydrogen peroxide. *Biochem J*, **128** (3), 617-630.
- 127 Schrader, M. and Fahimi, H.D. (2004) Mammalian peroxisomes and reactive oxygen species. *Histochem Cell Biol*, **122** (4), 383-393.
- 128 Bernhardt, R. (1996) Cytochrome P450: structure, function, and generation of reactive oxygen species. *Rev Physiol Biochem Pharmacol*, **127**, 137-221.
- 129 Xia, Y., Dawson, V.L., Dawson, T.M., Snyder, S.H., Zweier, J.L. (1996) Nitric oxide synthase generates superoxide and nitric oxide in arginine-depleted cells leading to peroxynitrite-mediated cellular injury. *Proc Natl Acad Sci U S A*, **93** (13), 6770-6774.
- 130 Riley, P.A. (1994) Free radicals in biology: oxidative stress and the effects of ionizing radiation. *Int J Radiat Biol*, **65** (1), 27-33.
- 131 Cadet, J., Douki, T., Gasparutto, D., Ravanat, J.-L. (2003) Oxidative damage to DNA: formation, measurement and biochemical features. *Mutat Res*, **531** (1-2), 5-23.
- 132 Valko, M., Rhodes, C. J., Moncol, J., Izakovic, M., Mazur, M. (2006) Free radicals, metals and antioxidants in oxidative stress-induced cancer. *Chem Biol Interact*, **160** (1), 1-40.

- 133 Halliwell, B. and Cross, C.E. (1994) Oxygen-derived species: their relation to human disease and environmental stress. *Environ Health Perspect*, **102 Suppl 10**, 5-12.
- 134 Church, D.F. and Pryor, W.A. (1985) Free-radical chemistry of cigarette smoke and its toxicological implications. *Environ Health Perspect*, **64**, 111-126.
- 135 Duong, C., Seow, H.J., Bozinovski, S., Crack, P.J., Anderson, G.P., Vlahos, R. (2010) Glutathione peroxidase-1 protects against cigarette smoke-induced lung inflammation in mice. *Am J Physiol Lung Cell Mol Physiol*, **299** (3), L425-33.
- 136 Bradley, K.A., Badrinath, S., Bush, K., Boyd-Wickizer, J., Anawalt, B. (1998) Medical risks for women who drink alcohol. *J Gen Intern Med*, **13** (9), 627-639.
- 137 Purohit, V., Khalsa, J., Serrano, J. (2005) Mechanisms of alcohol-associated cancers: introduction and summary of the symposium. *Alcohol*, **35** (3), 155-160.
- 138 Navasumrit, P., Ward, T.H., Dodd, N.J., O'Connor, P.J. (2000) Ethanol-induced free radicals and hepatic DNA strand breaks are prevented in vivo by antioxidants: effects of acute and chronic ethanol exposure. *Carcinogenesis*, **21** (1), 93-99.
- 139 Andican, G., Gelisgen, R., Unal, E., Tortum, O.-B., Dervisoglu, S., Karahasanoglu, T., Burcak, G. (2005) Oxidative stress and nitric oxide in rats with alcohol-induced acute pancreatitis. *World J Gastroenterol*, **11** (15), 2340-2345.
- 140 Wu, D. and Cederbaum, A.I. (2003) Alcohol, oxidative stress, and free radical damage. *Alcohol Res Health*, **27** (4), 277-284.
- 141 Ioannou, G.N., Dominitz, J.A., Weiss, N.S., Heagerty, P.J., Kowdley, K.V. (2004) The effect of alcohol consumption on the prevalence of iron overload, iron deficiency, and iron deficiency anemia. *Gastroenterology*, **126** (5), 1293-1301.
- 142 Koop, D.R., Crump, B.L., Nordblom, G.D., Coon, M.J. (1985) Immunochemical evidence for induction of the alcohol-oxidizing cytochrome P-450 of rabbit liver microsomes by diverse agents: ethanol, imidazole, trichloroethylene, acetone, pyrazole, and isoniazid. *Proc Natl Acad Sci U S A*, **82** (12), 4065-4069.
- 143 Albano, E., Clot, P., Morimoto, M., Tomasi, A., Ingelman-Sundberg, M., French, S.W. (1996) Role of cytochrome P4502E1-dependent formation of hydroxyethyl free radical in the development of liver damage in rats intragastrically fed with ethanol. *Hepatology*, **23** (1), 155-163.
- 144 Sutandyo, N. (2010) Nutritional carcinogenesis. *Acta Med Indones*, **42** (1), 36-42.
- 145 Dix, T.A. and Aikens, J. (1993) Mechanisms and biological relevance of lipid peroxidation initiation. *Chem Res Toxicol*, **6** (1), 2-18.
- 146 Marnett, L.J. (1999) Lipid peroxidation-DNA damage by malondialdehyde. *Mutat Res*, **424** (1-2), 83-95.
- 147 Benedetti, A., Comporti, M., Esterbauer, H. (1980) Identification of 4-hydroxynonenal as a cytotoxic product originating from the peroxidation of liver microsomal lipids. *Biochim Biophys Acta*, **620** (2), 281-296.
- 148 Pryor, W.A. and Stanley, J.P. (1975) Letter: A suggested mechanism for the production of malonaldehyde during the autoxidation of polyunsaturated fatty acids. Nonenzymatic production of prostaglandin endoperoxides during autoxidation. *J Org Chem*, **40** (24), 3615-3617.
- 149 Basu, A.K. and Marnett, L.J. (1983) Unequivocal demonstration that malondialdehyde is a mutagen. *Carcinogenesis*, **4** (3), 331-333.
- 150 Fong, K.L., McCay, P.B., Poyer, J.L., Keele, B.B., Misra, H. (1973) Evidence that peroxidation of lysosomal membranes is initiated by hydroxyl free radicals produced during flavin enzyme activity. *J Biol Chem*, **248** (22), 7792-7797.
- 151 Svingen, B.A., Buege, J.A., O'Neal, F.O., Aust, S.D. (1979) The mechanism of NADPH-dependent lipid peroxidation. The propagation of lipid peroxidation. *J Biol Chem*, **254** (13), 5892-5899.
- 152 Roubal, W.T. and Tappel, A.L. (1966) Polymerization of proteins induced by free-radical lipid peroxidation. *Arch Biochem Biophys*, **113** (1), 150-155.
- 153 Nielsen, H. (1981) Covalent binding of peroxidized phospholipid to protein: III. Reaction of individual phospholipids with different proteins. *Lipids*, **16** (4), 215-222.
- 154 Girotti, A.W. (1985) Mechanisms of lipid peroxidation. *J Free Radic Biol Med*, **1** (2), 87-95.
- 155 Quinn, M.T., Parthasarathy, S., Fong, L.G., Steinberg, D. (1987) Oxidatively modified low density lipoproteins: a potential role in recruitment and retention of monocyte/macrophages during atherogenesis. *Proc Natl Acad Sci U S A*, **84** (9), 2995-2998.

- 156 Breen, A.P. and Murphy, J.A. (1995) Reactions of oxyl radicals with DNA. *Free Radic Biol Med*, **18** (6), 1033-1077.
- 157 Aruoma, O.I., Halliwell, B., Gajewski, E., Dizdaroglu, M. (1989) Damage to the bases in DNA induced by hydrogen peroxide and ferric ion chelates. *J Biol Chem*, **264** (34), 20509-20512.
- 158 Lesko, S.A., Lorentzen, R.J., Ts'o, P.O. (1980) Role of superoxide in deoxyribonucleic acid strand scission. *Biochemistry*, **19** (13), 3023-3028.
- 159 Blakely, W.F., Fuciarelli, A.F., Wegher, B.J., Dizdaroglu, M. (1990) Hydrogen peroxide-induced base damage in deoxyribonucleic acid. *Radiat Res*, **121** (3), 338-343.
- 160 Pryor, W.A. (1988) Why is the hydroxyl radical the only radical that commonly adds to DNA? Hypothesis: it has a rare combination of high electrophilicity, high thermochemical reactivity, and a mode of production that can occur near DNA. *Free Radic Biol Med*, **4** (4), 219-223.
- 161 Sagher, D. and Strauss, B. (1983) Insertion of nucleotides opposite apurinic/aprimidinic sites in deoxyribonucleic acid during in vitro synthesis: uniqueness of adenine nucleotides. *Biochemistry*, **22** (19), 4518-4526.
- 162 Wallace, S.S. (1998) Enzymatic processing of radiation-induced free radical damage in DNA. *Radiat Res*, **150** (5 Suppl), S60-79.
- 163 Caldecott, K.W. (2003) Protein-protein interactions during mammalian DNA single-strand break repair. *Biochem Soc Trans*, **31** (Pt 1), 247-251.
- 164 Fraga, C.G., Shigenaga, M.K., Park, J.W., Degan, P., Ames, B.N. (1990) Oxidative damage to DNA during aging: 8-hydroxy-2'-deoxyguanosine in rat organ DNA and urine. *Proc Natl Acad Sci U S A*, **87** (12), 4533-4537.
- 165 Wood, M.L., Dizdaroglu, M., Gajewski, E., Essigmann, J.M. (1990) Mechanistic studies of ionizing radiation and oxidative mutagenesis: genetic effects of a single 8-hydroxyguanine (7-hydro-8-oxoguanine) residue inserted at a unique site in a viral genome. *Biochemistry*, **29** (30), 7024-7032.
- 166 Moriya, M. (1993) Single-stranded shuttle phagemid for mutagenesis studies in mammalian cells: 8-oxoguanine in DNA induces targeted G.C--T.A transversions in simian kidney cells. *Proc Natl Acad Sci U S A*, **90** (3), 1122-1126.
- 167 Shibutani, S., Bodepudi, V., Johnson, F., Grollman, A.P. (1993) Translesional synthesis on DNA templates containing 8-oxo-7,8-dihydrodeoxyadenosine. *Biochemistry*, **32** (17), 4615-4621.
- 168 Kalam, M.A., Haraguchi, K., Chandani, S., Loechler, E.L., Moriya, M., Greenberg, M.M., Basu, A.K. (2006) Genetic effects of oxidative DNA damages: comparative mutagenesis of the imidazole ring-opened formamidopyrimidines (Fapy lesions) and 8-oxo-purines in simian kidney cells. *Nucleic Acids Res*, **34** (8), 2305-2315.
- 169 Zuo, S., Boorstein, R.J., Teebor, G.W. (1995) Oxidative damage to 5-methylcytosine in DNA. *Nucleic Acids Res*, **23** (16), 3239-3243.
- 170 Evans, J., Maccabee, M., Hatahet, Z., Courcelle, J., Bockrath, R., Ide, H., Wallace, S. (1993) Thymine ring saturation and fragmentation products: lesion bypass, misinsertion and implications for mutagenesis. *Mutat Res*, **299** (3-4), 147-156.
- 171 Dypbukt, J.M., Thor, H., Nicotera, P. (1990) Intracellular Ca²⁺ chelators prevent DNA damage and protect hepatoma 1C1C7 cells from quinone-induced cell killing. *Free Radic Res Commun*, **8** (4-6), 347-354.
- 172 Sodum, R.S. and Chung, F.L. (1988) 1,N²-ethenodeoxyguanosine as a potential marker for DNA adduct formation by trans-4-hydroxy-2-nonenal. *Cancer Res*, **48** (2), 320-323.
- 173 Mao, H., Schnetz-Boutaud, N.C., Weisenseel, J.P., Marnett, L.J., Stone, M.P. (1999) Duplex DNA catalyzes the chemical rearrangement of a malondialdehyde deoxyguanosine adduct. *Proc Natl Acad Sci U S A*, **96** (12), 6615-6620.
- 174 Spencer, J.P., Whiteman, M., Jenner, A., Halliwell, B. (2000) Nitrite-induced deamination and hypochlorite-induced oxidation of DNA in intact human respiratory tract epithelial cells. *Free Radic Biol Med*, **28** (7), 1039-1050.
- 175 Levine, R.L. (1983) Oxidative modification of glutamine synthetase. II. Characterization of the ascorbate model system. *J Biol Chem*, **258** (19), 11828-11833.
- 176 Welch, K.D., van Eden, M.E., Aust, S.D. (2001) Modification of ferritin during iron loading. *Free Radic Biol Med*, **31** (8), 999-1006.
- 177 Berlett, B.S. and Stadtman, E.R. (1997) Protein oxidation in aging, disease, and oxidative stress. *J Biol Chem*, **272** (33), 20313-20316.
- 178 Go, Y.-M., Roede, J.R., Walker, D.I., Duong, D.M., Seyfried, N.T., Orr, M., Liang, Y., Pennell, K.D., Jones, D.P. (2013) Selective targeting of the cysteine proteome by thioredoxin and glutathione redox systems. *Mol Cell Proteomics*, **12** (11), 3285-3296.

- 179 Stadtman, E.R. (2004) Role of oxidant species in aging. *Curr Med Chem*, **11** (9), 1105-1112.
- 180 Ray, P.D., Huang, B.-W., Tsuji, Y. (2012) Reactive oxygen species (ROS) homeostasis and redox regulation in cellular signaling. *Cell Signal*, **24** (5), 981-990.
- 181 Garrison, W.M. (1987) Reaction Mechanisms in the Radiolysis of Peptides, Polypeptides, and Proteins. *Chem. Rev*, **87**, 381-398.
- 182 Uchida, K., Kato, Y., Kawakishi, S. (1990) A novel mechanism for oxidative cleavage of prolyl peptides induced by the hydroxyl radical. *Biochem Biophys Res Commun*, **169** (1), 265-271.
- 183 Monnier, V.M. (1990) Nonenzymatic glycosylation, the Maillard reaction and the aging process. *J Gerontol*, **45** (4), B105-11.
- 184 Uchida, K. and Stadtman, E.R. (1993) Covalent attachment of 4-hydroxynonenal to glyceraldehyde-3-phosphate dehydrogenase. A possible involvement of intra- and intermolecular cross-linking reaction. *J Biol Chem*, **268** (9), 6388-6393.
- 185 Peskin, A.V. and Winterbourn, C.C. (2001) Kinetics of the reactions of hypochlorous acid and amino acid chloramines with thiols, methionine, and ascorbate. *Free Radic Biol Med*, **30** (5), 572-579.
- 186 Ischiropoulos, H. (1998) Biological tyrosine nitration: a pathophysiological function of nitric oxide and reactive oxygen species. *Arch Biochem Biophys*, **356** (1), 1-11.
- 187 Alvarez, B., Rubbo, H., Kirk, M., Barnes, S., Freeman, B.A., Radi, R. (1996) Peroxynitrite-dependent tryptophan nitration. *Chem Res Toxicol*, **9** (2), 390-396.
- 188 Kettle, A.J. (1996) Neutrophils convert tyrosyl residues in albumin to chlorotyrosine. *FEBS Lett.*, **379** (1), 103-106.
- 189 Stadtman, E.R. and Levine, R.L. (2003) Free radical-mediated oxidation of free amino acids and amino acid residues in proteins. *Amino Acids*, **25** (3-4), 207-218.
- 190 Dukan, S., Farewell, A., Ballesteros, M., Taddei, F., Radman, M., Nystrom, T. (2000) Protein oxidation in response to increased transcriptional or translational errors. *Proc Natl Acad Sci U S A*, **97** (11), 5746-5749.
- 191 Knebel, A., Rahmsdorf, H.J., Ullrich, A., Herrlich, P. (1996) Dephosphorylation of receptor tyrosine kinases as target of regulation by radiation, oxidants or alkylating agents. *EMBO J*, **15** (19), 5314-5325.
- 192 Abate, C., Patel, L., Rauscher, F.J.3., Curran, T. (1990) Redox regulation of fos and jun DNA-binding activity in vitro. *Science*, **249** (4973), 1157-1161.
- 193 Lee, Z.-W., Kwon, S.-M., Kim, S.-W., Yi, S.-J., Kim, Y.-M., Ha, K.-S. (2003) Activation of in situ tissue transglutaminase by intracellular reactive oxygen species. *Biochem Biophys Res Commun*, **305** (3), 633-640.
- 194 Rhee, S.G., Bae, Y.S., Lee, S.R., Kwon, J. (2000) Hydrogen peroxide: a key messenger that modulates protein phosphorylation through cysteine oxidation. *Sci STKE*, **2000** (53), pe1.
- 195 Grune, T., Reinheckel, T., Davies, K.J. (1996) Degradation of oxidized proteins in K562 human hematopoietic cells by proteasome. *J Biol Chem*, **271** (26), 15504-15509.
- 196 Urushitani, M., Kurisu, J., Tsukita, K., Takahashi, R. (2002) Proteasomal inhibition by misfolded mutant superoxide dismutase 1 induces selective motor neuron death in familial amyotrophic lateral sclerosis. *J Neurochem*, **83** (5), 1030-1042.
- 197 Friguet, B., Stadtman, E.R., Szewda, L.I. (1994) Modification of glucose-6-phosphate dehydrogenase by 4-hydroxy-2-nonenal. Formation of cross-linked protein that inhibits the multicatalytic protease. *J Biol Chem*, **269** (34), 21639-21643.
- 198 Dröge, W. (2002) Free radicals in the physiological control of cell function. *Physiol Rev*, **82** (1), 47-95.
- 199 Janssen-Heininger, Y.M.W., Mossman, B.T., Heintz, N.H., Forman, H.J., Kalyanaram, B., Finkel, T., Stampler, J.S., Rhee, S.G., van der Vliet, A. (2008) Redox-based regulation of signal transduction: principles, pitfalls, and promises. *Free Radic Biol Med*, **45** (1), 1-17.
- 200 Lee, S.R., Kwon, K.S., Kim, S.R., Rhee, S.G. (1998) Reversible inactivation of protein-tyrosine phosphatase 1B in A431 cells stimulated with epidermal growth factor. *J Biol Chem*, **273** (25), 15366-15372.
- 201 Chiarugi, P. (2005) PTPs versus PTKs: the redox side of the coin. *Free Radic Res*, **39** (4), 353-364.
- 202 Giannoni, E., Buricchi, F., Raugei, G., Ramponi, G., Chiarugi, P. (2005) Intracellular reactive oxygen species activate Src tyrosine kinase during cell adhesion and anchorage-dependent cell growth. *Mol Cell Biol*, **25** (15), 6391-6403.

- 203 Simon, A.R., Rai, U., Fanburg, B.L., Cochran, B.H. (1998) Activation of the JAK-STAT pathway by reactive oxygen species. *Am J Physiol*, **275** (6 Pt 1), C1640-52.
- 204 Schmid, E., Hotz-Wagenblatt, A., Hacj, V., Droge, W. (1999) Phosphorylation of the insulin receptor kinase by phosphocreatine in combination with hydrogen peroxide: the structural basis of redox priming. *FASEB J*, **13** (12), 1491-1500.
- 205 Santoro, M., Carlomagno, F., Romano, A., Bottaro, D.P., Dathan, N.A., Grieco, M., Fusco, A., Vecchio, G., Matoskova, B., Kraus, M.H. (1995) Activation of RET as a dominant transforming gene by germline mutations of MEN2A and MEN2B. *Science*, **267** (5196), 381-383.
- 206 Schreck, R., Rieber, P., Baeuerle, P.A. (1991) Reactive oxygen intermediates as apparently widely used messengers in the activation of the NF-kappa B transcription factor and HIV-1. *EMBO J*, **10** (8), 2247-2258.
- 207 Galter, D., Mihm, S., Droge, W. (1994) Distinct effects of glutathione disulphide on the nuclear transcription factor kappa B and the activator protein-1. *Eur J Biochem*, **221** (2), 639-648.
- 208 Rainwater, R., Parks, D., Anderson, M.E., Tegtmeyer, P., Mann, K. (1995) Role of cysteine residues in regulation of p53 function. *Mol Cell Biol*, **15** (7), 3892-3903.
- 209 Suc, I., Meilhac, O., Lajoie-Mazenc, I., Vandaele, J., Jurgens, G., Salvayre, R., Negre-Salvayre, A. (1998) Activation of EGF receptor by oxidized LDL. *FASEB J*, **12** (9), 665-671.
- 210 Parola, M., Robino, G., Marra, F., Pinzani, M., Bellomo, G., Leonarduzzi, G., Chiarugi, P., Camandola, S., Poli, G., Waeg, G., Gentilini, P., Dianzani, M.U. (1998) HNE interacts directly with JNK isoforms in human hepatic stellate cells. *J Clin Invest*, **102** (11), 1942-1950.
- 211 Wartenberg, M., Diederhagen, H., Hescheler, J., Sauer, H. (1999) Growth stimulation versus induction of cell quiescence by hydrogen peroxide in prostate tumor spheroids is encoded by the duration of the Ca(2+) response. *J Biol Chem*, **274** (39), 27759-27767.
- 212 Yang, K.D. and Shaio, M.F. (1994) Hydroxyl radicals as an early signal involved in phorbol ester-induced monocytic differentiation of HL60 cells. *Biochem Biophys Res Commun*, **200** (3), 1650-1657.
- 213 Sauer, H., Rahimi, G., Hescheler, J., Wartenberg, M. (1999) Effects of electrical fields on cardiomyocyte differentiation of embryonic stem cells. *J Cell Biochem*, **75** (4), 710-723.
- 214 Velarde, V., La Cerda, P.M. de, Duarte, C., Arancibia, F., Abbott, E., Gonzalez, A., Moreno, F., Jaffa, A.A. (2004) Role of reactive oxygen species in bradykinin-induced proliferation of vascular smooth muscle cells. *Biol Res*, **37** (3), 419-430.
- 215 Luo, Y., Zou, P., Zou, J., Wang, J., Zhou, D., Liu, L. (2011) Autophagy regulates ROS-induced cellular senescence via p21 in a p38 MAPKalpha dependent manner. *Exp Gerontol*, **46** (11), 860-867.
- 216 Chen, Y., Azad, M.B., Gibson, S.B. (2009) Superoxide is the Major Reactive Oxygen Species Regulating Autophagy. *Cell Death Differ*, **16** (16), 1040-1052.
- 217 Ryter, S.W., Kim, H.P., Hoetzel, A., Park, J.W., Nakahira, K., Wang, X., Choi, A.M.K. (2007) Mechanisms of cell death in oxidative stress. *Antioxid Redox Signal*, **9** (1), 49-89.
- 218 Ott, M., Gogvadze, V., Orrenius, S., Zhivotovsky, B. (2007) Mitochondria, oxidative stress and cell death. *Apoptosis*, **12** (5), 913-922.
- 219 Morgan, M.J., Kim, Y.-S., Liu, Z. (2007) Lipid rafts and oxidative stress-induced cell death. *Antioxid Redox Signal*, **9** (9), 1471-1483.
- 220 Yamamoto, K., Ichijo, H., Korsmeyer, S.J. (1999) BCL-2 is phosphorylated and inactivated by an ASK1/Jun N-terminal protein kinase pathway normally activated at G(2)/M. *Mol Cell Biol*, **19** (12), 8469-8478.
- 221 Inoshita, S., Takeda, K., Hatai, T., Terada, Y., Sano, M., Hata, J., Umezawa, A., Ichijo, H. (2002) Phosphorylation and inactivation of myeloid cell leukemia 1 by JNK in response to oxidative stress. *J Biol Chem*, **277** (46), 43730-43734.
- 222 Kagan, V.E., Tyurin, V.A., Jiang, J., Tyurina, Y.Y., Ritov, V.B., Amoscato, A.A., Osipov, A.N., Belikova, N.A., Kapralov, A.A., Kini, V., Vlasova, I.I., Zhao, Q., Zou, M., Di, P., Svistunenko, D.A., Kurnikov, I.V., Borisenko, G.G. (2005) Cytochrome c acts as a cardiolipin oxygenase required for release of proapoptotic factors. *Nat Chem Biol*, **1** (4), 223-232.
- 223 Sauer, H., Wartenberg, M., Hescheler, J. (2001) Reactive oxygen species as intracellular messengers during cell growth and differentiation. *Cell Physiol Biochem*, **11** (4), 173-186.
- 224 Rigutto, S., Hoste, C., Grasberger, H., Milenkovic, M., Communi, D., Dumont, J.E., Corvilain, B., Miot, F., Deken, X. de (2009) Activation of dual oxidases Duox1 and Duox2: differential regulation mediated by camp-dependent protein kinase and protein kinase C-dependent phosphorylation. *J Biol Chem*, **284** (11), 6725-6734.

- 225 Griffioen, A.W. and Molema, G. (2000) Angiogenesis: potentials for pharmacologic intervention in the treatment of cancer, cardiovascular diseases, and chronic inflammation. *Pharmacol Rev*, **52** (2), 237-268.
- 226 Luczak, K., Balcerczyk, A., Soszynski, M., Bartosz, G. (2004) Low concentration of oxidant and nitric oxide donors stimulate proliferation of human endothelial cells in vitro. *Cell Biol Int*, **28** (6), 483-486.
- 227 Yasuda, M., Ohzeki, Y., Shimizu, S., Naito, S., Ohtsuru, A., Yamamoto, T., Kuroiwa, Y. (1999) Stimulation of in vitro angiogenesis by hydrogen peroxide and the relation with ETS-1 in endothelial cells. *Life Sci*, **64** (4), 249-258.
- 228 Huang, S.-S. and Zheng, R.-L. (2006) Biphasic regulation of angiogenesis by reactive oxygen species. *Pharmazie*, **61** (3), 223-229.
- 229 Neufeld, G., Cohen, T., Gengrinovitch, S., Poltorak, Z. (1999) Vascular endothelial growth factor (VEGF) and its receptors. *FASEB J*, **13** (1), 9-22.
- 230 Chua, C.C., Hamdy, R.C., Chua, B.H. (1998) Upregulation of vascular endothelial growth factor by H₂O₂ in rat heart endothelial cells. *Free Radic Biol Med*, **25** (8), 891-897.
- 231 McCord, J.M. and Fridovich, I. (1969) Superoxide dismutase. An enzymic function for erythrocyte hemocuprein. *J Biol Chem*, **244** (22), 6049-6055.
- 232 Zelko, I.N., Mariani, T.J., Folz, R.J. (2002) Superoxide dismutase multigene family: a comparison of the CuZn-SOD (SOD1), Mn-SOD (SOD2), and EC-SOD (SOD3) gene structures, evolution, and expression. *Free Radic Biol Med*, **33** (3), 337-349.
- 233 Culotta, V.C., Yang, M., O'Halloran, T.V. (2006) Activation of superoxide dismutases: putting the metal to the pedal. *Biochim Biophys Acta*, **1763** (7), 747-758.
- 234 Crapo, J.D., Oury, T., Rabouille, C., Slot, J.W., Chang, L.Y. (1992) Copper,zinc superoxide dismutase is primarily a cytosolic protein in human cells. *Proc Natl Acad Sci U S A*, **89** (21), 10405-10409.
- 235 Sturtz, L.A., Diekert, K., Jensen, L.T., Lill, R., Culotta, V.C. (2001) A fraction of yeast Cu,Zn-superoxide dismutase and its metallochaperone, CCS, localize to the intermembrane space of mitochondria. A physiological role for SOD1 in guarding against mitochondrial oxidative damage. *J Biol Chem*, **276** (41), 38084-38089.
- 236 Vijayvergiya, C., Beal, M.F., Buck, J., Manfredi, G. (2005) Mutant superoxide dismutase 1 forms aggregates in the brain mitochondrial matrix of amyotrophic lateral sclerosis mice. *J Neurosci*, **25** (10), 2463-2470.
- 237 Valentine, J.S., Doucette, P.A., Zittin Potter, S. (2005) Copper-zinc superoxide dismutase and amyotrophic lateral sclerosis. *Annu Rev Biochem*, **74**, 563-593.
- 238 Shibata, N. (2001) Transgenic mouse model for familial amyotrophic lateral sclerosis with superoxide dismutase-1 mutation. *Neuropathology*, **21** (1), 82-92.
- 239 Marklund, S.L. (1982) Human copper-containing superoxide dismutase of high molecular weight. *Proc Natl Acad Sci U S A*, **79** (24), 7634-7638.
- 240 Marklund, S.L., Holme, E., Hellner, L. (1982) Superoxide dismutase in extracellular fluids. *Clin Chim Acta*, **126** (1), 41-51.
- 241 Marklund, S.L. (1984) Extracellular superoxide dismutase and other superoxide dismutase isoenzymes in tissues from nine mammalian species. *Biochem J*, **222** (3), 649-655.
- 242 Nozik-Grayck, E., Suliman, H.B., Piantadosi, C.A. (2005) Extracellular superoxide dismutase. *Int J Biochem Cell Biol*, **37** (12), 2466-2471.
- 243 Marklund, S.L. (1992) Regulation by cytokines of extracellular superoxide dismutase and other superoxide dismutase isoenzymes in fibroblasts. *J Biol Chem*, **267** (10), 6696-6701.
- 244 MacMillan-Crow, L.A., Crow, J.P., Thompson, J.A. (1998) Peroxynitrite-mediated inactivation of manganese superoxide dismutase involves nitration and oxidation of critical tyrosine residues. *Biochemistry*, **37** (6), 1613-1622.
- 245 Weisiger, R.A. and Fridovich, I. (1973) Mitochondrial superoxide simutase. I. Site of synthesis and intramitochondrial localization. *J Biol Chem*, **248** (13), 4793-4796.
- 246 Warner, B.B., Stuart, L., Gebb, S., Wispe, J.R. (1996) Redox regulation of manganese superoxide dismutase. *Am J Physiol*, **271** (1 Pt 1), L150-8.
- 247 Thongphasuk, J., Oberley, L.W., Oberley, T.D. (1999) Induction of superoxide dismutase and cytotoxicity by manganese in human breast cancer cells. *Arch Biochem Biophys*, **365** (2), 317-327.
- 248 Hussain, S.P., Amstad, P., He, P., Robles, A., Lupold, S., Kaneko, I., Ichimiya, M., Sengupta, S., Mechanic, L., Okamura, S., Hofseth, L.J., Moake, M., Nagashima, M., Forrester, K.S., Harris,

- C.C. (2004) p53-induced up-regulation of MnSOD and GPx but not catalase increases oxidative stress and apoptosis. *Cancer Res*, **64** (7), 2350-2356.
- 249 Dhar, S.K. and St Clair, D.K. (2012) Manganese superoxide dismutase regulation and cancer. *Free Radic Biol Med*, **52** (11-12), 2209-2222.
- 250 Carlouz, A. and Touati, D. (1986) Isolation of superoxide dismutase mutants in *Escherichia coli*: is superoxide dismutase necessary for aerobic life? *EMBO J*, **5** (3), 623-630.
- 251 van Loon, A.P., Pesold-Hurt, B., Schatz, G. (1986) A yeast mutant lacking mitochondrial manganese-superoxide dismutase is hypersensitive to oxygen. *Proc Natl Acad Sci U S A*, **83** (11), 3820-3824.
- 252 Li, Y., Huang, T.T., Carlson, E.J., Melov, S., Ursell, P.C., Olson, J.L., Noble, L.J., Yoshimura, M.P., Berger, C., Chan, P.H., Wallace, D.C., Epstein, C.J. (1995) Dilated cardiomyopathy and neonatal lethality in mutant mice lacking manganese superoxide dismutase. *Nat Genet*, **11** (4), 376-381.
- 253 Lebovitz, R.M., Zhang, H., Vogel, H., Cartwright, J., JR, Dionne, L., Lu, N., Huang, S., Matzuk, M.M. (1996) Neurodegeneration, myocardial injury, and perinatal death in mitochondrial superoxide dismutase-deficient mice. *Proc Natl Acad Sci U S A*, **93** (18), 9782-9787.
- 254 Reaume, A.G., Elliott, J.L., Hoffman, E.K., Kowall, N.W., Ferrante, R.J., Siwek, D.F., Wilcox, H.M., Flood, D.G., Beal, M.F., Brown, R.H., JR, Scott, R.W., Snider, W.D. (1996) Motor neurons in Cu/Zn superoxide dismutase-deficient mice develop normally but exhibit enhanced cell death after axonal injury. *Nat Genet*, **13** (1), 43-47.
- 255 Carlsson, L.M., Jonsson, J., Edlund, T., Marklund, S.L. (1995) Mice lacking extracellular superoxide dismutase are more sensitive to hyperoxia. *Proc Natl Acad Sci U S A*, **92** (14), 6264-6268.
- 256 Lee, Y.H., Lin, Q., Boelsterli, U.A., Chung, M.C.M. (2010) The Sod2 mutant mouse as a model for oxidative stress: a functional proteomics perspective. *Mass Spectrom Rev*, **29** (2), 179-196.
- 257 Strassburger, M., Bloch, W., Sulyok, S., Schuller, J., Keist, A.F., Schmidt, A., Wenk, J., Peters, T., Wlaschek, M., Krieg, T., Hafner, M., Kümin, A., Werner, S., Müller, W., Scharffetter-Kochanek, K. (2005) Heterozygous deficiency of manganese superoxide dismutase results in severe lipid peroxidation and spontaneous apoptosis in murine myocardium in vivo. *Free Radic Biol Med*, **38** (11), 1458-1470.
- 258 Kokoszka, J.E., Coskun, P., Esposito, L.A., Wallace, D.C. (2001) Increased mitochondrial oxidative stress in the Sod2 (+/-) mouse results in the age-related decline of mitochondrial function culminating in increased apoptosis. *Proc Natl Acad Sci U S A*, **98** (5), 2278-2283.
- 259 Ikegami, T., Suzuki, Y., Shimizu, T., Isono, K., Koseki, H., Shirasawa, T. (2002) Model mice for tissue-specific deletion of the manganese superoxide dismutase (MnSOD) gene. *Biochem Biophys Res Commun*, **296** (3), 729-736.
- 260 Cyr, A.R., Brown, K.E., McCormick, M.L., Coleman, M.C., Case, A.J., Watts, G.S., Futscher, B.W., Spitz, D.R., Domann, F.E. (2013) Maintenance of mitochondrial genomic integrity in the absence of manganese superoxide dismutase in mouse liver hepatocytes. *Redox Biol*, **1** (1), 172-177.
- 261 Case, A.J. and Domann, F.E. (2012) Manganese superoxide dismutase is dispensable for post-natal development and lactation in the murine mammary gland. *Free Radic Res*, **46** (11), 1361-1368.
- 262 Parajuli, N., Marine, A., Simmons, S., Saba, H., Mitchell, T., Shimizu, T., Shirasawa, T., Macmillan-Crow, L.A. (2011) Generation and characterization of a novel kidney-specific manganese superoxide dismutase knockout mouse. *Free Radic Biol Med*, **51** (2), 406-416.
- 263 Shimizu, T., Nojiri, H., Kawakami, S., Uchiyama, S., Shirasawa, T. (2010) Model mice for tissue-specific deletion of the manganese superoxide dismutase gene. *Geriatr Gerontol Int*, **10 Suppl 1**, S70-9.
- 264 Nojiri, H., Shimizu, T., Funakoshi, M., Yamaguchi, O., Zhou, H., Kawakami, S., Ohta, Y., Sami, M., Tachibana, T., Ishikawa, H., Kurosawa, H., Kahn, R.C., Otsu, K., Shirasawa, T. (2006) Oxidative stress causes heart failure with impaired mitochondrial respiration. *J Biol Chem*, **281** (44), 33789-33801.
- 265 Jones, M.K., Zhu, E., Sarino, E.V., Padilla, O.R., Takahashi, T., Shimizu, T., Shirasawa, T. (2011) Loss of parietal cell superoxide dismutase leads to gastric oxidative stress and increased injury susceptibility in mice. *Am J Physiol Gastrointest Liver Physiol*, **301** (3), G537-46.
- 266 Misawa, H., Nakata, K., Matsuura, J., Moriwaki, Y., Kawashima, K., Shimizu, T., Shirasawa, T., Takahashi, R. (2006) Conditional knockout of Mn superoxide dismutase in postnatal motor

- neurons reveals resistance to mitochondrial generated superoxide radicals. *Neurobiol Dis*, **23** (1), 169-177.
- 267 Lustgarten, M.S., Jang, Y.C., Liu, Y., Muller, F.L., Qi, W., Steinhilber, M., Brooks, S.V., Larkin, L., Shimizu, T., Shirasawa, T., McManus, L.M., Bhattacharya, A., Richardson, A., van Remmen, H. (2009) Conditional knockout of Mn-SOD targeted to type IIB skeletal muscle fibers increases oxidative stress and is sufficient to alter aerobic exercise capacity. *Am J Physiol Cell Physiol*, **297** (6), C1520-32.
- 268 Loew, O. (1900) A new enzyme of general occurrence in organisms. *Science*, **11** (279), 701-702.
- 269 Kirkman, H.N. and Gaetani, G.F. (2007) Mammalian catalase: a venerable enzyme with new mysteries. *Trends Biochem Sci*, **32** (1), 44-50.
- 270 Takahara, S. and Miyamoto, H. (1948) The progressive, necrotic dental maxillitis that was considered to be the cause of the lack of catalase in the blood. *Okayama Igakkai zasshi*, **60** (1-2), 90; passim.
- 271 Goth, L., Rass, P., Pay, A. (2004) Catalase enzyme mutations and their association with diseases. *Mol Diagn*, **8** (3), 141-149.
- 272 Shriner, S.E., Linford, N.J., Martin, George M, Treuting, P., Ogburn, C.E., Emond, M., Coskun, P.E., Ladiges, W., Wolf, N., van Remmen, H., Wallace, D.C., Rabinovitch, P.S. (2005) Extension of murine life span by overexpression of catalase targeted to mitochondria. *Science*, **308** (5730), 1909-1911.
- 273 Kryukov, G.V., Castellano, S., Novoselov, S.V., Lobanov, A.V., Zehab, O., Guigo, R., Gladyshev, V.N. (2003) Characterization of mammalian selenoproteomes. *Science*, **300** (5624), 1439-1443.
- 274 Brigelius-Flohe, R. (2006) Glutathione peroxidases and redox-regulated transcription factors. *Biol Chem*, **387** (10-11), 1329-1335.
- 275 Drevet, J.R. (2006) The antioxidant glutathione peroxidase family and spermatozoa: a complex story. *Mol Cell Endocrinol*, **250** (1-2), 70-79.
- 276 Brigelius-Flohe, R. and Maiorino, M. (2013) Glutathione peroxidases. *Biochim Biophys Acta*, **1830** (5), 3289-3303.
- 277 Björnstedt, M., Xue, J., Huang, W., Akesson, B., Holmgren, A. (1994) The thioredoxin and glutaredoxin systems are efficient electron donors to human plasma glutathione peroxidase. *J Biol Chem*, **269** (47), 29382-29384.
- 278 Yant, L.J., Ran, Q., Rao, L., van Remmen, H., Shibatani, T., Belter, J.G., Motta, L., Richardson, A., Prolla, T.A. (2003) The selenoprotein GPX4 is essential for mouse development and protects from radiation and oxidative damage insults. *Free Radic Biol Med*, **34** (4), 496-502.
- 279 Imai, H., Hirao, F., Sakamoto, T., Sekine, K., Mizukura, Y., Saito, M., Kitamoto, T., Hayasaka, M., Hanaoka, K., Nakagawa, Y. (2003) Early embryonic lethality caused by targeted disruption of the mouse PHGPx gene. *Biochem Biophys Res Commun*, **305** (2), 278-286.
- 280 Cheng, W.H., Ho, Y.S., Valentine, B.A., Ross, D.A., Combs, G.F., JR, Lei, X.G. (1998) Cellular glutathione peroxidase is the mediator of body selenium to protect against paraquat lethality in transgenic mice. *J Nutr*, **128** (7), 1070-1076.
- 281 Krehl, S., Loewinger, M., Florian, S., Kipp, A.P., Banning, A., Wessjohann, L.A., Brauer, M.N., Iori, R., Esworthy, R.S., Chu, F.-F., Brigelius-Flohe, R. (2012) Glutathione peroxidase-2 and selenium decreased inflammation and tumors in a mouse model of inflammation-associated carcinogenesis whereas sulforaphane effects differed with selenium supply. *Carcinogenesis*, **33** (3), 620-628.
- 282 Hanschmann, E.-M., Godoy, J.R., Berndt, C., Hudemann, C., Lillig, C.H. (2013) Thioredoxins, glutaredoxins, and peroxiredoxins--molecular mechanisms and health significance: from cofactors to antioxidants to redox signaling. *Antioxid Redox Signal*, **19** (13), 1539-1605.
- 283 Arnér, E.S. and Holmgren, A. (2000) Physiological functions of thioredoxin and thioredoxin reductase. *Eur J Biochem*, **267** (20), 6102-6109.
- 284 Sabens, E.A. and Mielal, J.J. (2009) Glutaredoxin and Thioredoxin Enzyme Systems: Catalytic Mechanisms and Physiological Functions: Chapter 7, in *Glutathione and sulfur amino acids in human health and disease* (eds R. Masella and G. Mazza), John Wiley, Hoboken, N.J, pp. 121-156.
- 285 Powis, G. and Montfort, W.R. (2001) Properties and biological activities of thioredoxins. *Annu Rev Biochem Biomol Struct*, **30**, 421-455.
- 286 Arnér, E.S.J. (2009) Focus on mammalian thioredoxin reductases--important selenoproteins with versatile functions. *Biochim Biophys Acta*, **1790** (6), 495-526.

- 287 Matsui, M., Oshima, M., Oshima, H., Takaku, K., Maruyama, T., Yodoi, J., Taketo, M.M. (1996) Early embryonic lethality caused by targeted disruption of the mouse thioredoxin gene. *Dev Biol*, **178** (1), 179-185.
- 288 Bondareva, A.A., Capecchi, M.R., Iverson, S.V., Li, Y., Lopez, N.I., Lucas, O., Merrill, G.F., Prigge, J.R., Siders, A.M., Wakamiya, M., Wallin, S.L., Schmidt, E.E. (2007) Effects of thioredoxin reductase-1 deletion on embryogenesis and transcriptome. *Free Radic Biol Med*, **43** (6), 911-923.
- 289 Nonn, L., Williams, R.R., Erickson, R.P., Powis, G. (2003) The absence of mitochondrial thioredoxin 2 causes massive apoptosis, exencephaly, and early embryonic lethality in homozygous mice. *Mol Cell Biol*, **23** (3), 916-922.
- 290 Jakupoglu, C., Przemeczek, G.K.H., Schneider, M., Moreno, S.G., Mayr, N., Hatzopoulos, A.K., Angelis, M.H. de, Wurst, W., Bornkamm, G.W., Brielmeier, M., Conrad, M. (2005) Cytoplasmic thioredoxin reductase is essential for embryogenesis but dispensable for cardiac development. *Mol Cell Biol*, **25** (5), 1980-1988.
- 291 Conrad, M., Jakupoglu, C., Moreno, S.G., Lippl, S., Banjac, A., Schneider, M., Beck, H., Hatzopoulos, A.K., Just, U., Sinowatz, F., Schmahl, W., Chien, K.R., Wurst, W., Bornkamm, G.W., Brielmeier, M. (2004) Essential role for mitochondrial thioredoxin reductase in hematopoiesis, heart development, and heart function. *Mol Cell Biol*, **24** (21), 9414-9423.
- 292 Lincoln, D.T., Ali Emadi, E.M., Tonissen, K.F., Clarke, F.M. (2003) The thioredoxin-thioredoxin reductase system: over-expression in human cancer. *Anticancer Res*, **23** (3B), 2425-2433.
- 293 Lincoln, D.T., Al-Yatama, F., Mohammed, F.M.A., Al-Banaw, A.G., Al-Bader, M., Burge, M., Sinowatz, F., Singal, P.K. (2010) Thioredoxin and thioredoxin reductase expression in thyroid cancer depends on tumour aggressiveness. *Anticancer Res*, **30** (3), 767-775.
- 294 Ho, Y.-S., Xiong, Y., Ho, D.S., Gao, J., Chua, B.H.L., Pai, H., Mielal, J.J. (2007) Targeted disruption of the glutaredoxin 1 gene does not sensitize adult mice to tissue injury induced by ischemia/reperfusion and hyperoxia. *Free Radic Biol Med*, **43** (9), 1299-1312.
- 295 Yang, Y.F. and Wells, W.W. (1991) Identification and characterization of the functional amino acids at the active center of pig liver thioltransferase by site-directed mutagenesis. *J Biol Chem*, **266** (19), 12759-12765.
- 296 Mailloux, R.J., Xuan, J.Y., Beauchamp, B., Jui, L., Lou, M., Harper, M.-E. (2013) Glutaredoxin-2 is required to control proton leak through uncoupling protein-3. *J Biol Chem*, **288** (12), 8365-8379.
- 297 Pretsch, W. (1999) Glutathione reductase activity deficiency in homozygous Gr1a1Neu mice does not cause haemolytic anaemia. *Genet Res*, **73** (1), 1-5.
- 298 Cheng, N.-H., Zhang, W., Chen, W.-Q., Jin, J., Cui, X., Butte, N.F., Chan, L., Hirschi, K.D. (2011) A mammalian monothiol glutaredoxin, Grx3, is critical for cell cycle progression during embryogenesis. *FEBS J*, **278** (14), 2525-2539.
- 299 Wingert, R.A., Galloway, J.L., Barut, B., Foott, H., Fraenkel, P., Axe, J.L., Weber, G.J., Dooley, K., Davidson, A.J., Schmidt, B., Paw, B.H., Shaw, G.C., Kingsley, P., Palis, J., Schubert, H., Chen, O., Kaplan, J., The Tübingen 2000 Screen Consortium, Zon, L.I. (2005) Deficiency of glutaredoxin 5 reveals Fe-S clusters are required for vertebrate haem synthesis. *Nature*, **436** (7053), 1035-1039.
- 300 Camaschella, C., Campanella, A., Falco, L. de, Boschetto, L., Merlini, R., Silvestri, L., Levi, S., Iolascon, A. (2007) The human counterpart of zebrafish shiraz shows sideroblastic-like microcytic anemia and iron overload. *Blood*, **110** (4), 1353-1358.
- 301 Chae, H.Z., Kim, H.J., Kang, S.W., Rhee, S.G. (1999) Characterization of three isoforms of mammalian peroxiredoxin that reduce peroxides in the presence of thioredoxin. *Diabetes Res Clin Pract*, **45** (2-3), 101-112.
- 302 Rhee, S.G., Kang, S.W., Chang, T.S., Jeong, W., Kim, K. (2001) Peroxiredoxin, a novel family of peroxidases. *IUBMB Life*, **52** (1-2), 35-41.
- 303 Flohe, L., Budde, H., Hofmann, B. (2003) Peroxiredoxins in antioxidant defense and redox regulation. *Biofactors*, **19** (1-2), 3-10.
- 304 Neumann, C.A., Krause, D.S., Carman, C.V., Das, S., Dubey, D.P., Abraham, J.L., Bronson, R.T., Fujiwara, Y., Orkin, S.H., van Etten, R.A. (2003) Essential role for the peroxiredoxin Prdx1 in erythrocyte antioxidant defence and tumour suppression. *Nature*, **424** (6948), 561-565.
- 305 Lee, T.-H., Kim, S.-U., Yu, S.-L., Kim, S.H., Park, D.S., Moon, H.-B., Dho, S.H., Kwon, K.-S., Kwon, H.J., Han, Y.-H., Jeong, S., Kang, S.W., Shin, H.-S., Lee, K.-K., Rhee, S.G., Yu, D.-Y. (2003) Peroxiredoxin II is essential for sustaining life span of erythrocytes in mice. *Blood*, **101** (12), 5033-5038.

- 306 Li, L., Shoji, W., Takano, H., Nishimura, N., Aoki, Y., Takahashi, R., Goto, S., Kaifu, T., Takai, T., Obinata, M. (2007) Increased susceptibility of MER5 (peroxiredoxin III) knockout mice to LPS-induced oxidative stress. *Biochem Biophys Res Commun*, **355** (3), 715-721.
- 307 Iuchi, Y., Okada, F., Tsunoda, S., Kibe, N., Shirasawa, N., Ikawa, M., Okabe, M., Ikeda, Y., Fujii, J. (2009) Peroxiredoxin 4 knockout results in elevated spermatogenic cell death via oxidative stress. *Biochem J*, **419** (1), 149-158.
- 308 Wang, X., Phelan, S.A., Forsman-Semb, K., Taylor, E.F., Petros, C., Brown, A., Lerner, C.P., Paigen, B. (2003) Mice with targeted mutation of peroxiredoxin 6 develop normally but are susceptible to oxidative stress. *J Biol Chem*, **278** (27), 25179-25190.
- 309 Keen, J.H. and Jakoby, W.B. (1978) Glutathione transferases. Catalysis of nucleophilic reactions of glutathione. *J Biol Chem*, **253** (16), 5654-5657.
- 310 Tew, K.D. (1994) Glutathione-associated enzymes in anticancer drug resistance. *Cancer Res*, **54** (16), 4313-4320.
- 311 Zakharyan, R.A., Sampayo-Reyes, A., Healy, S.M., Tsapralis, G., Board, P.G., Liebler, D.C., Aposhian, H.V. (2001) Human monomethylarsonic acid (MMA(V)) reductase is a member of the glutathione-S-transferase superfamily. *Chem Res Toxicol*, **14** (8), 1051-1057.
- 312 Coles, B., Nowell, S.A., MacLeod, S.L., Sweeney, C., Lang, N.P., Kadlubar, F.F. (2001) The role of human glutathione S-transferases (hGSTs) in the detoxification of the food-derived carcinogen metabolite N-acetoxy-PhIP, and the effect of a polymorphism in hGSTA1 on colorectal cancer risk. *Mutat Res*, **482** (1-2), 3-10.
- 313 Berhane, K., Widersten, M., Engstrom, A., Kozarich, J.W., Mannervik, B. (1994) Detoxication of base propenals and other alpha, beta-unsaturated aldehyde products of radical reactions and lipid peroxidation by human glutathione transferases. *Proc Natl Acad Sci U S A*, **91** (4), 1480-1484.
- 314 Morel, F., Rauch, C., Petit, E., Piton, A., Theret, N., Coles, B., Guillouzo, A. (2004) Gene and protein characterization of the human glutathione S-transferase kappa and evidence for a peroxisomal localization. *J Biol Chem*, **279** (16), 16246-16253.
- 315 Jakobsson, P.J., Morgenstern, R., Mancini, J., Ford-Hutchinson, A., Persson, B. (1999) Common structural features of MAPEG -- a widespread superfamily of membrane associated proteins with highly divergent functions in eicosanoid and glutathione metabolism. *Protein Sci*, **8** (3), 689-692.
- 316 Hayes, J.D., Flanagan, J.U., Jowsey, I.R. (2005) Glutathione transferases. *Annu Rev Pharmacol Toxicol*, **45**, 51-88.
- 317 Dorion, S., Lambert, H., Landry, J. (2002) Activation of the p38 signaling pathway by heat shock involves the dissociation of glutathione S-transferase Mu from Ask1. *J Biol Chem*, **277** (34), 30792-30797.
- 318 Adler, V., Yin, Z., Fuchs, S.Y., Benezra, M., Rosario, L., Tew, K.D., Pincus, M.R., Sardana, M., Henderson, C.J., Wolf, C.R., Davis, R.J., Ronai, Z. (1999) Regulation of JNK signaling by GSTp. *EMBO J*, **18** (5), 1321-1334.
- 319 Manevich, Y., Feinstein, S.I., Fisher, A.B. (2004) Activation of the antioxidant enzyme 1-CYS peroxiredoxin requires glutathionylation mediated by heterodimerization with pi GST. *Proc Natl Acad Sci U S A*, **101** (11), 3780-3785.
- 320 Fang, J., Wang, S., Zhang, S., Su, S., Song, Z., Deng, Y., Cui, H., Wang, H., Zhang, Y., Qian, J., Gu, J., Liu, B., Li, P., Zhang, R., Liu, X., Wang, Z. (2013) Association of the glutathione s-transferase m1, t1 polymorphisms with cancer: evidence from a meta-analysis. *PLoS One*, **8** (11), e78707.
- 321 Hashibe, M., Brennan, P., Strange, R.C., Bhisey, R., Cascorbi, I., Lazarus, P., Oude Ophuis, M.B., Benhamou, S., Foulkes, W.D., Kato, T., Coutelle, C., Romkes, M., Gaspari, L., Taioli, E., Boffetta, P. (2003) Meta- and pooled analyses of GSTM1, GSTT1, GSTP1, and CYP1A1 genotypes and risk of head and neck cancer. *Cancer Epidemiol Biomarkers Prev*, **12** (12), 1509-1517.
- 322 Sergentanis, T.N. and Economopoulos, K.P. (2010) GSTT1 and GSTP1 polymorphisms and breast cancer risk: a meta-analysis. *Breast Cancer Res Treat*, **121** (1), 195-202.
- 323 Gilliland, F.D., Li, Y.-F., Saxon, A., Diaz-Sanchez, D. (2004) Effect of glutathione-S-transferase M1 and P1 genotypes on xenobiotic enhancement of allergic responses: randomised, placebo-controlled crossover study. *Lancet*, **363** (9403), 119-125.
- 324 Ji, J.D. and Lee, W.J. (2013) Association between the polymorphisms of glutathione S-transferase genes and rheumatoid arthritis: a meta-analysis. *Gene*, **521** (1), 155-159.

- 325 Engle, M.R., Singh, S.P., Czernik, P.J., Gaddy, D., Montague, D.C., Ceci, J.D., Yang, Y., Awasthi, S., Awasthi, Y.C., Zimniak, P. (2004) Physiological role of mGSTA4-4, a glutathione S-transferase metabolizing 4-hydroxynonenal: generation and analysis of mGsta4 null mouse. *Toxicol Appl Pharmacol*, **194** (3), 296-308.
- 326 Ilic, Z., Crawford, D., Vakharia, D., Egner, P.A., Sell, S. (2010) Glutathione-S-transferase A3 knockout mice are sensitive to acute cytotoxic and genotoxic effects of aflatoxin B1. *Toxicol Appl Pharmacol*, **242** (3), 241-246.
- 327 Henderson, C.J., Smith, A.G., Ure, J., Brown, K., Bacon, E.J., Wolf, C.R. (1998) Increased skin tumorigenesis in mice lacking pi class glutathione S-transferases. *Proc Natl Acad Sci U S A*, **95** (9), 5275-5280.
- 328 Fernandez-Canon, J.M., Baetscher, M.W., Finegold, M., Burlingame, T., Gibson, K.M., Grompe, M. (2002) Maleylacetoacetate isomerase (MAAI/GSTZ)-deficient mice reveal a glutathione-dependent nonenzymatic bypass in tyrosine catabolism. *Mol Cell Biol*, **22** (13), 4943-4951.
- 329 Lim, C.E.L., Matthaei, K.I., Blackburn, A.C., Davis, R.P., Dahlstrom, J.E., Koina, M.E., Anders, M.W., Board, P.G. (2004) Mice deficient in glutathione transferase zeta/maleylacetoacetate isomerase exhibit a range of pathological changes and elevated expression of alpha, mu, and pi class glutathione transferases. *Am J Pathol*, **165** (2), 679-693.
- 330 Byrum, R.S., Goulet, J.L., Griffiths, R.J., Koller, B.H. (1997) Role of the 5-lipoxygenase-activating protein (FLAP) in murine acute inflammatory responses. *J Exp Med*, **185** (6), 1065-1075.
- 331 Trebino, C.E., Stock, J.L., Gibbons, C.P., Naiman, B.M., Wachtmann, T.S., Umland, J.P., Pandher, K., Lapointe, J.-M., Saha, S., Roach, M.L., Carter, D., Thomas, N.A., Durtschi, B.A., McNeish, J.D., Hambor, J.E., Jakobsson, P.-J., Carty, T.J., Perez, J.R., Audoly, L.P. (2003) Impaired inflammatory and pain responses in mice lacking an inducible prostaglandin E synthase. *Proc Natl Acad Sci U S A*, **100** (15), 9044-9049.
- 332 Henderson, C.J., Wolf, C.R., Kitteringham, N., Powell, H., Otto, D., Park, B.K. (2000) Increased resistance to acetaminophen hepatotoxicity in mice lacking glutathione S-transferase Pi. *Proc Natl Acad Sci U S A*, **97** (23), 12741-12745.
- 333 Cappellini, M.D. and Fiorelli, G. (2008) Glucose-6-phosphate dehydrogenase deficiency. *Lancet*, **371** (9606), 64-74.
- 334 Meister, A. (1995) Glutathione biosynthesis and its inhibition. *Methods Enzymol*, **252**, 26-30.
- 335 Manu Pereira, M., Gelbart, T., Ristoff, E., Crain, K.C., Bergua, J.M., Lopez Lafuente, A., Kalko, S.G., Garcia Mateos, E., Beutler, E., Vives Corrons, J.L. (2007) Chronic non-spherocytic hemolytic anemia associated with severe neurological disease due to gamma-glutamylcysteine synthetase deficiency in a patient of Moroccan origin. *Haematologica*, **92** (11), e102-5.
- 336 Shi, Z.Z., Osei-Frimpong, J., Kala, G., Kala, S.V., Barrios, R.J., Habib, G.M., Lukin, D.J., Danney, C.M., Matzuk, M.M., Lieberman, M.W. (2000) Glutathione synthesis is essential for mouse development but not for cell growth in culture. *Proc Natl Acad Sci U S A*, **97** (10), 5101-5106.
- 337 Yang, Y., Dieter, M.Z., Chen, Y., Shertzer, H.G., Nebert, D.W., Dalton, T.P. (2002) Initial characterization of the glutamate-cysteine ligase modifier subunit Gclm(-/-) knockout mouse. Novel model system for a severely compromised oxidative stress response. *J Biol Chem*, **277** (51), 49446-49452.
- 338 Erasmus, E. and Mienie, L.J. (2008) Glutathione Synthetase Deficiency, in *Encyclopedia of molecular mechanisms of disease* (ed F. Lang), Springer, Berlin, London, pp. 726-727.
- 339 Ristoff, E., Mayatepek, E., Larsson, A. (2001) Long-term clinical outcome in patients with glutathione synthetase deficiency. *J Pediatr*, **139** (1), 79-84.
- 340 Lauterburg, B.H., Adams, J.D., Mitchell, J.R. (1984) Hepatic glutathione homeostasis in the rat: efflux accounts for glutathione turnover. *Hepatology*, **4** (4), 586-590.
- 341 DeLeve, L.D. and Kaplowitz, N. (1991) Glutathione metabolism and its role in hepatotoxicity. *Pharmacol Ther*, **52** (3), 287-305.
- 342 Githens, S. (1991) Glutathione metabolism in the pancreas compared with that in the liver, kidney, and small intestine. *Int J Pancreatol*, **8** (2), 97-109.
- 343 Bellomo, G., Vairetti, M., Stivala, L., Mirabelli, F., Richelmi, P., Orrenius, S. (1992) Demonstration of nuclear compartmentalization of glutathione in hepatocytes. *Proc Natl Acad Sci U S A*, **89** (10), 4412-4416.

- 344 Wahllander, A., Soboll, S., Sies, H., Linke, I., Muller, M. (1979) Hepatic mitochondrial and cytosolic glutathione content and the subcellular distribution of GSH-S-transferases. *FEBS Lett*, **97** (1), 138-140.
- 345 Meister, A. and Anderson, M.E. (1983) Glutathione. *Annu Rev Biochem*, **52**, 711-760.
- 346 Jones, D.P. (2002) Redox potential of GSH/GSSG couple: assay and biological significance. *Methods Enzymol*, **348**, 93-112.
- 347 Fiser, B., Jojart, B., Csizmadia, I.G., Viskolcz, B. (2013) Glutathione-hydroxyl radical interaction: a theoretical study on radical recognition process. *PLoS One*, **8** (9), e73652.
- 348 Packer, J.E., Slater, T.F., Willson, R.L. (1979) Direct observation of a free radical interaction between vitamin E and vitamin C. *Nature*, **278** (5706), 737-738.
- 349 Niki, E., Tsuchiya, J., Tanimura, R., Kamiya, Y. (1982) Regeneration of vitamin E from alpha-chromanoxyl radical by glutathione and vitamin C. *Chem. Lett.* (6), 789-792.
- 350 Niki, E., Saito, T., Kawakami, A., Kamiya, Y. (1984) Inhibition of oxidation of methyl linoleate in solution by vitamin E and vitamin C. *J Biol Chem*, **259** (7), 4177-4182.
- 351 Hazelton, G.A. and Lang, C.A. (1980) Glutathione contents of tissues in the aging mouse. *Biochem J*, **188** (1), 25-30.
- 352 Lauterburg, B.H., Smith, C.V., Hughes, H., Mitchell, J.R. (1984) Biliary excretion of glutathione and glutathione disulfide in the rat. Regulation and response to oxidative stress. *J Clin Invest*, **73** (1), 124-133.
- 353 Adams, J.D., JR, Lauterburg, B.H., Mitchell, J.R. (1983) Plasma glutathione and glutathione disulfide in the rat: regulation and response to oxidative stress. *J Pharmacol Exp Ther*, **227** (3), 749-754.
- 354 Asensi, M., Sastre, J., Pallardo, F.V., Lloret, A., Lehner, M., Garcia-de-la Asuncion, J., Vina, J. (1999) Ratio of reduced to oxidized glutathione as indicator of oxidative stress status and DNA damage. *Methods Enzymol*, **299**, 267-276.
- 355 Palmieri, B. and Sblendorio, V. (2007) Oxidative stress tests: overview on reliability and use. Part I. *Eur Rev Med Pharmacol Sci*, **11** (5), 309-342.
- 356 Samiec, P.S., Drews-Botsch, C., Flagg, E.W., Kurtz, J.C., Sternberg, P., JR, Reed, R.L., Jones, D.P. (1998) Glutathione in human plasma: decline in association with aging, age-related macular degeneration, and diabetes. *Free Radic Biol Med*, **24** (5), 699-704.
- 357 Cristalli, D.O., Arnal, N., Marra, F.A., Alaniz, M.J.T. de, Marra, C.A. (2012) Peripheral markers in neurodegenerative patients and their first-degree relatives. *J Neurol Sci*, **314** (1-2), 48-56.
- 358 Navarro, J., Obrador, E., Carretero, J., Petschen, I., Avino, J., Perez, P., Estrela, J.M. (1999) Changes in glutathione status and the antioxidant system in blood and in cancer cells associate with tumour growth in vivo. *Free Radic Biol Med*, **26** (3-4), 410-418.
- 359 IUPAC-IUB Joint Commission on Biochemical Nomenclature (JCBN) (1982) Nomenclature of tocopherols and related compounds. Recommendations 1981. *Eur J Biochem*, **123** (3), 473-475.
- 360 Sheppard, A.J., Pennington, J.A.T., Weihrauch, J.L. (1993) Analysis and distribution of vitamin E in vegetable oils and foods, in *Vitamin E in health and disease* (eds L. Packer and J. Fuchs), Dekker, New York, pp. 9-31.
- 361 Yoshida, Y., Niki, E., Noguchi, N. (2003) Comparative study on the action of tocopherols and tocotrienols as antioxidant: chemical and physical effects. *Chem Phys Lipids*, **123** (1), 63-75.
- 362 Burton, G.W., Joyce, A., Ingold, K.U. (1983) Is vitamin E the only lipid-soluble, chain-breaking antioxidant in human blood plasma and erythrocyte membranes? *Arch Biochem Biophys*, **221** (1), 281-290.
- 363 Cheeseman, K.H., Collins, M., Proudfoot, K., Slater, T.F., Burton, G.W., Webb, A.C., Ingold, K.U. (1986) Studies on lipid peroxidation in normal and tumour tissues. The Novikoff rat liver tumour. *Biochem J*, **235** (2), 507-514.
- 364 Ingold, K.U., Webb, A.C., Witter, D., Burton, G.W., Metcalfe, T.A., Muller, D.P. (1987) Vitamin E remains the major lipid-soluble, chain-breaking antioxidant in human plasma even in individuals suffering severe vitamin E deficiency. *Arch Biochem Biophys*, **259** (1), 224-225.
- 365 Niki, E. (1987) Antioxidants in relation to lipid peroxidation. *Chem Phys Lipids*, **44** (2-4), 227-253.
- 366 Packer, L. (1991) Protective role of vitamin E in biological systems. *Am J Clin Nutr*, **53** (4 Suppl), 1050S-1055S.
- 367 Sies, H., Stahl, W., Sundquist, A.R. (1992) Antioxidant functions of vitamins. Vitamins E and C, beta-carotene, and other carotenoids. *Ann N Y Acad Sci*, **669**, 7-20.

- 368 Brin, M.F., Pedley, T.A., Lovelace, R.E., Emerson, R.G., Gouras, P., MacKay, C., Kayden, H.J., Levy, J., Baker, H. (1986) Electrophysiologic features of abetalipoproteinemia: functional consequences of vitamin E deficiency. *Neurology*, **36** (5), 669-673.
- 369 Elias, E., Muller, D.P., Scott, J. (1981) Association of spinocerebellar disorders with cystic fibrosis or chronic childhood cholestasis and very low serum vitamin E. *Lancet*, **2** (8259), 1319-1321.
- 370 Howard, L., Ovesen, L., Satya-Murti, S., Chu, R. (1982) Reversible neurological symptoms caused by vitamin E deficiency in a patient with short bowel syndrome. *Am J Clin Nutr*, **36** (6), 1243-1249.
- 371 Rosenblum, J.L., Keating, J.P., Prensky, A.L., Nelson, J.S. (1981) A progressive neurologic syndrome in children with chronic liver disease. *N Engl J Med*, **304** (9), 503-508.
- 372 Sokol, R.J., Guggenheim, M.A., Iannaccone, S.T., Barkhaus, P.E., Miller, C., Silverman, A., Balistreri, W.F., Heubi, J.E. (1985) Improved neurologic function after long-term correction of vitamin E deficiency in children with chronic cholestasis. *N Engl J Med*, **313** (25), 1580-1586.
- 373 Gotoda, T., Arita, M., Arai, H., Inoue, K., Yokota, T., Fukuo, Y., Yazaki, Y., Yamada, N. (1995) Adult-onset spinocerebellar dysfunction caused by a mutation in the gene for the alpha-tocopherol-transfer protein. *N Engl J Med*, **333** (20), 1313-1318.
- 374 Ouahchi, K., Arita, M., Kayden, H., Hentati, F., Ben Hamida, M., Sokol, R., Arai, H., Inoue, K., Mandel, J.L., Koenig, M. (1995) Ataxia with isolated vitamin E deficiency is caused by mutations in the alpha-tocopherol transfer protein. *Nat Genet*, **9** (2), 141-145.
- 375 Hentati, A., Deng, H.X., Hung, W.Y., Nayer, M., Ahmed, M.S., He, X., Tim, R., Stumpf, D.A., Siddique, T., Ahmed (1996) Human alpha-tocopherol transfer protein: gene structure and mutations in familial vitamin E deficiency. *Ann Neurol*, **39** (3), 295-300.
- 376 Schuelke, M., Mayatepek, E., Inter, M., Becker, M., Pfeiffer, E., Speer, A., Hübner, C., Finckh, B. (1999) Treatment of ataxia in isolated vitamin E deficiency caused by alpha-tocopherol transfer protein deficiency. *J. Pediatr.*, **134** (2), 240-244.
- 377 Straub, O. (1987) *Key to carotenoids*, 2nd edn, Birkhäuser Verlag, Basel, Boston.
- 378 Stahl, W. and Sies, H. (2003) Antioxidant activity of carotenoids. *Mol Aspects Med*, **24** (6), 345-351.
- 379 Olson, J.A. and Krinsky, N.I. (1995) Introduction: the colorful, fascinating world of the carotenoids: important physiologic modulators. *FASEB J*, **9** (15), 1547-1550.
- 380 Conn, P.F., Lambert, C., Land, E.J., Schalch, W., Truscott, T.G. (1992) Carotene-oxygen radical interactions. *Free Radic Res Commun*, **16** (6), 401-408.
- 381 Packer, J.E., Mahood, J.S., Mora-Arellano, V.O., Slater, T.F., Willson, R.L., Wolfenden, B.S. (1981) Free radicals and singlet oxygen scavengers: reaction of a peroxy-radical with beta-carotene, diphenyl furan and 1,4-diazobicyclo (2,2,2)-octane. *Biochem Biophys Res Commun*, **98** (4), 901-906.
- 382 Chen, C.-H., Han, R.-M., Liang, R., Fu, L.-M., Wang, P., Ai, X.-C., Zhang, J.-P., Skibsted, L.H. (2011) Direct observation of the beta-carotene reaction with hydroxyl radical. *J Phys Chem B*, **115** (9), 2082-2089.
- 383 Burton, G.W. and Ingold, K.U. (1984) beta-Carotene: an unusual type of lipid antioxidant. *Science*, **224** (4649), 569-573.
- 384 Hill, T.J., Land, E.J., McGarvey, D.J., Schalch, W., Tinkler, J.H., Truscott, T.G. (1995) Interactions between Carotenoids and the CCl₃O₂.bul. Radical. *J. Am. Chem. Soc.*, **117** (32), 8322-8326.
- 385 Olson, J.A. (1989) Provitamin A function of carotenoids: the conversion of beta-carotene into vitamin A. *J Nutr*, **119** (1), 105-108.
- 386 Bendich, A. and Langseth, L. (1989) Safety of vitamin A. *Am J Clin Nutr*, **49** (2), 358-371.
- 387 McLaren, D.S. and Kraemer, K. (eds) (2012) *Manual on vitamin A deficiency disorders (VADD)*, Karger, Basel.
- 388 Awasthi, S., Peto, R., Read, S., Clark, S., Pande, V., Bundy, D. (2013) Vitamin A supplementation every 6 months with retinol in 1 million pre-school children in north India: DEVTA, a cluster-randomised trial. *Lancet*, **381** (9876), 1469-1477.
- 389 The Alpha-Tocopherol Beta Carotene Cancer Prevention Study Group (1994) The Effect of Vitamin E and Beta Carotene on the Incidence of Lung Cancer and Other Cancers in Male Smokers. *N Engl J Med*, **330** (15), 1029-1035.
- 390 Omenn, G.S., Goodman, G.E., Thornquist, M.D., Balmes, J., Cullen, M.R., Glass, A., Keogh, J.P., Meyskens, F.L., JR, Valanis, B., Williams, J.H., JR, Barnhart, S., Cherniack, M.G., Brodtkin,

- C.A., Hammar, S. (1996) Risk factors for lung cancer and for intervention effects in CARET, the Beta-Carotene and Retinol Efficacy Trial. *J Natl Cancer Inst*, **88** (21), 1550-1559.
- 391 Chatterjee, I.B. (1973) Evolution and the biosynthesis of ascorbic acid. *Science*, **182** (4118), 1271-1272.
- 392 Winkler, B.S. (1992) Unequivocal evidence in support of the nonenzymatic redox coupling between glutathione/glutathione disulfide and ascorbic acid/dehydroascorbic acid. *Biochim Biophys Acta*, **1117** (3), 287-290.
- 393 Meister, A. (1994) Glutathione-ascorbic acid antioxidant system in animals. *J Biol Chem*, **269** (13), 9397-9400.
- 394 Du, J., Cullen, J.J., Buettner, G.R. (2012) Ascorbic acid: chemistry, biology and the treatment of cancer. *Biochim Biophys Acta*, **1826** (2), 443-457.
- 395 Nishikimi, M. (1975) Oxidation of ascorbic acid with superoxide anion generated by the xanthine-xanthine oxidase system. *Biochem Biophys Res Commun*, **63** (2), 463-468.
- 396 Cabelli, D.E. and Bielski, B.H.J. (1983) Kinetics and mechanism for the oxidation of ascorbic acid/ascorbate by HO₂/O₂⁻ (hydroperoxyl/superoxide) radicals. A pulse radiolysis and stopped-flow photolysis study. *J. Phys. Chem.*, **87** (10), 1809-1812.
- 397 Rose, R.C. (1987) Ascorbic Acid Protection against Free Radicals. *Ann NY Acad Sci*, **498** (1 Third Confere), 506-508.
- 398 Dolberg, O.J., Elis, A., Lishner, M. (2010) Scurvy in the 21st century. *Isr Med Assoc J*, **12** (3), 183-184.
- 399 Pinnell, S.R. (1985) Regulation of collagen biosynthesis by ascorbic acid: a review. *Yale J Biol Med*, **58** (6), 553-559.
- 400 Jacobs, E.J., Connell, C.J., Patel, A.V., Chao, A., Rodriguez, C., Seymour, J., McCullough, M.L., Calle, E.E., Thun, M.J. (2001) Vitamin C and vitamin E supplement use and colorectal cancer mortality in a large American Cancer Society cohort. *Cancer Epidemiol Biomarkers Prev*, **10** (1), 17-23.
- 401 Jacobs, E.J., Connell, C.J., McCullough, M.L., Chao, A., Jonas, C.R., Rodriguez, C., Calle, E.E., Thun, M.J. (2002) Vitamin C, vitamin E, and multivitamin supplement use and stomach cancer mortality in the Cancer Prevention Study II cohort. *Cancer Epidemiol Biomarkers Prev*, **11** (1), 35-41.
- 402 Dawsey, S.P., Hollenbeck, A., Schatzkin, A., Abnet, C.C. (2014) A prospective study of vitamin and mineral supplement use and the risk of upper gastrointestinal cancers. *PLoS One*, **9** (2), e88774.
- 403 Pietta, P.G. (2000) Flavonoids as antioxidants. *J Nat Prod*, **63** (7), 1035-1042.
- 404 Morikawa, T., Yasuno, R., Wada, H. (2001) Do mammalian cells synthesize lipoic acid? Identification of a mouse cDNA encoding a lipoic acid synthase located in mitochondria. *FEBS Lett*, **498** (1), 16-21.
- 405 Shay, K.P., Moreau, R.F., Smith, E.J., Smith, A.R., Hagen, T.M. (2009) Alpha-lipoic acid as a dietary supplement: molecular mechanisms and therapeutic potential. *Biochim Biophys Acta*, **1790** (10), 1149-1160.
- 406 Suzuki, Y.J., Tsuchiya, M., Packer, L. (1991) Thiocctic acid and dihydrolipoic acid are novel antioxidants which interact with reactive oxygen species. *Free Radic Res Commun*, **15** (5), 255-263.
- 407 Scott, B.C., Aruoma, O.I., Evans, P.J., O'Neill, C., van der Vliet, A., Cross, C.E., Tritschler, H., Halliwell, B. (1994) Lipoic and dihydrolipoic acids as antioxidants. A critical evaluation. *Free Radic Res*, **20** (2), 119-133.
- 408 Haenen, G.R. and Bast, A. (1991) Scavenging of hypochlorous acid by lipoic acid. *Biochem Pharmacol*, **42** (11), 2244-2246.
- 409 Trujillo, M. and Radi, R. (2002) Peroxynitrite reaction with the reduced and the oxidized forms of lipoic acid: new insights into the reaction of peroxynitrite with thiols. *Arch Biochem Biophys*, **397** (1), 91-98.
- 410 Biewenga, G.P., Haenen, G.R., Bast, A. (1997) The pharmacology of the antioxidant lipoic acid. *Gen Pharmacol*, **29** (3), 315-331.
- 411 Ou, P., Tritschler, H.J., Wolff, S.P. (1995) Thiocctic (lipoic) acid: a therapeutic metal-chelating antioxidant? *Biochem Pharmacol*, **50** (1), 123-126.
- 412 Goralska, M., Dackor, R., Holley, B., McGahan, M.C. (2003) Alpha lipoic acid changes iron uptake and storage in lens epithelial cells. *Exp Eye Res*, **76** (2), 241-248.

- 413 Suh, J.H., Moreau, R., Heath, S.-H.D., Hagen, T.M. (2005) Dietary supplementation with (R)-alpha-lipoic acid reverses the age-related accumulation of iron and depletion of antioxidants in the rat cerebral cortex. *Redox Rep*, **10** (1), 52-60.
- 414 Yeldandi, A.V., Wang, X.D., Alvares, K., Kumar, S., Rao, M.S., Reddy, J.K. (1990) Human urate oxidase gene: cloning and partial sequence analysis reveal a stop codon within the fifth exon. *Biochem Biophys Res Commun*, **171** (2), 641-646.
- 415 Yeldandi, A.V., Yeldandi, V., Kumar, S., Murthy, C.V., Wang, X.D., Alvares, K., Rao, M.S., Reddy, J.K. (1991) Molecular evolution of the urate oxidase-encoding gene in hominoid primates: nonsense mutations. *Gene*, **109** (2), 281-284.
- 416 Ames, B.N., Cathcart, R., Schwiers, E., Hochstein, P. (1981) Uric acid provides an antioxidant defense in humans against oxidant- and radical-caused aging and cancer: a hypothesis. *Proc Natl Acad Sci U S A*, **78** (11), 6858-6862.
- 417 Santos, C.X., Anjos, E.I., Augusto, O. (1999) Uric acid oxidation by peroxynitrite: multiple reactions, free radical formation, and amplification of lipid oxidation. *Arch Biochem Biophys*, **372** (2), 285-294.
- 418 Becker, B.F. (1993) Towards the physiological function of uric acid. *Free Radic Biol Med*, **14** (6), 615-631.
- 419 Simic, M.G. and Jovanovic, S.V. (1989) Antioxidation mechanisms of uric acid. *J. Am. Chem. Soc.*, **111** (15), 5778-5782.
- 420 Wayner, D.D., Burton, G.W., Ingold, K.U., Barclay, L.R., Locke, S.J. (1987) The relative contributions of vitamin E, urate, ascorbate and proteins to the total peroxyl radical-trapping antioxidant activity of human blood plasma. *Biochim Biophys Acta*, **924** (3), 408-419.
- 421 Thomas, M.J. (1992) Urate causes the human polymorphonuclear leukocyte to secrete superoxide. *Free Radic Biol Med*, **12** (1), 89-91.
- 422 Davies, K.J., Sevanian, A., Muakkassah-Kelly, S.F., Hochstein, P. (1986) Uric acid-iron ion complexes. A new aspect of the antioxidant functions of uric acid. *Biochem J*, **235** (3), 747-754.
- 423 Lingeman, J.E. (2013) Pathogenesis of nephrolithiasis. *J Urol*, **189** (2), 417-418.
- 424 Shoji, A., Yamanaka, H., Kamatani, N. (2004) A retrospective study of the relationship between serum urate level and recurrent attacks of gouty arthritis: evidence for reduction of recurrent gouty arthritis with antihyperuricemic therapy. *Arthritis Rheum*, **51** (3), 321-325.
- 425 Perez-Ruiz, F., Atxotegi, J., Hernando, I., Calabozo, M., Nolla, J.M. (2006) Using serum urate levels to determine the period free of gouty symptoms after withdrawal of long-term urate-lowering therapy: a prospective study. *Arthritis Rheum*, **55** (5), 786-790.
- 426 Schumacher, H.R., JR (2008) The pathogenesis of gout. *Cleve Clin J Med*, **75 Suppl 5**, S2-4.
- 427 Joo, K., Kwon, S.-R., Lim, M.-J., Jung, K.-H., Joo, H., Park, W. (2014) Prevention of comorbidity and acute attack of gout by uric acid lowering therapy. *J Korean Med Sci*, **29** (5), 657-661.
- 428 Stocker, R., Yamamoto, Y., McDonagh, A., Glazer, A., Ames, B. (1987) Bilirubin is an antioxidant of possible physiological importance. *Science*, **235** (4792), 1043-1046.
- 429 Baranano, D.E., Rao, M., Ferris, C.D., Snyder, S.H. (2002) Biliverdin reductase: a major physiologic cytoprotectant. *Proc Natl Acad Sci U S A*, **99** (25), 16093-16098.
- 430 Stocker, R., Glazer, A.N., Ames, B.N. (1987) Antioxidant activity of albumin-bound bilirubin. *Proc Natl Acad Sci U S A*, **84** (16), 5918-5922.
- 431 Applegate, L.A., Luscher, P., Tyrrell, R.M. (1991) Induction of heme oxygenase: a general response to oxidant stress in cultured mammalian cells. *Cancer Res*, **51** (3), 974-978.
- 432 Vile, G.F., Basu-Modak, S., Waltner, C., Tyrrell, R.M. (1994) Heme oxygenase 1 mediates an adaptive response to oxidative stress in human skin fibroblasts. *Proc Natl Acad Sci U S A*, **91** (7), 2607-2610.
- 433 Motterlini, R., Foresti, R., Bassi, R., Green, C.J. (2000) Curcumin, an antioxidant and anti-inflammatory agent, induces heme oxygenase-1 and protects endothelial cells against oxidative stress. *Free Radic Biol Med*, **28** (8), 1303-1312.
- 434 Lin, Q., Weis, S., Yang, G., Weng, Y.-H., Helston, R., Rish, K., Smith, A., Bordner, J., Polte, T., Gaunitz, F., Dennery, P.A. (2007) Heme oxygenase-1 protein localizes to the nucleus and activates transcription factors important in oxidative stress. *J Biol Chem*, **282** (28), 20621-20633.
- 435 Lundvig, D.M.S., Immenschuh, S., Wagener, F.A.D.T.G. (2012) Heme oxygenase, inflammation, and fibrosis: the good, the bad, and the ugly? *Front Pharmacol*, **3**, 81.
- 436 Stocker, R., Bowry, V.W., Frei, B. (1991) Ubiquinol-10 protects human low density lipoprotein more efficiently against lipid peroxidation than does alpha-tocopherol. *Proc Natl Acad Sci U S A*, **88** (5), 1646-1650.

- 437 Lee, B.-J., Huang, Y.-C., Chen, S.-J., Lin, P.-T. (2012) Coenzyme Q10 supplementation reduces oxidative stress and increases antioxidant enzyme activity in patients with coronary artery disease. *Nutrition*, **28** (3), 250-255.
- 438 Sanoobar, M., Egtesadi, S., Azimi, A., Khalili, M., Jazayeri, S., Reza Gohari, M. (2013) Coenzyme Q10 supplementation reduces oxidative stress and increases antioxidant enzyme activity in patients with relapsing-remitting multiple sclerosis. *Int J Neurosci*, **123** (11), 776-782.
- 439 Nadjarzadeh, A., Shidfar, F., Amirjannati, N., Vafa, M.R., Motevalian, S.A., Gohari, M.R., Nazeri Kakhki, S.A., Akhondi, M.M., Sadeghi, M.R. (2014) Effect of Coenzyme Q10 supplementation on antioxidant enzymes activity and oxidative stress of seminal plasma: a double-blind randomised clinical trial. *Andrologia*, **46** (2), 177-183.
- 440 Sies, H. and Cadenas, E. (1985) Oxidative stress: damage to intact cells and organs. *Philos Trans R Soc Lond B Biol Sci*, **311** (1152), 617-631.
- 441 Cutler, R.G., Plummer, J., Chowdhury, K., Heward, C. (2005) Oxidative stress profiling: part II. Theory, technology, and practice. *Ann N Y Acad Sci*, **1055**, 136-158.
- 442 Harman, D. (2003) The free radical theory of aging. *Antioxid Redox Signal*, **5** (5), 557-561.
- 443 Harman D. (1956) Aging: a theory based on free radical and radiation chemistry. *J Gerontol*, **11** (3), 298-300.
- 444 Martin, I. and Grotewiel, M.S. (2006) Oxidative damage and age-related functional declines. *Mech Ageing Dev*, **127** (5), 411-423.
- 445 Tuppo, E.E.a.F.L.J. (2001) Free radical oxidative damage and Alzheimer's disease. *J Am Osteopath Assoc*, **101** (12 Suppl Pt 1), S11-5.
- 446 Ferretti, G., Bacchetti, T., Principi, F., DiLudovico, F., Viti, B., Angeleri, V.A., Danni, M., Provinciali, L. (2005) Increased levels of lipid hydroperoxides in plasma of patients with multiple sclerosis: a relationship with paraoxonase activity. *Mult Scler*, **11** (6), 677-682.
- 447 Kerr, S., Brosnan, M.J., McIntyre, M., Reid, J.L., Dominicczak, A.F., Hamilton, C.A. (1999) Superoxide anion production is increased in a model of genetic hypertension: role of the endothelium. *Hypertension*, **33** (6), 1353-1358.
- 448 Cave, A.C., Brewer, A.C., Narayanapanicker, A., Ray, R., Grieve, D.J., Walker, S., Shah, A.M. (2006) NADPH oxidases in cardiovascular health and disease. *Antioxid Redox Signal*, **8** (5-6), 691-728.
- 449 Dhalla, N.S., Temsah, R.M., Netticadan, T. (2000) Role of oxidative stress in cardiovascular diseases. *J Hypertens*, **18** (6), 655-673.
- 450 Elnakish, M.T., Hassanain, H.H., L Janssen, P.M., Angelos, M.G., Khan, M. (2013) Emerging role of oxidative stress in metabolic syndrome and cardiovascular diseases: Important Role of Rac/NADPH Oxidase. *J Pathol*.
- 451 Esser, P.R., Wolffe, U., Durr, C., Loewenich, F.D. von, Schempp, C.M., Freudenberg, M.A., Jakob, T., Martin, S.F. (2012) Contact sensitizers induce skin inflammation via ROS production and hyaluronic acid degradation. *PLoS One*, **7** (7), e41340.
- 452 Miesel, R., Hartung, R., Kroeger, H. (1996) Priming of NADPH oxidase by tumor necrosis factor alpha in patients with inflammatory and autoimmune rheumatic diseases. *Inflammation*, **20** (4), 427-438.
- 453 Rezaie, A., Parker, R.D., Abdollahi, M. (2007) Oxidative stress and pathogenesis of inflammatory bowel disease: an epiphenomenon or the cause? *Dig Dis Sci*, **52** (9), 2015-2021.
- 454 Weinberg, F., Hamanaka, R., Wheaton, W.W., Weinberg, S., Joseph, J., Lopez, M., Kalyanaraman, B., Mutlu, G.M., Budinger, G.R., Chandel, N.S. (2010) Mitochondrial metabolism and ROS generation are essential for Kras-mediated tumorigenicity. *Proc Natl Acad Sci U S A*, **107** (19), 8788-8793.
- 455 DeNicola, G.M., Karreth, F.A., Humpton, T.J., Gopinathan, A., Wei, C., Frese, K., Mangal, D., Yu, K.H., Yeo, C.J., Calhoun, E.S., Scrimieri, F., Winter, J.M., Hruban, R.H., Iacobuzio-Donahue, C., Kern, S.E., Blair, I.A., Tuveson, D.A. (2011) Oncogene-induced Nrf2 transcription promotes ROS detoxification and tumorigenesis. *Nature*, **475** (7354), 106-109.
- 456 Warburg, O. (1956) On the origin of cancer cells. *Science*, **123** (3191), 309-314.
- 457 Church, S.L., Grant, J.W., Ridnour, L.A., Oberley, L.W., Swanson, P.E., Meltzer, P.S., Trent, J.M. (1993) Increased manganese superoxide dismutase expression suppresses the malignant phenotype of human melanoma cells. *Proc Natl Acad Sci U S A*, **90** (7), 3113-3117.
- 458 Zhong, W., Oberley, L.W., Oberley, T.D., Yan, T., Domann, F.E., St Clair, D.K. (1996) Inhibition of cell growth and sensitization to oxidative damage by overexpression of manganese superoxide dismutase in rat glioma cells. *Cell Growth Differ*, **7** (9), 1175-1186.

- 459 Liu, R., Oberley, T.D., Oberley, L.W. (1997) Transfection and expression of MnSOD cDNA decreases tumor malignancy of human oral squamous carcinoma SCC-25 cells. *Hum Gene Ther*, **8** (5), 585-595.
- 460 Bostwick, D.G., Alexander, E.E., Singh, R., Shan, A., Qian, J., Santella, R.M., Oberley, L.W., Yan, T., Zhong, W., Jiang, X., Oberley, T.D. (2000) Antioxidant enzyme expression and reactive oxygen species damage in prostatic intraepithelial neoplasia and cancer. *Cancer*, **89** (1), 123-134.
- 461 van Remmen, H., Ikeno, Y., Hamilton, M., Pahlavani, M., Wolf, N., Thorpe, S.R., Alderson, N.L., Baynes, J.W., Epstein, C.J., Huang, T.-T., Nelson, J., Strong, R., Richardson, A. (2003) Life-long reduction in MnSOD activity results in increased DNA damage and higher incidence of cancer but does not accelerate aging. *Physiol Genomics*, **16** (1), 29-37.
- 462 Izutani, R., Asano, S., Imano, M., Kuroda, D., Kato, M., Ohyanagi, H. (1998) Expression of manganese superoxide dismutase in esophageal and gastric cancers. *J Gastroenterol*, **33** (6), 816-822.
- 463 Chung-man Ho, J., Zheng, S., Comhair, S.A., Farver, C., Erzurum, S.C. (2001) Differential expression of manganese superoxide dismutase and catalase in lung cancer. *Cancer Res*, **61** (23), 8578-8585.
- 464 Hu, Y., Rosen, D.G., Zhou, Y., Feng, L., Yang, G., Liu, J., Huang, P. (2005) Mitochondrial manganese-superoxide dismutase expression in ovarian cancer: role in cell proliferation and response to oxidative stress. *J Biol Chem*, **280** (47), 39485-39492.
- 465 Miranda, A., Janssen, L., Bosman, C.B., van Duijn, W., Oostendorp-van de Ruit, M.M., Kubben, F.J., Griffioen, G., Lamers, C.B., van Krieken, J.H., van de Velde, C.J., Verspaget, H.W. (2000) Superoxide dismutases in gastric and esophageal cancer and the prognostic impact in gastric cancer. *Clin Cancer Res*, **6** (8), 3183-3192.
- 466 Sutton, A., Khoury, H., Prip-Buus, C., Capanec, C., Pessayre, D., Degoul, F. (2003) The Ala16Val genetic dimorphism modulates the import of human manganese superoxide dismutase into rat liver mitochondria. *Pharmacogenetics*, **13** (3), 145-157.
- 467 Ambrosone, C.B., Freudenheim, J.L., Thompson, P.A., Bowman, E., Vena, J.E., Marshall, J.R., Graham, S., Laughlin, R., Nemoto, T., Shields, P.G. (1999) Manganese superoxide dismutase (MnSOD) genetic polymorphisms, dietary antioxidants, and risk of breast cancer. *Cancer Res*, **59** (3), 602-606.
- 468 Olson, S.H., Carlson, M.D.A., Ostrer, H., Harlap, S., Stone, A., Winters, M., Ambrosone, C.B. (2004) Genetic variants in SOD2, MPO, and NQO1, and risk of ovarian cancer. *Gynecol Oncol*, **93** (3), 615-620.
- 469 Kang, D., Lee, K.-M., Park, S.K., Berndt, S.I., Peters, U., Reding, D., Chatterjee, N., Welch, R., Chanock, S., Huang, W.-Y., Hayes, R.B. (2007) Functional variant of manganese superoxide dismutase (SOD2 V16A) polymorphism is associated with prostate cancer risk in the prostate, lung, colorectal, and ovarian cancer study. *Cancer Epidemiol Biomarkers Prev*, **16** (8), 1581-1586.
- 470 Sun, G.-G., Wang, Y.-D., Lu, Y.-F., Hu, W.-N. (2013) Different association of manganese superoxide dismutase gene polymorphisms with risk of prostate, esophageal, and lung cancers: evidence from a meta-analysis of 20,025 subjects. *Asian Pac J Cancer Prev*, **14** (3), 1937-1943.
- 471 Zejnilovic, J., Akev, N., Yilmaz, H., Isbir, T. (2009) Association between manganese superoxide dismutase polymorphism and risk of lung cancer. *Cancer Genet Cytogenet*, **189** (1), 1-4.
- 472 Hung, R.J., Boffetta, P., Brennan, P., Malaveille, C., Gelatti, U., Placidi, D., Carta, A., Hautefeuille, A., Porru, S. (2004) Genetic polymorphisms of MPO, COMT, MnSOD, NQO1, interactions with environmental exposures and bladder cancer risk. *Carcinogenesis*, **25** (6), 973-978.
- 473 Cao, M., Mu, X., Jiang, C., Yang, G., Chen, H., Xue, W. (2014) Single-nucleotide polymorphisms of GPX1 and MnSOD and susceptibility to bladder cancer: a systematic review and meta-analysis. *Tumour Biol*, **35** (1), 759-764.
- 474 Qiu, L.-X., Yao, L., Mao, C., Chen, B., Zhan, P., Yuan, H., Xue, K., Zhang, J., Hu, X.-C. (2010) Lack of association between MnSOD Val16Ala polymorphism and breast cancer risk: a meta-analysis involving 58,448 subjects. *Breast Cancer Res Treat*, **123** (2), 543-547.
- 475 Attatippaholkun, W. and Wikainapakul, K. (2013) Predominant genotypes and alleles of two functional polymorphisms in the manganese superoxide dismutase gene are not associated with Thai cervical or breast cancer. *Asian Pac J Cancer Prev*, **14** (6), 3955-3961.

- 476 Hurt, E.M., Thomas, S.B., Peng, B., Farrar, W.L. (2007) Molecular consequences of SOD2 expression in epigenetically silenced pancreatic carcinoma cell lines. *Br J Cancer*, **97** (8), 1116-1123.
- 477 Cullen, J.J., Weydert, C., Hinkhouse, M.M., Ritchie, J., Domann, F.E., Spitz, D., Oberley, L.W. (2003) The role of manganese superoxide dismutase in the growth of pancreatic adenocarcinoma. *Cancer Res*, **63** (6), 1297-1303.
- 478 Weydert, C., Roling, B., Liu, J., Hinkhouse, M.M., Ritchie, J.M., Oberley, L.W., Cullen, J.J. (2003) Suppression of the malignant phenotype in human pancreatic cancer cells by the overexpression of manganese superoxide dismutase. *Mol Cancer Ther*, **2** (4), 361-369.
- 479 Ough, M., Lewis, A., Zhang, Y., Hinkhouse, M.M., Ritchie, J.M., Oberley, L.W., Cullen, J.J. (2004) Inhibition of cell growth by overexpression of manganese superoxide dismutase (MnSOD) in human pancreatic carcinoma. *Free Radic Res*, **38** (11), 1223-1233.
- 480 Wheatley-Price, P., Asomaning, K., Reid, A., Zhai, R., Su, L., Zhou, W., Zhu, A., Ryan, D.P., Christiani, D.C., Liu, G. (2008) Myeloperoxidase and superoxide dismutase polymorphisms are associated with an increased risk of developing pancreatic adenocarcinoma. *Cancer*, **112** (5), 1037-1042.
- 481 Tang, H., Dong, X., Day, R.S., Hassan, M.M., Li, D. (2010) Antioxidant genes, diabetes and dietary antioxidants in association with risk of pancreatic cancer. *Carcinogenesis*, **31** (4), 607-613.
- 482 Zhang, J., Zhang, X., Dhakal, I.B., Gross, M.D., Kadlubar, F.F., Anderson, K.E. (2011) Sequence variants in antioxidant defense and DNA repair genes, dietary antioxidants, and pancreatic cancer risk. *Int J Mol Epidemiol Genet*, **2** (3), 236-244.
- 483 Nakhai, H., Sel, S., Favor, J., Mendoza-Torres, L., Paulsen, F., Duncker, G.I., Schmid, R.M. (2007) Ptf1a is essential for the differentiation of GABAergic and glycinergic amacrine cells and horizontal cells in the mouse retina. *Development*, **134** (6), 1151-1160.
- 484 Marino, S., Vooijs, M., van der Gulden, H., Jonkers, J., Berns, A. (2000) Induction of medulloblastomas in p53-null mutant mice by somatic inactivation of Rb in the external granular layer cells of the cerebellum. *Genes Dev*, **14** (8), 994-1004.
- 485 Ayala, J.E., Samuel, V.T., Morton, G.J., Obici, S., Croniger, C.M., Shulman, G.I., Wasserman, D.H., McGuinness, O.P. (2010) Standard operating procedures for describing and performing metabolic tests of glucose homeostasis in mice. *Dis Model Mech*, **3** (9-10), 525-534.
- 486 Andrikopoulos, S., Blair, A.R., Deluca, N., Fam, B.C., Proietto, J. (2008) Evaluating the glucose tolerance test in mice. *Am J Physiol Endocrinol Metab*, **295** (6), E1323-32.
- 487 Gabbi, C., Kim, H.-J., Hultenby, K., Bouton, D., Toresson, G., Warner, M., Gustafsson, J.-A. (2008) Pancreatic exocrine insufficiency in LXRbeta^{-/-} mice is associated with a reduction in aquaporin-1 expression. *Proc Natl Acad Sci U S A*, **105** (39), 15052-15057.
- 488 Dahlmann, B. and Reinauer, H. (1978) Purification and some properties of an alkaline proteinase from rat skeletal muscle. *Biochem J*, **171** (3), 803-810.
- 489 Schindelin, J., Arganda-Carreras, I., Frise, E., Kaynig, V., Longair, M., Pietzsch, T., Preibisch, S., Rueden, C., Saalfeld, S., Schmid, B., Tinevez, J.-Y., White, D.J., Hartenstein, V., Eliceiri, K., Tomancak, P., Cardona, A. (2012) Fiji: an open-source platform for biological-image analysis. *Nat Methods*, **9** (7), 676-682.
- 490 Mutterer, J. and Zinck, E. (2013) Quick-and-clean article figures with FigureJ. *J Microsc*, **252** (1), 89-91.
- 491 Hruban, R.H., Adsay, N.V., Albores-Saavedra, J., Compton, C., Garrett, E.S., Goodman, S.N., Kern, S.E., Klimstra, D.S., Kloppel, G., Longnecker, D.S., Luttges, J., Offerhaus, G.J. (2001) Pancreatic intraepithelial neoplasia: a new nomenclature and classification system for pancreatic duct lesions. *Am J Surg Pathol*, **25** (5), 579-586.
- 492 Young, L., Sung, J., Stacey, G., Masters, J.R. (2010) Detection of Mycoplasma in cell cultures. *Nat Protoc*, **5** (5), 929-934.
- 493 The Jackson Laboratory.
http://jaxmice.jax.org/protocolsdb/?p=116:2:4364220609002115::NO:2:P2_MASTER_PROTO_COL_ID,P2_JRS_CODE:3214,008179 (22 August 2014).
- 494 Clapcote, S.J. and Roder, J.C. (2005) Simplex PCR assay for sex determination in mice. *Biotechniques*, **38** (5), 702, 704, 706.
- 495 Pfaffl, M.W. (2001) A new mathematical model for relative quantification in real-time RT-PCR. *Nucleic Acids Res*, **29** (9), e45.
- 496 Garnett, M.J. and Marais, R. (2004) Guilty as charged: B-RAF is a human oncogene. *Cancer Cell*, **6** (4), 313-319.

- 497 Guo, M., Jia, Y., Yu, Z., House, M.G., Esteller, M., Brock, M.V., Herman, J.G. (2014) Epigenetic changes associated with neoplasms of the exocrine and endocrine pancreas. *Discov Med*, **17** (92), 67-73.
- 498 Thomson Reuters Pathway Maps. <http://lsresearch.thomsonreuters.com/maps/2208/> (22.08.14).
- 499 Melov, S., Schneider, J.A., Day, B.J., Hinerfeld, D., Coskun, P., Mirra, S.S., Crapo, J.D., Wallace, D.C. (1998) A novel neurological phenotype in mice lacking mitochondrial manganese superoxide dismutase. *Nat Genet*, **18** (2), 159-163.
- 500 Lenart, J., Dombrowski, F., Gorlach, A., Kietzmann, T. (2007) Deficiency of manganese superoxide dismutase in hepatocytes disrupts zoned gene expression in mouse liver. *Arch Biochem Biophys*, **462** (2), 238-244.
- 501 Lynn, S., Huang, E.J., Elchuri, S., Naeemuddin, M., Nishinaka, Y., Yodoi, J., Ferriero, D.M., Epstein, C.J., Huang, T.-T. (2005) Selective neuronal vulnerability and inadequate stress response in superoxide dismutase mutant mice. *Free Radic Biol Med*, **38** (6), 817-828.
- 502 Liang, L.-P., Waldbaum, S., Rowley, S., Huang, T.-T., Day, B.J., Patel, M. (2012) Mitochondrial oxidative stress and epilepsy in SOD2 deficient mice: attenuation by a lipophilic metalloporphyrin. *Neurobiol Dis*, **45** (3), 1068-1076.
- 503 Zhao, Y., Oberley, T.D., Chaiswing, L., Lin, S.-m., Epstein, C.J., Huang, T.-T., St Clair, D. (2002) Manganese superoxide dismutase deficiency enhances cell turnover via tumor promoter-induced alterations in AP-1 and p53-mediated pathways in a skin cancer model. *Oncogene*, **21** (24), 3836-3846.
- 504 Kohler, J.J., Cucoranu, I., Fields, E., Green, E., He, S., Hoying, A., Russ, R., Abuin, A., Johnson, D., Hosseini, S.H., Raper, C.M., Lewis, W. (2009) Transgenic mitochondrial superoxide dismutase and mitochondrially targeted catalase prevent antiretroviral-induced oxidative stress and cardiomyopathy. *Lab Invest*, **89** (7), 782-790.
- 505 Case, A.J., McGill, J.L., Tygrett, L.T., Shirasawa, T., Spitz, D.R., Waldschmidt, T.J., Legge, K.L., Domann, F.E. (2011) Elevated mitochondrial superoxide disrupts normal T cell development, impairing adaptive immune responses to an influenza challenge. *Free Radic Biol Med*, **50** (3), 448-458.
- 506 Lustgarten, M.S., Jang, Y.C., Liu, Y., Qi, W., Qin, Y., Dahia, P.L., Shi, Y., Bhattacharya, A., Muller, F.L., Shimizu, T., Shirasawa, T., Richardson, A., van Remmen, H. (2011) MnSOD deficiency results in elevated oxidative stress and decreased mitochondrial function but does not lead to muscle atrophy during aging. *Aging Cell*, **10** (3), 493-505.
- 507 Melov, S., Coskun, P., Patel, M., Tuinstra, R., Cottrell, B., Jun, A.S., Zastawny, T.H., Dizdaroglu, M., Goodman, S.I., Huang, T.T., Mizioro, H., Epstein, C.J., Wallace, D.C. (1999) Mitochondrial disease in superoxide dismutase 2 mutant mice. *Proc Natl Acad Sci U S A*, **96** (3), 846-851.
- 508 Robinson, K.M., Janes, M.S., Pehar, M., Monette, J.S., Ross, M.F., Hagen, T.M., Murphy, M.P., Beckman, J.S. (2006) Selective fluorescent imaging of superoxide in vivo using ethidium-based probes. *Proc Natl Acad Sci U S A*, **103** (41), 15038-15043.
- 509 Gerstner, B., DeSilva, T.M., Genz, K., Armstrong, A., Brehmer, F., Neve, R.L., Felderhoff-Mueser, U., Volpe, J.J., Rosenberg, P.A. (2008) Hyperoxia causes maturation-dependent cell death in the developing white matter. *J Neurosci*, **28** (5), 1236-1245.
- 510 Zielonka, J. and Kalyanaraman, B. (2010) Hydroethidine- and MitoSOX-derived red fluorescence is not a reliable indicator of intracellular superoxide formation: another inconvenient truth. *Free Radic Biol Med*, **48** (8), 983-1001.
- 511 Rosa, D.P., Martinez, D., Picada, J.N., Semedo, J.G., Marroni, N.P. (2011) Hepatic oxidative stress in an animal model of sleep apnoea: effects of different duration of exposure. *Comp Hepatol*, **10** (1), 1.
- 512 Termini, J. (2000) Hydroperoxide-induced DNA damage and mutations. *Mutat Res*, **450** (1-2), 107-124.
- 513 Russo, M.T., Luca, G. de, Degan, P., Bignami, M. (2007) Different DNA repair strategies to combat the threat from 8-oxoguanine. *Mutat Res*, **614** (1-2), 69-76.
- 514 Salazar, J.J. and van Houten, B. (1997) Preferential mitochondrial DNA injury caused by glucose oxidase as a steady generator of hydrogen peroxide in human fibroblasts. *Mutat Res*, **385** (2), 139-149.
- 515 Yakes, F.M. and van Houten, B. (1997) Mitochondrial DNA damage is more extensive and persists longer than nuclear DNA damage in human cells following oxidative stress. *Proc Natl Acad Sci U S A*, **94** (2), 514-519.

- 516 Hudson, E.K., Hogue, B.A., Souza-Pinto, N.C., Croteau, D.L., Anson, R.M., Bohr, V.A., Hansford, R.G. (1998) Age-associated change in mitochondrial DNA damage. *Free Radic Res*, **29** (6), 573-579.
- 517 Bennetts, L.E. and Aitken, R.J. (2005) A comparative study of oxidative DNA damage in mammalian spermatozoa. *Mol Reprod Dev*, **71** (1), 77-87.
- 518 Wang, J., Xiong, S., Xie, C., Markesbery, W.R., Lovell, M.A. (2005) Increased oxidative damage in nuclear and mitochondrial DNA in Alzheimer's disease. *J Neurochem*, **93** (4), 953-962.
- 519 Williams, M.D., van Remmen, H., Conrad, C.C., Huang, T.T., Epstein, C.J., Richardson, A. (1998) Increased oxidative damage is correlated to altered mitochondrial function in heterozygous manganese superoxide dismutase knockout mice. *J Biol Chem*, **273** (43), 28510-28515.
- 520 Wang, Y.-C., Lee, W.-C., Liao, S.-C., Lee, L.-C., Su, Y.-J., Lee, C.-T., Chen, J.-B. (2011) Mitochondrial DNA copy number correlates with oxidative stress and predicts mortality in nondiabetic hemodialysis patients. *J Nephrol*, **24** (3), 351-358.
- 521 Chan, S.W., Chevalier, S., Aprikian, A., Chen, J.Z. (2013) Simultaneous quantification of mitochondrial DNA damage and copy number in circulating blood: a sensitive approach to systemic oxidative stress. *Biomed Res Int*, **2013**, 157547.
- 522 Lee, H.-C. and Wei, Y.-H. (2005) Mitochondrial biogenesis and mitochondrial DNA maintenance of mammalian cells under oxidative stress. *Int J Biochem Cell Biol*, **37** (4), 822-834.
- 523 Guo, W., Jiang, L., Bhasin, S., Khan, S.M., Swerdlow, R.H. (2009) DNA extraction procedures meaningfully influence qPCR-based mtDNA copy number determination. *Mitochondrion*, **9** (4), 261-265.
- 524 Yoo, S.-E., Chen, L., Na, R., Liu, Y., Rios, C., van Remmen, H., Richardson, A., Ran, Q. (2012) Gpx4 ablation in adult mice results in a lethal phenotype accompanied by neuronal loss in brain. *Free Radic Biol Med*, **52** (9), 1820-1827.
- 525 Hinerfeld, D., Traini, M.D., Weinberger, R.P., Cochran, B., Doctrow, S.R., Harry, J., Melov, S. (2004) Endogenous mitochondrial oxidative stress: neurodegeneration, proteomic analysis, specific respiratory chain defects, and efficacious antioxidant therapy in superoxide dismutase 2 null mice. *J Neurochem*, **88** (3), 657-667.
- 526 Das, K.C. and Muniyappa, H. (2013) Age-dependent mitochondrial energy dynamics in the mice heart: role of superoxide dismutase-2. *Exp Gerontol*, **48** (9), 947-959.
- 527 Magnuson, M.A. and Osipovich, A.B. (2013) Pancreas-specific Cre driver lines and considerations for their prudent use. *Cell Metab*, **18** (1), 9-20.
- 528 Kawaguchi, Y., Cooper, B., Gannon, M., Ray, M., MacDonald, R.J., Wright, Christopher V E (2002) The role of the transcriptional regulator Ptf1a in converting intestinal to pancreatic progenitors. *Nat Genet*, **32** (1), 128-134.
- 529 Hoshino, M., Nakamura, S., Mori, K., Kawauchi, T., Terao, M., Nishimura, Y.V., Fukuda, A., Fuse, T., Matsuo, N., Sone, M., Watanabe, M., Bito, H., Terashima, T., Wright, Christopher V E, Kawaguchi, Y., Nakao, K., Nabeshima, Y.-I. (2005) Ptf1a, a bHLH transcriptional gene, defines GABAergic neuronal fates in cerebellum. *Neuron*, **47** (2), 201-213.
- 530 Obata, J., Yano, M., Mimura, H., Goto, T., Nakayama, R., Mibu, Y., Oka, C., Kawauchi, M. (2001) p48 subunit of mouse PTF1 binds to RBP-Jkappa/CBF-1, the intracellular mediator of Notch signalling, and is expressed in the neural tube of early stage embryos. *Genes Cells*, **6** (4), 345-360.
- 531 Sandbach, J.M., Coscun, P.E., Grossniklaus, H.E., Kokoszka, J.E., Newman, N.J., Wallace, D.C. (2001) Ocular pathology in mitochondrial superoxide dismutase (Sod2)-deficient mice. *Invest Ophthalmol Vis Sci*, **42** (10), 2173-2178.
- 532 Saborowski, M., Saborowski, A., Morris, John P 4th, Bosbach, B., Dow, L.E., Pelletier, J., Klimstra, D.S., Lowe, S.W. (2014) A modular and flexible ESC-based mouse model of pancreatic cancer. *Genes Dev*, **28** (1), 85-97.
- 533 Zhou, Q., Law, A.C., Rajagopal, J., Anderson, W.J., Gray, P.A., Melton, D.A. (2007) A multipotent progenitor domain guides pancreatic organogenesis. *Dev Cell*, **13** (1), 103-114.
- 534 Solar, M., Cardalda, C., Houbracken, I., Martin, M., Maestro, M.A., Medts, N. de, Xu, X., Grau, V., Heimberg, H., Bouwens, L., Ferrer, J. (2009) Pancreatic exocrine duct cells give rise to insulin-producing beta cells during embryogenesis but not after birth. *Dev Cell*, **17** (6), 849-860.
- 535 Reinert, R.B., Kantz, J., Misfeldt, A.A., Poffenberger, G., Gannon, M., Brissova, M., Powers, A.C. (2012) Tamoxifen-Induced Cre-loxP Recombination Is Prolonged in Pancreatic Islets of Adult Mice. *PLoS One*, **7** (3), e33529.

- 536 Hall, J.M., Couse, J.F., Korach, K.S. (2001) The multifaceted mechanisms of estradiol and estrogen receptor signaling. *J Biol Chem*, **276** (40), 36869-36872.
- 537 Dhar, S.K., Tangpong, J., Chaiswing, L., Oberley, T.D., St Clair, Daret K (2011) Manganese superoxide dismutase is a p53-regulated gene that switches cancers between early and advanced stages. *Cancer Res*, **71** (21), 6684-6695.
- 538 Case, A.J. and Domann, F.E. (2014) Absence of manganese superoxide dismutase delays p53-induced tumor formation. *Redox Biol*, **2**, 220-223.
- 539 Morton, J.P., Timpson, P., Karim, S.A., Ridgway, R.A., Athineos, D., Doyle, B., Jamieson, N.B., Oien, K.A., Lowy, A.M., Brunton, V.G., Frame, M.C., Evans, T.R.J., Sansom, O.J. (2010) Mutant p53 drives metastasis and overcomes growth arrest/senescence in pancreatic cancer. *Proc Natl Acad Sci U S A*, **107** (1), 246-251.
- 540 Vina, J., Sastre, J., Pallardo, F., Borras, C. (2003) Mitochondrial theory of aging: importance to explain why females live longer than males. *Antioxid Redox Signal*, **5** (5), 549-556.
- 541 Andren-Sandberg, A., Hoem, D., Backman, P.L. (1999) Other risk factors for pancreatic cancer: hormonal aspects. *Ann Oncol*, **10 Suppl 4**, 131-135.
- 542 Dorak, M.T. and Karpuzoglu, E. (2012) Gender differences in cancer susceptibility: an inadequately addressed issue. *Front Genet*, **3**, 268.
- 543 Bourhis, J., Lacaine, F., Augusti, M., Huguier, M. (1987) Protective effect of oestrogen in pancreatic cancer. *Lancet*, **2** (8565), 977.
- 544 Fernandez, E., La Vecchia, C., D'Avanzo, B., Negri, E. (1995) Menstrual and reproductive factors and pancreatic cancer risk in women. *Int J Cancer*, **62** (1), 11-14.
- 545 Kreiger, N., Lacroix, J., Sloan, M. (2001) Hormonal factors and pancreatic cancer in women. *Ann Epidemiol*, **11** (8), 563-567.
- 546 Prizment, A.E., Anderson, K.E., Hong, C.-P., Folsom, A.R. (2007) Pancreatic cancer incidence in relation to female reproductive factors: Iowa Women's Health Study. *JOP*, **8** (1), 16-27.
- 547 Sumi, C., Longnecker, D.S., Roebuck, B.D., Brinck-Johnsen, T. (1989) Inhibitory effects of estrogen and castration on the early stage of pancreatic carcinogenesis in Fischer rats treated with azaserine. *Cancer Res*, **49** (9), 2332-2336.
- 548 Velarde, M.C. (2014) Mitochondrial and sex steroid hormone crosstalk during aging. *Longev Healthspan*, **3** (1), 2.
- 549 Konduri, S. and Schwarz, R.E. (2007) Estrogen receptor beta/alpha ratio predicts response of pancreatic cancer cells to estrogens and phytoestrogens. *J Surg Res*, **140** (1), 55-66.
- 550 Jensen, E.V., Suzuki, T., Numata, M., Smith, S., DeSombre, E.R. (1969) Estrogen-binding substances of target tissues. *Steroids*, **13** (4), 417-427.
- 551 Kocanova, S., Mazaheri, M., Caze-Subra, S., Bystricky, K. (2010) Ligands specify estrogen receptor alpha nuclear localization and degradation. *BMC Cell Biol*, **11**, 98.
- 552 Xie, W., Duan, R., Chen, I., Samudio, I., Safe, S. (2000) Transcriptional activation of thymidylate synthase by 17beta-estradiol in MCF-7 human breast cancer cells. *Endocrinology*, **141** (7), 2439-2449.
- 553 Sun, G., Porter, W., Safe, S. (1998) Estrogen-induced retinoic acid receptor alpha 1 gene expression: role of estrogen receptor-Sp1 complex. *Mol Endocrinol*, **12** (6), 882-890.
- 554 Li, Z., Tuteja, G., Schug, J., Kaestner, K.H. (2012) Foxa1 and Foxa2 are essential for sexual dimorphism in liver cancer. *Cell*, **148** (1-2), 72-83.
- 555 Naugler, W.E., Sakurai, T., Kim, S., Maeda, S., Kim, K., Elsharkawy, A.M., Karin, M. (2007) Gender disparity in liver cancer due to sex differences in MyD88-dependent IL-6 production. *Science*, **317** (5834), 121-124.
- 556 Stein, B. and Yang, M.X. (1995) Repression of the interleukin-6 promoter by estrogen receptor is mediated by NF-kappa B and C/EBP beta. *Mol Cell Biol*, **15** (9), 4971-4979.
- 557 Guerra, C. and Barbacid, M. (2013) Genetically engineered mouse models of pancreatic adenocarcinoma. *Mol Oncol*, **7** (2), 232-247.
- 558 Pani, G., Bedogni, B., Anzevino, R., Colavitti, R., Palazzotti, B., Borrello, S., Galeotti, T. (2000) Deregulated manganese superoxide dismutase expression and resistance to oxidative injury in p53-deficient cells. *Cancer Res*, **60** (16), 4654-4660.
- 559 Drane, P., Bravard, A., Bouvard, V., May, E. (2001) Reciprocal down-regulation of p53 and SOD2 gene expression-implication in p53 mediated apoptosis. *Oncogene*, **20** (4), 430-439.
- 560 Dhar, S.K., Xu, Y., St Clair, Daret K (2010) Nuclear factor kappaB- and specificity protein 1-dependent p53-mediated bi-directional regulation of the human manganese superoxide dismutase gene. *J Biol Chem*, **285** (13), 9835-9846.

- 561 Irani, K., Xia, Y., Zweier, J.L., Sollott, S.J., Der, C.J., Fearon, E.R., Sundaresan, M., Finkel, T., Goldschmidt-Clermont, P.J. (1997) Mitogenic signaling mediated by oxidants in Ras-transformed fibroblasts. *Science*, **275** (5306), 1649-1652.
- 562 Ushio-Fukai, M. and Nakamura, Y. (2008) Reactive oxygen species and angiogenesis: NADPH oxidase as target for cancer therapy. *Cancer Lett*, **266** (1), 37-52.
- 563 Rajendran, P., Nandakumar, N., Rengarajan, T., Palaniswami, R., Gnanadhas, E.N., Lakshminarasiah, U., Gopas, J., Nishigaki, I. (2014) Antioxidants and Human Diseases. *Clin Chim Acta*.
- 564 Sayin, V.I., Ibrahim, M.X., Larsson, E., Nilsson, J.A., Lindahl, P., Bergo, M.O. (2014) Antioxidants accelerate lung cancer progression in mice. *Sci Transl Med*, **6** (221), 221ra15.
- 565 Banim, Paul J R, Luben, R., McTaggart, A., Welch, A., Wareham, N., Khaw, K.-T., Hart, A.R. (2013) Dietary antioxidants and the aetiology of pancreatic cancer: a cohort study using data from food diaries and biomarkers. *Gut*, **62** (10), 1489-1496.
- 566 Bjelakovic, G., Nikolova, D., Simonetti, R.G., Gluud, C. (2008) Systematic review: primary and secondary prevention of gastrointestinal cancers with antioxidant supplements. *Aliment Pharmacol Ther*, **28** (6), 689-703.
- 567 Heinen, M.M., Verhage, Bas A J, Goldbohm, R.A., van den Brandt, Piet A (2012) Intake of vegetables, fruits, carotenoids and vitamins C and E and pancreatic cancer risk in The Netherlands Cohort Study. *Int J Cancer*, **130** (1), 147-158.
- 568 Chandel, N.S. and Tuveson, D.A. (2014) The promise and perils of antioxidants for cancer patients. *N Engl J Med*, **371** (2), 177-178.
- 569 Pani, G., Colavitti, R., Bedogni, B., Fusco, S., Ferraro, D., Borrello, S., Galeotti, T. (2004) Mitochondrial superoxide dismutase: a promising target for new anticancer therapies. *Curr Med Chem*, **11** (10), 1299-1308.
- 570 HGNC. <http://www.genenames.org/> (22.08.14).

APPENDIX

Table Appendix.1: Gene symbols and names

Human Homologue	Mouse Homologue	Full Name	Common Synonyms
ADA	Ada	adenosine deaminase	-
AMY2A	Amy1	alpha-amylase (pancreatic)	-
BAX	Bax	BCL2-associated X protein	-
BCL2	Bcl2	B-cell CLL/lymphoma 2	-
BRAF	Braf	B-Raf proto-oncogene, serine/threonine kinase	-
BRCA2	Brca2	breast cancer 2, early onset	-
CASP3	Casp3	caspase 3, apoptosis-related cysteine peptidase	-
CAT	Cat	catalase	-
CCND1	Ccnd1	cyclin D1	B-cell CLL/lymphoma 1 (BCL1/Bcl1)
CDC25A	Cdc25a	cell division cycle 25A	-
CDKN1A	Cdkn1a	cyclin-dependent kinase inhibitor 1A	P21, p21CIP1, p21Cip1/Waf1
CDKN2A	Cdkn2a	cyclin-dependent kinase inhibitor 2A	p16INK4a, p19Arf
CK19	Ck19	cytokeratin 19	keratin 19 (KRT19/Krt19)
CYPA	Cypa	cyclophilin A	peptidylprolyl isomerase A (PPIA/Ppia)
DDR2	Ddr2	discoidin domain receptor tyrosine kinase 2	-
ERK1	Erk1	extracellular signal-regulated kinase 1	mitogen-activated protein kinase 3 (MAPK3/Mapk3), p44mapk
ERK2	Erk2	extracellular signal-regulated kinase 2	mitogen-activated protein kinase 1 (MAPK1/Mapk1), p41mapk
ESR1	Esr1	estrogen receptor 1	estrogen receptor alpha (ERA/Era)
ESR2	Esr2	estrogen receptor 2	estrogen receptor beta (ERB/Erb)
FSCN	Fscn	fascin	-
FOXA1	Foxa1	forkhead box A1	hepatocyte nuclear factor 3 alpha, (HNF3A/Hnf3a)
GADD45B	Gadd45b	growth arrest and DNA-damage-inducible beta	-
GCLC	Gclc	glutamate-cysteine ligase catalytic subunit	-
GCLM	Gclm	glutamate-cysteine ligase modifier subunit	-
GLRX	Glrx	glutaredoxin (thioltransferase)	-
GPX	Gpx	glutathione peroxidase	-
GSS	Gss	glutathione synthetase	-
GST	Gst	glutathione S-transferase	-
HMOX1	Hmox1	heme oxygenase (decycling) 1	HO-1
INS	Ins2	insulin	-
IL6	Il6	interleukin 6	-

JAK	<i>Jak</i>	Janus kinase	-
JARID1	<i>Jarid1</i>	<i>jumonji AT rich interactive domain 1</i>	lysine (K)-specific demethylase 5 (KDM5/Kdm5)
KRAS	<i>Kras</i>	<i>Kirsten rat sarcoma viral oncogene homolog</i>	-
MAO	<i>Mao</i>	<i>monoamine oxidase</i>	-
MAP3K5	<i>Map3k5</i>	<i>mitogen-activated protein kinase kinase kinase 5</i>	apoptosis signal regulating kinase 1 (ASK1/Ask1)
MAPK8	<i>Mapk8</i>	<i>mitogen-activated protein kinase 8</i>	JUN N-terminal kinase (JNK/Jnk), stress activated protein kinase (SAPK/Sapk)
MCL1	<i>Mcl1</i>	<i>myeloid cell leukemia 1</i>	-
MKI67	<i>Mki67</i>	<i>marker of proliferation Ki-67</i>	-
MPO	<i>Mpo</i>	<i>myeloperoxidase</i>	-
MSLN	<i>Msln</i>	<i>mesothelin</i>	-
MUC1	<i>Muc1</i>	<i>mucin 1</i>	-
MUC5	<i>Muc5</i>	<i>mucin 5</i>	-
NFKB	<i>Nfkb</i>	<i>nuclear factor of kappa light polypeptide gene enhancer in B-cells</i>	NF-kappaB, p50
NOS	<i>Nos</i>	<i>nitric oxide synthase</i>	-
NOX	<i>Nox</i>	<i>NADPH oxidase</i>	-
NOXA	<i>Noxa</i>	<i>Noxa</i>	phorbol-12-myristate-13-acetate-induced protein 1 (PMAIP1/Pmaip1)
p38	<i>p38</i>	<i>p38</i>	AHA1, activator of heat shock 90kDa protein ATPase homolog 1 (AHSA1/Ahsa1)
PAK1	<i>Pak1</i>	<i>p21 protein (Cdc42/Rac)-activated kinase 1</i>	-
PRDX	<i>Prdx</i>	<i>peroxiredoxin</i>	-
PSCA	<i>Psca</i>	<i>prostate stem cell antigen</i>	-
PTF1A	<i>Ptf1a</i>	<i>pancreas specific transcription factor 1a</i>	p48
PTPN1	<i>Ptpn1</i>	<i>protein tyrosine phosphatase non-receptor type 1</i>	Protein tyrosine phosphatase 1B (PTP1B/Ptp1b)
PTPN6	<i>Ptpn6</i>	<i>protein tyrosine phosphatase non-receptor type 6</i>	SH2-containing protein tyrosine phosphatase-1 (SHP-1/Shp-1)
PUMA	<i>Puma</i>	<i>p53 upregulated modulator of apoptosis</i>	BCL2 binding component 3 (BBC3/Bbc3)
RARA	<i>Rara</i>	<i>retinoic acid receptor alpha</i>	-
RET	<i>Ret</i>	<i>ret proto-oncogene</i>	-
SDHB	<i>Sdhb</i>	<i>succinate dehydrogenase complex, subunit B, iron sulfur (lp)</i>	-
SFN	<i>Sfn</i>	<i>stratifin</i>	14-3-3 sigma
SHC	<i>Shc</i>	<i>Src homology 2 domain-containing transforming protein 1</i>	p66
SMAD4	<i>Smad4</i>	<i>SMAD family member 4</i>	deleted in pancreatic carcinoma, locus 4 (DPC4/Dpc4)

SOD1	Sod1	superoxide dismutase 1	amyotrophic lateral sclerosis 1 (ALS1/Als1), Cu,Zn superoxide dismutase (Cu,Zn-SOD/Cu,Zn-Sod)
SOD2	Sod2	superoxide dismutase 2	Mn superoxide dismutase (Mn-SOD/Mn-Sod)
SOD3	Sod3	superoxide dismutase 3	extracellular superoxide dismutase (EC-SOD/EC-Sod)
SRC	Src	SRC proto-oncogene, non-receptor tyrosine kinase	-
STK11	Stk11	serine/threonine kinase 11	LKB1/Lkb1
TOP2A	Top2a	topoisomerase (DNA) II alpha 170kDa	-
TP53	Trp53	tumor protein p53	p53
TXN	Txn	thioredoxin	-
TXNRD	Txnrd	thioredoxin reductase	-
TYMS	Tyms	thymidylate synthetase	-
VEGF	Vegf	vascular endothelial growth factor	-
XDH	Xdh	xanthine dehydrogenase	xanthine oxidase (XO/Xo)

Common gene symbols and names were used in this theses. Most are taken from [570].

Table Appendix.2: Brands and companies.

Brand/Company	Location
abcam plc	Cambridge, U. K.
AlleMan Pharma GmbH	Rimbach, Germany
Altromin Spezialfutter GmbH & Co. KG	Lage, Germany
AppliChem GmbH	Darmstadt, Germany
BANDELIN electronic GmbH & Co. KG	Berlin, Germany
Bayer Vital GmbH	Leverkusen, Germany
B. Braun Melsungen AG	Melsungen, Germany
Bio-Rad Laboratories GmbH	Munich, Germany
Biozym Scientific GmbH	Oldendorf, Germany
BMG Labtech GmbH	Ortenberg, Germany
Brand GmbH + Co.	Wertheim, Germany
Carl Roth GmbH+Co. KG	Karlsruhe, Germany
Carl Zeiss AG	Oberkochen, Germany
Cayman Chemical	Ann Arbor, Michigan, U.S.A.
Cell Signaling Technologies, Inc.	Danvers, Massachusetts, U. S. A.
Corning, Inc.	Tewksbury, Massachusetts, U. S. A.
CP-Pharma-Handelsgesellschaft mbH	Burgdorf, Germany
Dako Deutschland GmbH	Hamburg, Germany
Developmental Studies Hybridoma Bank	Iowa City, Iowa, U.S.A.
Electron Microscopy Sciences	Hatfield, Pennsylvania, U.S.A.
ENZO Life Sciences, Inc.	Farmingdale, New York, U. S. A.
Eurofins Genomics GmbH	Ebersberg, Germany
Free Software Foundation	Boston, Massachusetts, U.S.A.
GE Healthcare UK Limited	Buckinghamshire, U. K.
GF Health Products, Inc.	Atlanta, Georgia, U. S. A.
GraphPad Software, Inc.	La Jolla, California, U.S.A

Greiner Bio-One GmbH	Frickenhausen, Germany
Heidolph Instruments, GmbH & Co. KG	Schwabach, Germany
J.T. Baker/Mallinckrodt Baker, Inc.	Griesheim, Germany
Konica minolta Medical Imaging USA, Inc.	Wayne, New Jersey, U. S. A.
Life Technologies GmbH	Darmstadt, Germany
Leica Biosystems Nußloch GmbH	Nußloch, Germany
Medite GmbH	Burgdorf, Germany
Merck KGaA	Darmstadt, Germany
Millipore Corporation	Temecula, California, U. S. A.
PEQLAB Biotechnologie GmbH	Erlangen, Germany
Promega GmbH	Mannheim, Germany
Qiagen GmbH	Hilden, Germany
Roche Diagnostics GmbH	Mannheim, Germany
ryma-pharm GmbH	Körle, Germany
Santa Cruz Biotechnology, Inc.	Santa Cruz, California, U. S. A.
Sarstedt AG & Co.	Nümbrecht, Germany
Scanbur A/S	Karlsunde, Denmark
Schubert & Weiss OMNILAB GmbH & Co. KG	Munich, Germany
Sigma-Aldrich Laborchemikalien GmbH	Taufkirchen, Germany
ssniff Spezialdiäten GmbH	Soest, Germany
ThermoFisher/Thermo Electron LED GmbH	Langenselbold, Germany
TPP Techno Plastic Products AG	Trasadingen, Switzerland
Vector Laboratories, Inc.	Burlingame, California, U. S. A.
Waldeck GmbH & Co. KG	Münster, Germany

ACKNOWLEDGEMENTS

First of all, I would like to thank Prof. Angelika Schnieke for readily agreeing to be my principal examiner and for her active contribution to this work as part of my Thesis Advisory Committee. Your advice and encouragement have always been of greatest value to me.

Further, I would like to especially thank Prof. Dr. Roland M. Schmid for accepting me as a Ph.D. student at his institute. Thank you for the guidance and support and in particular for sharing with me parts of your immense wisdom, experience, and enthusiasm. This was truly inspiring. Thank you also for enabling the many events, including the annual retreat, the hiking trips, and the Christmas parties that I could be part of in the last years. They sure made a great contribution to the excellent atmosphere within the 2. Medizinische Klinik.

Next, I would like to cordially thank my co-supervisor and main scientific advisor Dr. Henrik P. Einwächter. Thank you for the many helpful ideas, the vivid scientific discussions, and your continuous support.

Also, I would like to express my gratitude to PD Dr. Eike Gallmeier for the active participation as the third member of my Thesis Advisory Committee and Prof. Dr. Harald Luksch for agreeing to be head of the examination board.

Many thanks to the International Max Planck Research School for Molecular and Cellular Life Sciences (IMPRS-LS), especially the members of the Coordination Office Dr. Hans-Jörg Schäffer, Dr. Ingrid Wolf, and Maximiliane Reif for the high-end method and soft skill courses, the dedication, and the strong support throughout the entire time of my Ph.D..

Furthermore, I would like to thank Dr. Marina Lesina, Dr. Clara Lubeseder-Martellato, Thomas Briel, and Katharina Alexandrow for their invaluable methodological advice with the primary acinar explants and diverse immunohistochemistry protocols.

Many thanks to my fellow lab mates from AG Quante, Siveke, and Algül, especially Marc, Thomas, Flo, Bettina, Moritz, Anna, Chanty, Natasha, Marina, and Tobi, as well as my favorite technician Anja, for the great times, the coffee breaks, the beers and mulled wines, the 90ies music, your matter-of-course helpfulness and everything else. Also, I would like to thank all my friends from the MBT studies and the dormitory Wohnheim 3 in Freising for always cheering me up.

Finally, biggest thanks to my best friend Tina and my partner Uli for proofreading and revising my thesis and most importantly for all the tolerance, patience, support, and love. You were my rocks; I couldn't have accomplished this without you.

CURRICULUM VITAE

Persönliche Angaben

Name	Christin Ruoff
Geburtstag und -ort	14. März 1985 in Heilbronn (Neckar)
Staatsangehörigkeit	deutsch

Promotion

05/2010 – 11/2014	Doktorarbeit II. Medizinische Klinik u. Poliklinik, Klinikum rechts der Isar, Universitätsklinikum der TU München, München <i>“Role of Sod2 in Pancreatic Carcinogenesis”</i> Bedeutung eines pankreas-spezifischen Knockouts des antioxidanten Enzyms Sod2 für die Tumorentstehung und -progression in der Maus)
-------------------	---

Studium und Schule

10/2007 - 12/2009	Masterstudium der Molekularen Biotechnologie Technische Universität München, Freising Masterarbeit: <i>“Identification of Novel Long-Range Regulatory Elements for the Tumour Suppressor BRCA1”</i> (Note: 1,0) Abschluss: Master of Science in Molekularer Biotechnologie (Note: 1,0)
10/2004 - 07/2007	Bachelorstudium der Molekularen Biotechnologie Technische Universität München, Freising Bachelorarbeit: <i>“Construction of a cre Recombinase Gene under the Control of a Pancreas-Specific Promoter”</i> (Note: 1,3) Abschluss: Bachelor of Science in Molekularer Biotechnologie (Note: 1,7)
09/1995 - 06/2004	Schulbildung Zabergäu-Gymnasium Brackenheim, Brackenheim Abschluss: Allgemeine Hochschulreife (Note: 1,4)

Internationale Forschungserfahrung

03/2009 - 11/2009	Masterarbeit UQ Brisbane, SCMB, St Lucia, Australia
-------------------	---

Stipendien und Auszeichnungen

09/2014	Posterpreis und Reisestipendium 3rd International Conference on Tumor Microenvironment and Cellular Stress, Mykonos, Greece
03/2010 – 11/2014	Ph.D. Fellowship International Max Planck Research School for Molecular and Life Sciences (IMPRS-LS), Max-Planck-Institut für Biochemie, München
03/2009-07/2009	Stipendium für Masterarbeiten deutscher Graduerter im Ausland Deutscher Akademischer Austausch Dienst (DAAD)